Energy Management

Energy Management

Edited by
Francisco Maciá Pérez

Preface

Forecasts point to a huge increase in energy demand over the next 25 years, with a direct and immediate impact on the exhaustion of fossil fuels, the increase in pollution levels and the global warming that will have significant consequences for all sectors of society.

Irrespective of the likelihood of these predictions or what researchers in different scientific disciplines may believe or publicly say about how critical the energy situation may be on a world level, it is without doubt one of the great debates that has stirred up public interest in modern times.

The diverse and tragic events that have affected us recently —such as atmospheric phenomena, terrorist attacks, economic crises and ecological catastrophes— should help us to understand that the only possible response to these types of situations is to predict the possible scenarios that we might face in the short, medium and long term. In this way we may be prepared to prevent them or at least to mitigate their effects.

These arguments alone are enough to fully justify that the study of energy management issues should be seriously taking into account by researchers, whose initiatives must be called to become an important benchmark. Furthermore, there is a reason, even for the most sceptical, to take an interest in energy management: we are at an ideal moment in which set out new objectives for sectors that are fast reaching their limits. For example, for some time the end user has been more concerned about power consumption and overheating in a new microprocessor than its speed in gigahertz. Similarly, Internet service providers are seeking more processing power and storage capacity at the same time as a suitable location that assures them of a stable and continuous electricity supply for their installations. So that, if right decisions are made on time then these threats can be transformed into opportunities.

Whatever their motivations, many enterprises and governments have already started to develop energy management programs. For the moment, we can assume that we are still in the initial phases and that we are a little lost and bewildered, constantly asking ourselves what steps we should take or what measures we should adopt.

We should probably already be thinking about the design of a worldwide strategic plan for energy management across the planet. It would include measures to raise awareness, educate the different actors involved, develop policies, provide resources, prioritise actions and establish contingency plans. This process is complex and depends on political, social, economic and technological factors that are hard to take into account simultaneously. Then, before such a plan is formulated, studies such as those described in this book can serve to illustrate what Information and Communication Technologies have to offer in this sphere and, with luck, to create a reference to encourage investigators in the pursuit of new and better solutions.

Contents

Embedded Energy Management System for the ICT Saving Energy Consumption

Francisco Maciá-Pérez, Diego Marcos-Jorquera, Virgilio Gilart-Iglesias,
Juan Antonio Gil Martínez-Abarca, Luis Felipe Herrera-Quintero,
and Antonio Ferrándiz-Colmeiro

Computer Science Department. University of Alicante
Spain

1. Introduction

The importance of Information and Communication Technologies (ICT) in all areas of human activity in today's world is an indisputable fact. In the last years, there has been an exponential increase of the use of these technologies within the society, from its professional use in enterprises and organizations to its personal use in playful and everyday activities at home. In addition, the new ICT paradigms evolution together with the growing use of Internet have caused the apparition of new business models that require complex systems in order to support them, available 24 hours per day 7 days per week, with better quality of service, etc.

However, this growing use of ICT technologies together with the requirements of emerging business models is converting these technologies in one of the main responsible of the worldwide energy consumption increase. In this way, (Gartner press, 2007) determines that the emission rate of CO_2 originated from the ICT consumption is the 2% and predict that this energy consumption will grow in an exponential way in the next years if solutions are not adopted.

In fact, one part of this consumption is due to an inefficient use of the ICT technologies. According to the study described in (Mines et al., 2008), a great number of the ICT managers know the necessary measures that they have to realize in order to obtain a energy saving produced by the use of ICT in their organizations, however, usually this measures are not applied if they do not mean an economic benefit for the business. One of the main reasons of the inadequate energy consumption of ICT listed in the study is the lack of awareness of the users in relation to this energetic problem that involve an incorrect use of the ICT infrastructures. Some examples of this uses are to leave power on Personal Computers (PC's), printers, servers or network devices when is not necessary.

There is the paradox that one of the solutions with more repercussion nowadays in order to optimize the energy consumption of the ICT is the use of the same ICT. This approach is one of the main proposals of the European Union (Commission European Report, 2008) that pretend to promote an efficient use of the energy consumption through the use of the Information and Communications Technologies.

In consonance with this approach, our proposal consists of providing embedded IT management services in physical network devices (generally, small sized devices with simple services and low energy consumption), so that, in order to deploy those services, it is enough to select the specific device providing the service, and connecting it to the communications network. The device itself will obtain the minimum information required to activate the initial set up and, once this has been completed, execute the management tasks with minimal human intervention.

Obviously, from a functional point of view the services offered by these devices are totally compatible with the traditional network services and therefore their integration and interoperability are ensured.

By way of illustration and with the aim of arguing the motivating of the proposal, we suggest a specific management service that we named Energy Management System (EMS): a service for the ICT systems monitoring and consumption control of these same systems doing that the ICT resources will be available only when they are necessaries (in a proactive or scheduled way). Thus it will be possible to avoid processing and consumption during the downtimes. The goal of this service is to reduce and to optimize the energy consumption of the ICT infrastructures.

The basic function of the service will be to indicate to the embedded EMS device (eEMS) which equipment and which service or services of those equipments we wish to check in order to reduce the energy consumption. These actions will be done according to system global load or of the requirements defined by the user or system administrator.

In the following sections we provide a review of the current state of the art of the technologies involved; a description of the EMS service, hardware and software structure of the device in which it is embedded; the specification of the application protocol and its implementation as Web Service embedded in a specific network device and the test scenario in order to validate the proposal; and, finally, the conclusions on the research and the current lines of work.

2. Background

Increasing in the energy consumption has turned into a global problem. EU has ordered to the member states and industry to use the ICT to increase the energy efficiency as a mode to fight against climatic change and drive to economy recovery. According to European Union forecasts, through the ICT, the CO_2 emissions can be reduced up to 15% in 2020. For achieve this purpose, the saving energy is based on two mainly ways. On the one hand, to make aware population about how to use the energy. On the other hand, an improvement in control and management of the energy use in industries, offices and public places. In this document it is recommended that the ICT industry itself could be the pioneer reducing their own CO_2 emissions near to 20% in 2020 (European Union, 2008).

The majority of the proposals in order to reduce the ICT energetic consumption are focused on getting better design of the devices architectures. In (Moshnyaga & Tamaru, 1997) different design techniques of ICT devices architectures are described with the aim of reducing the energetic consumption of these devices. In this way the Green Grid (The green gird, 2009) is focused on the best practices and management approaches for lowering data centers energy consumption. The Department of Energy of USA released the Server Energy

Measurement Protocol (EnergyStar, 2009) that establishes a procedure for attaching an energy usage measurement to existing performance measurements for servers.

Another approach (Lawton, 2007) very used nowadays to reduce the ICT energetic consumption is the virtualization. This proposal is originated from the hypothesis that the majority of the servers in the data centers are working to the 20% of its capability. The use of virtualization systems such as VMWare enables to execute virtual machines inside an only server, making good use of its processing capability.

Fig. 1. Google´s Datacenter distribution.

In the same way, another alternative that takes an advantages of the virtualization for the reduction of power consumption of the DataCenters, as which it is produced by TIC's elements and its infrastructure(e.g refrigeration systems), basically it is the geographical distribution of DataCenters, under climatic zones that allows in dynamic way, move the computation to some places, where there exists a better conditions of temperature and also a places where the electricity's fees are lowest (Follow the moon). This approach is not oriented directly for the computation, besides, only this is applicable to a very big companies as Google.

However, in complex ICT environments with high availability requirements (replication, load balancing and clusterization), the proposals described previously are not enough to reduce the energetic consumption because the system management is not contemplated in a global way.

The use of embedded devices in order to provide services in a distributed environment is other of the solutions that allow decreasing the ICT infrastructures energetic consumption. In this sense, many of these devices include the Power over Ethernet (PoE) technology. This technology allows providing energy to the devices through of Ethernet wire (Deuty, 2004).

On the other hand, there are many proposals in order to monitor and control the energy consumption trough of ICT tools and applications. In (Pietilainen, 2003) several of these tools are described. These tools use emergent technologies such as Internet and distributed systems to control and to supervise energy consumption. This kind of tools is oriented to inspect the general energetic consumption in the buildings, and although they could be used to control the ICT specific consumption, these tools and applications do not include

features of proactive management, autonomy and inattention to optimize the consumption. In these cases, the person that manage the application is who once analyzed the information obtained has to take the decision and to execute it himself in order to optimize the consumption. In addition, these tools have to be executed in PC's, servers or more complex systems, and therefore, add an increase of the energetic consumption.

The early researches about the energy management consumption were mainly focused on embedded and notebook systems. In these studies, the way of manage dynamically the energy for extending battery life is based on switching devices to lower-power modes when there is a reduced demand of services. Static strategies of energy management can lead to poor performance or unnecessary energy consumption when there are wide variations in the rate of requests of services (Ren et al., 2005). Some researches have augured that operating systems should be able to both implement energy-conservation policies and manage power for server applications at the system level (beini et al., 1998). In (Lien et al., 2004) a system for saving energy in a web server clusters has been proposed by using dinamic server management. So, architecture for Dynamic Web-Server has beens presented for resources management in a server cluster. The goal was to allocate different numbers of servers for different service rates in a way that automatically adapts the server cluster to the Web requests and improves the energy efficiency. According to these proposals, in (Lien et al., 2004) a system for estimation of the energy consumption of streaming media centers has been proposed. All of the mentioned studies show the importance of to achieve saving energy consumption, specially, when the number of machines wired in networks is very high.

The use of network management systems can help to automate the maintenance activities, allowing an efficient use of the network resources, and to be used to reduce the energy consumption. The first open standards which attempted to address problems of ICT management in a global manner were SNMP and CMIP (RFC project, 2009), proposed by the IETF (Internet Engineering Task Force); both protocols being principally oriented towards network monitoring and control. The main inconvenience of these administration models was their dependence on the platform.

The use of multi-agent systems for computer network management provides a series of characteristics which favour automation and self reliance in maintenance processes (Du et al., 2003) (Guo et al., 2005). The creation of projects such as AgentLink III, the first Coordinated Action on based on Agents financed by the 6th European Commission Framework Programme, is a clear indicator of the considerable degree of interest in research into software agents.

In areas where automated handling of information and those where several devices are involved, such as industrial processes or domotics, there has been a trend in the development of autonomous management towards architectures designed for services for embedded systems (Topp et al., 2002) (Jammes et al., 2005). This final framework includes monitoring systems developed by third parties but residing with the client, who is responsible for their control and management. Along these lines we find proposals such as NAGIOS (NAGIOS, 2009), MON (MON, 2009), MUNIN/MONIT (MUNIT, 2009) (MONIT, 2009) or nPULSE (nPULSE, 2009) generic monitoring systems for network services for linux, with Web interface, highly configurable and based on open code which monitors the availability of network services and applications. The disadvantage of these proposals is based on the complexity of their installation and configuration in environments without

qualified system administrators, in addition to the complex systems and infrastructures required for their implementation.

The approach described in this research work is presented as a solution that bring together the advantages of the current network management systems oriented to the control of ICT energetic consumption together with the use of embedded devices that minimize the consumption of these management systems.

3. Energy Management Service

The main goal of the EMS is to manage the power on or power off of a set of elements in a communications network in terms of a planning or in a proactive manner, analyzing the status of the system that is managed.

The eEMS is the version of the management service that has been implemented in Web Service, and it has been embedded in a network device (known as eEMS Device) designed for this purpose (see fig. 2). This device is small in size, with low consumption, robust, transparent to existing ICT infrastructures and with minimum maintenance required from the system administrators.

The system administrator informs the eEMS device, by means of its *interface agents*, which of the network components require a power management. The eEMS device has sufficient knowledge of each device to carry out this task. This knowledge is included in *management agents* displaced to the device for this purpose. The *management agents* implement specific protocols for power on devices, as the Wake on LAN (WoL) standard, or for power off, as the shutdown in SNMP. In some cases, to take the decision to power off or power on a device, they utilize a set of *monitoring agents* that analyze applications, services or network traffic. In this way, if the device receives a request for manage a set of devices, it will request the adequate *monitoring agents* and *management agents* in a self sufficient manner in order to carry out this work. The *management and monitoring agents* are enough flexible to adapt to the possible different scenarios.

Thus, the eEMS device represents the core of the system. Figure 2 shows a diagram of the main elements and actors involved in the service, together with the existing relation between them. We may synthesise these as: eEMS Device, Network Components, Discovery Service, EMS Center, EMS Clients, a set of Software Agents and the EMS application protocol (EMSP). These elements shall subsequently be described in greater detail.

The eEMS device, as has been seen, is the cornerstone of the energy management service. It is designed in order to act as a proxy between the Wide Area Network (WAN) and Local Area Network (LAN) to which it provides support. This device provides a container in which different agents and applications ensure that the service can be executed.
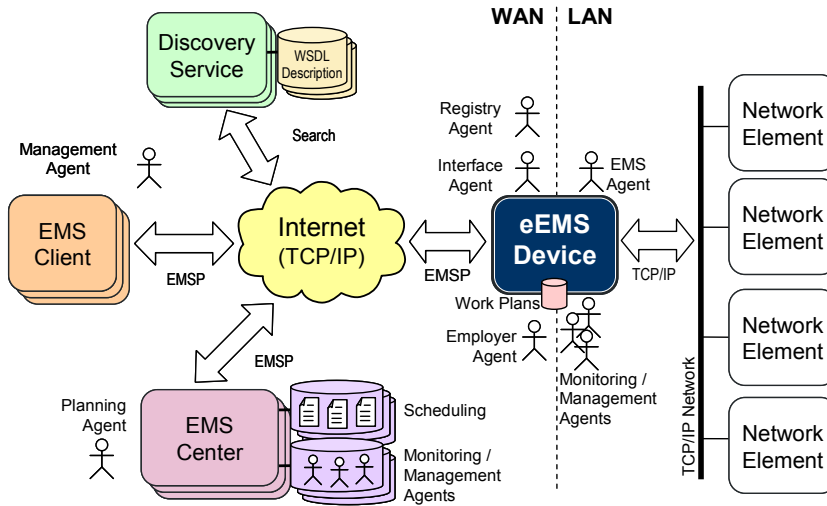
Fig. 2. Organization of functional elements of the EMS service.

In the proposal implementation, the device interface with the system administrators and with other management devices or management equipments is provided by agents acting as embedded Web Services (see *interface agent* in figure 2). From a functional point of view, this is the reason why an eEMS device can be to taken into account, simply, as if it were a Web Service. In this way, an eEMS device is responsible for collecting the management request from the WAN. These requests are based on EMSP protocol and encapsulated in SOAP (Simple Object Access Protocol) messages when they are sent to the Web Service Interface.

The Network Components are the goal of the network monitoring service and comprise all those devices connected to the TCP/IP network. This include PC's, servers, printers, routers and, in general, any device susceptive to power on or power off in a remote manner.

The Discovery Service comprises a standard Universal Description, Discovery and Integration (UDDI) registration service. It is responsible for maintaining the pages describing the EMS services in Web Service Description Language (WSDL) format, as well as facilitating that information to the clients wishing to access the service.

EMS Centers usually act as automated control panels for the eEMS devices distributed through Internet. This control is implemented through the *planning agents* who carry out, execute and verify all the previously established tasks on the eEMS devices. EMS Centres are also responsible for managing the repository of *monitoring and management agents* with the know-how of each device management. Although in large installations it is recommended that management and scheduling services are included, the existence of an EMS centre is not essential. Likewise, although each EMS centre can manage around a thousand eEMS devices, it is possible to use the number of EMS centers considered appropriate, and it is possible to create one hierarchy with these elements.

EMS Clients, through the *EMS agents*, provide the user with access to the EMS Centre (in order to manage work plans or query log files) and to the eEMS Devices (in order to manage particular devices). These clients are not necessary for the normal operating system; however, they avoid physical movements of the system administration staff.

Software agents. System functionality has been defined as a distributed application based on software agents, because this approach intrinsically includes aspects such as: communications, synchronization, updates, etc. Among the agents that have been defined in the system, the most important are the agents placed in the eEMS device, and as a result, they comprise the system core. Of these last agents, the *interface agents* are of prime importance as they allow the device to provide its functionality to external elements (see section).

The EMS protocol (EMSP) is a request-response application level protocol using SOAP messages. This protocol is used by the different system components in order to communicate between each other. In fact, as the application has been designed as a set of software agents, the protocol will be used by the software agents to communicate with each other (see section 5).

4. Software Agents

The software agents do not constitute a conventional multi-agent system because a generic context has not been defined for them, they do not use standard agent communication languages and they do not work collaborating to achieve a general target which is used by the agents to take its decisions. In fact, the set of software agents implement part of the functionality of a distributed application which has been designed to provide a network service; in this case, the monitoring service. The reason why agent approach is used lies in its simplicity to design distributed applications and to take into account aspects such as communication, mobility or software updates.

Each eEMS device comprises a set of agents that implement its interface with the system administrators or with others system elements (EMS clients or EMS centers). In order to guarantee the system's compatibility with a large range of technologies, several interface agents have been implemented. In this way, the *interface agent* provides a matching interface with Web Services-based applications. The *interface agent* can identify commands based on *EMSP protocol* and, from these commands, schedule the eEMS device work plan. *EMS agents*, *management agents* and *monitoring agents* are another type of agent placed in the eEMS device and designed to perform the energy management service. The first type of agents ensures execution of the scheduling, delegating the specific monitoring task to a *monitoring agent* and the specific management task to a *management agent*. In addition to these core agents, other agents are included in each eEMS device in order to perform auxiliary tasks. Thus, the *register agents* undertake to check the monitoring service in a Discovery Service; and the *employer agents* are responsible for locating the *management agents* or *monitoring agents* required by the eEMS device to carry out its task. These agents are mobile agents that, initially, can reside in an agent farm located in an EMS Centre.

CMD	ACTION	ARG	FUNCTION
SET	MODE		Reports the current operation mode.
		PASSIVE [port]	Sets the passive mode and, optionally, the listening port number.
		ACTIVE <ip> [:port]	Sets the active mode, specifying the EMS centerr's IP address and port number.
	RUN		Reports the current EMS service state.
		<STARTS STOP>	|Starts or stops the EMS service.
GET	SCHDL		Returns the list of scheduled tasks in the device.
	STATUS	[<host>[:port] [<service>]]	Returns the status of a specific service or a set of services.
PUT	SCHDL	<schdl-table>	Adds a task or a set of tasks to the scheduling.
MONITOR	ON	<host>:<port> <time> <service> [arguments]*	Establishes a monitoring rule for the address <host>:<port>, establishing the poliing time in seconds and the monitor that will be utilized as well as the arguments that this require.
	OFF	<host>:<port> <service>	Cancels a monitoring rule.
ALERT			Send an error alert.

Table 1. Main instructions of the EMS protocol.

Besides the agents located in each eEMS device, the distributed application is completed by other auxiliary agents located outside the device which, while not being crucial to the service, serve to make it more functional. As a result, the *client agents* reside in an EMS Client and are responsible for providing an appropriate interface for the administrators so that they can access the EMS Centre or an eEMS Device from any node connected to Internet. The *planning agents* reside in the EMS Centers and undertake the planning management of eEMS Devices.

5. EMS Protocol

The system agents, implemented in our prototype, communicate with each other by means of messages containing instructions capable of interpreting and executing. These instructions, together with their syntax and its pertinent response, come defined by the EMS Protocol or EMSP. When the agents specifically behave as Web Services, these commands will be incrusted inside the request and response SOAP messages. Web Services has been selected like communication protocol because it is an interoperable specification and that it permits to decouple totally the distinct actors of the system.

The EMS Protocol (EMSP) is a request-response application level protocol which gathers all monitoring service functionality through a set of instructions. The protocol has been defined as a request-response text-based application protocol. This enables it be easily adapted to different models, such as client-server (over basic protocols like HTTP, SMTP or telnet) and SOA (over protocols like SOAP).

The sequence diagram in figure 3 shows the basic service operation and the communication between the system software agents. The diagram comprises two blocks and is executed constantly in parallel mode. In the first block the device *interface agents* are on standby for

requests (from a *Planning Agent* or directly from a *Client Agent)*. When the interface agents receive a monitoring request, they add the task to the Work Plan database of the eEMS device. The second diagram block corresponds to the execution of the programmed tasks. In this case the *EMS Agent* is constantly checking the Work Plan database and selecting the suitable *Monitoring Agent* and the *Management Agent* to carry out the requested tasks.
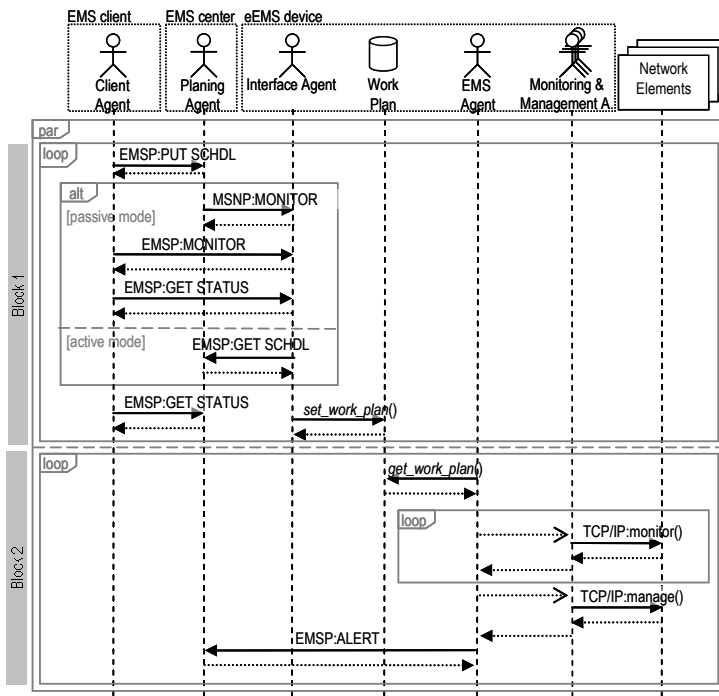
Fig. 3. Sequence diagram of the EMS main functionality.

Although it is not shown in this diagram, there is also a third block which concerns the contracting of the *Monitoring Agents*. When there is not a *Monitoring or Management Agent* able to deal with the service requested, the *EMS Agent* and the *Interface Agents* who have detected this lack may make a request to the *Employer Agent* programming it into its Work Plan. The *Employer Agent* then undertakes to obtain the *Monitoring Agents* required by the device. This agent is responsible for negotiating and validating the whole process. The *Monitoring & Management Agents* are mobile agents located in the agent repository in the EMS Centers.

6. eEMS Device Implementation and Test Scenario

In this section the implementation of an eEMS prototype device is presented (fig. 4). The hardware platform chosen for the prototype development is a *Lantronix Xport® AR™* device which has a 16 bit *DSTni-EX™* processor with 120MHz frequency reaching 30MIPS respectively (figure 4 shows an image of an eEMS device prototype connected to the service

network). The various memory modulates provided by this device undertake specific tasks according to their intrinsic features: the execution programmes and the dates handled by the device SRAM memory reside in the (1,25MB); the ROM memory (16KB) holds the system start up application and, finally, the flash memory, with 4MB, stores information which though non-volatile, is susceptible to change, such as the set up of the eEMS device or the system applications which may be updated. These capacities are sufficient for the memory requirements of the software developed for implementing the protocol.

Among other I/O interfaces, the device has a Fast Ethernet network interface which allows suitable external communications ratios. In addition, in order to ensure the correct system operation, there are several auxiliary elements such as: a watchdog which monitors the CPU and prevents it from blocking; and a PLL frequency divider required to set up the frequency of the system clock, with an adjustable clock signal (CLK) to optimise consumption or performance according to needs.

As a real time operating system, the device incorporates version 3 of the *Lantronix* OS, *Evolution OS™*. Through a confidentiality agreement with *Lantronix*, we have had access to the different modules of the system. Given the space restrictions, this has been crucial to develop a made-to-measure version of this OS. Salient elements of this version include, a TCP/IP stack together with several client-server application protocols (HTTP, TFTP, SNMP and telnet).

In the service layer, the implementation process has been conditioned by the limited characteristics of *XPort AR* device. Three service blocks are implemented: the middleware that provides the communication mechanisms of the monitoring service, the EMS service kernel with the implementation of EMS instructions, and the middleware platform that provides the execution of software agents.

The communication service middleware is upheld by standard protocols and technologies included in the *Evolution OS*. In the SOA based EMSP implementation (i.e., the Web Service interface), the cSOAP library was used for development, which is appropriate for these devices (cSOAP, 2009). However, some changes have been made to the original cSOAP library due to device limitations (restriction of memory use, proprietary libraries, etc.). These limitations have forced us to replace cSOAP XML parser, LibXML2 (over 1 MB in size), by another adapted XML parser with limited but sufficient functionalities to achieve our objective. Due to cSOAP limitations, only *RPC style* which uses the same protocol analyser used in the Client-Server version has been developed.
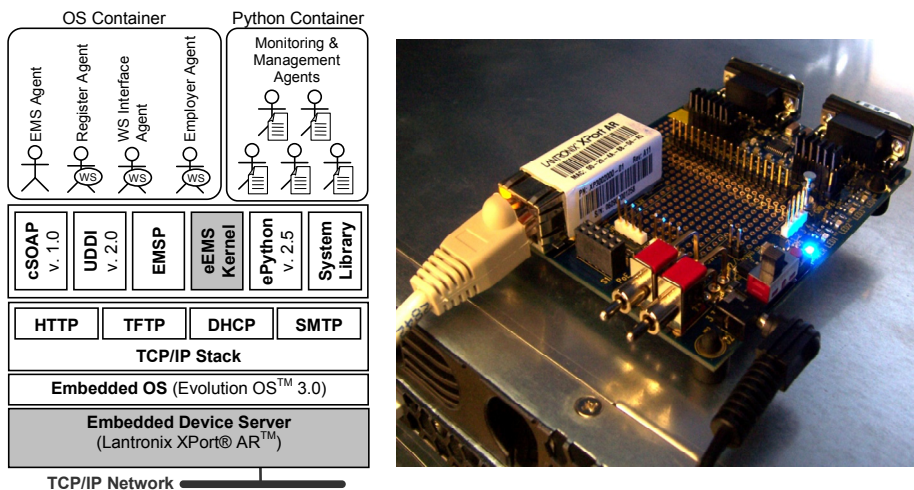
Fig. 4. eEMS device prototype architecture (left) and picture (right).

In addition, in order to register and to publish the services, an UDDI embedded version has been implemented based on UDDI version 2.0 which simply permits publishing the WSDL document associated with the monitoring service.

The EMS service kernel has been implemented as a functions library written in C language and offered as API for the others eEMS device modules. By means of this library, the intrinsic functionalities of the monitoring service are achieved.

In order to implement service agents, a division has been made in the implementation process between static and mobile agents. In the first case, an ad-hoc implementation for the *XPort AR* device has been developed in C language, using an operative system such as the agents' container. In the second case, in order to establish an execution framework for the mobile agents (the *monitoring agents*), a Python embedded engine (*ePython* version 2.5) has been adapted to the *XPort AR* features. These *monitoring agents* are implemented as *Python* text scripts.

In order to validate the proposal described in this research work the system and ICT infrastructures that support the Web applications of the Polytechnic University College at the University of Alicante have been chosen like test scenario (Fig. 5.). It is a replicated scenario that includes features of high availability and fault tolerance.

Fig. 5. Polytechnic University College Web Site.

The Web applications provide different services for the students around 9044, for the professors around 609, for the administration and services staff and for the external users. These applications are available during 24 hours per day and 7 days per week (inscription system, Web storage system, Web email system, management system, virtual classroom system, general information and others Web applications).

In the table 2, the system components are enumerated, describing the main services included and its infrastructures. This scenario is composed by 10 machines that gives to the users all that them need.

Service Type	Server Model	Number
Apache Web Server	Asus RS120-E4/PA2	3
Apache Tomcat Application Server	Asus RS120-E4/PA2	3
MySQL Database	Asus RS120-E4/PA2	2
OpenLDAP service directory	Asus RS120-E4/PA2	2

Table 2. The Polytechnic University College at the University of Alicante test scenario components.

In figure 6 is showed the chart that include the accesses average of all users to the applications of the Polytechnic University College and the amount of Web traffic transferred in one day. Based on the information displayed in the chart the consumption optimization strategy of the resources has been defined.
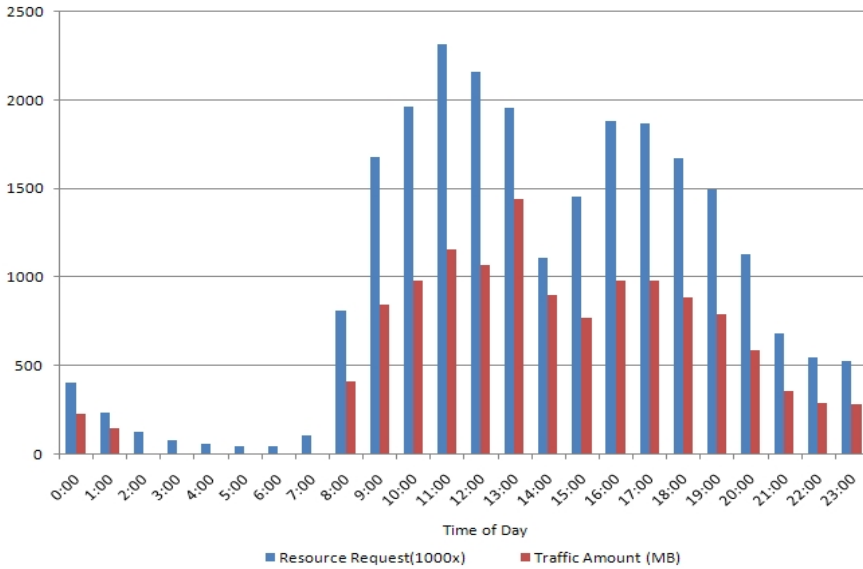
Fig. 6. Average of user requests and amount traffic per day.

In the eEMS device a scheduling has been established that define the time intervals in which all servers have to be power on, also we have considered the traffic by these, due to this variable offers what users needs, and therefore is possible to know when there is more or not information processing into the servers that causes an increment or a diminution of energy consumption. This scheduling has been realized according to the information obtained of the users' accesses to the different applications. In the critical periods the scheduling will obligate to maintain the systems at full performance. Out of the defined periods, the eEMS, in an automatic way, will be responsible of analyzing the information traffic, the request number and accesses to the different applications. In function of the analysis, the eEMS will send the adequate commands sequence in order to power on or power off different system nodes, that is, the system capacity level will be maintained in a dynamic way based on the petition.

The eEMS is able to manage all of the machines that take part into the infrastructure; the number of machines that is power on depends of the traffic that is generated by the users at the time of day. In our scenario there is always 7 machines turn it on due to the system needs to give support to critical applications, however there is several time of day that the eEMS systems keep power off some machines. In a normal infrastructure, there is always 10 machines that are power on and some machines are not been using by the users for that reason the energy consumption is higher. The eEMS allows to use the system in a more efficient way obtaining energy consumption saving. During one week several tests have been realized using the management service and as a result a 13,7% reduction of the energy consumption has been observed in relation to the system without the eEMS device (see table 3 and 4).

Service Type	Server Model	Energy Consumption Average with EMS (wh)		
		Minimum	Average	Maximum
Apache Web Server	Asus RS120-E4/PA2	195,04	660,87	885
Apache Tomcat Application Server	Asus RS120-E4/PA2	195,04	603,79	885
MySQL Database	Asus RS120-E4/PA2	195,04	466,67	590
OpenLDAP service directory	Asus RS120-E4/PA2	97,52	359	590

Table 3. Energy Consumption with the EMS system.

Service Type	Server Model	Energy Consumption Average without EMS (wh)		
		Minimum	Average	Maximum
Apache Web Server	Asus RS120-E4/PA2	292,56	700	885
Apache Tomcat Application Server	Asus RS120-E4/PA2	292,56	700	885
MySQL Database	Asus RS120-E4/PA2	195,04	466,67	590
OpenLDAP service directory	Asus RS120-E4/PA2	195,04	466,67	590

Table 4. Energy Consumption without EMS system.

The energetic saving has not been better (see figure 7) because in this scenario there was one requirement of faults tolerance that obligate to have, minim, two servers to support each service. Obviously, if the system is more complex and there are more replicated nodes for each service the energetic saving will be greater.
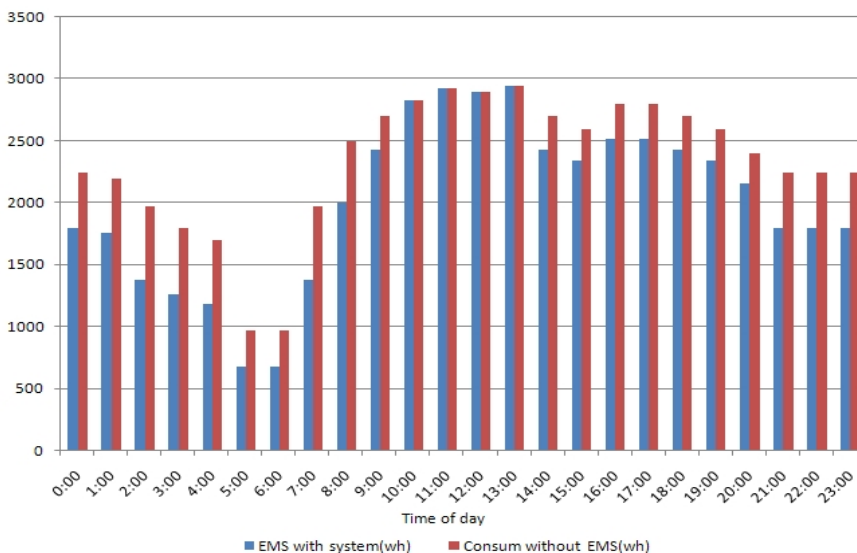

Fig. 7. Relation between energy consumption with the EMS system and without it.

Also, we considerer to highlighted, that the embedded device chosen include the PoE technology, when the eEMS is included in the system its consumption is practically negligible. If the network infrastructures where the eEMS is connected do not support PoE technology, the consumption of *XPort AR* where the service EMS is included would be only 0,957W.

7. Conclusion

In this paper we have presented an energy management system for the ICT infrastructures designed to saving the energy consumption. This system is totally complementary with others approaches oriented to the energy saving and is enough flexible to adapt to different scenarios. One of the most relevant aspects of this system consists of providing these embedded management services in network devices with small size, simple, low power consumption, adjusted costs, autonomous, designed with safety criteria and robustness, and compatible with the traditional network services through the standard protocols such as: SOAP, SMTP or HTTP. In order to validate the proposal, a functional prototype has been designed and implemented. The prototype has been used in a real scenario where we have obtained satisfied results.

We are currently working with other embedded network services and integrating them all in a model based on Semantic Web Services, so that in future they will not only be compatible with existing services, but also with new services or setups which were not considered in the initial design.

8. Acknowledgments

9. References

Beini, L; Boglio, A.; Cavalluci, S. & Riccó. B. (1998). Monitoring system activity for OS-directed dynamic power management. *International Symposium on Low Power Electronics and Design*. ISLPED'98 pp: 185 – 190, 1998 ISBN: 1-58113-059-7.

Commission European Report: Addressing the challenge of energy efficiency through Information and Communication Technologies, COM (2008) 241 final, Available from http://ec.europa.eu

cSOAP: http://csoap.sourceforge.net/ (URL).

Deuty, S. (2004). Exploring the options for distributed and point of load power in telecomm and network applications. *Telecommunications Energy Conference, 2004*. INTELEC 2004. 26th Annual International, pp 223- 229, ISBN: 0-7803-8458-X Chicago, September 2004, United States of America.

Du, T.C.; Li, E.Y. & Chang, A.P. (2003). Mobile Agents in Distributed Network Management. *In Communications at the ACM*, 46(7), pp127-132. ISSN:0001-0782, New York, July 2003, United Sates Of America.

Energy Star: http://www.energystar.gov/ (URL)

European Union. (2008). Addressing the challenge of energy efficiency through Information and Communication Technologies. http://eur-lex.europa.eu/LexUriServ/ LexUriServ.do?uri=COM:2008:0241:FIN:EN:PDF (URL)

Gartner press release: Gartner Estimates ICT Industry Accounts for 2 Percent of Global CO2 Emissions. Gartner Symposium/ITxpo 2007 Emerging Trends, April 26, (2007) Available from http://www.gartner.com/it/page.jsp?id=503867

Guo, J.; Liao, Y. & Parviz, B. (2005). An Agent-Based Network management system. *Presented at the 2005 Internet and Multimedia Applications.*

Jammes, F.; Smit, H.; Martinez-Lastra, J.L. & Delamer, I.M. (2005). Orchestration of Service-Oriented Manufacturing Processes. *Proc. of the 10th IEEE International Conference on Emerging Technologies and Factory Automation*, ETFA 2005, ISBN 0-7803-9401-1, Catania, September 19-22, 2005, Italy

Lawton, G. (2007). Powering Down the Computing Infrastructure. Computer, vol. 40, no. 2, pp. 16-19, IEEE Computer Society, ISSN: 0018-9162.

Lien, C.H.; Bai, Y.W.; Lin, M.B. & P.-A. Chen. (2004) The saving of energy in web server clusters by utilizing dynamic sever management. *Proceedings. 12th IEEE International Conference on Networs.* vol. 1, pp. 253–257. ISBN: 0-7803-8783-X. Hyderabad,December 2004,India

Lien, C.H.; Bai, Y.W. & Lin, M. B. (2007). Estimation by Software for the Power Consumption of Streaming Media Servers. *IEEE Transactions on Instrumentation and Measurement*. vol.56 no.5, pp: 1859-1870 . ISSN: 0018-9456. Braunschweig, October 2007, Germany

Mines, C.; Ferrusi, C.; Brown, E.; Lee, C. & Van-Metre, E. (2008).: The dawn of green IT services. A market overview of sustainability consulting for IT organizations. Forrester Research Report. (2008)

MON: http://www.kernel.org/software/mon/ (URL)

MONIT: http://www.tildeslash.com/monit/ (URL)

MUNIN: http://munin.projects.linpro.no/ (URL)

NAGIOS: http://nagios.org (URL)

Moshnyaga, G. V. & Tamaru, K. (1997). Energy Saving Techniques for Architecture Design of Portable Embedded Devices. *10Th annual IEEE International ASIC Conference and Exhibit*. ISBN: 0-7803-4283-6, New York, September 1997, United States of America.

nPULSE: http://www.horsburgh.com/h_npulse.html (URL)

Pietilainen, J. (2003). Improved Building Energy Consumption with the Help of Modern ICT. *ICEBO. International Conference for Enhanced Building operations*. California, October 2003, United States of America.

Ren, Z.; Krogh, B. H. & Marculescu, R. (2005). Hierarchical adaptive dynamic power management. *IEEE Transactions on Computers*, vol. 54, no. 4, pp. 409–420. ISSN:0018-9340.

RFC Project: http://www.rfc.net (URL)

The Green Grid: http://www.thegreengrid.org/ (URL)

Topp, U.; Muller, P.; Konnertz, J. & Pick, A. (2002). Web based Service for Embedded Devices, LNCS vol. 2593, 2002, pp. 141-153. ISBN 978-3-540-00745-6

Distributed Energy Management Using the Market-Oriented Programming

Toshiyuki Miyamoto
Osaka University
Japan

1. Introduction

This chapter discusses energy planning in a small district composed of a set of corporate entities. Although the term "energy planning" has a number of different meanings, the energy planning in this chapter stands for finding a set of energy sources and conversion devices so as to meet the energy demands of all the tasks in an optimal manner. Since reduction of CO_2 emissions which are the main factor of global warming is one of the most important problems in the 21st century about preservation of the earth environment, recent researches on energy planning consider reducing impacts to the environment(Cormio et al., 2003; Dicorato et al., 2008; Hiremath et al., 2007).

On the other hand, corporate entities with energy conversion devices become possible to sale surplus energy by deregulation about energy trading. Normally conversion devices have non-linear characteristics; its efficiency depends on the operating point. By selling energy to other entities, one may have an opportunity to operate its devices at a more efficient point.

We suppose a small district, referred to be a "group", that composed of independent plural corporate entities, referred to be "agents", and in the group trading of electricity and heat energies among agents are allowed. We also suppose that a cap on CO_2 emissions is imposed on each agent. Each agent performs energy planning under the constraints on CO_2 emissions and by considering energy trading in the group.

An agent may take various actions for reduction: use of alternative and renewable energy sources, use of or replacement to highly-efficient conversion devices, purchase of emission credits, and so on. Use of alternative and renewable energy sources and purchase of emission credits are easier ways to reduce CO_2 emissions. However, there is no guarantee to get sufficient amount of such energy or credit at an appropriate price, because the amount of such energy and credit is limited and their prices are resolved in the market. On the other hand, installing a highly-efficient conversion device comes expensive.

Another way to reduce CO_2 emissions is energy trading among agents. Suppose that one agent is equipped with an energy conversion device such as boilers, co-generation systems, etc. If he operates his device according to his energy demands only, the operating point of the device cannot be the most efficient one. Energy trading among agents makes it possible to seek efficient use of devices, and as a result to reduce CO_2 emissions.

When we attempt to minimize energy cost under the constraints on CO_2 emissions in the group, it is not difficult by considering the entire group as one agent. But it is another matter

whether each agent will accept the centralized optimal solution because agents are independent. Therefore, we adopt a cooperative energy planning method instead of total optimization. By this method, we want to reduce energy consumption considering the amount of the CO_2 emissions in the entire group without undermining the economic benefit to each agent.

A software system in the control center in a power grid to control and optimize the performance of the generation and/or transmission system is known as an energy management system (EMS). We are considering a distributed software system that performs energy planning in the group. We call such a energy planning system for the group a distributed energy management system (DEMS).

Corresponding mathematical formulation of the energy planning is known as the unit commitment (UC) problem(Padhy, 2004; Sheble & Fahd, 1994). Although the goal of our research is solving the UC problem and deciding the allocation of traded energies in DEMSs, the main topic of this chapter is to discuss how to find an optimal energy allocation. In order to make the problem simple, we consider the UC problem with only one time period and all of the energy conversion devices are active. Most methods for the UC problem solve in centralized manner. But as mentioned before we cannot apply any centralized method. Nagata et al. (2002) proposed a multi-agent based method for the UC problem. But they did not consider energy trading among agents.

The interest of this chapter is how to decide the allocation of traded energies through coordination among agents. In DEMSs, an allocation that minimize the cost of a group is preferred; a sequential auction may be preferred. Therefore, we propose to apply the market-oriented programming (MOP)(Wellman, 1993) into DEMSs.

The MOP is known as a multi-agent protocol for distributed problem solving, and an optimal resource allocation for a set of computational agents is derived by computing general equilibrium of an artificial economy. Some researches, which uses the MOP, have been reported in the fields of the supply chain management(Kaihara, 2001), B2B commerce(Kaihara, 2005), and so on. Maiorano et al. (2003) discuss the *oligopolistic* aspects of an electricity market.

This chapter is organized as follows. Section 2 introduces the DEMSs and an example group. An application of the MOP into DEMSs is described in Section 3. The bidding strategy of agents and an energy allocation method based on the MOP is described. In Section 4, computational evaluation of the MOP method is performed comparing with three other methods. The first comparative method is an multi-items and multi-attributes auction-based method. The second one is called the individual optimization method, and this method corresponds to a case where internal energy trading is not allowed. The last one is the whole optimization method.

2. Distributed Energy Management Systems

2.1 Introduction

A software system in the control center in a power grid to control and optimize the performance of the generation and/or transmission system is known as an energy management system (EMS). This chapter addresses an operations planning problem of an EMS in independent corporate entities. Each of them demands electricity and heat energies, and he knows their expected demand curves. Moreover a cap on CO_2 emissions is imposed on each entity, and it is not allowed to exhaust CO_2 more than their caps. Some (or all) entities are equipped with energy conversion devices such as turbines; they perform optimal planning of purchasing primal energy and operating energy conversion devices in order to satisfy energy demands and constraints on CO_2 emissions.

We suppose a small district, referred to be a "group", that composed of independent plural corporate entities, referred to be "agents", and in the group trading of electricity and heat energies among agents is allowed. In the case of co-generation systems, demands should be balanced between electricity and heat in order to operate efficiently. Even when demands from himself are not balanced, if an agent was possible to sell surplus energy in the group, efficiency of the co-generation system might be increased. Normally conversion devices have non-linear characteristics; its efficiency depends on the operating point. By selling energy to other entities, one may have an opportunity to operate its devices at a more efficient point. There is a merit for consumers that they are possible to obtain energies at a low price.

It is possible to consider the whole group to be one agent, and to perform optimization by a centralized method, referred to be a "whole optimization". The whole optimization comes up with a solution which gives the lower bound of group cost; since each agent is independent, there exists another problem that each agent accepts the solution by the whole optimization or not.

The DEMS is a software (multi-agent) system that seeks optimal planning of purchasing primal energy and operating energy conversion devices in order to satisfy energy demands and constraints on CO_2 emissions by considering energy trading in the group. The cost for each agent is defined by the difference between the total cost of purchased energy and the income of sold energy; the cost of the group is defined by the sum of agent's costs. We are expecting that the group cost is minimized as a result of profit-seeking activities of agents.

Generally, energy demands are time varying and cost arises at starting conversion devices up. Although the goal of our research is solving the UC problem and deciding the allocation of traded energies in DEMSs, the main topic of this chapter is to discuss how to find an optimal energy allocation. In order to make the problem simple, we consider the UC problem with only one time period and all of the energy conversion devices are active.

In DEMSs, since a cap on CO_2 emissions is imposed on each agent, it is necessary that a producer is able to impute his overly-emitted CO_2 to consumers in energy trading. Therefore, we employ not only the unit price but also the CO_2 emission basic unit for energy trading. The CO_2 emission basic unit means the amount of CO_2 emitted by energy consumption of one unit. Power companies and gas companies calculate CO_2 emission basic unit of their selling energies in consideration of relative proportions of their own energy conversion devices or constituents of products, and companies have been made them public. Consumers are possible to calculate their CO_2 emissions came from their purchased energy. Note that CO_2 emission basic unit is considered just as one of attributes of a energy in DEMSs, and its value could be decided independent of relative proportions of energy conversion devices or constituents of products.

In a group, agents are connected by electricity grids and heat pipelines; they are able to transmit energies via these facilities. The electricity grid connects each pair of agents, but the heat pipeline is laid among a subset of agents. We do not take capacities of electricity grids and heat pipelines into account; also no wheeling charge is considered.
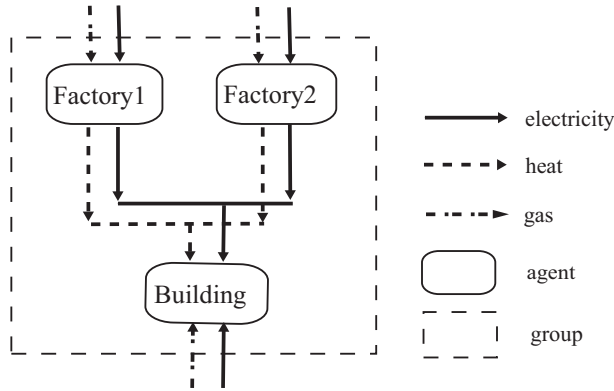
2.2 Example Group

Fig. 1. An example group
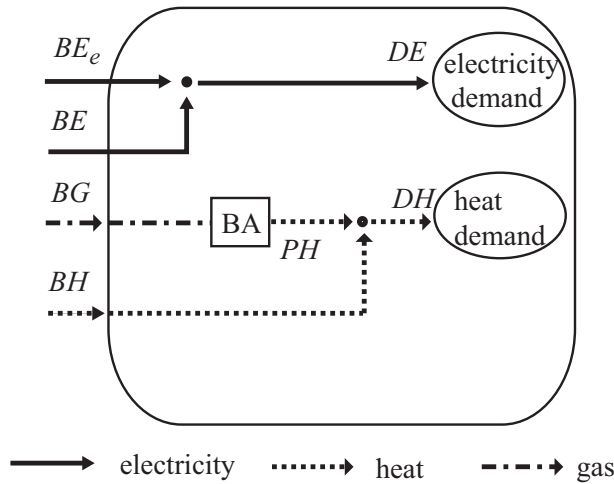
Fig. 2. A building model

Figure 1 depicts an example group that is a subject of this chapter. This group is composed of three agents: Factory1, Factory2, and Building. The arrows indicate energy flows; two factories purchase electricity and gas from outside of the group and sell electricity and heat in the group, and Building purchases electricity, gas and heat from both of inside and outside of the group.

Composition of each agent is shown in Fig. 2 and Fig. 3. BA is a boiler and GT is a gas-turbine. BE_e and BE express electricity purchased from outside and inside of the group, respectively. BG expresses gas purchased from outside of the group; BH expresses heat purchased from

Fig. 3. A factory model

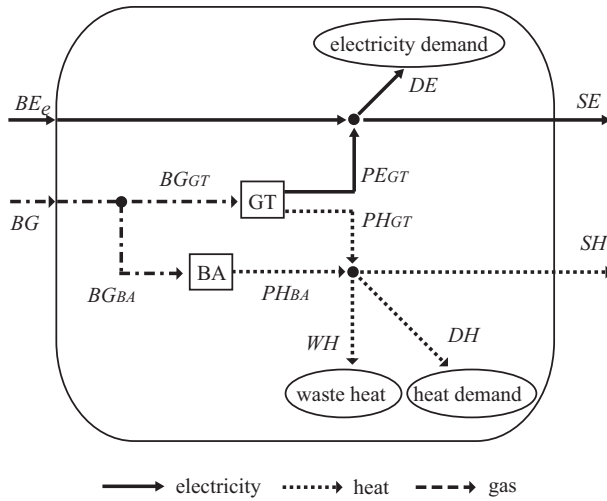inside of the group. PH is the produced heat and PE is the generated electricity. DE, DH, and WH express electricity demand, heat demand, and waste heat, respectively. Building tries to meet his electricity demand by purchasing electricity from inside and outside of the group, and he tries to meet his heat demand by producing heat with his boiler and by purchasing heat in the group. Factories tries to meed his electricity demand by generating electricity with his gas-turbine and by purchasing electricity from outside of the group, and he tried to meet his heat demand by producing heat with his boiler and/or gas-turbine.

3. Application of the Market-Oriented Programming into DEMSs

3.1 Market-Oriented Programming
The Market-Oriented Programming (MOP)(Wellman, 1993) is a method for constructing a virtual perfect competitive market on computers, computing a competitive equilibrium as a result of the interaction between agents involved in the market, and deriving the Pareto optimum allocation of goods. For formulation of the MOP, it is necessary to define (1) goods, (2) agents, and (3) agent's bidding strategies.

A market is opened for each good, and the value (unit price) of a good is managed by the market. Each agent cannot control the value, and he makes bids by the quantity of goods in order to maximize his own profit under the presented values. Each market updates the value in compliance with market principles (Fig. 4). Namely, when the demand exceeds the supply, the market raises the unit price; when the supply exceeds the demand, the market lowers the unit price. The change of unit price is iterated until the demand is equal to the supply in all markets; the state is called an equilibrium.
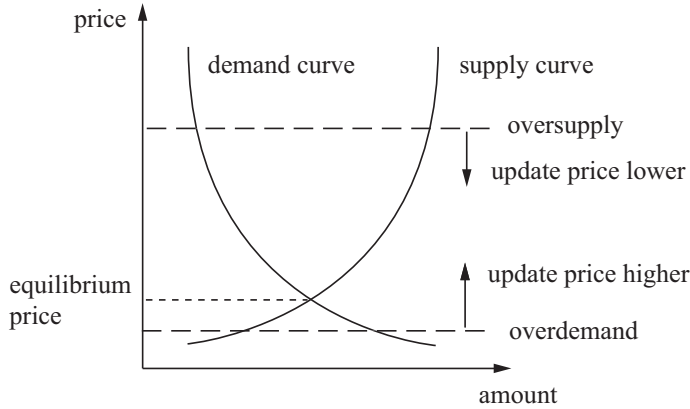
Fig. 4. Price updating in the market

3.2 Formulation of Markets

For the formulation of MOP, we define (1) goods (2) agents, and (3) agent's bidding strategies as follows:

(1) goods

Electricity and heat traded in the group are goods.

(2) agents

A corporate entity in the group is an agent, and an agent that has energy converters such as turbines can become a producer or a consumer, but it cannot be a producer and a consumer at the same time.

(3) agent's bidding strategies

Bidding strategies will be described in Section 3.3.

3.3 Bidding Strategies

Let $\mathcal{P} = \{p_1, \cdots, p_n\}$ be a set of agents. The set $\mathcal{E}$ of electricity energies is defined as follows:

$$\mathcal{E} = \{E_{ij} | p_i, p_j \in \mathcal{P}\} \cup \{E_{ei} | p_i \in \mathcal{P}\}, \tag{1}$$

where E_{ij} denotes electricity supplied from agent p_i to agent p_j, and E_{ei} denotes electricity that agent p_i purchased from outside of the group. The electricity E_{ij} is a pair $(\alpha_{E_{ij}}, \beta_{E_{ij}})$; $\alpha_{E_{ij}}$ is the unit price, and $\beta_{E_{ij}}$ is the CO_2 emissions basic unit of E_{ij}. The electricity E_{ei} is also a pair $(\alpha_{E_{ei}}, \beta_{E_{ei}})$. There exists only one kind of electricity in outside of the group, i.e. $\forall i, j, \alpha_{E_{ei}} = \alpha_{E_{ej}}$ and $\beta_{E_{ei}} = \beta_{E_{ej}}$.

The set of heat energies is represented by $\mathcal{H} = \{H_{ij}\}$, $(i, j = 1, \cdots, n, i \neq j)$, where H_{ij} denotes heat that is supplied from agent p_i to agent p_j. Also the heat H_{ij} is a pair $(\alpha_{H_{ij}}, \beta_{H_{ij}})$; $\alpha_{H_{ij}}$ is the unit price, and $\beta_{H_{ij}}$ is the CO_2 emissions basic unit.

$\mathcal{K} = \{K_{wi}\}$, $(i = 1, \cdots, n)$ represents the set of other energies, such as gas, that are supplied to agent p_i from outside of the group. K_{wi} is a pair $(\alpha_{K_{wi}}, \beta_{K_{wi}})$; $\alpha_{K_{wi}}$ is the unit price, and $\beta_{K_{wi}}$ is the CO_2 emissions basic unit.

The amount of traded electricity $E \in \mathcal{E}$ is expressed by a map $Q : \mathcal{E} \to \mathbb{R}^+$, where $\mathbb{R}^+$ is the set of non-negative real numbers. Here the following equations must hold for purchased electricity BE_i and sold electricity SE_i of agent p_i:

$$BE_i \quad = \sum_{j \neq i \vee j = e} Q(E_{ji}), \text{and} \tag{2}$$

$$SE_i \quad = \sum_{j \neq i \vee j = e} Q(E_{ij}). \tag{3}$$

The amount of traded heat $H \in \mathcal{H}$ is expressed by a map $R : \mathcal{H} \to \mathbb{R}^+$. The following equations must hold for purchased heat BH_i and sold heat SH_i of agent p_i:

$$BH_i \quad = \sum_{j \neq i} R(H_{ji}), \text{and} \tag{4}$$

$$SH_i \quad = \sum_{j \neq i} R(H_{ij}). \tag{5}$$

BK_{wi}, DE_i, DH_i, and WH_i express the amount of purchased energy K_{wi}, the demand, the head, and the waste heat of agent p_i, respectively.

The cost J_i of agent p_i is calculated by the following equation:

$$
\begin{aligned}
J_i \quad = \quad & \sum_{j \neq i \vee j = e} \alpha_{E_{ji}} \cdot Q(E_{ji}) + \sum_{j \neq i} \alpha_{H_{ji}} \cdot R(H_{ji}) + \sum_{K_{wi} \in \mathcal{K}} \alpha_{K_{wi}} \cdot BK_{wi} \\
& - \sum_{j \neq i} \alpha_{E_{ij}} \cdot Q(E_{ij}) - \sum_{j \neq i} \alpha_{H_{ij}} \cdot R(H_{ij}).
\end{aligned}
\tag{6}
$$

The CO_2 emissions CO_{2i} of agent p_i is calculated by the following equation:

$$
\begin{aligned}
CO_{2i} \quad = \quad & \sum_{j \neq i \vee j = e} \beta_{E_{ji}} \cdot Q(E_{ji}) + \sum_{j \neq i} \beta_{H_{ji}} \cdot R(H_{ji}) + \sum_{K_{wi} \in \mathcal{K}} \beta_{K_{wi}} \cdot BK_{wi} \\
& - \sum_{j \neq i} \beta_{E_{ij}} \cdot Q(E_{ij}) - \sum_{j \neq i} \beta_{H_{ij}} \cdot R(H_{ij}).
\end{aligned}
\tag{7}
$$

Let K_i be the cap on CO_2 emissions for agent p_i. Then the following equation must hold.

$$CO_{2i} \leq K_i \tag{8}$$

Let $\mathcal{U}_i = \{u_1, \cdots, u_m\}$ be the set of energy conversion devices of agent p_i. Each device has input-output characteristic function:

$$\Gamma_k : \mathbb{R}^{+\{IE_k, IH_k, IK_{wik}\}} \to \mathbb{R}^{+\{OE_k, OH_k\}}, \tag{9}$$

where IE_k is the amount of input electricity, IH_k is the amount of input heat, IK_{wik} is the amount of input energy K_{wi}, OE_k is the amount of output electricity, and OH_k is the amount of output heat for device u_k. The form of a characteristic function depends on the conversion device; in the case of gas boiler it could be expressed by the following function:

$$OH_k = p(IK_{wik})^b + d, \tag{10}$$

where p, b, and d are parameters. For adding constraints on output range, inequality can be used:

$$\underline{OH_K} \leq OH_k \leq \overline{OH_k}, \tag{11}$$

where $\underline{OH_K}$ and $\overline{OH_k}$ are the minimum output and the maximum output, respectively.
The following energy balance equations for each energy must hold in each agent.

$$BE_i + \sum_{k=1}^{m} OE_k \quad = \quad DE_i + SE_i + \sum_{k=i}^{m} IE_k \tag{12}$$

$$BH_i + \sum_{k=1}^{m} OH_k \quad = \quad DH_i + SH_i + WH_i + \sum_{k=i}^{m} IH_k \tag{13}$$

$$\forall K_{wi} \in \mathcal{K} : BK_{wi} \quad = \quad \sum_{k=i}^{m} IK_{wik} \tag{14}$$

Agent p_i will decide his bids for the markets by solving the following minimization problem.

$$\begin{aligned} \min \quad & J_i & (15)\\ \text{s.t.} \quad & (8), (12), (13), (14) \\ & \forall u_k \in \mathcal{U}_i : \Gamma_k \end{aligned}$$

Each agent finds the amount of purchased/sold energies and input energies for his conversion devices that minimize his own cost under the constraints of energy balance, the cap on CO_2 emissions, characteristics of devices.
Bidding strategies of agents introduced in Section 2.2 could be expressed as follows.
Building

$$\begin{aligned} \min \quad & \alpha_{BE_e} BE_e + \alpha_{BE} BE + \alpha_{BG} BG + \alpha_{BH} BH & (16)\\ \text{s.t.} \quad & PH = p_{BA} BG^{b_{BA}} - d_{BA} & (17)\\ & BE_e + BE = DE & (18)\\ & BH + PH = DH & (19)\\ & \beta_{BE_e} BE_e + \beta_{BE} BE + \beta_{BG} BG + \beta_{BH} BH \leq K_{\text{Building}} & (20) \end{aligned}$$

Factory

$$\begin{aligned} \min \quad & \alpha_{BE_e} BE_e + \alpha_{BG} BG - \alpha_{SE} SE - \alpha_{SH} SH & (21)\\ \text{s.t.} \quad & PE_{GT} = p_{GT_E} (BG_{GT})^{b_{GT_E}} - d_{GT_E} & (22)\\ & PH_{GT} = p_{GT_H} (BG_{GT})^{b_{GT_H}} - d_{GT_H} & (23)\\ & PH_{BA} = p_{BA} (BG_{BA})^{b_{BA}} - d_{BA} & (24)\\ & BE_e + PE_{GT} = DE + SE & (25)\\ & PH_{GT} + PH_{BA} = DH + SH + WH & (26)\\ & BG = BG_{GT} + BG_{BA} & (27)\\ & \beta_{BE_e} BE_e + \beta_{BG} BG - \beta_{SE} SE - \beta_{SH} SH \leq K_{\text{Factoriy}} & (28) \end{aligned}$$

3.4 Demand-Supply Curves

It is know that one of necessary conditions for the convergence of the MOP is convexity of the production possibility set(Wellman, 1993). The characteristic function of energy conversion devices is important of the convexity. For example, when the function is given by Equation (10), the parameter b must hold that $b < 1$. A typical example of demand-supply curves in DEMSs is shown in Fig. 5. There exist two characteristics in DEMSs.
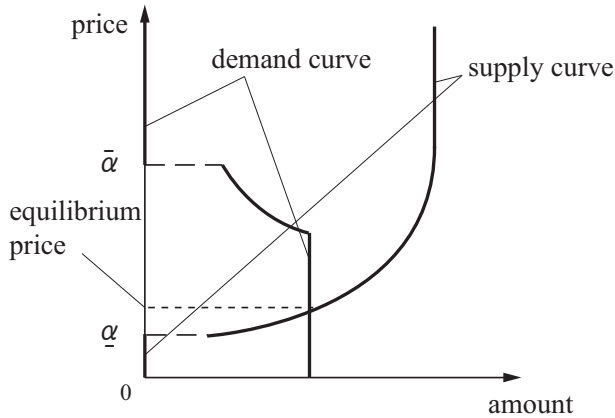

Fig. 5. Demand-supply curves in DEMSs

The first characteristic is that the demand (resp. supply) curve has a gap in the amount between 0 and some positive value at the price $\bar{\alpha}$ (resp. $\underline{\alpha}$). This is caused by that agents tries to maximize their economic profits. Namely, $\bar{\alpha}$ and $\underline{\alpha}$ are marginal prices so that agents are able to make a profit. It is profitable for a consumer to purchase the energy in the group when the price is lower than $\bar{\alpha}$, then he will bid a positive value. If the price is higher than $\bar{\alpha}$, it is profitable to purchase the energy from outside of the group, then his bid will become 0. Similarly, a producer will not supply energy in the group when the price is lower than $\underline{\alpha}$.

The second characteristic is that there exists a upper limit of the amount for both of the demand and the supply curves. The upper limit for the demand curve comes from the energy demand of consumers, and the upper limit for the supply curve comes from capacities of energy conversion devices.

3.5 Execution Procedure

Due to the characteristics described in Section 3.4, a case may happen that no crossing exists, therefore a simple MOP procedure does not converge to the equilibrium.

There exist two types for such a situation.

1. Over-demand at $\bar{\alpha}$ (Fig. 6)

   When producers are not able to supply enough energy to meet the demand of consumer agents, the demand exceeds the supply even at (just below of) $\bar{\alpha}$. At the next turn, the price becomes a little bit higher than $\bar{\alpha}$, then the demand becomes 0. Therefore vibration of price may appear.
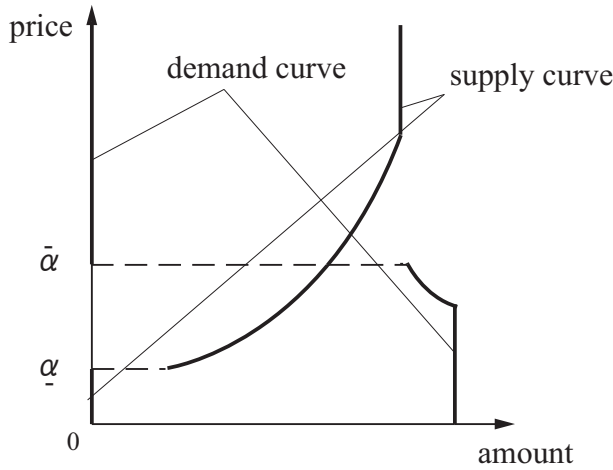
Fig. 6. Over-demand at $\bar{\alpha}$

In this case, the supplied energy is shared among consumer agents and the shortage must be managed by other methods. By introducing a cap on the demand in the MOP procedure, we realize that.

2. Over-supply at $\underline{\alpha}$ (Fig. 7)

When suppliers produce an ample of energy, the amount of the supply may exceeds the demands at (just above of) $\underline{\alpha}$. At the next turn, the price becomes a little bit lower than $\underline{\alpha}$, then the supply becomes 0. Also in this case, vibration of price may appear.

This kind of situation may occur when a supplier hold a co-generation system and his heat demand is not much. He operate the co-generation system in order to meet the electricity demand. But at the same time, plenty of heat will also produced. He may sell the heat even if the price is 0, but may not sell when the price becomes negative.

In this case, the energy demand is shared among producer agents and the rest is dumped. By introducing a cap on the supply in the MOP procedure, we realize that.

The idea described above 1. and 2. is realized by the following procedure, see Fig. 8. In the following the consumer is denoted by p_{con}, and the set of producers is denoted by $\mathcal{S}$.

At **Step1**, one market is established for each energy and for each consumer. The initial value is a pair (α_0, β_0), where α_0 is the initial unit price and β_0 is the initial CO_2 emissions basic unit. In each market, $d = \infty$, and $s_{p_i} = \infty$ for each $p_i \in \mathcal{S}$.

At **Step2**, the market presents 3-tuple (α, β, d) to the consumer, and (α, β, s_{p_i}) to producer $p_i \in \mathcal{S}$, where, α is the unit price, β is the CO_2 emissions basic unit, d is the upper bound of the demand, and s_{p_i} is the upper bound of the supply.

At **Step3**, the consumer and the producer decide the amount of the demand and the supply based on the condition that the market presents, respectively. The bidding strategy described in Section 3.3 is used for the decision.

At **Step4**, the market updates the price or the upper bound according to the supply and the demand. The bid amount by the consumer is denoted by $bid_{p_{con}}$, and the bid amount by the
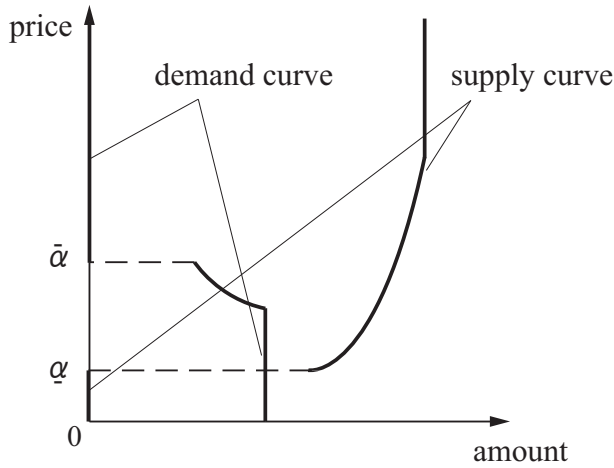
Fig. 7. Over-supply at $\underline{\alpha}$

producer p_i is denoted by bid_{p_i}. At **Case 2.3** and **Case 3.3**, the value of α is updated according to the equality (29):

$$\alpha := \alpha + \gamma(bid_{com} - \sum_i bid_{sup_i}), \tag{29}$$

where $\gamma > 0$ is a parameter. The equality (29) raises the unit price when over-demand, and lowers it when over-supply.

Steps from 2 to 4 are repeated until the condition of **Step4**-**Case 1** holds in all markets.

4. Computational Experiments

4.1 Energy Trading Decision Methods

This section introduces other energy allocation methods briefly.

4.1.1 Individual Optimization

Under the individual optimization method, each agent purchases energy only from outside of the group, and optimizes its running plan of conversion devices. By using this method, we can calculate group cost and cost for each agent under a condition that internal energy trading is not used.

4.1.2 Whole Optimization

The whole optimization method considers the group as one agent, and does optimization for the whole group. In this case the cap on emissions is imposed on the whole group. We can calculate lower bound cost for the group by using this method. This lower bound is optimal, and we cannot get better plan than that. With this method, we can get an energy purchase and running plan of devices, but we cannot get cost and CO_2 emission for each agent.

Step 1 Establish Markets

Step 2 Present Conditions

Step 3 Bid

Step 4 Update Condition

    Case 1 $bid_{p_{con}} = \Sigma_{p_i \in \mathcal{S}} bid_{p_i}$

        If this condition holds in all markets, the MOP procedure finishes.

    Case 2 $bid_{p_{con}} < \Sigma_{p_i \in \mathcal{S}} bid_{p_i}$

        Case 2.1 $d < \Sigma_{p_i \in \mathcal{S}} bid_{p_i}$

            The market raises d.

        Case 2.2 $d \geq \Sigma_{p_i \in \mathcal{S}} bid_{p_i} \wedge \alpha \leq \underline{\alpha}$

            The market lowers s_{p_i} for each $p_i \in \mathcal{S}$. The value of s_{p_i} is decided in proportion to bid_{p_i} and under the constraint of an equality $\Sigma_{p_i \in \mathcal{S}} s_{p_i} = bid_{p_{con}}$.

        Case 2.3 $d \geq \Sigma_{p_i \in \mathcal{S}} bid_{p_i} \wedge \alpha > \underline{\alpha}$

            The market lowers α.

    Case 3 $bid_{com} > \Sigma_{p_i \in \mathcal{S}} bid_{p_i}$

        Case 3.1 $bid_{p_{con}} > \Sigma_{p_i \in \mathcal{S}} s_{p_i}$

            The market raises s_{p_i} for each $p_i \in \mathcal{S}$.

        Case 3.2 $bid_{p_{con}} \leq \Sigma_{p_i \in \mathcal{S}} s_{p_i} \wedge \alpha \geq \overline{\alpha}$

            The market lowers d. The value of d is $\Sigma_{p_i \in \mathcal{S}} s_{p_i}$.

        Case 3.3 $bid_{p_{con}} \leq \Sigma_{p_i \in \mathcal{S}} s_{p_i} \wedge \alpha < \overline{\alpha}$

            The market raises α.

    The MOP procedure goes back to **Step2**.

Fig. 8. Execution procedure

4.1.3 Multi-attribute and Multi-item Auction

Miyamoto et al. (2007) proposed an energy trading decision method based on English auction protocol(David et al., 2002). This method is a multi-attribute auction because it uses two attributes: unit price and CO_2 emission basic unit. Also it is a multi-item auction because energy demands could be divided into several demands with small energy amount.

This method expresses energy value by

$$\nu = \lambda\alpha + \mu\beta, \tag{30}$$

where α is unit price, β is CO_2 emission basic unit, and λ and μ are parameters. A consumer shows three items: amount of energy demand, λ and μ. Producers bid three items: their amount of energy supply, α, and β. After some iterations, winning producers get rights to supply.

When an agent holds a conversion device, such as a gas turbine, that is able to produce more than one types of energy, electricity trading and heat trading are inseparable for the agent. Therefore, in (Miyamoto et al., 2007) we adopted a sequential method; we decide electricity trading first and then decide heat trading.

4.2 Configuration

In the following experiments, we used parameters shown in Tables 1 and 2.

α_{BE_e}[yen/kWh]	10.39
β_{BE_e}[kg-CO$_2$/kWh]	0.317
α_{BG}[yen/m^3]	28.6
β_{BG}[kg-CO$_2$/m^3]	1.991

Table 1. Unit price and CO$_2$ emission basic unit of electricity and gas from outside of the group

	Building	Factory 1	Factory 2
p_{BA}	35.03	37.22	37.02
b_{BA}	0.85	0.85	0.85
d_{BA}	5000	8000	8000
$\overline{PH_{BA}}$	10000	10000	5000
p_{GT_E}	-	17.91	16.32
b_{GT_E}	-	0.85	0.85
d_{GT_E}	-	6000	6200
$\overline{PE_{GT}}$	-	50000	30000
p_{GT_H}	-	31.84	25.87
b_{GT_H}	-	0.85	0.85
d_{GT_H}	-	2200	2200

Table 2. Parameters of energy conversion devices

Table 1 shows unit price and CO$_2$ emission basic unit of electricity and gas purchased from outside of the group. These values are taken from Web pages of power and gas company in Japan.

Table 2 shows parameters of conversion devices, where $\overline{PH_{BA}}$ is the maximum output heat of the boiler, and $\overline{PE_{GT}}$ is the maximum output electricity of the gas-turbine.

4.3 Ex1: Evaluation of Concurrent Evolution

This experiment is done in order to evaluate the concurrent evolution of electricity and heat trading. Table 3 shows energy demands and the cap on CO$_2$ emissions for each agent.

	Building	Factory 1	Factory 2
DE[kWh]	12000	40000	20000
DH[Mcal]	10000	30000	15000
K[kg-CO$_2$]	7500	20000	15000

Table 3. Ex1: energy demands and caps on emissions

Experimental results are shown in Tables 4, 5, 6, and 7.

By the auction method (Table 5), the producer agent assumes that amount of heat trade is zero when the agent calculate a bid for electricity auction. The agent cannot allow for emissions reduction through heat trading, and electricity sales of Factory 2 resulted in only 4748.1[kWh]. The agent cannot produce further electricity due to the caps.

	Factory 1	Factory 2	Building	total
BE_e[kWh]	51.4	0.0	2000.0	2051.4
BG[m^3]	10802.9	9195.3	342.5	20340.7
BE[kWh]	-	-	10000.0	10000.0
BH[Mcal]	-	-	10000.0	10000.0
SE[kWh]	0.0	10000.0	-	10000.0
SH[Mcal]	6747.2	3252.8	-	10000.0
CO_2[kg-CO_2]	20000.0	14402.7	6745.9	41148.6
cost[yen]	309497.0	159258.5	134302.6	603058.1

Table 4. Ex1: energy allocation by the MOP method

	Factory 1	Factory 2	Building	total
BE_e[kWh]	2303.3	1840.5	6704.6	10848.4
BG[m^3]	10357.1	7240.9	342.5	17940.5
BE[kWh]	-	-	5295.4	5295.4
BH[Mcal]	-	-	10000.0	10000.0
SE[kWh]	547.3	4748.1	-	5295.4
SH[Mcal]	9999.0	1.0	-	10000.0
CO_2[kg-CO_2]	20000.0	15000.0	4158.4	39158.4
cost[yen]	320144.3	184830.9	120837.9	625813.1

Table 5. Ex1: energy allocation by the auction method

	Factory 1	Factory 2	Building	total
BE_e[kWh]	0.0	0.0	0.0	0.0
BG[m^3]	13152.0	7331.0	342.5	20825.5
BE[kWh]	-	-	12000.0	12000.0
BH[Mcal]	-	-	10000.0	10000.0
SE[kWh]	8760.0	3240.0	-	12000.0
SH[Mcal]	10000.0	0.0	-	10000.0
CO_2[kg-CO_2]	-	-	-	41463.6
cost[yen]	-	-	-	595609.3

Table 6. Ex1: energy allocaiton by the whole optimization method

On the other hand, Factory 2 succeeded to sell electricity of 10000[kWh] by the MOP method (Table 4), because the agent could take emissions reduction through heat trading into consideration. This trade could not be achieved through sequential method such as the auction method. The MOP method succeeded to obtain better solution by deciding electricity and heat trade concurrently.

The whole optimization method worked out an optimal solution (Table 6), and Factory 1 which has the most efficient gas turbine produced most electricity and heat for Building. As a result, the group does not buy any electricity from the outside. As for group costs, we can say that group cost by the MOP method is not so different from cost by the whole optimization. Note that this method cannot decide the cost and CO_2 emissions for each agent.

	Factory 1	Factory 2	Building	total
BE_e[kWh]	7780.0	0.0	12000.0	19780.0
BG[m^3]	8806.0	6463.0	1247.0	16516.0
BE[kWh]	-	-	0.0	0.0
BH[Mcal]	-	-	0.0	0.0
SE[kWh]	0.0	0.0	-	0.0
SH[Mcal]	0.0	0.0	-	0.0
CO_2[kg-CO_2]	19999.0	12867.8	6286.8	39153.6
cost[yen]	332685.8	184841.8	160344.2	677871.8

Table 7. Ex1: energy allocation by the individual optimization method

The resulting plan by the individual optimization was expensive because internal energy trading was not used. The result (Table 7) shows effectiveness of the internal energy trading.

4.4 Ex2: Evaluation for Consumer's Demand Change

This experiment is done in order to evaluate efficiency of the methods under a change of consumer's demands. Energy demands and caps on CO_2 emissions for each agent are shown in Table 8. We fixed electricity demand and increased head demand by 10000[Mcal] of Building who is a consumer in the group. In this case, factories begin to start their boiler as electricity demand increases. In order to exclude influences of emissions constraints, the cap on emissions for Building was set enough large as 35000[kg-CO_2].

	Building	Factory 1	Factory 2
DE[kWh]	12000	40000	20000
DH[Mcal]	10000~110000	30000	15000
K[kg-CO_2]	35000	30000	20000

Table 8. Ex2: energy demands and caps on emissions

4.4.1 Comparison on Group Cost

Figure 9 shows transitions of group costs by each method when heat demand of Building changes.

Costs by all methods except the individual optimization are constant until 90000[Mcal]. This is because heat was over produced in order to produce electricity and internal trading of heat does not effect the group costs. When heat demand exceeds 100000[Mcal], agents have to start their boiler to meet the heat demand, and then the group costs increases.

In comparison to the individual optimization, which does not use internal trading, other three methods succeeded to reduce the group costs. This result shows that it is possible to reduce a group cost by introducing internal energy trading. For every heat demands, the MOP method obtains near optimal solutions, and they were better than the solutions by the auction method. This is an effect of the concurrent evolution.

4.4.2 Comparison on Agent Costs

Figure 10 shows transitions of CO_2 emissions for each agent by the MOP method, and Fig. 11 shows transitions by the auction method.
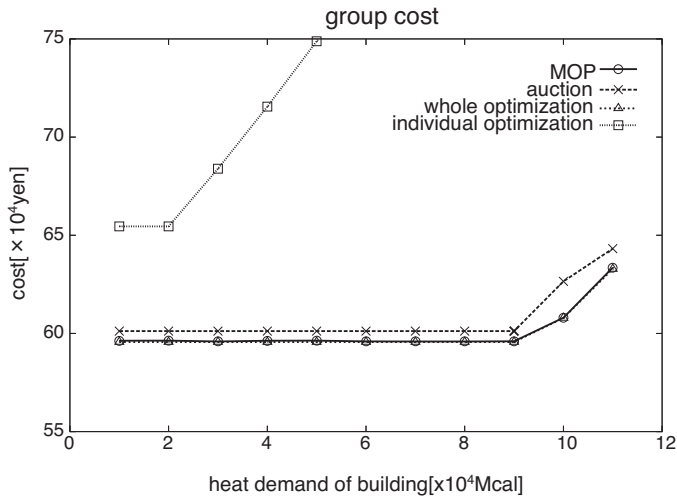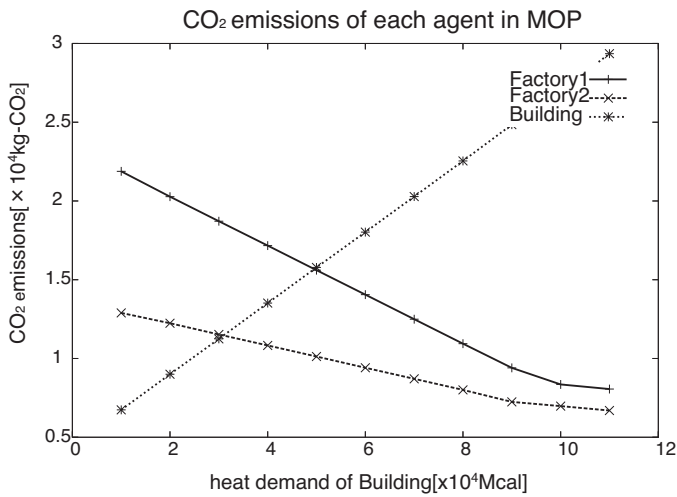
Fig. 9. Ex2: transition of group cost

Fig. 10. Ex2: transition of CO_2 emissions by the MOP method

As depicted in Fig. 10, by the MOP method emissions by Building increases linearly, and emissions of Factories 1 and 2 decease as heat demand increases. In this experiment, since CO_2 emission basic unit of heat is fixed as a positive value[1], emissions by consumers increases as heat demand increases, and producers can reduce their emissions by shifting emissions to the consumer.

---

[1] Actually the value is the same with a basic unit calculated by assuming that Building use its own boiler.
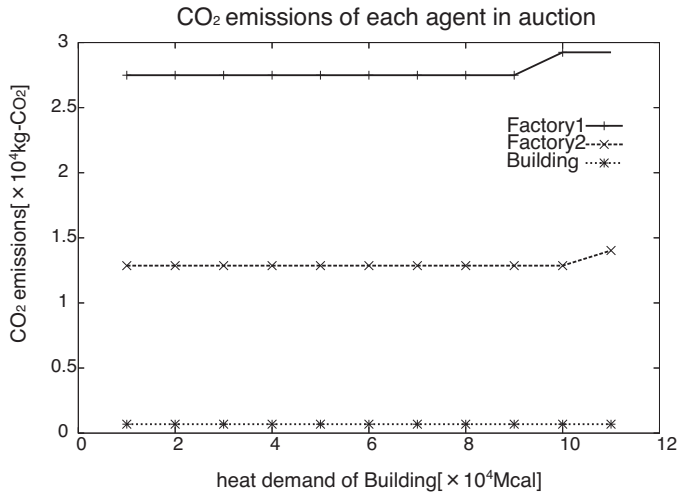
Fig. 11. Ex2: transition of CO_2 emissions by the auction method

On the other hand, as depicted in Fig. 11, by the auction method emissions by each agent were constant. In the auction method, producers can decide CO_2 emission basic unit for their bid. In this experiment, since caps on emissions for each agent was large enough, producers chose zero as CO_2 emission basic unit for their bids in order to reduce costs. As a result, CO_2 emissions by Factory 1 and 2 stayed at high level, and emissions by Building stayed at low level.

The MOP method at this point does not include a mechanism to change a value of CO_2 emission basic unit dynamically. This may cause a situation that results by the MOP becomes worse than the auction method when a cap on emissions for a producer is small. In order to confirm this prospect, the next experiment is done by changing caps on emissions for a producer.

4.5 Ex3: Evaluation on Caps on Emissions Change

	Building	Factory 1	Factory 2
DE[kWh]	12000	40000	20000
DH[Mcal]	10000	30000	15000
K[kg-CO_2]	7500	20000	11000~20000

Table 9. Ex3: energy demands and caps on emissions

Energy demands and caps on CO_2 emissions for each agent are shown in Table 9. We fixed the cap on CO_2 emissions for Factory 1 as 20000[kg-CO_2], and changed the cap for Factory 2.

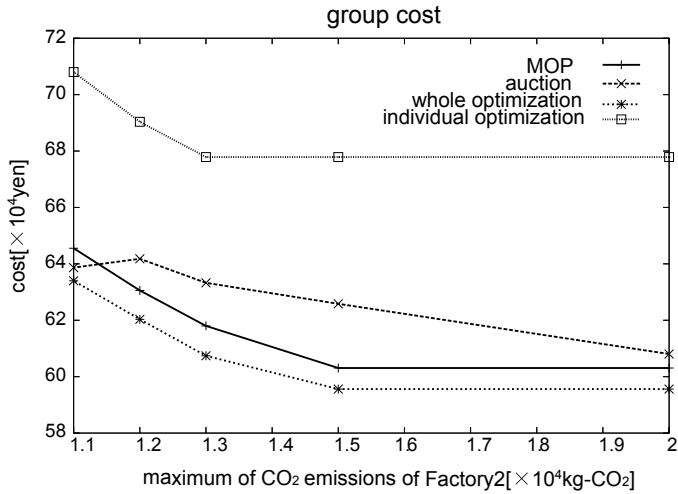### 4.5.1 Comparison on Group Cost

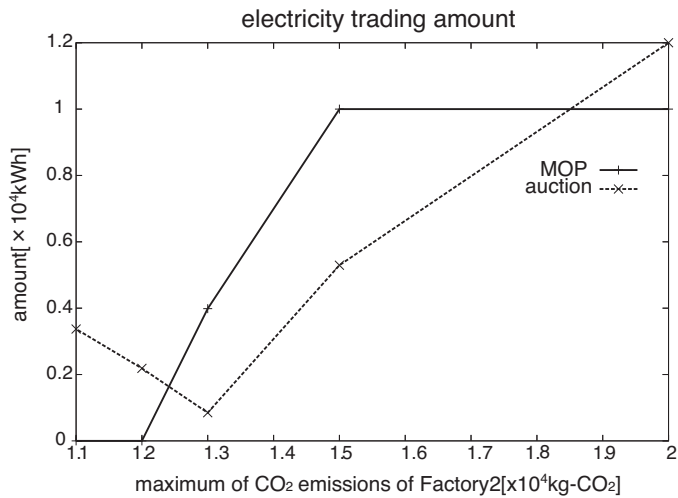Fig. 12. Ex3: transition of group cost

Fig. 13. Ex3: transitions of electricity trade of Factory2

Figure 12 shows transitions of group costs by each method when the cap on emissions for Factory 2 changes.

As depicted in Fig. 12, group costs by the MOP method are lower than the costs by the auction method when the caps on emissions for Factory 2 is larger than or equals to 12000[kg-CO$_2$]. The group cost by the auction method, however, becomes low when the cap is 11000[kg-CO$_2$]. Figure 13 shows transitions of electricity trade of Factory 2 by the MOP and the auction methods. When the cap was 11000[kg-CO$_2$], electricity was not traded internally by the MOP method, but was traded by the auction method. Since the MOP method at this point does not include a mechanism to change a value of CO$_2$ emission basic unit dynamically, Factory 2 chose zero as its supply for electricity market when the cap was less than or equals to 12000[kg-CO$_2$].

In the auction method, producers can decide CO$_2$ emission basic unit for their bid. Table 10 show combinations of unit price and CO$_2$ emission basic unit of bids by Factory 2. The table shows that Factory 2 selected a scheme to reduce emissions by setting unit price as zero and emission basic unit as a positive value when the cap was less than or equals to 12000[kg-CO$_2$]. As a result, the auction method succeeded to trade electricity internally for every cases.

	Factory 1		Factory 2	
$K_{Factory2}$	α	β	α	β
20000	0	0.9577	8.7153	0
15000	0	0.9577	8.7153	0
13000	0	0.9577	8.7153	0
12000	0	0.9577	0	1.1149
11000	0	0.9577	0	0.9577

Table 10. Ex3: change of unit price and CO$_2$ emission basic unit

As described above, we found that the MOP method at this point may lose an opportunity to deal internally in same special cases such as the cap on emissions for a producer is small.

4.6 Ex4: Evaluation on CO$_2$ Emissions Reduction

This experiment is done in order to evaluate possibility of CO$_2$ emissions reduction by the methods. Energy demands and caps on CO$_2$ emissions for each agent are shown in Table 11.

	Building	Factory 1	Factory 2
DE[kWh]	12000	40000	20000
DH[Mcal]	10000	30000	15000

Table 11. Ex4: energy demands and caps on emissions

Table 12 shows caps on CO$_2$ emissions for each agent, and CO$_2$ emissions basic units which were used for the MOP method. At first, we calculated minimal CO$_2$ emissions by using the individual optimization method for each agent. Values of this emissions were the caps at the first step, then the caps are decreased in the same rate r%. We evaluated whether each method is able to obtain a feasible solution. In case of the MOP method, we decreased also the CO$_2$ emissions basic unit in the same rate, so that Building meets the cap constraint.

$r[\%]$	$K_{Factory1}$	$K_{Factory2}$	$K_{Building}$	β_E	β_H
0	16999	11000	6286	0.317	0.226
1	16829	10890	6223	0.313	0.223
2	16659	10780	6161	0.310	0.221
3	16489	10670	6098	0.307	0.219
4	16319	10560	6035	0.304	0.216
5	16149	10450	5972	0.301	0.214
6	15979	10340	5909	0.297	0.212
7	15809	10230	5846	0.294	0.210

Table 12. Ex4: caps on CO_2 emissions and basic units

$r[\%]$	MOP	Auction	Whole
1	-	725400	710533
2	-	727623	717715
3	-	-	725179
4	-	-	732999
5	-	-	741153
6	-	-	749876
7	-	-	-

Table 13. Ex4: group costs when emissions basic units in Table 12 are used

$r[\%]$	MOP	Auction	Whole
1	710927	725400	710533
2	718397	727623	717715
3	725862	-	725179
4	733687	-	732999
5	741854	-	741153
6	751673	-	749876
7	-	-	-

Table 14. Ex4: group costs when $\beta_E = 0.502$, $\beta_H = 0.020$

Group costs by each method when emissions basic units in Table 12 were used are shown in Table 13. The whole optimization method succeeded to reduce CO_2 emissions of 6% from the individual optimization. This shows that by using internal energy trading it is possible to reduce CO_2 of maximally 6% in this case. The auction method succeeded to reduce emissions in 2%, and the MOP method failed to reduce.

In the case of this example, Factories have to operate their gas turbine further to produce electricity for internal trade, and then their emissions increases. On the other hand, since Factories have overly produced heat, internal trade of heat does not increase their emissions. Factories need to shift their emissions onto selling electricity.

Therefore, we set CO_2 emissions basic unit of electricity (resp. heat) as 0.502[kg-CO_2/kWh] (resp. 0.020[kg-CO_2/m^3]), and examined again. Results are shown in Table 14. In this case,

the MOP method succeeded to reduce emissions in 6%, and the group cost was close to that of the optimal solution. The auction method is not able to reduce further since Factories cannot allow for heat trade. The result shows that the MOP method is effective also for CO_2 emissions reduction.

The above discussion suggests to develop CO_2 emissions basic unit control mechanism in the MOP method. To do that, we have to develop the following two methods: 1) a method to sense a situation where basic unit should be adjusted, and 2) a method to adjust the basic unit. Our resent research considers how to realize the CO_2 emissions basic unit control mechanism(Sugimoto et al., 2008a;b).

5. Conclusion

This chapter considered energy management in a group which is composed of plural corporate entities. Entities perform optimal planning of purchasing primal energy and operating energy conversion devices in order to satisfy energy demands. Moreover a cap on CO_2 emissions is imposed on each entity, and it is not allowed to exhaust CO_2 more than their caps. This chapter discussed effectiveness the energy trading in the group.

In order to make the problem simple, we supposed the UC problem with only one time period and all of the energy conversion devices were active, and we discussed how to decide energy allocation among entities. So far, we had proposed an auction based method(Miyamoto et al., 2007), but the method had a problem on efficiency. Therefore we proposed the MOP based method for deciding energy allocation. In order to decide energy allocation in DEMSs, we formulated the group, and showed the MOP based execution procedure.

Next this chapter compared energy trading decision methods by computational experiments. The proposed MOP method succeeded to obtain better solutions than the previous auction method. We, however, found a necessity to develop CO_2 emissions basic unit control mechanism in the MOP method.

Directions of next research includes a) the CO_2 emissions basic unit control mechanism(Sugimoto et al., 2008a), b) groups with plural consumers(Sugimoto et al., 2008b), and c) planning over plural periods.

6. References

Cormio, C., Dicorato, M., Minoia, A. & Trovato, M. (2003). A regional energy planning methodology including renewable energy sources and environmental constraints, *Renewable and Sustainable Energy Reviews* **Vol.7**: 99–130.

David, E., Schwartz, R. & Kraus, S. (2002). An english auction protocol for multi-attribute items, *Lecture Notes in Computer Science* **Vol.2531**: 52–68.

Dicorato, M., Forte, G. & Trovato, M. (2008). Environmental-constrained energy planning using energy-efficiency and distributed-generation facilities, *Renewable Energy* **Vol.33**: 1297–1313.

Hiremath, R., Shikha, S. & Ravindranath, N. (2007). Decentralized energy planning; modeling and application – a review, *Renewable and Sustainable Energy Reviews* **Vol.11**: 729–752.

Kaihara, T. (2001). Supply chain management with market economics, *Intl. J. of PRODUCTION ECONOMICS* **Vol.73**(No.1): 5–14.

Kaihara, T. (2005). A study on resource allocation with buying behavior in b to b commerce, *Elec. Eng. in JAPAN* **Vol.153**(No.1): 63–72.

Maiorano, A., Song, Y. & Trovato, M. (2003). Modelling and analysis of electricity markets, *Operation of Market-oriented Power Systems*, Springer, pp. 13–49.

Miyamoto, T., Kitayama, T., Kumagai, S., Mori, K., Kitamura, S. & Sindo, S. (2007). An energy trading system with consideration of co_2 emissions, *Electrical Engineering in Japan* **Vol.162**(No.4): 1513–1521.

Nagata, T., Ohono, M., Kubokawa, J., Sasaki, H. & Fujita, H. (2002). A multi-agent approach to unit commitment problems, *Proceedings of the IEEE Power Engineering Society Transmission and Distribution Conference*, pp. 64–69.

Padhy, N. P. (2004). Unit commitment – a bibliographical survey, *IEEE Transactions on Power Systems* **Vol.19**: 1196–1205.

Sheble, G. B. & Fahd, G. N. (1994). Unit commitment literature synopsis, *IEEE Transactions on Power Systems* **Vol.9**: 128–135.

Sugimoto, Y., Miyamoto, T., Kumagai, S., Mori, K., Kitamura, S. & Yamamoto, T. (2008a). Co2 emission basic unit control mechanism in a distributed energy management system using the market oriented programming, *Proceedings of ICSET 2008*, pp. 583–588.

Sugimoto, Y., Miyamoto, T., Kumagai, S., Mori, K., Kitamura, S. & Yamamoto, T. (2008b). An energy distribution decision method in distributed energy management systems with several agents, *Proceedings of the 17th IFAC World Congress*, pp. 664–669.

Wellman, M. P. (1993). A market-oriented programming environment and its application to distributed multi-commodity flow problems, *Journal of Artificial Intelligence Research* **Vol.1**: 1–23.

Efficient Energy Management to Prolong Lifetime of Wireless Sensor Network

Hung-Chin Jang and Hon-Chung Lee
National Chengchi University
Taiwan, R.O.C.

1. Introduction

Since the batteries in a wireless sensor network are either hard to charged or replaced, how to efficiently utilize limited energy in a wireless sensor network has become an important issue. Those operations for a sensor to consume energy are target detection, data transmission and reception, data processing, etc. Among others data transmission consumes most of the energy, and it heavily depends on the transmission distance and the transmitted data amount. In the literature those methods have been devoted to energy saving problems can be categorized into shortening transmission distance (Heinzelman et al., 2000), reducing transmitted data amount (Klein, 1993), scheduling radio transceivers (Busse et al., 2006), scheduling sensing components (Huang & Tseng, 2003), adjusting transmission range (Wang, 2004), and adjusting detection range (Cardei et al., 2006). Our approach focuses on adjusting the detection range of each sensor in order to reduce the overlaps among detection ranges while keep the detection ability above a predefined threshold. If we can largely reduce the overlaps among detection ranges and effectively decrease the amount of duplicate data then we will be able to save energy more efficiently. Meguerdichian et al. (2001) exploited the coverage problem in wireless ad-hoc sensor networks in terms of Voronoi diagram and Delaunay triangulation. In this paper we propose a Voronoi dEtection Range Adjustment (VERA) method that utilizes distributed Voronoi diagram to delimit the responsible detection range of each sensor. Then we use Genetic Algorithm to optimize the most suitable detection range of each sensor. Simulations show that VERA outperforms Maximum Detection Range, *K*-covered (Huang & Tseng, 2003), and Greedy (Cardei et al., 2006) methods in reducing the overlaps among detection ranges, minimizing energy consumption, and prolonging network lifetime.

This paper is organized as follows. Section 2 has a detailed survey on the related work. Section 3 introduces a five-step framework of our proposed methodology, which includes position determination, detection range partition, grid structure establishment, detection power minimization, and detection power adjustment. Section 4 presents system simulations and results. Finally, section 5 offers brief concluding remarks.

2. Related work

In a wireless sensor network, wireless transmission consists of three major operations: (1) convert data into radio waves, (2) amplify radio waves until reaching the receiving sensors, (3) receiving sensors receive data. The amount of energy consumed in each of the three operations is proportional to the transmitted data amount. Furthermore, the amount of energy consumed in operation (2) is inversely proportional to the square of the distance between two communicating sensors. Both of them imply energy consumption can be effectively reduced by shortening the transmission distance and reducing the transmitted data amount.

Much research has been devoted to energy saving problem in the literature. Those approaches can be classified into shortening transmission distance, reducing transmitted data amount, scheduling radio transceivers, scheduling sensing components, adjusting transmission range and adjusting detection range.

Heinzelman's work (Heinzelman et al., 2000) focuses on shortening the transmission distance in order to reduce energy consumption. Given that sensor A has data to be forwarded to sensor C, if there exists a sensor B such that $[dist(A,C)]^2 \geq [dist(A,B)]^2 + [dist(B,C)]^2$ then the original routing path "sensor A $\rightarrow$ sensor C" will be changed to "sensor A $\rightarrow$ sensor B $\rightarrow$ sensor C". Klein's work (Klein, 1993) is based on data fusion. Klein assumed the data collected by those sensors within the same area should be quite similar (redundant). For example, the collected temperatures from sensors of the same area are about the same. Once all these similar data forwarded to a responding sensor, it fuses these data before forwarding to the next stop. This may thus mitigate energy consumption by reducing transmitted data amount. Data fusion usually works with clustering. Sensors in a clustering structure are classified into different clusters according to their locations. Each cluster has a cluster head that is responsible for collecting, fusing and forwarding data. Due to overloaded workload of cluster head, it usually consumes the most energy than the other cluster members. To prolong the lifetime of the whole sensor network, all cluster members should take turns to serve as the cluster head. Energy saving can also be achieved through scheduling. Sensor is made of different components, e.g., sensing component, processor, transceiver, memory and battery. Each component can be individually enabled to operation. Those components of a sensor that are not in operations can be turned off temporarily for the sake of energy saving. This can be realized through scheduling of radio transceivers and sensing components. Scheduling of radio transceivers means to turn the transceivers on (operating mode) and off (sleep mode). Those transceivers that are not responsible for transmitting and relaying data could be turned off while other components, like sensing components and processors, function normally. Busse et al. (2006) proposed a Topology and Energy Control Algorithm (TECA). In TECA, each sensor in a cluster, after functioning for a while, has to determine whether it should turn off its transceiver or not. This decision is made according to the role it plays in the cluster. If a sensor serves as a cluster head or bridge (the one connecting nodes between two clusters) then it keeps, otherwise, turns it off. Even if a sensor moves to sleep mode, it still listens to the messages from the cluster. Once, a sensor is called to serve as a cluster head (or bridge), it resumes itself from sleep mode and turns on its transceiver. Sensing components can be scheduled in a similar way. A sensor turns off those sensing components that are not on duty. Such sensor can still transmit and forward data. Huang & Tseng (2003) proposed a *K*-covered method that is able to cover a sensor field in a 2D or 3D space with least number of sensors. With scheduling, it may come

to another energy saving problem. Each component of a sensor may be turned on and off frequently. Restarting sensor components from sleep mode frequently may consume more energy than that saved by staying in sleep mode. Some researchers proposed adjusting the communication range of each sensor to just enough short distance. This adjustment is usually based on optimization. Wang (2004) proposed adjusting the transmission power of each sensor in order to reduce the communication range of each sensor and thus save much energy. His method should work under the precondition of no broken connections. Detection range adjustment is an alternative approach without extra power consumption due to restarting sensors. In the recent years active sensors, like microwave sensors, are able to proactively detect moving objects by using microwave, laser, ultrasonic, etc. This also makes energy saving possible by simply adjusting sensing power and detection range. Cardei et al. (2006) proposed a Greedy algorithm to solve target coverage problem by adjusting detection range. Area coverage problem means how to use limited sensors to cover the whole area, while target coverage problem considers only how to cover all targets in that area. Cardei et al., first, randomly deployed several targets in a sensing field, then generated set covers to fully cover those targets. Each set cover is formed by several sensors, and each sensor is allowed to join different set covers. All these set covers are then used to monitor all targets in turn.

3. Methodology

We assume that there are n sensors, S_1, S_2,…,S_n, randomly deployed to cover a detection field, F. Each sensor is able to adjust its detection power, K_i, and connect to all those neighbours within its transmission range. The detection power corresponds to a detection range, D_i. The detection ability of each sensor must be greater than a threshold, α ($0<\alpha<1$). The aim of this research is to minimize the overlaps of detection ranges in order to minimize the total detection power, ΣK_i, of the whole network.

The proposed methodology can be divided into five steps. The first step is position determination, which is used to determine the position of each sensor. The second step is detection range partition, where each sensor uses Voronoi diagram algorithm to delimit its responsible detection range. The third step is grid structure establishment, where each grid point corresponding to an area is used to calculate the detection probability of that area. The fourth step is detection (sensing) power minimization, where we use Genetic Algorithm to minimize the total detection power of the whole network. The final step is detection (sensing) power adjustment. This adjustment is based on the results of detection power minimization. Fig. 1 shows the framework of the five-step methodology.
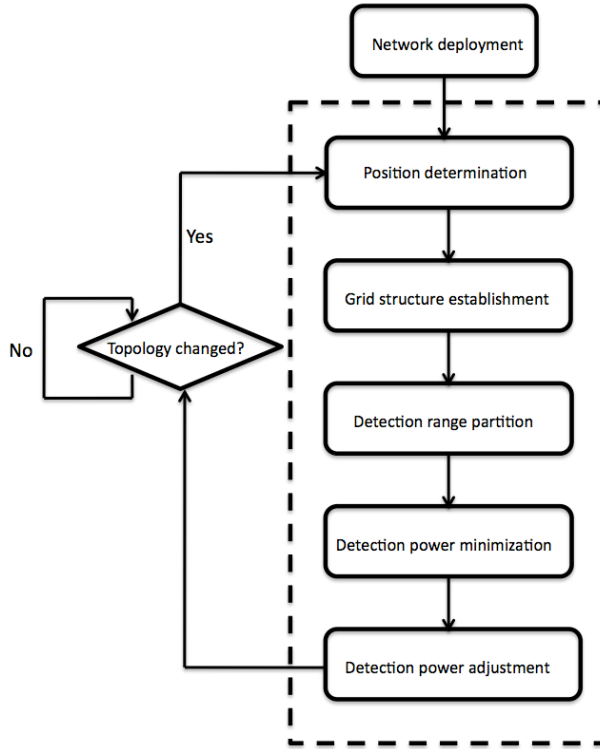
Fig. 1. Framework of the five-step methodology

Before proposing the framework of five-step methodology, we introduce some useful formulae.

3.1 Related formulae
Free space loss of radio wave

$$\text{Free space loss} = 20\log\frac{4\pi d}{\lambda} \qquad (1)$$

Where λ is the wavelength and d is the transmitted distance. Free space loss is the attenuation rate of a transmitted radio wave.

Detection power, E_i, of sensor S_i to a target

$$\text{Pr} = Pt + Gain - 20\log\frac{8\pi d}{\lambda} \qquad (2)$$

Where Pt is the emitted detection power of a sensor, *Gain* is antenna gain, d is the distance between sensor and target, and Pr is the radio power received by the sensor from a target.

In a wireless sensor network, a detection process consists of a sensor transmitting a detection radio wave and receiving bounced back radio wave. A larger Pr indicates higher detection ability of a sensor to a target. In addition to Pr, the detection energy of sensor S_i to a target also includes the thermal noise, N_i, generated by electronic component of sensor S_i. Thus the total detection energy, E_i, to a target is the sum of Pr and N_i.

$$E_i = Pr + N_i \qquad (3)$$

Detection probability, $P_i(u)$, of a node at position u by sensor S_i

$$P_i(u) = prob[E_i(u) > \beta] = prob[\Pr(u) + N_i > \beta] \qquad (4)$$

$P_i(u)$ is the detection probability that an event occurs at position u detected by sensor S_i. β is a threshold used to determine whether an event is triggered. As the detected energy is larger than β, a corresponding event is triggered. Otherwise, the detected energy is thought to be a thermal noise.

Conjunctive detection probability

$$P(u) = 1 - [\prod (1 - P_i(u))] \qquad (5)$$

On the other hand, a position u might be covered by more than one detection range of different sensors. Let an event occur at a position, u, the probability that all sensors do not detect is $\prod (1 - P_i(u))$. Therefore, the conjunctive detection probability, $P(u)$, of all sensors is $1 - [\prod (1 - P_i(u))]$.

With all the related formulae, we introduce each step of the proposed methodology in the following subsections.

3.2 Position determination
The first step is to determine the position of each sensor. If each sensor is equipped with a GPS, the system could have the absolute position of each sensor. However, this kind of sensors will be limited to being placed in an outdoor environment. Besides, it makes sensor bigger and consumes more energy. In the proposed method, we consider the position of each sensor in terms of relative position. These positions can be calculated by either one of AOA (Angle of Arrival), TDOA (Time Difference of Arrival) and RSSI (Received Signal Strength Indicator) methods. If each sensor knows only the relative positions between itself and its neighbours, it will not be able to compute the Voronoi diagram of the whole network. On the other hand, if all sensors send their positions to base stations, it will consume huge bandwidth and transmission energy. This problem will be solved by improving the Voronoi diagram in the following subsection.

3.3 Detection range partition
After position determination, each sensor will be able to know the relative positions of its 1-hop neighbours. The next step is to determine the responsible detection range of each sensor. Meguerdichian et al. (2001) exploited the coverage problem in wireless ad-hoc sensor networks in terms of Voronoi diagram and Delaunay triangulation. In this research,

we employ Voronoi diagram to delimit the responsible detection range of each sensor. Voronoi diagram can be used to divide an area into sub-areas. In a Voronoi diagram, it holds the property that the nearest site of any point x in a sub-area $V(P_i)$ must be P_i (site).

Definition *: Voronoi diagram*

Let P = {P_1, P_2,...,P_n}, n $\geqq$ 2, P is a set of nodes in an area, and P_1, P_2, ..., P_n are sites.

$V(P_i)$={x: P_i-x $\leqq$ P_j-x, $\forall j \neq i$}

$V(P)$={$V(P_1)$, $V(P_2)$,......, $V(P_n)$}

$V(P)$ is called a Voronoi diagram.

Fig. 2. shows the Voronoi diagram formed by three sites P_1, P_2, P_3. The nearest site of a random point x in the sub-region $V(P_1)$ must be P_1. The same principle applies to both $V(P_2)$ and $V(P_3)$. Fig. 3 shows the sub-regions of random deployed sensors using Voronoi diagram.
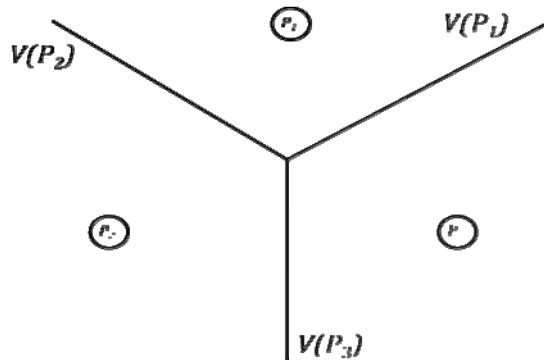
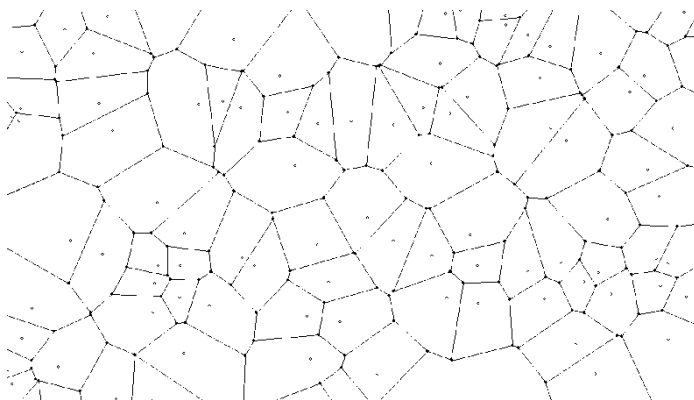Fig. 2. The Voronoi diagram formed by three sites (P_1, P_2, P_3)

Fig. 3. Sub-regions of random deployed sensors using Voronoi diagram

Next, we determine the responsible detection range of each sensor. Fig. 4 shows part of the Voronoi diagram formed by sensor A and its neighbours, where the quadrangle is the sub-region of sensor A. Fig. 5 shows the case when the responsible detection range covers the sub-region of sensor A. Fig. 6 shows another case when the detection range does not fully cover the sub-region of sensor A due to its limited sensing power. In such case the responsible detection range is equal to its maximum detection range.
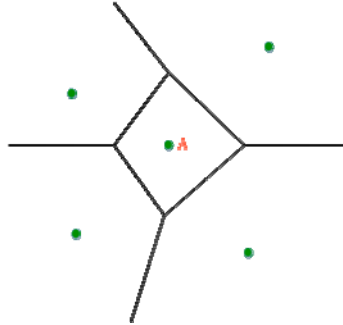

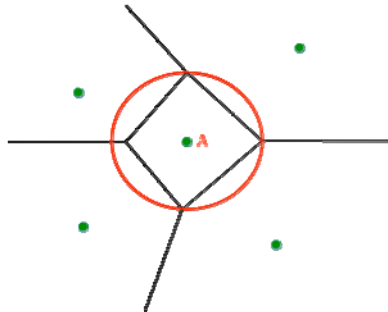Fig. 4. Sub-regions formed by sensor A and its neighbours

Fig. 5. The responsible detection range covers the sub-region of sensor A
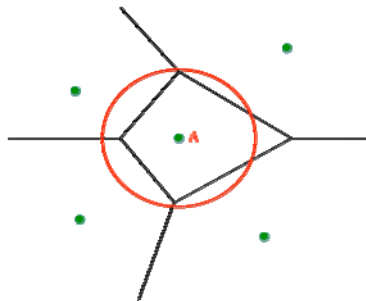

Fig. 6. The sub-region of sensor A is larger than its maximum detection range

Besides, it can be proved that if the maximum transmission distance between two sensors is greater than twice the maximum detection range of each sensor then the responsible

detection ranges of the two sensors do not overlap. Fig. 7 shows that sensor A and B are not neighbours to each other. Though their sub-regions are overlapped, their responsible detection ranges do not overlap.
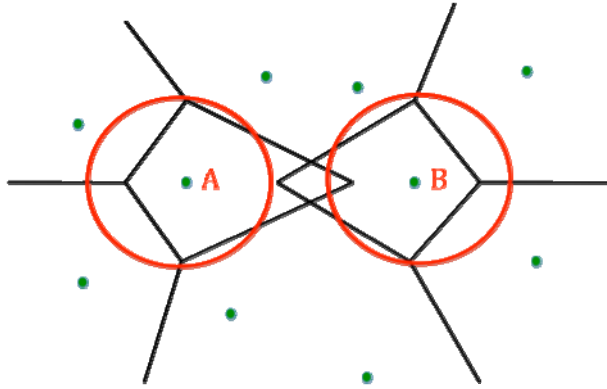

Fig. 7. The sub-regions of sensors A and B overlap, but their responsible detection ranges do not overlap

3.4 Grid structure establishment

To make sure that the detection ability of each sensor is greater than a predefined threshold, α, we create a grid structure for detection field, F. In a grid structure, each grid point represents a target. In Fig. 8, the solid circles are sensors and each vertex of a square is a grid point.
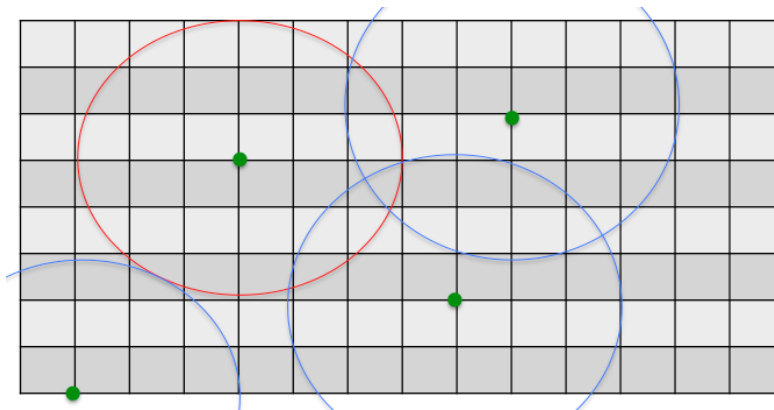

Fig. 8. Grid structure of a target detection area

Assume that there are m grid points in the responsible detection range of sensor S_i. Let $P(u)$ be the conjunctive detection probability, Γ be the threshold of detection probability of the grid point u. We define G_i to be the set of those u whose $P(u)$ is smaller than Γ, that is $G_i=\{u \mid u \in S_i, P(u) \leqq \Gamma\}$. We also define $1-\dfrac{|G_i|}{m}$ to be the detection ability of sensor S_i.

The greater $1 - \frac{|G_i|}{m}$, the higher detection ability of sensor S_i. In addition, we set another threshold, α, for S_i. While reducing the overlaps of detection ranges, the system should keep the detection ability above the threshold α.

Fig. 9 shows the detection ability of sensor S_i. There are 29 grid points spread in distinct locations. We assume the threshold of the detection ability, Γ, is 0.7. Since the detection abilities of the grid points A, B, C, D and E are less then 0.7, all these five points belong to set G_i. We can thus compute the detection ability of S_i, $1 - \frac{|G_i|}{m}$, is 24/29.
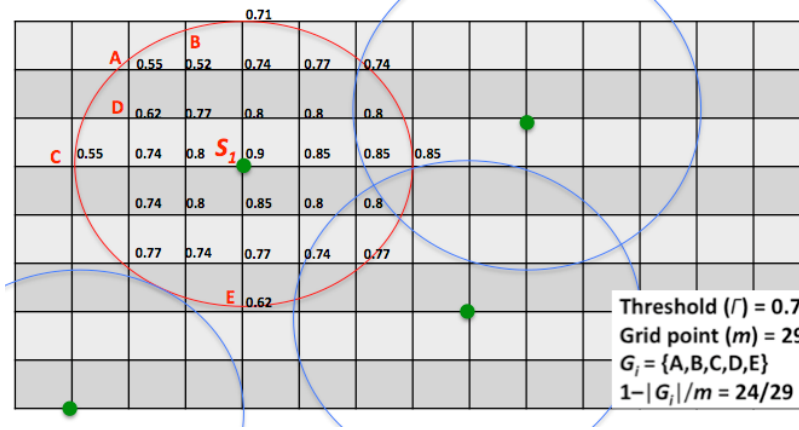

Fig. 9. Detection ability of sensor S_i

3.5 Detection power minimization

After establishing the grid structure, our goal is to minimize the detection power, K_i, or equivalently the, P_t. We use a Genetic Algorithm (GA) to do the minimization. GAs are the methods used to find exact or approximate solutions to optimization and search problems. GAs are often used to solve those problems of high-complexity, like NP-problem, in limited time. Fig. 10 shows the operation flow of genetic algorithms.

Chromosome encoding: encode species into chromosome string according to the attributes of the problem domain. Each chromosome string is thought of as a problem solution.

Objective function: used to evaluate a chromosome string, determine the adaptation degree (fitness) of a chromosome string. In general, the higher adaptation degree of a chromosome string, the better solution.

Selection: select highly evaluated chromosome strings as parents of offersprings. A highly evaluated chromosome string usually has higher probability being selected.

Genetic operations: can be either Crossover or Mutation. Crossover is used to produce better chromosome strings (offsprings) by exchanging sub-strings of parents. Mutation is different from crossover in that it changes (e.g., 0→1, 1→0) very few codes of parents to escape from local optimum. Mutation occurs much less frequent than crossover does.

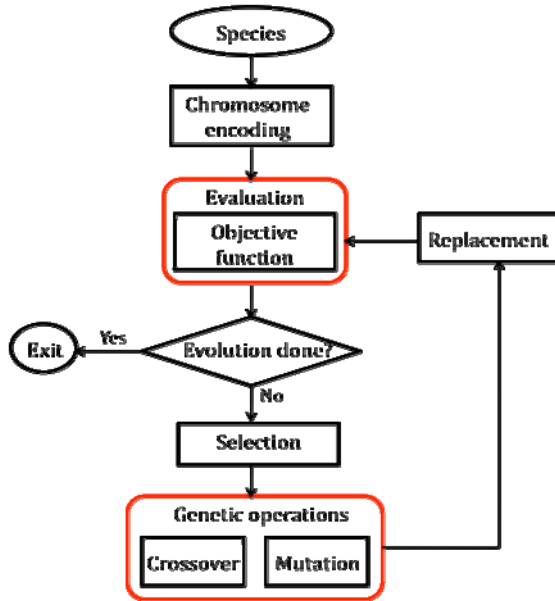*Replacement*: replace old chromosome strings (parents) by new chromosome strings (offsprings).

Fig. 10. Operation flow of genetic algorithms.

Chromosome encoding

First, we encode the detection powers of sensors, S_1, S_2,…,S_n, into a chromosome string, $K_1, K_2,…,K_n$. Then we generate a set of initial solutions (chromosome strings) as shown in Fig. 11.
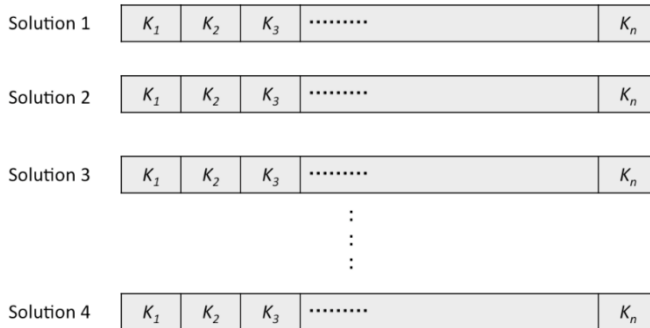

Fig. 11. Encoded chromosome strings

Evaluation

Chromosome string encoding is followed by evaluation. The system objective is to minimize the Total Detection Power (*TDP*). In addition, there are two constraints. One (7) is to constrain the detection power, K_i, the other (8) is to make sure the detection ability of the sensor is greater than a predefined threshold, *a*.

Objective function

$$Min \sum K_i \tag{6}$$

Constraints

$$Max\_K_i \geqq K_i \geqq 0 \tag{7}$$

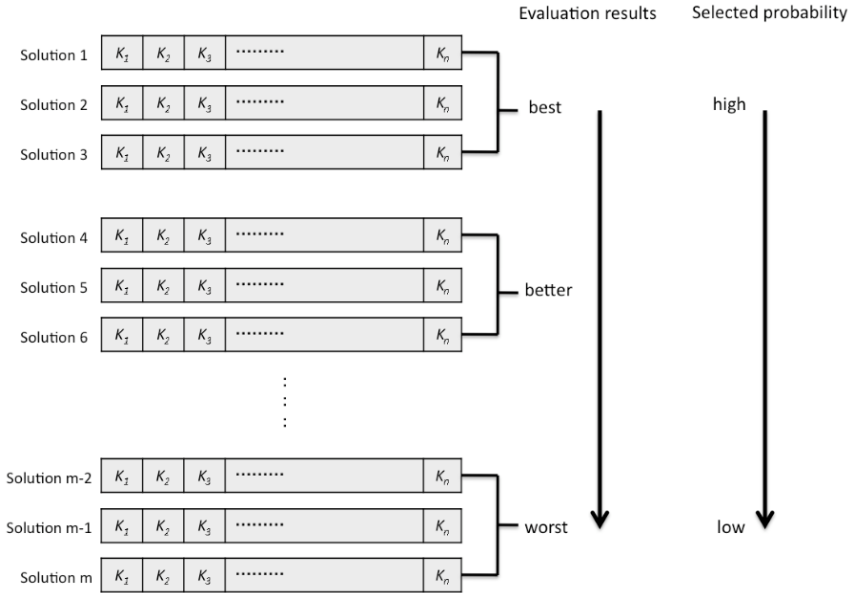$$1 - \frac{|G_i|}{m} > \alpha \tag{8}$$

Fig. 12. The relation between chromosome strings categories and selected probabilities.

Selection

In selection, we classify all chromosome strings into different categories. All those chromosome strings belonging to the same category have similar evaluations. The categories of higher evaluations will have higher probability being selected. Fig. 12 shows the relation between chromosome strings categories and selected probabilities.

Crossover

We design the crossover operation to be two-point crossover. We first randomly choose two positions in a chromosome strings. The offsprings are then produced by exchanging the sub-strings that lie between the two positions. Fig. 13 shows an example of two-point crossover.
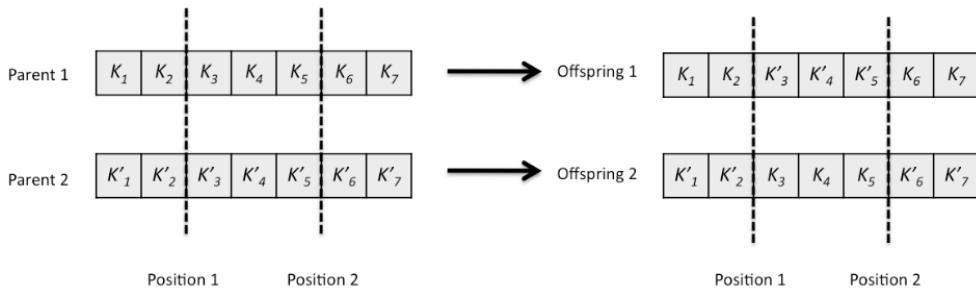
Fig. 13. Example of two-point crossover

Mutation

In mutation, we random choose very few K_i's (low probability) by increasing or decreasing their sensing power. Fig. 14 is an example of mutation. In this example, we random choose elements K_2, K_3, K_4 from parent. K_2 and K_3 become K_2'and K_3' by increasing their sensing powers. On the contrary, K_4becomes K_4' by decreasing its sensing power.
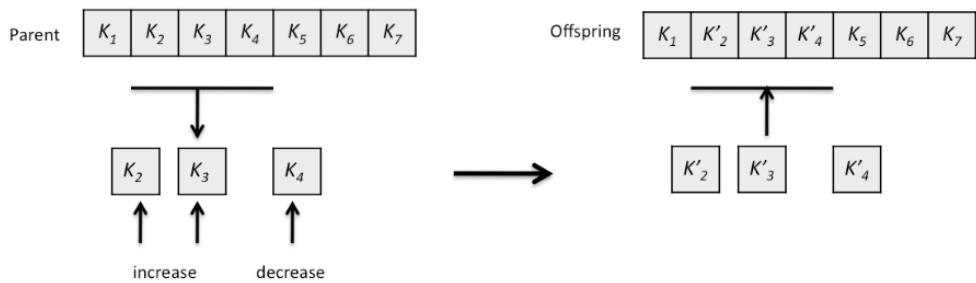
Fig. 14. Example of mutation.

Replacement

As new offsprings are produced, those chromosome string with low evaluation results will be replaced by the new offsprings with high evaluation results.

3.6 Detection power adjustment

Eventually, the optimum will be reached after several iterations of Genetic Algorithm. Each sensor then sets the corresponding value in the optimal chromosome string as its detection power. All these values of detection power will be propagated to each of their neighbours through message exchanges. Each sensor will then adjust its detection power according to both the received values and the value computed by its own. At the end of this step, all the detection powers of sensors are determined. Afterwards the optimization process won't be triggered only if some sensors are damaged or the network topology is changed.

3.7 Procedure

The procedure of the proposed methodology is illustrated as follows.

1. *Sensor S exchanges messageswith its neighbours and computesthe relative positions of its neighbours.*
2. *Use Voronoi diagram algorithm to calculate the responsible detection ranges of S.*
3. *Establishgrid structure (m grid points) of S.*
4. *Encode chromosome, with Length = n, Element$_i$ = detection power K of sensor S$_i$, |chromosome| = X.*
5. **forall** *chromosomes***do**
6. **Evaluate function** *(chromosome)*
7. **end for**
8. **while** *Evolution is not finished***do**
9. *operation = random(Crossover ||Mutation)*
10. **if** *operation == Crossover* **then**
11. *select two chromosomes asparents according to the evaluation resultsof TDP randomly exchange some elements to produce offsprings*
12. **else**
13. *select a chromosome as parent according to the evaluation result of TDP randomly change some elements to produce offspring(max_K$_i$≧K$_i$≧0)*
14. **end if**
15. **Evaluate function***(offspring)*
16. **if***(the TDP of evaluation result of offspring is better than their parents) andDetection ability of offspring > a***then**
17. *replace parents by offsprings*
18. **else**
19. *replace parents by offsprings with lower probability and give up offspring's with higher probability*
20. **end if**
21. **end while**

Evaluate function*(chromosome)*
1. **for all** *grid point u of sensor S*
2. **for all** *detection power K$_i$ in the chromosome*
3. $\text{Pr} = K_i + \dfrac{Gain}{I} - 20\log\dfrac{8\pi d}{\lambda}$
4. $P_i(u) = prob[\text{Pr} + N_i > \beta]$
5. **end for**
6. $P(u) = 1 - [\prod_{i}^{n}(1 - P_i(u))]$
7. $G = \{u \mid u \in S_i, P(u) \leq \Gamma\}$
8. **end for**
9. *Detection ability* $= 1 - \dfrac{|G|}{m}$
10. $TDP = \sum K_i$

4. Simulations and results

Simulations are based on the following parameters setting: there are 30 to 100 sensors with the same capability randomly deployed in a detection field of 100×100 m^2. The detection power of each sensor is adjustable, the maximum detection power is 15dBm, the detection range is between 0 to 20 meters, the transmission range is 40 meters, the frequency of detection radio wave is 10.525MHz, the sensitivity is -85dBm, the antenna gain is $8dBm$, the threshold of detection ability (*a*) is 0.8. In performance comparisons, VERA method is further separated into VERA1 (VERA with $\Gamma = 0.7$) and VERA2 (VERA with $\Gamma \approx 0$). VERA1 and VERA2 are compared with MDR (Maximum Detection Range), *K*-covered (*K* = 1), and Greedy algorithm by simulations. MDR is an algorithm simply used to maximize detection range without any enhancements on detection range adjustment. *K*-covered and Greedy algorithms are those proposed by (Huang & Tseng, 2003) and (Cardei et al., 2006), respectively. Five simulations are conducted to verify the performances against overlaps of detection ranges, duplicate data amount, total energy consumption, network lifetime and average detection probability.
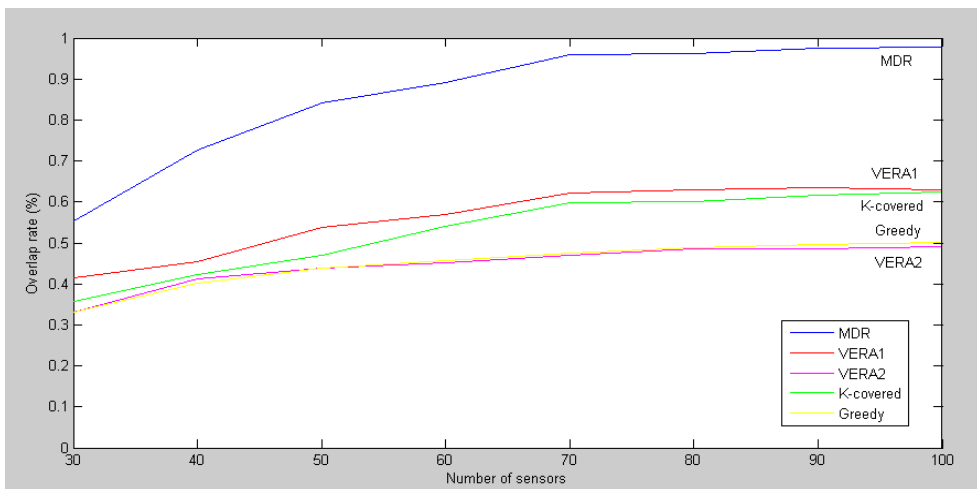

Fig. 15. Comparisons of the ratios of overlapped detection range

Fig. 15 shows the comparisons of the ratios of overlapped detection range of the five methods. As the number of sensors is increased between 30 and 70, the ratios of overlaps of each method increase constantly. This is because when the number of sensors is smaller than 70, there is no sufficient number of sensors to cover the whole detection field. As the number goes beyond 70, the ratios of overlaps of MDR approximate 1.0 because MDR does nothing to detection range adjustment. Whereas the ratios of VERA1 and *K*-covered stay around 0.6, and those of VERA2 and Greedy stay around 0.5, respectively.

In the second simulation, we define the proportion of duplicate data to be the ratio of the duplicate data amount to the number of detected events. Fig. 16 shows the comparisons of the portions of duplicate data amount of the five methods. It shows that the proportions of VERA1, VERA2 and Greedy are very close to one other. VERA1 has larger duplicate data amount and larger number of detected events. Since there is no detection ability limit on VERA2 and Greedy, it results in smaller duplicate data amount and smaller number of

detected events. *K*-covered has higher portion of duplicate data due to having more overlaps and smaller number of detected events.
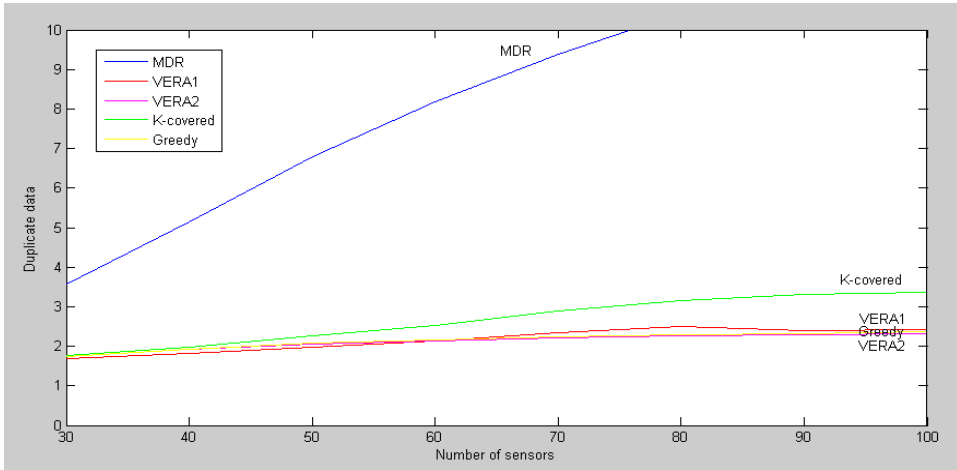
Fig. 16. Comparisons of the portions of duplicate data amount

Fig. 17 shows the comparisons of total energy consumptions of the five methods per round. Since MDR is unable to adjust detection range, the total energy consumption is increased as the number of sensors is increased. As the number of sensors is below 63, the total energy consumption of *K*-covered is less than that of Greedy since *K*-covered has less information exchange than that of Greedy, and *K*-covered has less data needs to be relayed to base stations. As the number of sensors is larger than 63, *K*-cover increases the number of data relays quickly resulting in more energy consumption. Since VERA1 and VERA2 have less information exchange than that of the others, and VERA2 uses less detection power than that of VERA1, therefore VERA2 has the best energy consumption performance.
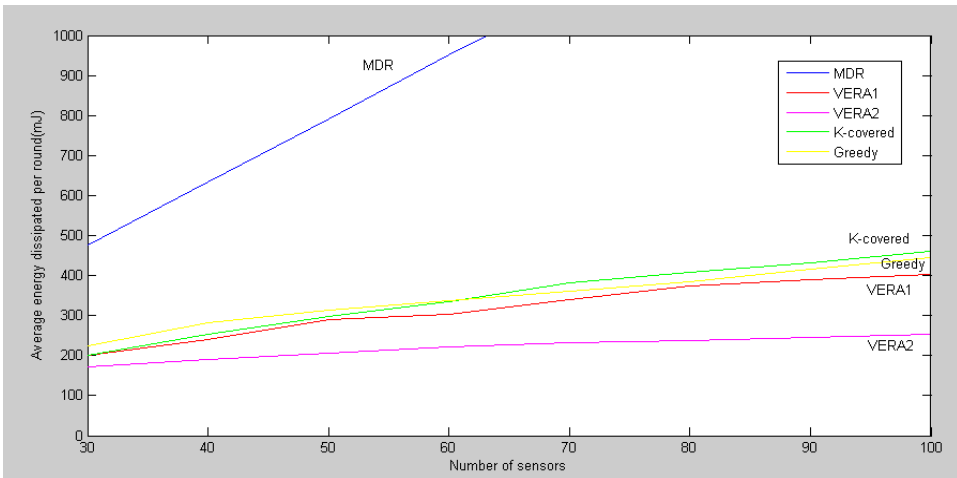
Fig. 17. Comparisons of total energy consumption per round

Fig. 18 shows the comparisons of network lifetime of VERA, *K*-covered and Greedy methods. At the time the sensor network is deployed at its early stage, there must have many sensors using very high detection powers to reach the borders of detection field. It shows that there are many sensors died at the end of the first 220 rounds. Comparing the number of rounds that the last sensor died, we have VERA2 (940 rounds) > Greedy (890 rounds) > *K*-covered (880 rounds) > VERA1 (700 rounds). Comparing the number of rounds that the last ten sensors survived, we have VERA2 (700 rounds) > Greedy (680 rounds) > *K*-covered (670 rounds) > VERA1 (650 rounds).
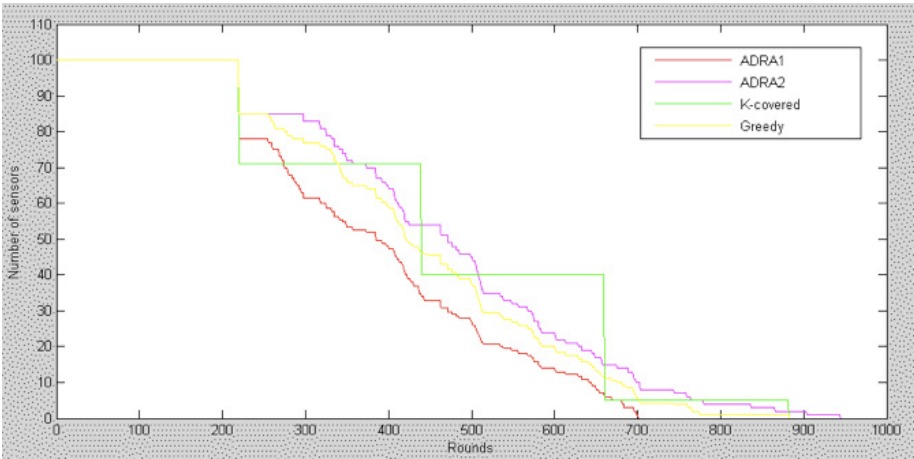
Fig. 18. Comparisons of network lifetime

Fig. 19 shows the comparisons of average detection probability of the detection field of the five methods. As the number of sensors is greater than 70, the average detection probability of VERA1 is very close to 0.7. It is 10% higher than that of *K*-covered, VERA2 and Greedy. The average detection probability of MDR is almost 0.9 due to its maximum detection power.

Fig. 19. Comparisons of average detection probability of the detection field

5. Conclusions

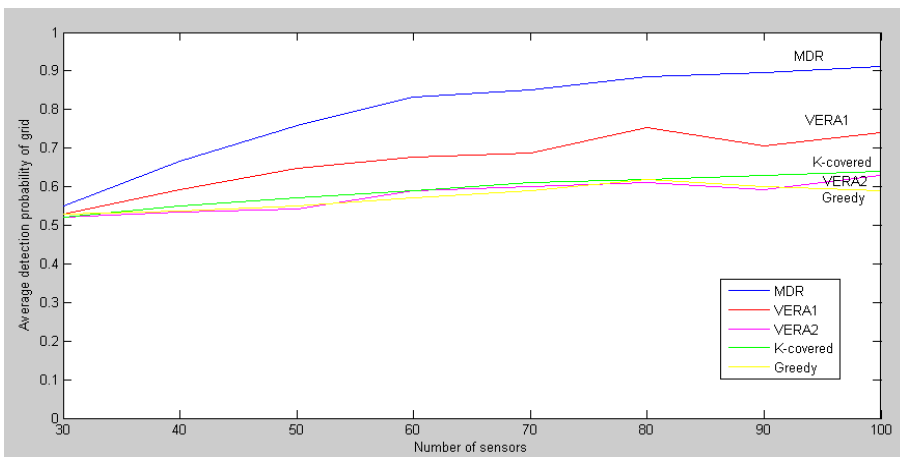In this paper we introduced a framework of five-step methodology to carry out detection range adjustment in a wireless sensor network. These steps are position determination, detection range partition, grid structure establishment, detection power minimization, and detection power adjustment. We proposed a Voronoi dEtection Range Adjustment (VERA) method that utilizes distributed Voronoi diagram to delimit the responsible detection range of each sensor. All these adjustments are under the guarantee that the detection abilities of sensors are above a predefined threshold. We then use Genetic Algorithm to optimize the optimal detection range of each sensor.

Simulations show that the proposed VERA outperforms Maximum Detection Range, *K*-covered and Greedy methods in terms of reducing the overlaps of detection range, minimizing the total energy consumption, and prolonging network lifetime, etc.

6. References

Busse, M.; Haenselmann, T. & Effelsberg, W. (2006). TECA: a topology and energy control algorithm for wireless sensor networks, *Proceedings of the 9th ACM International Symposium on Modeling Analysis and Simulation of Wireless and Mobile Systems (MSWiM '06)*, Oct. 2006.

Cardei, M., Wu, J. & Lu, M. (2006). Improving Network Lifetime using Sensors with Adjustable Sensing Ranges, *International Journal of Sensor Networks (IJSNet)*, Vol. 1, No.1/2, (2006) 41-49.

Heinzelman, W.R.; Chandrakasan, A.; & Balakrishnan, H. (2000). Energy-efficient communication protocol for wireless microsensor networks, *Proceedings of the 33rd International Conference on System Sciences (HICSS '00)*, Jan. 2000.

Huang, C.-F. & Tseng, Y.-C. (2003). The coverage problem in a wireless sensor network, *ACM Int'l Workshop on Wireless Sensor Networks and Applications (WSNA)*, 2003.

Klein, L. (1993). Sensor and data fusion concepts and applications, In: SPIE Optical Engineering Press.

Meguerdichian, S.; Koushanfar, F.; Potkonjak, M. & Srivastava, M. B. (2001). Coverage problems in wireless ad-hoc sensor networks, *IEEE INFOCOM*, pp. 1380–1387, 2001.

Wang, S.C.; Wei, D.S.L.; & Kuo, S.Y. (2004). SPT-based power-efficient topology control for wireless ad hoc networks, *Proceedings of the 2004 Military Communications Conference (MILCOM'04)*, Oct. 2004.

Motor Energy Management based on Non-Intrusive Monitoring Technology and Wireless Sensor Networks

Hu Jingtao
Key Laboratory of Industrial Informatics
Shenyang Institute of Automation, Chinese Academy of Sciences
China

1. Introduction

Induction motors are widely used in industry as essential driving machines. There are many motor driven systems in plants, such as pumping systems, compressed air systems, and fan systems, etc. These motor driven systems use over 70% of the total electric energy consumed by industry. Because of the oversized installation or under-loaded conditions, motors generally operate at low efficiency which results in wasted energy. To improve the motor energy usage in industry, motor energy management should be done.

The motor energy management is based on the motor energy usage evaluation and condition monitoring. Over the years, many methods have been proposed. But these methods are too intrusive for in-service motor monitoring, because they need either expensive speed and/or torque transducers, or an accurate motor equivalent circuit. Non-intrusive methods should be developed.

Another problem comes from the communication network. Energy usage evaluation and condition monitoring systems in industrial plants are usually implemented with wired communication networks. Because of the high cost of installation and maintenance of these cables, it is desired to look for a low-cost, robust, and reliable communication network.

This paper presents a motor energy management system based on non-intrusive monitoring technologies and wireless sensor networks. In the following sections, some key technologies for motor energy management are discussed. At first, a three-layer system architecture is proposed to build a motor energy management system. And an in-service motor condition monitoring system based on non-intrusive monitoring technologies and wireless sensor networks is presented. Then wireless sensor networks and its application in motor energy management are discussed. The design and implementation of a WSN node are presented. Thirdly, non-intrusive motor current signature analysis technology is introduced to make motor energy usage evaluation. Applying the efficiency estimation method introduced, a front-end device used to monitor motors is developed. At last, the motor monitoring and energy management system is deployed in a laboratory and some tests are made to verify the design. The system is also applied in a plant to monitor four pumping motors.

2. In-Service Motor Monitoring and Energy Management System

2.1 Motor Energy Management Architecture

Motor energy management is a complicated program which embodies optimal design, operation, and maintenance of motor driven systems to use energy efficiently. The system optimization is based on the motor condition monitoring, energy usage evaluation, and energy saving analysis. Such work is so complex that before developing a motor energy management system, we need to construct a system architecture to guide the system development.

This paper presents a three-layer system architecture which is composed of a data acquisition platform, a condition monitoring platform, an energy consumption and saving analysis platform, a communication platform, and a motor energy data management platform, as illustrated in Fig. 1.
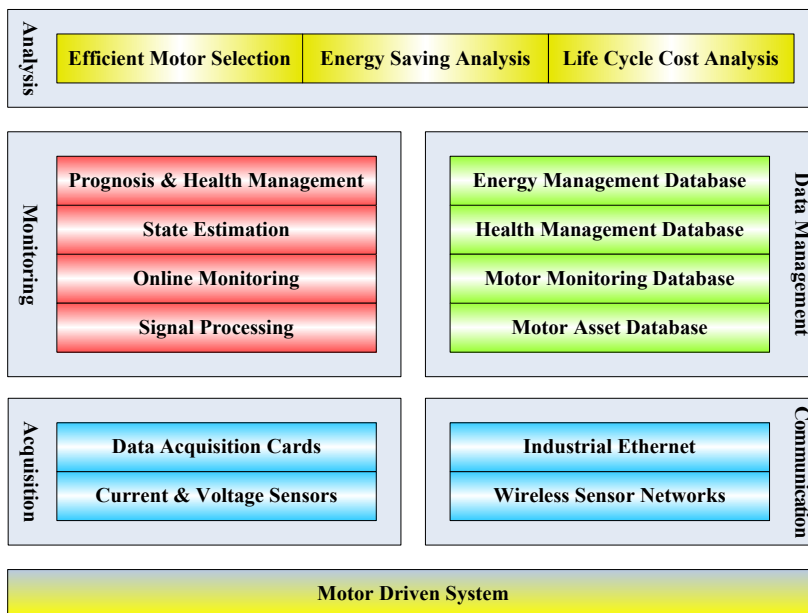
Fig. 1. Motor energy management architecture

The need of data acquisition comes first to monitor the operation of a motor driven system. We need data acquisition cards to collect raw signals coming from sensors, such as current and voltage sensors, and transmit them to the monitoring system over a communication network. There are many ways to build a network, such as field bus, industrial Ethernet, and wireless sensor networks. The data acquisition and communication platforms form the base of a motor energy management system.

Upon the data acquisition is the motor condition monitoring platform. Based on the digital signal processing (DSP) technologies, the operation conditions of motors are monitored, and the health state and the energy usage of motors are evaluated. Such functions need data management abilities. So some databases are created and maintained, including motor asset database, motor monitoring database, health management database, and energy

management database, etc. The condition monitoring platform and data management platform form the main body of a motor energy management system.

At the top level are some applications to make motor energy management. To replace the inefficient motors currently used, motor selection can be made based on the energy usage evaluation of the motors. Energy saving analysis and life cycle cost analysis can be done for the replacement. That's the energy consumption and saving analysis platform.

2.2 In-Service Motor Monitoring System

An in-service motor monitoring and energy management system was developed based on the architecture presented in section 2.1. The system has two subsystems: a data acquiring and analysis subsystem deployed at the motor control centre (MCC), and a condition monitoring and energy management subsystem running at a central supervisory station (CSS), as illustrated in Fig. 2.
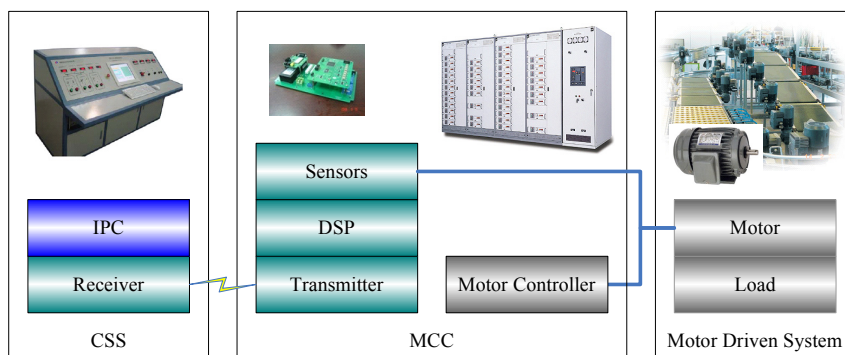
Fig. 2. In-service motor monitoring and energy management system

The data acquiring and analysis subsystem consists of some front-end devices which are used to acquire data and analyze the motors conditions. One front-end device is composed of three parts: a sensor unit, a processing unit and a communication unit.

The sensor unit is used to detect the line current and line voltage signals from the power supplied to a motor. Only the current and voltage sensors are used. Without any other sensors, the motor system is disturbed minimally.

The processing unit based on digital signal processing technologies gathers and analyzes those signals to determine the condition of motors. Some signal processing and inferential models are used to evaluate the energy and health conditions of the motors, as illustrated in Fig. 3.

The communication unit is used to send the results to the condition monitoring and energy management subsystem running at a central supervisory station, which gathers and stores the analysis results, evaluates the energy usage, and analyzes the energy savings. Here the communication is based on the wireless sensor networks.

The condition monitoring and energy management subsystem has a friendly graphic user interface (GUI). The condition of a motor is monitored on the main screen by 8 parameters, including the rotor speed, torque, current root-mean-square, voltage root-mean-square, power factor, input power, output power, and efficiency. They are displayed in two ways:

instantaneous values and iscillograms, as illustrated in Fig. 4. For multi-motors monitored, one can selected which motor's condition is displayed by a drop-down box on the screen.
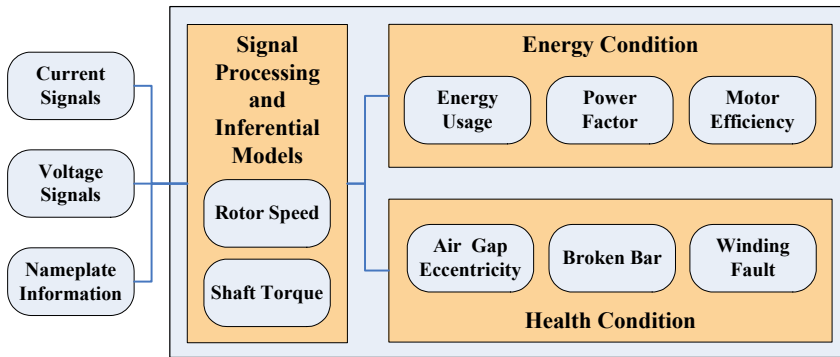
Fig. 3. Functions of the processing unit

All the data are stored in the database and can be restored to make further analysis. Furthermore, motor performance could be analyzed and six performance curves could be obtained. They are efficiency-rotor speed, torque-rotor speed, input power-rotor speed, output power-rotor speed, torque-output power, and efficiency-output power curves, as illustrated in Fig. 5.
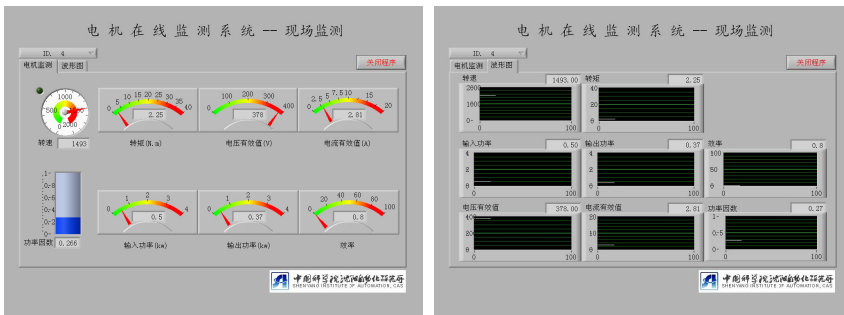
Fig. 4. In-service motor condition monitoring (Left: Instant values, Right: Iscillograms)
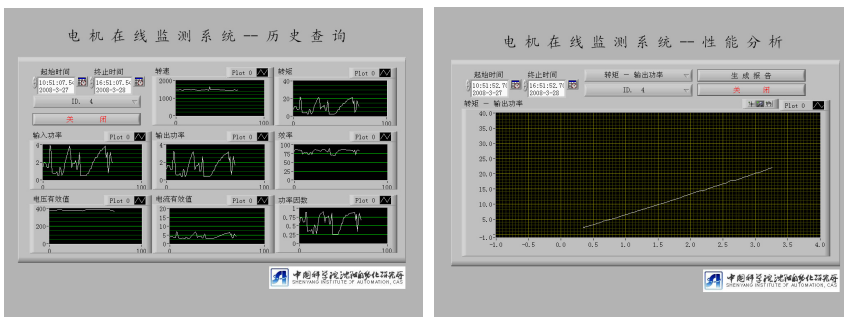
Fig. 5. Motor condition analysis (Left: History data, Right: Performance analysis)

3. Applying Wireless Sensor Networks in Motor Energy Management

The energy evaluation system in industrial plants is usually implemented with wired communication networks so far. Because of the high cost of installation and maintenance of these cables, it is desired to look for a low-cost, robust, and reliable communication network. The wireless sensor networks (WSN) is a self-organized network of small sensor nodes with communication and calculation abilities. As an open architecture, self-configuring, robust, and low cost network, it is suitable to meet the requirement.

Harish Ramanurthy et al. (2005) proposed a wireless smart sensor platform which is an attempt to develop a generic platform with 'plug-and-play' capability to support hardware interface, payload and communications needs of multiple inertial and position sensors, and actuators/motors used in instrumentation systems and predictive maintence applications.

James E. Hardy et al. (2005) discussed the robust, self-configuring wireless sensors networks for energy management and concluded that WSN can enable energy savings, diagnostics, prognostics, and waste reduction and improve the uptime of the entire plant.

Nathan Ota and Paul Wright (2006) discussed the application trends in wireless sensor networks for manufacturing. WSNs can make an impact on many aspects of predictive maintenance (PdM) and condition-based monitoring. WSNs enable automation of manual data collection. PdM applications of WSNs enable increased frequency of sampling. Condition-based monitoring applications benefit from more sensing points and thus a higher degree of automation.

Bin Lu et al. (2005) and Jose A Getierrze et al. (2006) applied wireless sensor networks in industrial plant energy management systems. A simplified prototype WSN system was developed using the prototype WSN sensors devices, which were composed of a sensor unit, an A/D conversion unit, and a radio unit. However, because the IEEE 802.15.4 standard is designed to provide relaxed data throughput, it is not acceptable in some real-time cases for the large amount of raw data to be transmitted from the motor control centre to the central supervisory station.

3.1 Wireless sensor networks

The WSN is a self-organized network with dynamic topology structure, which is broadly applied in the areas of military, environment monitoring, medical treatment, space exploration, business, and household automation (YU HAIBIN et al., 2006).

The IEEE802.15.4 standard is the physical layer and MAC sub-layer protocol for WSN, which supports three frequency bands with 27 channels as shown in Fig. 6. The 2.4GHz band defines 16 channels with a data rate of 250KBps. It is available worldwide to provide communication with large data throughput, short delay, and short working cycle. The 915MHz band in North America defines 10 channels with a data rate of 40Kbps. And the 868MHz band in Europe defines only 1 channel with a data rate of 20Kbps. They provide communication with small data throughput, high sensitivity, and large scales.

The IEEE 802.15.4 supports two network topologies as shown in Fig. 7. The star topology is simple and easy to implement. But it can only cover a small area. The peer-to-peer topology, on the other hand, can cover a large area with multiple links between nodes. But it is difficult to implement because of its network complexity.

An IEEE 802.15.4 data packet, called physical layer protocol data unit (PPDU), consists of a five-byte synchronization header (SHR) which contains a preamble and a start of packet

delimiter, a one-byte physical header (PHR) which contains a packer length, and a payload field, or physical layer service data unit (PSDU), which length varies from 2 to 127 bytes depending on the application demand, as shown in Fig. 8.
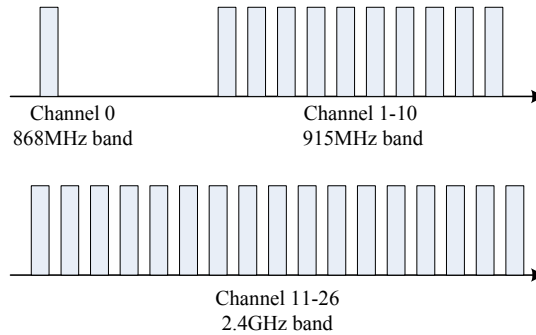
Fig. 6. IEEE 802.15.4 frequency bands and channels
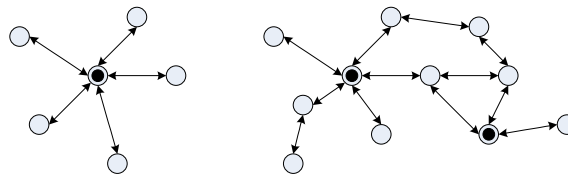
Fig. 7. Star (L) and peer-to-peer (R) topologies

Preamble	Start of packet delimiter	PSDU Length	PHY layer payload
4bytes	1 byte	1 byte	2-127 bytes
SHR		PHR	PSDU

Fig. 8. IEEE 802.15.4 packet structure

3.2 Design and implement of WSN nodes

A WSN node is implemented with a Cirronet ZMN2400HP wireless module to build a communication network between MCC and CSS. The ZMN2400HP consists of an 8-bit Atmel Mega128 microcontroller, which has 128KB flash memory, 4KB EEPROM and 4KB internal SRAM, and a Chipcon CC2420 radio chip, which is compatible with the IEEE 802.15.4 standard and works at 2.4 GHz band. A more detailed structure of the node is shown in Fig. 9.
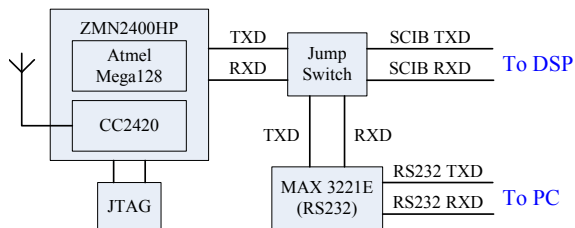
Fig. 9. Design of WSN nodes

Generally there are three kinds of nodes in a wireless sensor network: transmitter nodes, which have both sensing and wireless communicating capabilities, the receiver nodes, which have both wireless and wire communicating capability, and relay nodes which have only the wireless communicating capability to relay the data packets in the case that the distances between the transmitter and receiver nodes are beyond the communication range.

In the in-service motor monitoring system, most of the WSN nodes are transmitter ones used as the communication unit of the front-end device in the MCC, to transmit the processing results to the CSS. As a few receiver and relay nodes are used in the system, all of the three kinds of nodes are implemented based on the same hardware structure to simplify the design. Those full-capability nodes can be configured to act as transmitter, receiver or relay nodes. This gives the reason why the communication unit is separated from the signal processing unit in the design of the front-end devices.

Power consumption is the dominating factor in the design of WSN nodes. However in this specific application, the power consumption is no longer a problem to be considered because the WSN nodes are installed at such locations as a MCC or a CSS, where the power supply is available. So the WSN nodes are designed to be powered by AC/DC converters.

Additionally, as the WSN nodes are used either with the processing unit or individually, it is designed to be supplied either by the processing unit or an AC/DC converter.

3.3 Communication protocol

Generally the data transmitting is initiated by the front-end devices. When the signal processing unit gets the results ready, it makes an interrupt request to the communication unit, which acknowledges the request and receives the data through the asynchronous serial ports and then transmits them to the CSS. There are nine kinds of communication packets, as illustrated in Table 1.

There are two kinds of data transmitting which are initiated by the CSS. The first one is the raw data transmitting. When more detailed analysis needs to be made, the raw currents data must be sent to the CSS, where the raw data are processed and analyzed by the more powerful PC. When this situation occurs, a raw data request is sent by the CSS to a given front-end device, which then gathers some raw data and divides them into several packets to send to the CSS one by one. Each time, the front-end device waits for an acknowledge packet sent back by the CCS before continuing to send the next one. The raw data transmitting ends when the CSS gets the last packet and sends back an ending packet.

Type	Description	Direction
0x00	Processing results request	CSS → Nodes
0x11	Raw data request	CSS → FED
0x12	Configuration	CSS → FED
0x13	Raw data acknowledge	CSS → FED
0x14	Raw data ending acknowledge	CSS → FED
0x21	Processing data	FED → CSS
0x22	Raw data	FED → CSS
0x23	Configuration acknowledge	FED → CSS
0x2A	Log data	Nodes → CSS

Note: FED stands for "front-end devices"

Table 1. Communication packet types

The second data transmitting initiated by the CSS is the configuration. A configuration packet is sent to the front-end devices which guided them to configure the processing parameters, such as the motor poles, motor slots, current and/or voltage sensors errors, etc. Additionally, some log data are transmitted, including the conditions of the nodes, repeaters (routers), and coordinators. When the network fails, the log data are stored in the EEPROM temporarily and sent to the CSS as soon as the connection is rebuilt.

3.4 Motor monitoring network management

The central WSN node used at CSS is called a coordinator, which manages all the nodes in the network by an ID table. A node registers to the coordinator by reporting its ID after it powers on or resets. The coordinator communicates with each node in the ID table in turn to get the processing results from the front-end devices. In this way, the communicating conflict can be avoided. If the coordinator couldn't receive any data from a node in a given period of time, it deletes its ID from the table.

The ID table is defined as follows:

```
    typedef struct
    {
        // node ID
        USIGN8 ucNodeID;
        // node address
        USIGN16 uNodeShortAddr;
        // request fail counter
        USIGN8 ucReqFailCounter;
    }NODE_ID;

    typedef struct
    {
        // node counter
        USIGN8 nodeNum;
        NODE_ID nodeId[MAX_NODE_NUM];
    }NODE_ID_TABLE;
```

The ID table is updated according to the combination of three conditions as described in Table 2. Here condition 1 (C1) is that the node ID is in the table. Condition 2 (C2) is that the node address is in the table. Condition 3 (C3) is that the node address changed.

C1	C2	C3	Update
N	N	-	Add new node ID
N	Y	-	Set the node ID in the record
Y	N	-	Set the node address in the record
Y	Y	Y	Set new node address in the record
Y	Y	N	No action

Table 2. ID table updating

To maintain the network alive, some abnormal conditions are detected and handled. A communication unit of the front-end device, also called a front-end node, resets its main CPU and the CC2420 chip and searches for the network again in three cases. First, it can't connect to the network in a given period of time after it powered on. Second, it can't receive the acknowledgement when it tries to register its ID to the coordinator at CSS after connecting to the network. Last, it doesn't receive the processing results request in a given period of time during a connecting session.

A repeater (router) transmits data between the front-end nodes and the coordinator. It's more complex to judge a repeater's condition because both the front-end nodes and the coordinator could reset in some cases. Some actions are made according to the combination of five conditions as described in Table 3. Here condition 1 (C1) is that the repeater has received data from the coordinator. Condition 2 (C2) is that the repeater has received data from front-end nodes. Condition 3 (C3) is that the repeater has got an overtime during transmitting data with the coordinator. Condition 4 (C4) is that the repeater has got an overtime during transmitting data with front-end nodes. And condition 5 (C5) is that the repeater has got an overtime during registering to the network.

The coordinator handles abnormal situations in two cases. It resets its main CPU and CC2420 chip to rebuild the network if no nodes register to it in a given period of time when network initiating or all IDs are deleted from its records.

C1	C2	C3	C4	C5	Action
N	N	-	-	N	Wait for data
				Y	Reset
N	Y	-	N	-	Wait for data
			Y		Reset
Y	N	N	-	-	Wait for data
		Y			Reset
Y	Y	N	N	-	No
		N	Y		Reset
		Y	N		Reset
		Y	Y		Reset

Table 3. Repeater abnormal processing

4. Non-intrusive Motor Energy Usage Condition Monitoring

The motor energy usage condition monitoring plays an important role in the motor energy management. And the efficiency estimation is the key for the motor energy usage monitoring and evaluation.

The motor efficiency is defined as the ratio of the motor shaft output power P_O to the input power P_I as (1), and the difference between them is the power losses which are classified as stator copper loss W_S, rotor copper loss W_R, core loss W_C, friction and windage loss W_{FW}, and stray load loss W_{LL}, as given by (2).

$$\eta = \frac{P_O}{P_I} \times 100\%$$
(1)

$$W_L = P_I - P_O = W_S + W_R + W_C + W_{FW} + W_{LL}$$
(2)

Over the years, many methods have been proposed to determine the motor efficiency. Generally they can be divided into three groups: direct detection, indirect detection, and inference methods. The direct detection methods measure the motor input and output power with power meters and calculate the motor efficiency directly. The indirect detection methods, also known as segregated loss methods, measure losses by various tests, such as load test, no-load test, and locked-rotor test, etc. The motor efficiency is then obtained by loss analysis. Many direct and indirect methods have been adopted by some international standards such as IEEE 112-B, IEC 34-2, and JEC 37. The Chinese national standard for motor efficiency determination is GB1032-2005. The methods defined in the standards are agreement. The main difference of them is how to determine the stray load loss.

The inference methods determine the motor efficiency with estimation models after some simple experiments. The slip method (John S. Hus, 1998) presumed that the percentage of the load is proportional to the ratio of the measured slip to the full-load slip. Thus the motor efficiency is approximated using (3). The current method (John S. Hus, 1998) assumed that the percentage of load is proportional to the ratio of the measured current to full-load current. The motor efficiency is approximated using (4). Both of the methods are simple and low-intrusive, but poor precise. Some improvements have been made to give a more accurate efficiency estimate.

$$\eta = \frac{slip}{slip_{rated}} \cdot \frac{P_{O,rated}}{P_I}$$
(3)

$$\eta = \frac{I}{I_{rated}} \cdot \frac{P_{O,rated}}{P_I}$$
(4)

4.1 Non-intrusive Motor Efficiency Estimation

The methods described above are bench testing which requires the motor to be tested in a laboratory environment that may be different from the original working site. Another disadvantage is that they require the motor to be removed from service. They cannot be directly used for the in-service motors.

The motor current signature analysis (MCSA) method is a non-intrusive testing method to evaluate the condition of motors by processing the motor stator current and voltage signals collected at the power supply while a motor is running. The motor is tested in situ, that means motor's original working condition is maintained. As no sensors are need to place in

motors, it's also called the sensorless method. The MCSA method can be used to estimate motor efficiency and diagnose motor faults.

Bin Lu (2006) made a survey of efficiency estimation methods of in-service induction motors, and classified more than 20 of the most important methods into 9 categories according to their physical properties. Based on the survey results, he proposed the air gap torque method, one of the reference methods, as one of candidates for the nonintrusive in-service motor efficiency estimation.

The motor efficiency can be defined as (5) in terms of the shaft torque and the rotor speed, since the output power is the product of them. This is the basic principle of torque methods. But it's difficult, even impossible in most cases, to measure the shaft torque while a motor is in service.

$$\eta = \frac{T_{shaft} \cdot \omega_r}{P_I} \tag{5}$$

J. Hsu & B.P. Scoggins (1995) proposed an air gap torque (AGT) method which takes the output shaft torque as the air gap torque less the torque losses associate with friction, windage, and stray load losses caused by rotor currents. The motor efficiency can be obtained by (6) where the air gap torque (T_{AG}) is calculated using (7) from the motor instantaneous input line currents and voltages.

$$\eta = \frac{T_{AG} \cdot \omega_r - \left(L_{FW} + L_S \right)}{P_I} \tag{6}$$

$$T_{AG} = \frac{Poles}{2\sqrt{3}} \left\{ (i_A - i_B) \cdot \int \left[u_{CA} - R(i_C - i_A) \right] dt - (i_C - i_A) \cdot \int \left[u_{AB} - R(i_A - i_B) \right] dt \right\} \tag{7}$$

As the rotor speed (ω_r) and stator resistance (R) measurements are required and a no-load test must be run to measure losses L_{FW} and L_S, the AGT method is still a highly intrusive method difficult to use in the in-service motor monitoring. To overcome these problems, a "nonintrusive" method is developed by making the following improvements to the original AGT method (Bin Lu, 2006).

a) Without direct measurement, the rotor speed is estimated from motor current spectrum analysis extracting slot harmonics from stator currents.
b) The stator resistance is estimated from the input line voltages and phase currents using an on-line DC signal injection method.
c) The losses are estimated from empirical values using only motor nameplate data. The friction and windage loss is 1.2% of the rated output power; and the stray-load loss is estimated from the recommended values in IEEE standard 112.

4.2 Rotor Speed estimation

The main approach for speed estimation in induction motors uses the machine model to design observers (M.A. Gallegos et al., 2006). Luenberger observers, model reference adaptive systems, adaptive observers, Kalman filtering techniques, and estimation based on parasitic effects are some techniques to deal with the problem of speed estimation.

Rotor slot harmonics spectrum estimation technique is a kind of sensorless speed detection method. The rotor slot produces harmonic components in the air gap field, which modulate the flux interlacing on the stator with a frequency proportional to the rotor speed. Thus the speed can be estimated using the slot harmonics frequency (f_{sh}) by (8) (Azzeddine Ferrah at al., 1992).

$$n = \frac{60}{z_r}\left(f_{sh} \pm f_1\right) \tag{8}$$

We developed a rotor speed estimator based on slot harmonics spectrum estimation, as illustrated in Fig. 10. (X.Z. Che & J.T. Hu et al, 2008)
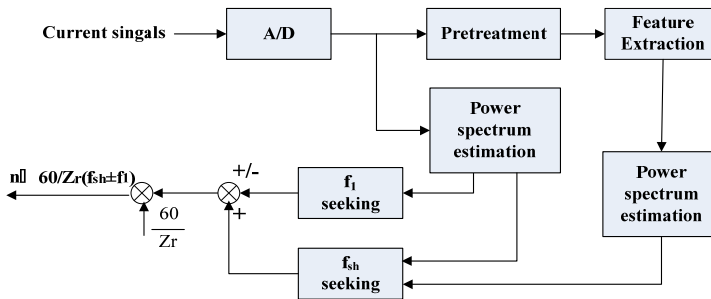

Fig. 10. Rotor speed estimation based on slot harmonics spectrum estimation

To extract feature more accurately, pretreatment is made before spectrum analysis. First, a band-pass filter is designed based on Chebyshev uniform approximation to filter out the fundamental component and upper and lower frequency noise signals. And then frequency aliasing is used to enhance the slot harmonics signal. The slot harmonics appear in the spectrum at $2f_1$ intervals, so the raw signals are downsampled to $2f_1$. Here f_1 is the original sampling frequency. As the sampling frequency is lower than the slot harmonics frequency after the downsampling, the frequency aliasing occurs that enhances the paired slot harmonics and weakens noises.

After the pretreatment, the frequency offset of the slot harmonics in the aliasing spectrum is detected with maximum entropy spectrum estimation, which is a modern power spectrum estimation method based in AR model. The frequency with the max amplitude in the aliasing spectrum is the frequency offset of the slot harmonics. Then the slot harmonics frequency is determined by matching the offset on the original spectrum.

4.3 Design and implement of motor monitoring front-end devices

Based on the non-intrusive efficiency estimation method mentioned above, the front-end device is developed with the digital signal processing (DSP) techniques. It is divided into three parts: sensing, signal processing and communication unit, as shown in Fig. 11
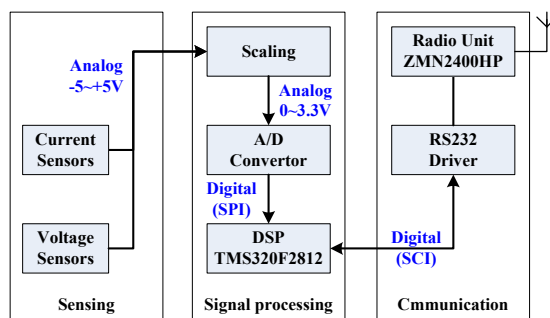
Fig. 11. The design of the front-end device

The three parts of the front-end devices are designed and implemented separately on individual PCB's. When constructing the front-end devices, the signal processing unit and the communication unit are mounted on the sensing unit and linked by cables with each other, as shown in Fig. 12. The flexible design could meet the requirement for different sensors while different motors are monitored. And moreover the sensing unit could be omitted in the case that the current and voltage sensors are already equipped in the MCC in industrial plants. In that case, the communication unit can be mounted on the signal processing unit.

The sensing unit consists of two current sensors and two voltage sensors. Both of them are highly accurate Hall effect ones. In the prototype devices used in the laboratory, the current sensor is HNC025A with 0-36 amps RMS current range, $\pm$ 0.6% accuracy, and <0.2% linearity, and the voltage sensor is HNV025A with 100-2500V volts RMS current range, $\pm$ 0.6% accuracy, and <0.2% linearity.

Fig. 12. Implementation of the sensing, processing and communication unit

The signal processing unit contains three main subunits. The -5v - +5v analogue voltage signals coming from the sensing unit are firstly scaled into analogue signals in the range of 0-3.3 volts to meet the requirement of the ADC chip. And then a 12-bit 8-channel ADC is used to sample the analogue waveforms at a certain frequency , which can be configured as 2, 4 or 8 KHz in the prototype devices, and convert them into digital signals.

The kernel of the signal processing unit is a 32-bit fixed-point DSP chip TMS320F2812, which has 128KB flash memory, 18KB internal SRAM. It controls the signal processing and spectrum estimation programs running in a μcOS/II system.

In order to evaluate the energy usage, 8 motor condition parameters are estimated and/or calculated, including the current root mean square (I_{rms}), the voltage root mean square (U_{rms}), the input power (P_I), the power factor ($\cos\varphi$), the rotor speed (ω_r), the shaft torque (T_{Shaft}), the output power (P_O), and the efficiency (η), as shown in Fig. 13.
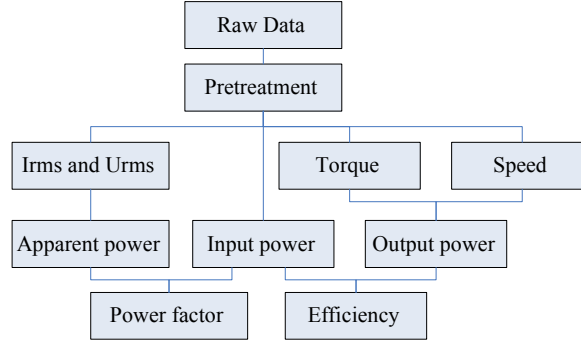

Fig. 13. Motor condition parameters calculation

The output power is calculated from rotor speed and shaft torque. The rotor speed is estimated by the method described in section 4.2. The shaft torque is obtained by subtracting the torque losses associated with the friction and windage loss L_{FW} and rotor stray-load loss L_S from the calculated air-gap torque, as given by (9). In this implement, the combined losses of L_{FW} and L_S are assumed to be 3.5% of rated output power from empirical values. And the stator resistance is assumed to be the same as the resistance measured at cool state. Other parameters can be obtained by (10)-(13). At last, the motor efficiency is calculated by (1).

$$T_{shaft} = T_{AG} - \frac{L_{FW}}{\omega_r} - \frac{L_S}{\omega_r} \tag{9}$$

$$I_{rms} = \sqrt{\frac{1}{N}\sum_{m=1}^{N} i_m^2} \tag{10}$$

$$U_{rms} = \sqrt{\frac{1}{N}\sum_{m=1}^{N} u_m^2} \tag{11}$$

$$P_I = \frac{1}{N}\sum_{m=1}^{N} u_m i_m \tag{12}$$

$$\cos\varphi = \frac{P}{S} = \frac{P}{\sqrt{3}\cdot U \cdot I} \tag{13}$$

5. Laboratory Test and Plant Application

The system are tested in the laboratory with four Y100L2-4 induction motors (4-pole, 3KW, 380V, 6.8A) with four 4KW DC generators as their loads, and applied in a plant to monitor four pumping motors as illustrated in Fig. 14.

In the CCS, a WSN receiver node is used as a coordinator of the network. Four front-end devices are installed in the MCC to acquire the current and voltage signals of the four test motors. When started, they search and connect to the coordinator automatically to setup a star wireless network. Then the coordinator sends a query packet to one of the 4 front-end nodes every second and receives a data packet sent back on the request. In this way, the motor monitoring results are successfully transmitted to the CSS constantly.

The motors are tested from no load to full load with intervals of 12.5% load. And signals are sampled and analyzed for 120 seconds at each load point. That means totally 4 (motors) * 9 (load point per motor) * 120 (seconds per load point) / 3 (seconds for one packet) = 1440 packets are transmitted from 4 front-end devices to the CCS. As only one packet is sent to the coordinator from one of the 4 front-end monitoring devices every second, the data throughput is enough to transmit the data packets, and there is no packet lost in the laboratory test.

Fig. 14. Laboratory testing system (L) and the pumping motors in a plant (R)

5.1 Data throughput over the WSN

As described in section 3.1, the PSDU length can vary from 2 to 127 bytes in a IEEE 802.15.4 data packet. In the proposed system, the PSDU is totally 32 bytes long with 1-byte motor ID, 1-byte frame type, 2-byte counting number, 4-byte voltage, 4-byte current, 4-byte speed, 4-byte torque, 4-byte input power, 4-byte output power, 2-byte efficiency, and 2-byte power factor. Apparently, one result can be transmitted in one data packet.

To meet the requirement of signal processing, 4 channels of current and voltage signals are sampled synchronously at 4KHz frequency for 1 second to get 50 cycles of 50Hz waveforms. Another 2 seconds are spent on calculating and transmitting the results. So every 3 seconds, a data packet is sent to the CSS from one front-end device.

That transmitting time and data throughput requirement is enough to be implemented in an IEEE 802.15.4 WSN with the standard latency 6-60 ms and data throughput 250KBps.

To check the maximum communication abilities between the WSN nodes, a simple test is made in which real size data packets are continuously sent from a transmitter to a receiver in 300ms with each packet sent within an specified interval (Is). The packets sent from the transmitter (Ps) and the packets received by the receiver (Pr) are counted. Then the real receiving interval (Ir), average packets received per second (Pa), and the packets lost rate (Lr) are calculated. The test results are illustrated in Table 4.

Is	Ps	Pr	Ir	Pa	Lr
0.100	2976	2976	0.0101	9.92	0.0000%
0.050	5887	5887	0.0051	19.62	0.0000%
0.030	9691	9691	0.0031	32.30	0.0000%
0.025	11567	11567	0.0026	38.56	0.0000%
0.020	14310	14310	0.0021	47.70	0.0000%
0.015	18791	18790	0.0016	62.63	0.0053%
0.010	22577	19537	0.0015	65.12	13.4650%
0.005	29718	18851	0.0016	62.84	36.5671%

Table 4. Communication abilities test

From the test results, it can be seen that the minimum packets receiving interval is about 0.015 seconds. In other words, maximum 66.7 packets can be received every second on average. If the transmitter sends packets faster than that, the communication becomes worse with packets lost rate getting higher.

5.2 Motor efficiency estimation

The test results on motor No.3 and 4 are listed in Table 5 and 6 with estimated values and measured values. The estimated values vs. measured values of speed, torque, and efficiency of motor No. 3 are figured in Fig. 15 to 17.

The detection errors are large when the loads are under 25%. That's because the electromagnetic characteristic of the motor ferromagnetic slope the power factor curve under no load or light loads conditions. Another reason is that the motor load-efficiency curve is sloping in that section and the speed estimation error is enlarged in efficiency calculation process.

Generally the average loads of in-service motors are above 50%, so the larger errors under no load or light loads condition have little effects on the application of the monitoring system in plants.

Loads (%)	speed(r/min)		torque(N.m)		efficiency	
	Estimation	Measurement	Estimation	Measurement	Estimation	Measurement
0	1498.75	1495.80	1.25	1.16	41.40%	43.26%
12.5	1491.50	1494.00	2.75	2.46	62.50%	62.58%
25.0	1482.00	1483.80	5.75	5.34	79.30%	76.82%
37.5	1469.00	1470.60	8.72	9.34	80.10%	85.61%
50.0	1459.50	1460.40	12.00	11.94	84.80%	83.37%
62.5	1450.25	1451.40	14.50	13.69	85.20%	79.72%
75.0	1443.25	1443.00	16.25	16.43	84.00%	84.44%
87.5	1436.75	1435.20	17.50	17.07	82.80%	79.92%
100	1428.50	1428.60	18.50	19.49	81.20%	75.93%

Table 5. Test results on motor No. 3

Loads (%)	speed(r/min)		torque(N.m)		efficiency	
	Estimation	Measurement	Estimation	Measurement	Estimation	Measurement
0	1499.50	1496.40	2.50	1.30	76.20%	43.81%
12.5	1498.75	1492.80	3.25	2.54	72.70%	61.56%
25.0	1478.50	1485.00	6.25	5.61	81.60%	77.54%
37.5	1472.25	1471.80	9.00	9.08	82.80%	84.05%
50.0	1460.75	1462.20	12.00	11.83	85.90%	91.48%
62.5	1450.25	1449.00	14.00	14.33	82.00%	84.27%
75.0	1439.50	1441.00	16.25	16.41	84.40%	85.53%
87.5	1434.00	1434.00	17.75	17.82	84.00%	84.14%
100	1426.75	1427.40	18.75	19.08	82.40%	83.39%

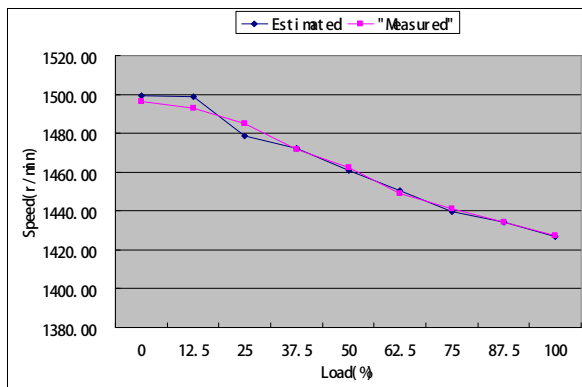Table 6. Test results on motor No. 4

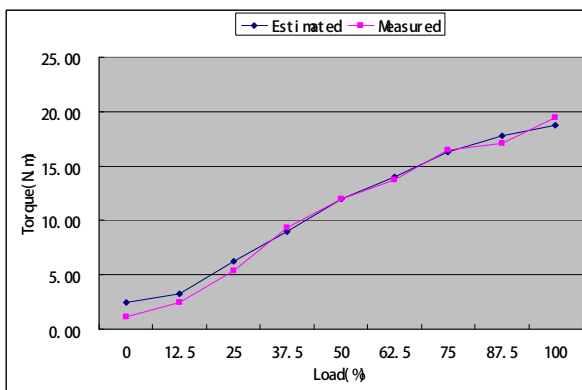Fig. 15. Estimated vs. Measured Speed Values of Motor No. 3

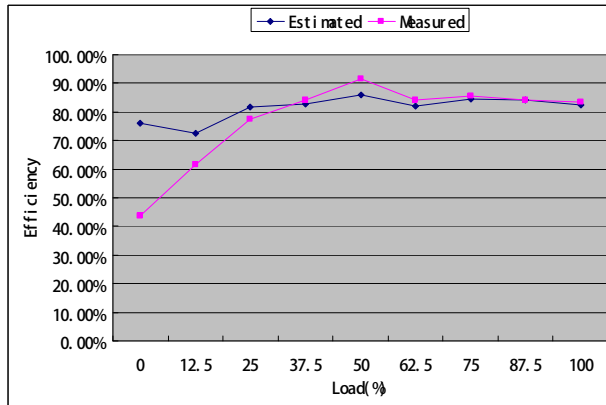Fig. 16. Estimated vs. Measured Torque Values of Motor No.3

Fig. 17. Estimated vs. Measured Efficiency Values of Motor No.3

6. Conclusion

This paper proposes a motor energy management architecture, which is composed of a data acquisition platform, a condition monitoring platform, an energy consumption and saving analysis platform, a communication platform, and a motor energy data management platform.

Under the guidance of the architecture, an in-service motor monitoring and energy management system is developed based on non intrusive monitoring technologies and wireless sensor networks. The system has two subsystems: a data acquiring and analysis subsystem, and a condition monitoring and energy management subsystem.

To evaluate the in-service motor energy usage, motor efficiency estimation methods are discussed. And a motor monitoring front-end device is developed with the implement of the methods introduced. The device is designed as three separate units, including a sensing unit, a processing unit, and a communication unit. Such a flexible design could meet various requirements in the application.

The wireless sensor network is a self-organized network with dynamic topology. As a low-cost, robust, and reliable communication network, it is used to connect the front-end devices with the central supervisory station. A WSN node is designed and implemented for the in-service motor monitoring system, which can also be used as a unit of the front-end device.

The laboratory tests and plant application show that the system can help the plant managers to improve motor-driven systems.

7. References

U.S. Department of Energy (2007), Sensors & Automation 2007 Annual Portfolio Review, Rosemont, Illinois, June 2007.

Electrical Industrial Association of China (2006), The New Trend of Motor Energy-saving, *Electrical Industry*, April 2006, pp. 50-52

Ramamurthy, H.; Prabhu, B.S.; Gadh, R. & Madni, A.M., Smart sensor platform for industrial monitoring and control, *Sensors, 2005 IEEE,* Oct. 30 2005-Nov. 3 2005, pp.1116-1119

James E. Hardy; Wayne W. Manges; Jose A. Guitierrez & Phani Teja V. Kuruganti (2005), Wireless Sensors and Networks for Advanced Energy Management, *2005 ACEEE Summer Study on Energy Efficiency in Industry*, West Point, New York, July 2005

Nathan Ota & Paul Wright (2006), Trends in wireless sensor networks for Manufacturing, *Int. J. Manufacturing Research*, Vol. 1, No. 1, (2006), pp. 3-17

Bin LU; Long Wu; Thomas G. Habetler; Ronald G. Harley & Jose A. Gutierrez (2005), On the Application of Wireless Sensor Network in Condition Monitoring and Energy Evaluation for Electric Machines, *Proceedings of the 31st Annual Conference of the IEEE Industrial Electronics Society (IECON'05)*, pp.2674-2679, Raleigh, NC, Nov. 2005.

Jose A. Gutierrez; David B. Durocher & Bin Lu (2006), Applying Wireless Sensor Networks in Industrial Plant Energy Evaluation and Planning Systems, *Conference Record of the 2006 IEEE IAS Pulp and Paper Conference*, pp.1-7, Jun. 2006

Yu Haibin; Zeng Peng & Liang Wei (2006), *Intelligent Wireless Sensor Networks*, Li Wei; Tian Shiying & Yao Qingshuang, (1st Ed), Science Press, ISBN 7-03-016453-9, Beijing

John S. Hsu; John D. Kueck; Mitchell Olszewski; Don A. Casada; Pedro J. Otaduy & Leon M. Tolbert, Comparision of Induction Motor Field Efficiency Evaluation Methods, *IEEE Transactions on Industry Applications,* pp.117-125, Vol. 34, No. 1, Jan./Feb. 1998.

B. Lu; T. G. Habetler & R. G. Harley (2006), A Survey of Efficiency-Estimation Methods for In-Servce Induction Motors, *IEEE Trans. Industry Applications,* pp.924-933, vol. 42, no. 4, Jul./Aug. 2006.

Bin Lu; Thomas G. Habetler & Ronald G. Harley (2006), A Nonintrusive and In-Service Motor Efficiency Estimation Method using Air-Gap Torque with Considerations of Condition Monitoring, *Conference Record of the 2006 IEEE Industry Applications Conference,* pp.1533 – 1540, Volume 3, Oct. 2006

J. hsu & B.P. Scoggins (1995), Field Test of Motor Efficiency and Load Changes through Air-gap Torque, *IEEE Transctions on Energy Convers,* pp.477-483, vol. 10, no.3, Sep. 1995.

M.A. Gallegos; R. Alvarez & C.A. Nunez (2006), A survey on speed estimtion for sensorless control of induction motors, *10th IEEE International Power Electronics Congress,* pp.1-6, Oct. 2006.

Azzeddine Ferrah; Kerth J. Bradley & Greg M. Asher (1992), an FFT-Based Novel Approach to Noninvasive Speed Measurement in Induction Motor Drives, *IEEE Transaction on Instrumentation and Measurement*, pp. 797-802, Vol. 41, No. 6, Dec. 1992

X.Z. Che; J.T. Hu & Q.J. Guo (2008), An Slot Harmonics Detection-Based Approach to Speed Estimation in a Sensorless Induction Motor, *Chinese Journal of Scientific Instrument*, pp. 414-417, Vol.29, No.4S, 2008(4)

Home energy management problem: towards an optimal and robust solution

Duy Long Ha, Stéphane Ploix, Mireille Jacomino and Minh Hoang Le
G-SCOP lab (Grenoble Institute of Technology)
France

1. Introduction

A home automation system basically consists of household appliances linked via a communication network allowing interactions for control purposes (Palensky & Posta, 1997). Thanks to this network, a load management mechanism can be carried out: it is called *distributed control* in (Wacks, 1993). Load management allows inhabitants to adjust power consumption according to expected comfort, energy price variation and CO_2 equivalent rejection. For instance, during the consumption peak periods when power plants rejecting higher quantities of CO_2 are used and when energy price is high, it could be possible to decide to delay some services, to reduce some heater points or to run requested services even so according to weather forecasts and inhabitant requests. Load management is all the more interesting that local storage and production means exist. Indeed, battery, photovoltaic panels or wind mills provide additional flexibilities. Combining all these elements lead to systems with many degrees of freedom that are very complex to manage by users.

The objective of this study is to setup a general mathematical formulation that makes it possible to design optimized building electric energy management systems able to determine the best energy assignment plan, according to given criteria. A building energy management system consists in two aspects: the load management and the local energy production management. (House & Smith, 1995) and (Zhou & Krarti, 2005) have proposed optimal control strategies for HVAC (Home Ventilation and Air Conditioning) system taking into account the natural thermal storage capacity of buildings that shift the HVAC consumption from peak-period to off-peak period. Zhou & Krarti (2005) has shown that this control strategy can save up to 10% of the electricity cost of a building. However, these approaches do not take into account the energy resource constraints, which generally depend on the autonomy needs of off-grid systems (Muselli et al., 2000) or on the total power production limits of the suppliers in grid connected systems.

The household load management problem can be formulated as a assignment problem where energy is considered as a resource shared by appliances, and tasks are energy consumptions of appliances. Ha et al. (2006a) presents a three-layers household energy control system that is both able to satisfy the maximum available electrical power constraint and to maximize user satisfaction criteria. This approach carries out more reactivity to adapt consumption to the energy provider requirements. Ha et al. (2006b) proposes a global solution for the household load management problem. In order to adapt the consumption to the available energy, the home automation system controls the appliances in housing by determining the

starting time of services and also by computing the temperature set points of HVAC systems. This problem has been formulated as a multi-objective constraint satisfaction problem and has been solved by a dynamic Tabu Search. This approach can carry out the coordination of appliance consumptions of HVAC system and of services in making it possible to set up a compromise between the cost and the user comfort criteria.

With an energy production management production point of view, Henze & Dodier (2003) has proposed an adaptive optimal control for an off-grid PV-hybrid system using a quadratic cost function and a Q-learning approach. It is more efficient than conventional control but it requires to be trained beforehand with actual data covering a long time period. Generally speaking, studies in literature focus only on one aspect of the home energy management problem: the load management or the local energy production but not on the joined load and production management problem.

This chapter formulates the global approach for the building energy management problem as a scheduling problem that takes into account the load consumption and local energy production points of view. The optimization problem of the building energy management is modeled using both continuous and discrete variables: it is modeled as a mixed integer linear problem.

2. Problem description

In this chapter, energy is restricted to electricity consumption and production. Each service is depicted by an amount of consumed/produced electrical power; it is supported by one or several appliances.

2.1 The concept of service

Housing with appliances aims at providing comfort to inhabitants thanks to services which can be decomposed into three kinds: the end-user services that produce directly comfort to inhabitants, the intermediate services that manage energy storage and the support services that produce electrical power to intermediate and end-user services. Support services deal with electric power supplying thanks to conversion from a primary energy to electricity. *Fuel cells based generators*, *photovoltaic power suppliers*, *grid power suppliers* such as EDF in France, belong to this class. Intermediate services are generally achieved by electrochemical batteries. Among the end-user services, well-known services such as *clothe washing*, *water heating*, *specific room heating*, *cooking in oven* and *lighting* can be found.

A service with index i is denoted $SRV(i)$. Appliances are just involved in services: they are not central from an inhabitant point of view. Consequently, they are not explicitly modelled.

2.2 Caracterisation of services

Let us assume a given time range for anticipating the energy needs (typically 24 hours). A service is qualified as *permanent* if its energetic consumption/production/storage covers the whole time range of energy assignment plan, otherwise, the service is named *temporary service*. The following table gives some examples of services according to this classification.

	temporary services	permanent services
support services	photovoltaic panels	power provider
intermediate services	-	storage
end-user services	washing	room heating

The services can also be classified according to the way their behavior can be modified.

Whatever the service is, an end-user, an intermediate or a support service can be modifiable or not. A service is qualified as *modifiable by a home automation system* if the home automation system is capable to modify its behavior (the starting time for example).

There are different ways of modifying services. Sometimes, modifiable services can be considered as continuously modifiable such as the temperature set points in *room heating services* or the shift of a washing. Some other services may be modified discretely such as the interruption of a *washing service*. The different ways of modifying services can be combined: for instance, a washing service can be considered both as interruptible and as continuously shiftable. A service modeled as discretely modifiable contains discrete decision variables in its model whereas a continuously modifiable service contains continuous decision variables. Of course, a service may contain both discrete and continuous decision variables.

A service can also be characterized by the way it is known by a home automation system. The consumed or produced power may be observable or not. Moreover, for end-user services, the impact of a service on the inhabitant comfort may be known or not.

Obviously, a service can be taken into account by a home automation system if it is at least observable. Some services are indirectly observable. Indeed, all the not observable services can be gathered into a virtual non modifiable service whose consumption/production is deduced from a global power meter measurement and from the observable service consumptions and productions. In addition, a service can be taken into account for long term schedulings if it is predictable. In the same way as for observable services, all the unpredictable services can be gathered into a global no-modifiable predictable service. A service can be managed by a home automation system if it is observable and modifiable. Moreover, it can be long-term managed if it is predictable and modifiable.
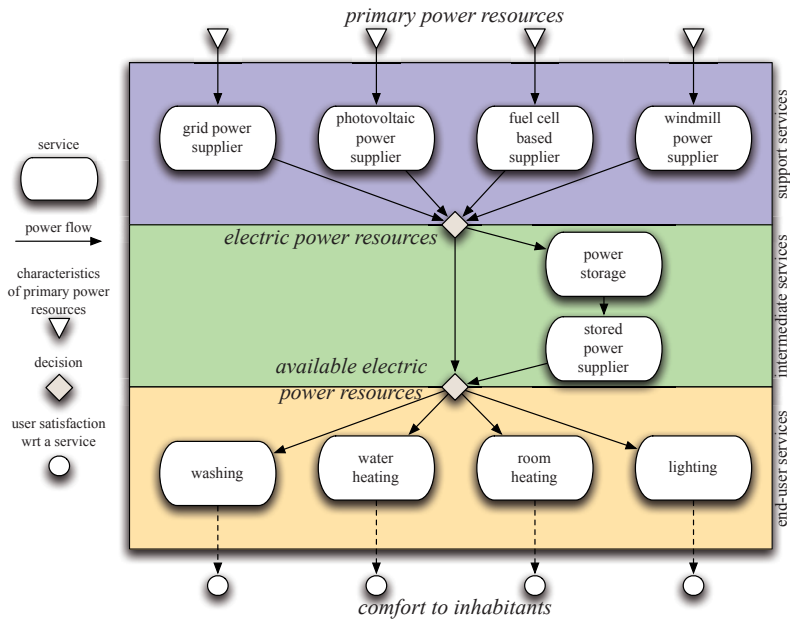

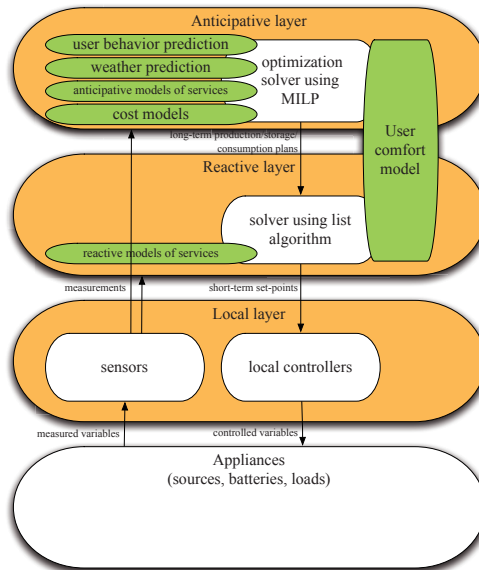Fig. 1. Structure of services in housing

Fig. 2. Schema of the 3 layers control mechanism

2.3 Principle of control mechanism

An important issue in home automation problems is the uncertainties in the model data. For instance, solar radiation, outdoor temperature or services requested by inhabitants may not be predicted with accuracy. In order to solve this issue, a three-layer architecture is presented in this chapter: a local layer, a reactive layer and an anticipative layer (see figure 2).

The *anticipative layer* is responsible for scheduling end-user, intermediate and support services taking into account predicted events and costs in order to avoid as much as possible the use of the *reactive layer*. The prediction procedure forecasts various informations about future user requests but also about available power resources and costs. Therefore, it uses information from predictable services and manage continuously modifiable and shiftable services. This layer has slow dynamics and includes predictive models with learning mechanisms, including models dealing with inhabitant behaviors. This layer also contains a predictive control mechanism that schedules energy consumption and production of end-user services several hours in advance. This layer computes plans according to available predictions. The sampling period of the anticipative layer is denoted Δ. This layer relies on the most abstract models.

The *reactive layer* has been detailed in (Abras et al., 2006). Its objective is to manage adjustments of energy assignment in order to follow up a plan computed by the upper *anticipative layer* in spite of unpredicted events and perturbations. Therefore, this layer manages modifiable services and uses information from observable services (comfort for end-user services and power for others). This layer is responsible for decision-making in case of violation of predefined constraints dealing with energy and inhabitant comfort expectations: it performs arbitrations between services. The set-points determined by the plan computed by the upper *anticipative layer* are dynamically adjusted in order to avoid user dissatisfaction. The control actions may be dichotomic in enabling/disabling services or more gradual in adjusting
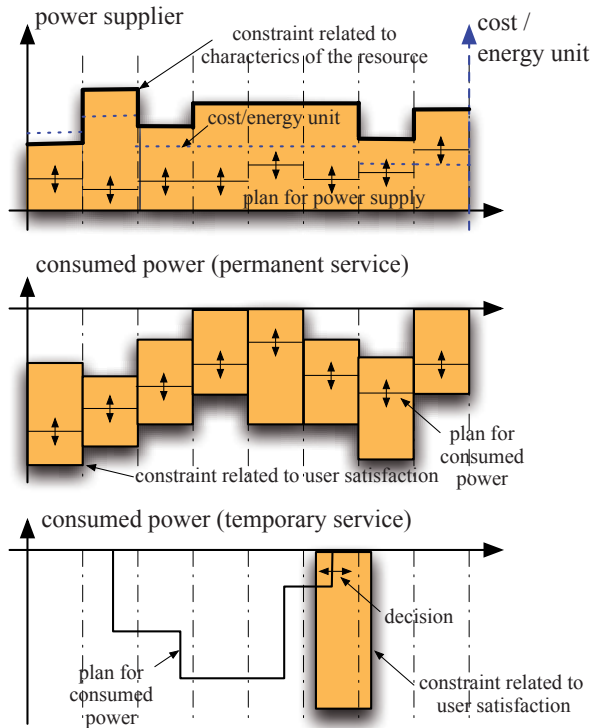
Fig. 3. Plans computed by the anticipative mechanism

set-points such as reducing temperature set point in room heating services or delaying a temporary service. Actions of the reactive layer have to remain transparent for the plan computed by the anticipative layer: it can be considered as a fast dynamic unbalancing system taking into account actual housing state, including unpredicted disturbances, to satisfy energy, comfort and cost constraints. If the current state is too far from the computed plan, the anticipative layer has to re-compute it.

The *local layer* is composed of devices together with their existing local control systems generally embedded into appliances by manufacturers. It is responsible for adjusting device controls in order to reach given set points in spite of perturbations. This layer abstracts devices and services for upper layers: fast dynamics are hidden by the controllers of this level. This layer is considered as embedded into devices: it is not detailed into this chapter.

This chapter mainly deals with the scheduling mechanism of the anticipative layer, which computes anticipative plans as shown in figure 3.

3. Modeling services

Modeling services can be decomposed into two aspects: the modeling of the behaviors, which depends on the types of involved models, and the modeling of the quality of the execution of services, which depends on the types of service. Whatever the type of model it is, it has to be

defined all over a time horizon $K\Delta$ for anticipative problem solving composed of K sampling periods lasting Δ each.

3.1 Modeling behavior of services

In order to model the behavior of the different kinds of services in housing, three different types of models have been used: discrete events are modeled by finite state machines, continuous behaviors are modeled by differential equations and mixed discrete and continuous evolutions are modeled by hybrid models that combine the two previous ones.

Using finite state machines (FSM)

A finite state machine dedicated to a service SRV is composed of a finite number of states $\{\mathcal{L}_m; m \in \{1, ..., M\}\}$ and a set of transitions between those states $\{\mathcal{T}_{p,q} \in \{0, 1\}; (p, q) \in S \subset \{1, ..., M\}^2\}$. Each state $\mathcal{L}_m$ of a service SRV is linked to a phase characterized by a maximal power production $P_m > 0$ or consumption $P_m < 0$.

A transition triggers a state change. It is described by a condition that has to be satisfied to be enabled. The condition can be a change of a state variable measured by a sensor, a decision of the antipative mechanism or an elapsed time for phase transition. If it exists a transition between the state $\mathcal{L}_m$ and $\mathcal{L}_{m'}$ then $\mathcal{T}_{m,m'} = 1$, otherwise $\mathcal{T}_{m,m'} = 0$. An action can be associated to each state: it may be a modification of a set-point or an on/off switching. As an example, let's consider a washing service.

The service provided by a washing machine may be modeled by a FSM with 4 states: the first state is the *stand-by* state $\mathcal{L}_1$ with a maximal power of $P_1 = -5W$ (it is negative because it deals with consumed power). The transition towards the next state is triggered by the anticipative mechanism. The second state is the *water heating* state $\mathcal{L}_2$ with $P_2 = -2400W$. The transition to the next state is triggered after τ_2 time units. The next state corresponds to the *washing* characterized by $\mathcal{P}_3 = -500W$. And finally, after a given duration τ_3 depending on the type of washing (i.e. the type of requested service), the spin-drying state is reached with $\mathcal{P}_3 = -1000W$. After a given duration τ_4, the *stand-by* state is finally recovered. Considering that the initial state is $\mathcal{L}_1$, this behavior can be formalized by:

$$\begin{cases} (state = \mathcal{L}_1) \wedge (t = t_{start}) & \rightarrow state = \mathcal{L}_2 \\ (state = \mathcal{L}_2) \wedge (t = t_{start+\tau_2}) & \rightarrow state = \mathcal{L}_3 \\ (state = \mathcal{L}_3) \wedge (t = t_{start+\tau_2+\tau_3}) & \rightarrow state = \mathcal{L}_4 \\ (state = \mathcal{L}_4) \wedge (t = t_{start+\tau_2+\tau_3+\tau_4}) & \rightarrow state = \mathcal{L}_1 \end{cases} \tag{1}$$

Using differential equations

In buildings, thermal phenomena are continuous phenomena. In particular, the thermal behavior of a HVAC system can be modeled by state space models:

$$\begin{cases} \frac{dx_c(t)}{dt} = A_c x_c(t) + B_c u_c(t) + F_c p_c(t) \\ y_c(t) = C x_c(t) \end{cases} \tag{2}$$

$x_c(t)$ contains state variables, usually temperature. $u_c(t)$ contains controlled input variables such as energy flows. $p_c(t)$ contains known but uncontrolled input variables such as outside temperature or solar radiance. A first order state space thermal model relevant for control purpose has been proposed in Nathan (2001) but the second order model based on an electric

analogy proposed in Madsen (1995) has been preferred for our control purpose because it models the dynamic of indoor temperature. For a room heating service $SRV(i)$, it yields:

$$\begin{cases} \frac{d}{dt}\begin{bmatrix} T_{in}(i,t) \\ T_{env}(i,t) \end{bmatrix} = A_c \begin{bmatrix} T_{in}(i,t) \\ T_{env}(i,t) \end{bmatrix} + B_c \begin{bmatrix} P(i,t) \end{bmatrix} + F_c \begin{bmatrix} T_{out}(i,t) \\ \phi_s(i,t) \end{bmatrix} \\ T_{in}(i,t) = C_c \begin{bmatrix} T_{in}(i,t) \\ T_{env}(i,t) \end{bmatrix} \end{cases} \tag{3}$$

with $A_c = \begin{bmatrix} \frac{-1}{r_{in}c_{env}} & \frac{1}{r_{in}c_{env}} \\ \frac{1}{r_{in}c_{in}} & -\frac{r_{env}+r_{in}}{r_{env}r_{in}c_{in}} \end{bmatrix}$, $B_c = \begin{bmatrix} 0 \\ \frac{1}{-c_{in}} \end{bmatrix}$, $F_c = \begin{bmatrix} 0 & 0 \\ \frac{1}{r_{env}c_{in}} & \frac{w}{c_{in}} \end{bmatrix}$ and $C_c = \begin{bmatrix} 1 & 0 \end{bmatrix}$

This model allows a rather precise description of the dynamic variations of indoor temperature with:

- T_{in}, T_{out}, T_{env} the respective indoor, outdoor and housing envelope temperatures
- c_{in}, c_{env} the thermal capacities of first indoor environment and second the envelope of the housing
- r_{in}, r_{env} thermal resistances
- w the equivalent surface of the windows
- P the power consumed by the thermal generator, $P \leq 0$. In this chapter, this flow is assumed to correspond to an electric energy flow.
- ϕ_s the energy flow generated by the solar radiance

In order to solve the anticipative problem, continuous time models have to be discretized according to the anticipation period Δ. Equation (2) modelling service $SRV(i)$ becomes:

$$\forall k \in \{1, \ldots, K\},$$
$$\begin{bmatrix} T_{in}(i,k+1) \\ T_{env}(i,k+1) \end{bmatrix} = A_i \begin{bmatrix} T_{in}(i,k) \\ T_{env}(i,k) \end{bmatrix} + B_i \begin{bmatrix} E(i,k) \end{bmatrix} + F_i \begin{bmatrix} T_{out}(i,k) \\ \phi_s(i,k) \end{bmatrix} \tag{4}$$

with $A_i = e^{A_c\Delta}$, $B_i = (e^{A_c\Delta} - I_n)A_c^{-1}\Delta^{-1}B_c$, $F_i = (e^{A_c\Delta} - I_n)A_c^{-1}F_c$, $E(i,k) = P(i,k)\Delta$ and $E(i,k) \leq 0$.

Using hybrid models
Some services cannot be modeled by a finite state machine nor by differential equations. Both approaches have to be combined: the resulting model is then based on a finite state machine where each state $\mathcal{L}_m$ actually becomes a set of states which evolution is depicted by a differential equation.
An electro-chemical storage service supported by a battery may be modeled by a hybrid model (partially depicted in figure 4). $x(t)$ stands for the quantity of energy inside the battery and $u(t)$ the controlled electrical power exchanged with the grid network.

Using static models
Power sources are usually modelled by static constraints. Local intermittent power resources, such as photovoltaic power system or local electric windmill, and power suppliers are considered here. Using weather forecasts, it is possible to predict the power production $w(i,k)$

during each sampling period $[k\Delta, (k+1)\Delta]$ of a support service $SRV(i)$. The available energy for each sampling period k is then given by:

$$E(i,k) = w(i,k)\Delta \ \forall k \in \{1, ..., K\} \tag{5}$$

with $w(i,k) \geq 0$

According to the subscription between inhabitants and a power supplier, the maximum available power is given. It may depends on time. For a service of power supply $SRV(i)$, it can be modelled by the following constraint:

$$E(i,k) \leq p_{max}(i,k)\Delta \ \forall k \in \{1, ..., K\} \tag{6}$$

where $p_{max}(i,k)$ stands for the maximum available power.

3.2 Modeling quality of the execution of services

Depending on the type of service, the quality of the service achievement may be assessed in different ways. End-user services provide comfort to inhabitants, intermediate services provide autonomy and support services provide power that can be assessed by its cost and its impact on the environment. In order to evaluate these qualities different types of criteria have been introduced.

End-user services

Generally speaking, modifiable permanent services use to control a physical variable: the user satisfaction depends on the difference between an expected value and an actual one. Let's consider for example the HVAC controlling a temperature. A flat can usually be split into several HVAC services related to rooms (or thermal zones) assumed to be independent.

According to the comfort standard 7730 (AFNOR, 2006), three qualitative categories of thermal comfort can be distinguished: A, B and C. In each category, (AFNOR, 2006) proposes typical value ranges for temperature, air speed and humidity of a thermal zone that depends on the type of environment: office, room,... These categories are based on an aggregated criterion named Predictive Mean Vote (PMV) modelling the deviation from a neutral ambience. The absolute value of this PMV is an interesting index to evaluate the quality of a HVAC service. In order to simplify the evaluation of the PMV, typical values for humidity and air speed are used. Therefore, only the ambient temperature corresponding to the neutral value of PMV (PMV=0) is dynamically concerned. Under this assumption, an ideal temperature T_{opt} is obtained. Depending on the environment, an acceptable temperature range coming from
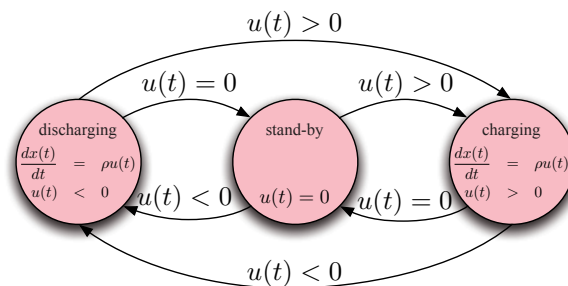

Fig. 4. Hybrid model of a battery

the standard leads to an interval $[T_{min}, T_{max}]$. For instance, in an individual office in category A, with typical air speed and humidity conditions, the neutral temperature is $T_{opt} = 22°C$ and the acceptable range is $[21°C, 23°C]$.

Therefore, considering the HVAC service $SRV(i)$, the discomfort criterion $D(i,k)$, which is more usable than comfort criterion here, is modelled by the following formula where assumptions are depicted by two parameters a_1 and a_2:

$$D(i,k) = |PMV(T_{in}(i,k))| = \begin{cases} a_1 \times \dfrac{(T_{opt} - T_{in}(i,k))}{T_{opt} - T_{Min}} & \text{if } T_{in}(i,k) \leq T_{opt} \\ a_2 \times \dfrac{(T_{in}(i,k) - T_{opt})}{T_{Max} - T_{opt}} & \text{if } T_{in}(i,k) > T_{opt} \end{cases} \qquad (7)$$

The global comfort criterion is defined as following:

$$D(i) = \sum_{k=1}^{K} D(i,k) \qquad (8)$$

Generally speaking, modifiable temporary end-user services do not aim at controlling a physical variable. Temporary services such as washing are expected by inhabitants to finished at a given time. Therefore, the quality of achievement of a temporary service depends on the amount of time it is shifted. Therefore, in the same way as for permanent services, a user dissatisfaction criterion for a service $SRV(i)$ is defined by:

$$D(i) = \begin{cases} \dfrac{f(i) - f_{opt}(i)}{f_{max}(i) - f_{opt}(i)} & \text{if } f(i) > f_{opt}(i) \\ \dfrac{f_{opt}(i) - f(i)}{f_{opt}(i) - f_{min}(i)} & \text{if } f(i) \leq f_{opt}(i) \end{cases} \qquad (9)$$

where f_{opt} stands for the requested end time and f_{min} and f_{max} stand respectively for the minimum and maximum acceptable end time.

Intermediate services

Intermediate services are composed of two kinds of services: the *power storage services*, which store energy to be able to face difficult situations such as off-grid periods, and then lead to the availability of the *stored power supplier services* (see figure 1). A power storage service $SRV(i)$ and a stored power service $SRV(j); j \neq i$ are associated to each storage system.

The quality of a *power storage service* has to be evaluated: it is related to the amount of stored energy. This quality is called *autonomy*.

Let us consider a electric storage system modelled by a power storage service $SRV(i)$ and by a stored power supplier service $SRV(j)$. The stock $E^{stock}(k)$ of the storage system is modelled by:

$$E^{stock}(k) = E^{stock}_{initial} - \sum_{\zeta=1}^{k} (E(i,\zeta) + E(j,\zeta)) \qquad (10)$$

with $E(i,\zeta) \leq 0$ and $E(j,\zeta) \geq 0$.

Let P_{ref} be the reference power taken into account for the computation of the autonomy duration $\tau_{autonomy}$. The autonomy objective $A(k)$ can be defined by:

$$A(k) = \sum_{k \in \{1,...,K\}} E^{stock}(k) \qquad (11)$$

Depending on the inhabitant expectations, autonomy can also be formulated by constraints to be satisfied at any sample time: $P_{ref}\tau_{autonomy} - E^{stock}(k) = 0$, $\forall k \in \{1, \ldots, K\}$.

Let's now focus on *stored power supplier* service. What is the quality for this service i.e. the service that provides stored energy to the housing. It is not a matter of economy nor of ecology because costs is already taken into account when power production services provide power to the storage system. It is not also a matter of stored energy: there is no quality of service defined for *stored power supplier* service.

Support services

Support services dealing with power resources do not interact directly with inhabitants. However, inhabitants do care about their cost and their environmental impact. These two aspects have to be assessed.

In most cases, the economical criterion corresponds to the cost of the provided, stored or sold energy. This cost may contain depreciation of the device used to produce power.

Let $SRV(0)$ be a photovoltaic support service and $SRV(1)$ be a power supplier service. Let's examine the case of power provider such as EDF in France. Energy is sold at a given price $C(1, k)$ to the customer for each consumed kWh at time k. In order to promote photovoltaic production, power coming from photovoltaic plants is bought by the supplier at higher price $C(0, k) > C(1, k)$.

Different power metering principles can be subscribed with a French power supplier. Only the most widespread principle is addressed. The energy cost is thus given by the following equation:

$$C(k) = C(1, k)E(1, k) - C(0, k)E(0, k), \ \forall k \in \{1, \ldots, K\} \quad (12)$$

The equivalent mass of carbon dioxide rejected in the atmosphere has been used as ecological criterion for a support service. This criterion is easy to establish for most power devices: photovoltaic cells, generator and even for energy coming from power suppliers. Powernext energy exchange institution publishes the equivalent mass of carbon dioxide rejected in the atmosphere per power unit in function of time (see http://www.powernext.fr). For instance, in France, electricity coming from the grid network produces $66g/kWh$ of CO_2 during off-peak periods and $383g/kWh$ during peak period (Angioletti & Despretz, 2003). Energy coming from photovoltaic panels is considered as free of CO_2 rejection (grey energy is not taken into account). For each support service $SRV(i)$, a CO_2 rejection rate $\tau_{CO2}(i, k)$ can be defined as the equivalent volume of CO_2 rejected per kWh. Therefore, the total rejection for a support service $SRV(i)$ during the sampling period k is given by $\tau_{CO2}(i, k)E(i, k)$ where $E(i, k)$ corresponds to the energy provided by the support service $SRV(i)$ during the sampling period k.

4. Formulation of the anticipative problem as a linear problem

The formulation of the energy management problem contains both behavioral models with discrete and continuous variables, differential equation and finite state models, and quality models with nonlinearities such as in the PMV model. In order to get mixed linear problems which can be solved by well known efficient algorithms, transformations have to be done. The ones that have been used are summarized in the next section.

4.1 Transformation tools

Basically, a proposition denoted $\mathcal{X}$ is either *true* or *false*. It can result from the combination of propositions thanks to connecting operators such as "$\wedge$"(and), "$\vee$"(or), "$\oplus$" (exclusive or), "$\neg$"

(not), "$\rightarrow$" (implies), "$\leftrightarrow$" (if and only if),... Whatever the proposition $\mathcal{X}$ is, it can be associated to a binary variable $\delta \in \{0,1\}$ such as: $\mathcal{X} = (\delta = 1)$.

Therefore, (Williams, 1993) has shown that, in integer programming, connecting operators may be modelled by:

$$\begin{array}{lcl} \neg \mathcal{X} & \leftrightarrow & \delta = 0 \\ \mathcal{X}_1 \wedge \mathcal{X}_2 & \leftrightarrow & \delta_1 + \delta_2 = 2 \\ \mathcal{X}_1 \vee \mathcal{X}_2 & \leftrightarrow & \delta_1 + \delta_2 \geq 1 \\ \mathcal{X}_1 \oplus \mathcal{X}_2 & \leftrightarrow & \delta_1 + \delta_2 = 1 \\ \mathcal{X}_1 \rightarrow \mathcal{X}_2 & \leftrightarrow & \delta_1 - \delta_2 \leq 0 \\ \mathcal{X}_1 \leftrightarrow \mathcal{X}_2 & \leftrightarrow & \delta_1 - \delta_2 = 0 \end{array} \tag{13}$$

According to (Bemporad & Morari, 1998), the transformation into a standard linear problem can be achieved using lower and upper bounds of $dom(f(x); x \in dom(x)) = dom(ax - b; x \in dom(x)) \subset [m, M]$. Then, Binary variables can be connected to linear conditions as follows:

$$\delta = (ax - b \leq 0) \leftrightarrow \left\{ \begin{array}{l} ax - b \leq M(1 - \delta) \\ ax - b > m\delta \end{array} \right. \tag{14}$$

Consider for instance the statement $a_1 x \leq b_1 \leftrightarrow a_2 x' \leq b_2$. Using the previous transformation, it can be formulated as:

$$\left\{ \begin{array}{l} a_1 x - b_1 \leq M(1 - \delta) \\ a_1 x - b_1 \leq m\delta \\ a_2 x' - b_2 \leq M(1 - \delta) \\ a_2 x' - b_2 \leq m\delta \end{array} \right.$$

with $dom(a_1 x - b_1; x \in dom(x)) \cup dom(a_2 x' - b_2; x' \in dom(x')) \subset [m, M]$.

In many cases, such as in presence of absolute values like in PMV evaluation, products of discrete and continuous variables appear. They have to be reformulated in order to get mixed linear problems. Auxiliary variables may be used for this purpose. First consider the product of 2 binary variables δ_1 and δ_2: $\delta_3 = \delta_1 \times \delta_2$. It can be transformed into a discrete linear problem:

$$\delta_3 = \delta_1 \times \delta_2 \leftrightarrow \left\{ \begin{array}{lcl} -\delta_1 + \delta_3 & \leq & 0 \\ -\delta_2 + \delta_3 & \leq & 0 \\ \delta_1 + \delta_2 - \delta_3 & \leq & 1 \\ \delta_1, \delta_2, \delta_3 \in \{0,1\} & & \end{array} \right. \tag{15}$$

Consider now the product of a binary variable with a continuous variable: $z = \delta \times x$ where $\delta \in \{0,1\}$ and $x \in [m, M]$. It means that $\delta = 0 \rightarrow z = 0$ and $\delta = 1 \rightarrow z = x$. Therefore, the semi-continuous variable z can be transformed into a mixed linear problem:

$$z = \delta \times x \leftrightarrow \left\{ \begin{array}{lcl} z & \leq & M \times \delta \\ z & \geq & m\delta \\ z & \leq & x - m(1 - \delta) \\ z & \geq & x - M(1 - \delta) \end{array} \right. \tag{16}$$

These transformations can now be used to remove nonlinearities from the PMV computations, time shifting of services and power storage.

4.2 Linearization of PMV

Generally speaking, behavioral models of HVAC systems is given by Eq. (2) and an example is given by (3). Model (4) is already linear but nonlinearities come up with the absolute value of the PMV evaluation. Let's introduce a binary variable $\delta_a(k)$ satisfying $\delta_a(k) = 1 \leftrightarrow T_{in}(k) \leq T_{opt}$ $\forall k$. Then, the PMV function (7) can be reformulated into a mixed linear form for every service $SRV(i)$:

$$
\begin{aligned}
|PMV(T_{i,a}(k))| &= \delta_a(k) \times a_1 \times \frac{(T_a(i,k) - T_{opt})}{T_{opt} - T_{Min}} + (1 - \delta_a(k)) \times a_2 \times \frac{(T_{opt} - T_a(k))}{T_{Max} - T_{opt}} \\
&= F_1 \delta_a(k) + F_2 T_a(k) + F_3 z_a(k) + F_4
\end{aligned}
\tag{17}
$$

Using eq. (14) to transform the absolute value, the equivalent form of the condition that contains $T_a(k) \leq T_{opt}$ is given by:

$$
\begin{cases}
T_a(k) - T_{opt} \leq (T_{max} - T_{opt})(1 - \delta_a(k)) \\
T_a(k) - T_{opt} \geq \epsilon + (T_{min} - T_{opt} - \epsilon)\delta_a(k)
\end{cases}
\tag{18}
$$

A semi-continuous variable $z_a(k)$ is added to take place of the product $\delta_a(k) \times T_{in}(k)$ in eq. (17). According to eq. (16), the transformation of $z_a(k) \triangleq \delta_a(k) \times T_{in}(k)$ leads to:

$$
\begin{cases}
z_a(k) & \leq (T_{max} - T_{opt})\delta_a(k) \\
z_a(k) & \geq (T_{min} - T_{opt})\delta_a(k) \\
z_a(k) & \leq T_{in}(k) - (T_{min} - T_{opt})(1 - \delta_a(k)) \\
z_a(k) & \geq T_{in}(k) - (T_{max} - T_{opt})(1 - \delta_a(k))
\end{cases}
\tag{19}
$$

After the linearization of PMV, let's now consider the linearization of the time shifting of services.
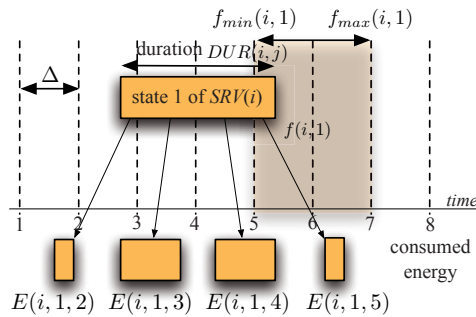
4.3 Formalizing time shifting

Fig. 5. Shift of temporary services

Temporary services are modelled by finite state machines. The consumption of a state can be shifted such as task in scheduling problems. The starting and ending times of services can be synchronized to an anticipative period such as in (Duy Ha, 2007). It leads to a discrete-time formulation of the problem. However, this approach is both a restriction of the solution space and an approximation because the length of a time service has to be a multiple of Δ. The general case has been considered here.

In the scientific literature, continuous time formulations of scheduling problems exist (Castro & Grossmann, 2006; Pinto & Grossmann, 1995; 1998). However, these results concerns scheduling problems with disjunctive resource constraints. Instead of computing the starting time of tasks, the aim is to determine the execution sequence of tasks on shared resources. In energy management problems, the matter is not restricted to determine such sequence because several services can be achieved at the same time.

An alternative formulation based on transformations (14) and (16), suitable for the energy management in housings, is introduced.

Temporary services can be continuously shifted. Let $DUR(i,j)$, $f(i,j)$ and $p(i,j)$ be respectively the duration of the state j of service $SRV(i)$, the ending time and the power related to the service $SRV(i)$ during the state j. $f(i,j)$ is defined according to inhabitant comfort models: they correspond to extrema in the comfort models presented in section 3.2.

According to (Esquirol & Lopez, 1999), the potential consumption/production duration (effective duration if positive) $d(i,j,k)$ of a service $SRV(i)$ in state j during a sampling period $[k\Delta, (k+1)\Delta]$ is given by (see figure 5):

$$d(i,j,k) = \min(f(i,j), (k+1)\Delta) - \max(f(i,j) - DUR(i,j), k\Delta) \tag{20}$$

Therefore, the consumption/production energy $E(i,j,k)$ of the service $SRV(i)$ in state j during a sampling period $[k\Delta, (k+1)\Delta]$ is given by:

$$E(i,j,k) = \begin{cases} d(i,j,k)p(i,j) & \text{if } d(i,j,k) > 0 \\ 0 & \text{otherwise} \end{cases} \tag{21}$$

$E(i,j,k)$ can be modelled using a binary variable: $\delta_{t0}(i,j,k) = (d(i,j,k) \geq 0)$ and a semi-continuous variable $z_{t0}(i,j,k) = \delta_{t0}(i,j,k)d(i,j,k)$ such as in (14) and in (16). It leads to the following inequalities:

$$d(i,j,k) \leq \delta_{t0}(i,j,k)K\Delta \tag{22}$$
$$d(i,j,k) > (\delta_{t0}(i,j,k) - 1)K\Delta \tag{23}$$
$$E(i,j,k) = z_{t0}(i,j,k)p(i,j) \tag{24}$$
$$z_{t0}(i,j,k) \leq \delta_{t0}(i,j,k)K\Delta \tag{25}$$
$$z_{t0}(i,j,k) \geq -\delta_{t0}(i,j,k)K\Delta \tag{26}$$
$$z_{t0}(i,j,k) \leq d(i,j,k) + (1 - \delta_{t0}(i,j,k))K\Delta \tag{27}$$
$$z_{t0}(i,j,k) \geq d(i,j,k) - (1 - \delta_{t0}(i,j,k))K\Delta \tag{28}$$

But the model still contains nonlinear functions min and max in the expression of $d(i,j,k)$. Therefore, equation (20) has to be transformed into a mixed-linear form. Let's introduce 2 binary variables $\delta_{t1}(i,j,k)$ and $\delta_{t2}(i,j,k)$ defined by:

$$\delta_{t1}(i,j,k) = (f(i,j) - k\Delta \geq 0)$$
$$\delta_{t2}(i,j,k) = (f(i,j) - DUR(i,j) - k\Delta \geq 0)$$

Using (14), it yields:

$$f(i,j) - k\Delta \leq \delta_{t1}(i,j,k)K\Delta \tag{29}$$
$$f(i,j) - k\Delta \geq (\delta_{t1}(i,j,k) - 1)K\Delta \tag{30}$$
$$f(i,j) - DUR(i,j) - k\Delta \leq \delta_{t2}(i,j,k)K\Delta \tag{31}$$
$$f(i,j) - DUR(i,j) - k\Delta \leq (\delta_{t2}(i,j,k) - 1)K\Delta \tag{32}$$

Therefore, min and max of equation (20) become:

$$f_{min}(i,j,k) = \delta_{t1}(i,j,k+1)(k+1)\Delta + (1 - \delta_{t1}(i,j,k+1))\,f(i,j) \tag{33}$$
$$s_{max}(i,j,k) = \delta_{t2}(i,j,k)(f(i,j) - DUR(i,j)) + (1 - \delta_{t2}(i,j,k))\,k\Delta \tag{34}$$

with $\min(f(i,j),(k+1)\Delta) = f_{min}(i,j,k)$ and $\max(f(i,j) - DUR(i,j),k\Delta) = s_{max}(i,j,k)$.
The duration $d(i,j,k)$ can then be evaluated:

$$d(i,j,k) = f_{min}(i,j,k) - s_{max}(i,j,k) \tag{35}$$

Equations (22) to (35) model the time shifting of a temporary service.
Let's now consider nonlinearities inherent to power storage services modelled by hybrid models.

4.4 Linearization of power storage
A storage service $SRV(i)$ with a maximum capacity of E_{stock}^{max} can be modelled at time k by:

$$E_{stock}(i,k) = max(min(E_{stock}^{max}, E_{stock}(i,k-1) + E(i,k-1)),0)$$

Let's define the following binary variables: $\delta_1(i,k) = (E_{stock}(i,k) \leq E_{stock}^{max})$ and $\delta_2(i,k) = (E_{stock}(i,k) \geq 0)$. Using (14), it yields:

$$E_{stock}(i,k) - E_{stock}^{max} \quad \leq \quad (1 - \delta_1(i,k))\,E_{stock}^{max} \tag{36}$$
$$E_{stock}(i,k) - E_{stock}^{max} \quad > \quad -\delta_1(i,k)E_{stock}^{max} \tag{37}$$
$$E_{stock}(i,k) \quad \leq \quad \delta_2(i,k)E_{stock}^{max} \tag{38}$$
$$E_{stock}(i,k) \quad > \quad (\delta_2(i,k) - 1)\,E_{stock}^{max} \tag{39}$$

The stored energy can then be written:

$$E_{stock}(i,k) \quad = \quad \delta_1(i,k-1)\delta_2(i,k-1)\,(E_{stock}(i,k-1) + E(i,k-1))\ldots$$
$$\cdots + (1 - \delta_1(i,k))E_{stock}^{max}$$

With variables $\delta_3(i,k) = \delta_1(i,k)\delta_2(i,k)$, $z_1(i,k) = \delta_3(i,k)E_{stock}(i,k)$ and $z_2(i,k) = \delta_3(i,k)E(i,k)$ and using transformations (15) and (16), the energy $E_{stock}(i,k)$ can be rewritten into a linear form:

$$E_{stock}(i,k) = z_1(i,k-1) + z_2(i,k-1) + (1 - \delta_1(i,k))E_{stock}^{max} \tag{40}$$

The following constraints must be satisfied:

$$-\delta_1(i,k) + \delta_3(i,k) \quad \leq \quad 0 \tag{41}$$
$$-\delta_2(i,k) + \delta_3(i,k) \quad \leq \quad 0 \tag{42}$$
$$\delta_1(i,k) + \delta_2(i,k) - \delta_3(i,k) \quad \leq \quad 1 \tag{43}$$
$$z_1(i,k) \quad \leq \quad \delta_3(i,k)E_{stock}^{max} \tag{44}$$
$$z_1(i,k) \quad \geq \quad -\delta_3(i,k)E_{stock}^{max} \tag{45}$$
$$z_1(i,k) \quad \leq \quad E_{stock}(i,k) + (1 - \delta_3(i,k))E_{stock}^{max} \tag{46}$$
$$z_1(i,k) \quad \geq \quad E_{stock}(i,k) - (1 - \delta_3(i,k))E_{stock}^{max} \tag{47}$$
$$z_2(i,k) \quad \leq \quad \delta_3(i,k)E_{stock}^{max} \tag{48}$$
$$z_2(i,k) \quad \geq \quad -\delta_3(i,k)E_{stock}^{max} \tag{49}$$
$$z_2(i,k) \quad \leq \quad E(i,k) + (1 - \delta_3(i,k))E_{stock}^{max} \tag{50}$$
$$z_2(i,k) \quad \geq \quad E(i,k) - (1 - \delta_3(i,k))E_{stock}^{max} \tag{51}$$

Equations (40) to (51) are a linear model of a power storage service.

Main services have been modelled by mixed integer linear form. Other services can be modelled in the same way. Let's now focus on how to solve the resulting mixed integer linear problem.

5. Solving approach

Anticipative control in home energy management can be formulated as an multicriteria mixed-linear programming problem represented by a set of constraints and optimization criteria.

5.1 Problem summary

In a actual problem, the number of constraints is so large they cannot be detailed in this chapter. Nevertheless, the fundamental modelling and transformation principles have been presented in sections 3 and 4.

HVAC services are representative examples of permanent services. They have been modelled by equations like (4) and (19). The decision variables are heating powers $\Phi_s(i, k)$.

Temporary services, such as clothe washing, are modelled by equations like (22) to (35). The decision variables are the ending times: $f(i, j)$.

Storage services are modelled by equations like (40) to (51). The decision variables are energy exchange with the storage systems: $E(i, j)$.

Power supplier services are modelled by equations like (5). There is no decision variable for these services.

These results can be adapted to fit most situations. If necessary, more details about modelling can be found in (Duy Ha, 2007). As a summary, the following constraints may be encountered:

- linearized behavioral models of services
- linearized comfort models related to end-user services

In addition, a constraint modelling the production/consumption balance has to be added. Generally speaking, this constraint can be written:

$$\forall k \in \{1, \ldots, K\}, \ \sum_{i \in \mathcal{I}} E(i, k) = 0 \tag{52}$$

where $\mathcal{I}$ contains the indexes of available predictable services.

If there is a grid power supplier modelled by a support service $SRV(0)$, the imported energy can be adjusted to effective needs (it is also true for fuel cells based support services). Therefore, $E(0, k)$ has to be set to the maximum available energy for a sampling period: $E(0, k) = P^{max}(0, k)\Delta$ where $P^{max}(0, k)$ stands for the maximum available power during sampling period k. Consequently, (52) becomes:

$$\forall k \in \{1, \ldots, K\}, \ \sum_{i \in \mathcal{I}} E(i, k) \geq 0 \tag{53}$$

All the predictable but not modifiable services provide data to the optimization problem. Their indexes are contained in $\mathcal{I}^{modifiable} \subset \mathcal{I}$. Decision variables are all related to predictable and modifiable services: they may be binary or continuous decision variables. The problem to be solved is thus a mixed-linear programming problem. Moreover, the optimization problem is a multi-criteria problem using the following criteria: economy, dissatisfaction, CO2eq and autonomy criteria.

Economy criterion is given by (12) when there is only a grid power supplier and a photo-voltaic power supplier. Depending of the predictable support services $\mathcal{I}^{support*}$ excluding photovoltaic power supplier and on the existence of photovoltaic power supplier $SRV(0)$,

$$J^{autonomy} = \sum_{k=1}^{K} \left(\sum_{i \in \mathcal{I}^{support*}} C(i,k)E(i,k) - C(0,k)E(0,k) \right) \tag{54}$$

where $C(i,k)$ stands for the kWh cost of the support service i.

Dissatisfaction criterion comes from expressions like (7) and (9). Let $\mathcal{I}^{end-user} \subset \mathcal{I}$ be the indexes of predictable end-user services. The comfort criteria may be given by:

$$J^{discomfort} = \sum_{i \in \mathcal{I}^{end-user}} sum_{k \in \{1,\dots,K\}} D(i,k) \tag{55}$$

The autonomy criterion comes from (11). It is given by:

$$J^{autonomy} = sum_{k \in \{1,\dots,K\}} A(k) \tag{56}$$

If there are several storage systems, the respective $A(k)$ have to be summed up in the criterion $J^{autonomy}$.

Finally, the CO2 equivalent rejection can be computed like the autonomy criteria:

$$J^{CO2eq} = \sum_{k=1}^{K} \sum_{i \in \mathcal{I}^{support}} \tau_{CO2}(i,k)E(i,k) \tag{57}$$

where $\tau_{CO2}(i,k)$ stands for the CO2 equivalent volume rejection for 1 kWh consummed by the support service i and $\mathcal{I}^{support}$ gathers the indexes of predictable support services.

All these criteria can be aggregated into a global criterion. α-criterion approaches can also be used.

5.2 Decomposition into subproblems

In section 2.2, services have been split into permanent and temporary services. Let $\mathcal{I}^{temporary}$ be the indexes of modifiable and predictable temporary services. It is quite usual in housing that some modifiable and predictable temporary services cannot occur at the same time, whatever the solution is. Using this property, the search space can be reduced.

Let's defined the horizon of a service.

Definition 1. *The horizon of a service $SRV(i)$, denoted $H(SRV(i))$, is a time interval in which $SRV(i)$ may consume or produce energy.*

The horizon of a service $SRV(i)$ is denoted: $[\underline{H}(SRV(i)), \overline{H}(SRV(i))] \subseteq [0, K\Delta]$. A permanent service has an horizon equal to $[0, K\Delta]$. A temporary service $SRV(i)$ has an horizon given by $\underline{H}(SRV(i)) = s_{min}(i)$ (the earliest starting of the service) and $\overline{H}(SRV(i)) = f_{max}(i)$ (the latest ending of the service).

Only predictable and modifiable services are considered in the following because they contain decision variables. Two predictable and modifiable services may interact if and only if there is a non empty intersection between their horizons.

Definition 2. *Two predictable and modifiable services $SRV(i)$ and $SRV(j)$ are in direct temporal relation if $H(SRV(i)) \bigcap H(SRV(j)) \neq \emptyset$. The direct temporal relation between $SRV(i)$ and $SRV(j)$ is denoted $\overbrace{SRV(i), SRV(j)} = 1$ if it exists, and $\overbrace{SRV(i), SRV(j)} = 0$ otherwise.*

If $H(SRV(i)) \bigcap H(SRV(j)) = \varnothing$, $SRV(i)$ and $SRV(j)$ are said temporally independent. Even if two services $SRV(i)$ and $SRV(j)$ are not in direct temporal relation, it may exists an indirect relation that can be found by transitivity. For instance, consider an additional service $SRV(l)$. If $\overbrace{SRV(i), SRV(l)} = 1$, $\overbrace{SRV(i), SRV(l)} = 1$ and $\overbrace{SRV(i), SRV(j)} = 0$, $SRV(i)$ and $SRV(j)$ are said to be indirect temporal relation.

Direct temporal relations can be represented by a graph where nodes stands for predictable and modifiable services and edges for direct temporal relations. If the direct temporal relation graph of modifiable and predictable services is not connected, the optimization problem can be split into independent sub-problems. The global solution corresponds to the union of sub-problem solutions (Diestel, 2005). This property is interesting because it may lead to important reduction of the problem complexity.

6. Application example of the mixed-linear programming

After the decomposition into independent sub-problems, each sub-problem related to a specific time horizon can be solved using Mixed-Linear programming. The open source solver GLKP (Makhorin, 2006) has been used to solve the problem but commercial solver such as CPLEX (ILOG, 2006) can also be used. Mixed-Linear programming solvers combined a branch and bound (Lawler & Wood, 1966) algorithm for binary variables with linear programming for continuous variables.

Let's consider a simple example of allocation plan computation for a housing for the next 24h with an anticipative period $\Delta = $1h. The plan starts at 0am. Energy coming from a grid power supplier has to be shared between 3 different end-user services:

- $SRV(1)$ is a room HVAC service whose model is given by (3). According to the inhabitant programming, the room is occupied from 6pm to 6am. Out of the occupation periods, the inhabitant dissatisfaction $D(1, k)$ is not taken into account. Room HVAC service is thus considered here as a permanence service. The thermal behavior is given by:

$$\begin{bmatrix} T_{in}(1, k+1) \\ T_{env}(1, k+1) \end{bmatrix} = \begin{bmatrix} 0.299 & 0.686 \\ 0.203 & 0.794 \end{bmatrix} \begin{bmatrix} T_{in}(1, k) \\ T_{env}(1, k) \end{bmatrix} + \begin{bmatrix} 1.264 \\ 0.336 \end{bmatrix} E(1, k) + \begin{bmatrix} 0.015 & 0.44 \\ 0.004 & 0.116 \end{bmatrix} \begin{bmatrix} T_{ext}(k) \\ \phi_s(1, k) \end{bmatrix}$$

$$(58)$$

The comfort model of service $SRV(1)$ in period k is

$$D(1, k) = \begin{cases} \dfrac{22 - T_{in}(i, k)}{5} & \text{if } T_{in}(i, k) \leq 22 \\ \dfrac{T_{in}(i, k) - 22}{5} & \text{if } T_{in}(i, k) > 22 \end{cases} \qquad (59)$$

The global comfort of service $SRV(1)$ is the sum of comfort model of the whole period:

$$D(1) = \sum_{k=1}^{K} D(1, k) \qquad (60)$$

- Service $SRV(2)$ corresponds to an electric water heater. It is considered as a temporary preemptive service. Its horizon is given by $H(SRV(2)) = [3, 22]$. The maximal power consumption is 2kW and 3.5kWh can be stored within the heater.

- $SRV(3)$ corresponds to a cooking in an oven that lasts 1h. It is considered as a temporary and modifiable but not preemptive service. It just can be shifted providing that the following comfort constraints are satisfied: $f_{min}(3) = 9 : 30am$, $f_{max}(3) = 5pm$, $f_{opt} = 2pm$ where f_{min}, f_{max} and f_{opt} stand respectively for the earliest acceptable ending time, the latest acceptable ending time and the preferred ending time. The cooking requires $2kW$. The global comfort of service $SRV(2)$ is:

$$D(3) = \begin{cases} \dfrac{f(3) - 14}{3} & \text{if} \quad f(3) > 14 \\ \dfrac{2(14 - f(3))}{9} & \text{if} \quad f(3) \leq 14 \end{cases} \tag{61}$$

- $SRV(4)$ is a grid power supplier. There is 2 prices for the kWh depending on the time of day. The cost is defined by a function $C(4, k)$. The energy used is modelled by $E(4, k)$. The maximum subscribed power is $E_{max}(4) = 4kW$.

The consumption/production balance leads to:

$$\sum_{i=1}^{3} E(i, k) \leq E_{max}(4) \tag{62}$$

The objective here is to minimize the economy criterion while keeping a good level of comfort for end-user services. The decision variables correspond to:

- the power consumed by $SRV(1)$ that correspond to a room temperature
- the interruption $SRV(2)$
- the shifting of service $SRV(3)$

The chosen global criterion to be minimized is:

$$J = \sum_{k=1}^{K} (E(4, k)C(4, k)) + D(1) + D(3) \tag{63}$$

The analysis of temporal relations points out a strongly connected direct temporal relation graph: the problem cannot be decomposed. The problem covering 24h yields a mixed-linear program with 470 constraints with 40 binary variables and 450 continuous variables. The solving with GLPK led to the result drawn in figure 6 after 1.2s of computation with a 3.2Ghz Pentium IV computer. Figure 6 points out that the power consumption is higher when energy is cheaper and that the temperature in the room is increased before the period where energy is costly in order to avoid excessive inhabitant dissatisfaction where the room is occupied.

In this case of study, a basic energy management is also simulated. In assuming that: the service $SVR(1)$ is managed by the user; the heater is turned on when the room is occupied and turned off in otherwise. The set point temperature is set to 22řC. The the water heating service $SVR(2)$ is turned on by the signal of off-peak period (when energy is cheaper). The cooking service $SVR(3)$ is programmed by user and the ending of service is 2pm. The result of this simulation is presented in figure 8.

The advanced management reaches the objective of reducing the total cost of power consumption (-22%). The dissatisfactions of the services $SVR(1)$ and $SVR(3)$ reach a good level in comparison with the basic management strategy. Indeed, a 1řC shift from the desired temperature during one period leads to a dissatisfaction of 0.2 and a dissatisfaction of 0.22 corresponds to
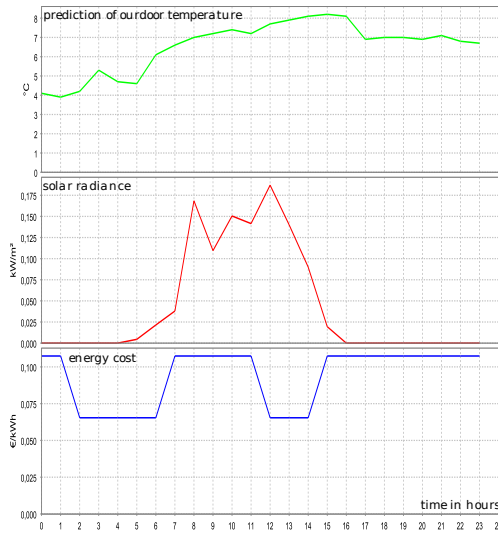
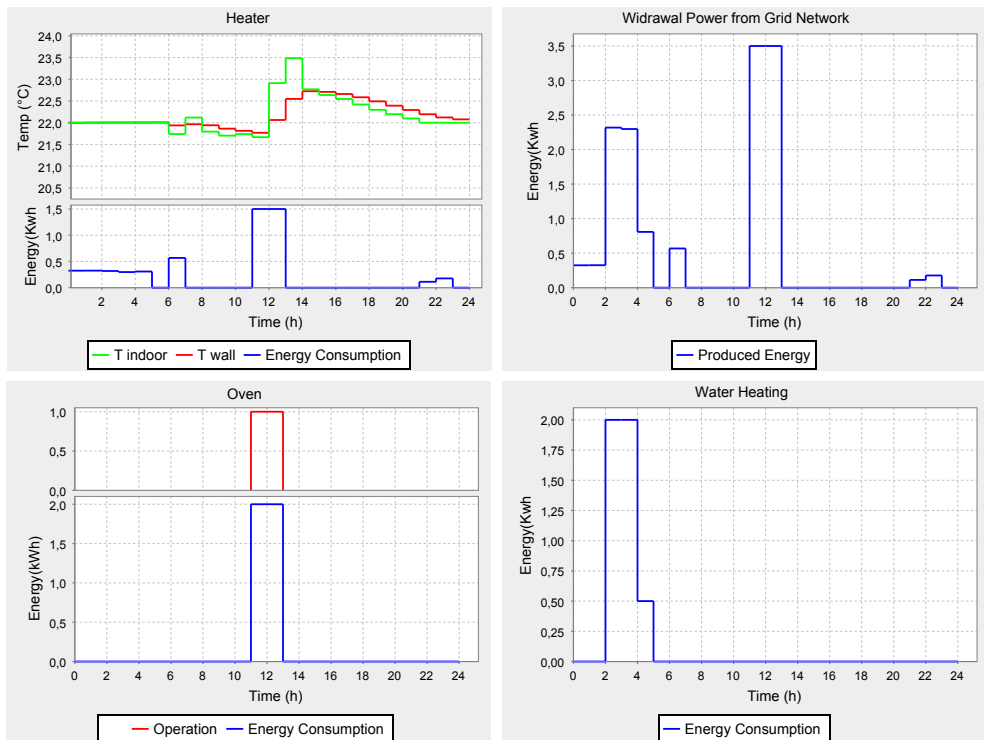Fig. 6. Considered weather and energy cost forecasts

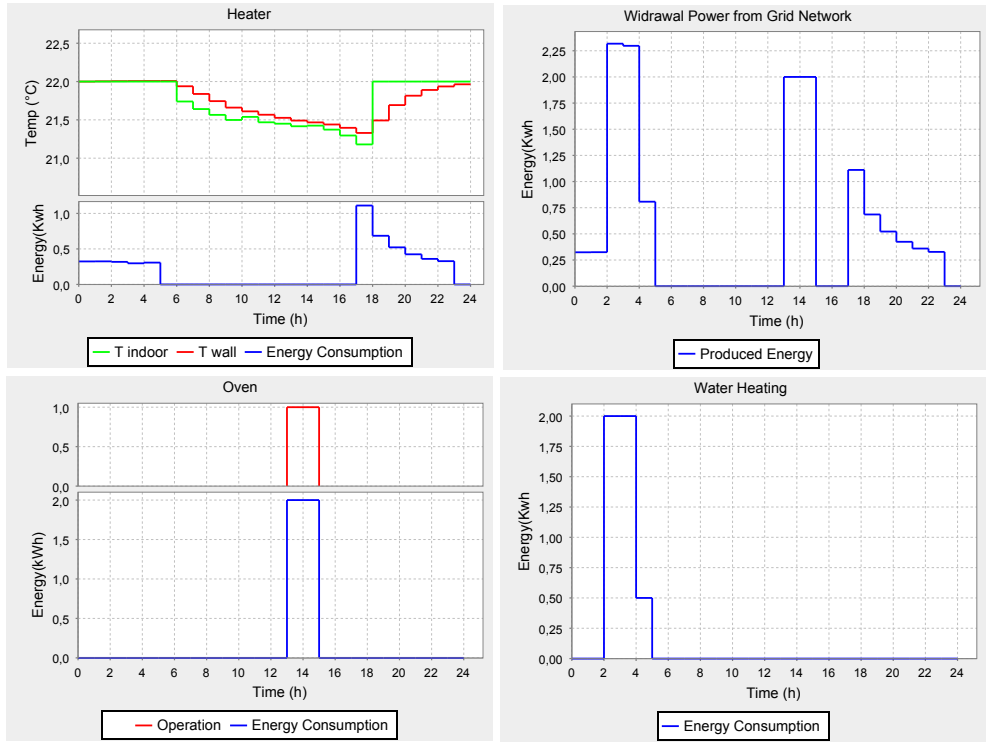Fig. 7. Results of the advanced energy management strategy computed by GLPK

Fig. 8. Results of the basic energy management strategy

a 1 hour delay for the cooking service. The basic management lead to an important dissatisfaction regarding the service $SVR(1)$, the heater is turned on only when the room is occupied. It lead to a dissatisfaction in period $[6pm, 7pm]$. The cooking service $SVR(3)$ is shifted one hour sooner by the advanced management strategy for getting the off-peak tariff. The total energy consumption of advanced management is slightly higher than the one of basic management strategy(+3%) but in terms of carbon dioxid emission, an important reduction (-65%) is observed. Thanks to an intelligent energy management strategy, economical cost and environmental impact of the power consumption have been reduced.

In addition, different random situations have been generated to get a better idea of the performance (see table 1). The computation time highly increases with the number of binary variables. Examples 3 and 4 show that the computation time does not only depend on the

Strategy of energy management	Total cost	Energy consumption	CO2 emission	$D(1)$	$D(3)$
Basic management	1.22euros	13.51kWh	3452.2g	0.16	0.00
Advanced management	0.95euros	13.92kWh	1216.2g	0.20	0.22

Table 1. Comparison between the two strategies of energy management

number of constraints and of variables. Example 5 fails after one full computation day with an *out of memory* message (there are 12 services in this example).

Mixed-linear programming manages small size problems but is not very efficient otherwise. The hybrid meta-heuristic has to be preferred in such situations.

Example number	Number of variables	Number of constraints	Computation time
1	201 continuous, 12 binary	204	1.2s
2	316 continuous, 20 binary	318	22s
3	474 continuous, 24 binary	479	144s
4	474 continuous, 24 binary	479	32m
5	1792 continuous, 91 binary	1711	>24h

Table 2. Results of random problems computed using GLPK

7. Taking into account uncertainties

Many model parameters used for prediction, such as predicting the weather information, are uncertain. The uncertainties are also present in the optimization criterion. For example, the criterion corresponding to thermal sensation depends on air speed, the metabolism of the human body that are not known precisely.

7.1 Sources of uncertainties in the home energy management problem

There are two main kinds of uncertainties. The first one comes from the outside like the one related to weather prediction or to the availability of energy resources. The second one corresponds to the uncertainty which come from inside the building. Reactive layer of the control mechanism manages uncertainties but some of them can be taken into account during the computation of robust anticipative plans.

The weather prediction naturally contains uncertainties. It is difficult to predict precisely the weather but the outside temperature or the level of sunshine can be predicted with confident intervals. The weather prediction has a significant impact on the local production of energy in buildings. In literature, effective methods to predict solar radiation during the day are proposed. Nevertheless, the resulting predictions may be very different from the measured values. It is indeed difficult to predict in advance the cloud in the sky. Uncertainties about the prediction of solar radiation have a direct influence on the consumption of services such as heating or air conditioning systems. Moreover, it can also influence the total available energy resource if the building is equipped with photovoltaic panels.

The disturbances exist not only outside the building but also in the building itself. A home energy management system requires sensors to get information on the status of the system. But some variables must be estimated without sensor: for example metabolism of the body of the inhabitants or the air speed in a thermal zone. More radically, there are energy activities that occur without being planned and change the structure of the problem. In the building, the user is free to act without necessarily preventing the energy management system. The consumption of certain services such as cooking, lighting, specifying the duration and date of execution remain difficult to predict. The occupation period of the building, which a strong energy impact, also varies a lot.

Through a brief analysis, sources of uncertainties are numerous, but the integration of all

sources of uncertainties in the resolution may lead to very complex problem. All the uncertainties cannot be taken into account at the same time in the anticipative mechanism: it is better to deal firstly with disturbances that has a strong energy impact. The sources of uncertainty have been classified according to two types of disturbances:

- The first type of uncertainty corresponds to those who change the information on the variables of the problem of energy allocation. The consequence of such disturbances is generally a deterioration of the actual result compared to the computed optimal solution.

- The second type corresponds to the uncertainties that cause the most important disturbances. They change the structure of the problem by adding and removing strong constraints. The consequence in the worst case is that the current solution is no longer relevant.

In both cases, the reactive mechanism will manage the situations in decreasing user satisfaction. If the anticipative plan is robust, it will be easier for the reactive mechanism to keep user satisfaction high.

7.2 Modelling uncertainty

A trail of research for the management of uncertainties is stochastic optimization, which amounts to represent the uncertainties by random variables. These studies are summarized in Greenberg & Woodruf (1998). Billaut et al. (2005b) showed three weak points of these stochastic methods in the general case:

- The adequate knowledge of most problems is not sufficient to infer the law of probability, especially during initialization.

- The source of disturbances generally leads to uncertainty on several types of data at once. The assumption that the disturbances are independent of each other is difficult to satisfy.

- Even if you come to deduce a stochastic model, it is often too complex to be used or integrated in a optimization process.

An alternative approach to modelling uncertainty is the method of intervals for continuous variables: it is possible to determine an interval pillar of their real value. You can find this approach to the problem of scheduling presented in Dubois et al. (2003; 2001). Aubry et al. (2006); Rossi (2003) have used the *all scenarios-method* to model uncertainty in a problem of load-balancing of parallel machines. The combination of three types of models (stochastic model, scenario model, interval model) is also possible according to Billaut et al. (2005b). In the context of the home energy management problem, stochastic methods have not been used because ensuring an average performance of the solution is not the target. For example, an average performance of user's comfort can lead to a solution which is very unpleasant at a time and very comfortable at another time. The methods based on intervals appear to be an appropriate method to this problem because it is a min-max approach. For example, uncertainty about weather prediction as the outside temperature T_{ext} can be modelled by an interval $T_{ext} \in \left[\underline{T_{ext}}, \overline{T_{ext}} \right]$. The modelling of an unpredictable cooking whose duration is $p \in [0.5h, 3h]$ and the execution date is in the interval $s(i) \in [18h, 22h]$. Similarly, the uncertainty of the period of occupation of the building or other types of disturbances can be modelled.

7.3 Introduction to multi-parametric programming

The approach taking into account uncertainties is to adopt a three-step procedure like scheduling problems presented in Billaut et al. (2005a):

- Step 0: Solving the problem in which the parameters are set to predict their most likely value.

- Step 1: Solving the problem, where uncertainties are modelled by intervals, to get a family of solutions.

- Step 2: Choosing a robust solution from among those which have been computed at step 1.

The main objective is to seek a solving method for step 1. A parametric approach may be chosen for calculating a family of solutions that will be used by step 2.

The parametric programming is a method for solving optimization problem that characterizes the solution according to a parameter. In this case, the problem depends on a vector of parameters and is referred to as a Multi-Parametric programming (MP). The first method for solving parametric programming was proposed in Gass & Saaty (1955), then a method for solving muti-parametric has been presented in Gal & J.Nedoma (1972). Borrelli (2002); Borrelli et al. (2000) have introduced an extension of the multi-parametric programming for the multi-parametric mixed-integer programming: a geometric method programming. The multi-parametric programming is used to define the variables to be optimized according to uncertainty variables.

Formally, a MP-MILP is defined as follows: let x_c be the set of continuous variables, and x_d be the set of discrete variables to be optimized. The criterion to be minimized can be written as:

$$J(x_c, x_d) = Ax_c + Bx_d$$
$$\text{subject to}$$
$$\begin{bmatrix} F & G & H \end{bmatrix} \begin{bmatrix} x_c \\ \theta \\ x_d \end{bmatrix} \leq W \tag{64}$$

where θ is a vector of uncertain parameters.

Definition 1 A polytope is defined by the intersection of a finite number of bounded half-spaces. An admissible region P is a polytope of $\begin{bmatrix} x_c \\ \theta \end{bmatrix}$ on which each point can generate an admissible solution to the problem 64. $\begin{bmatrix} x_c \\ \theta \end{bmatrix}$ belongs to a family of polytopes defined by the values of $x_d \in dom(x_d)$:

$$P(x_d) = \left\{ (x_c, \theta) \mid \begin{bmatrix} F & G & H \end{bmatrix} \begin{bmatrix} x_c \\ \theta \\ x_d \end{bmatrix} \leq W \right\} \tag{65}$$

In this family of polytopes, the optimal regions are defined as follows:

Definition 2 The optimal region $P^*(x_d) \subseteq P$ is the subset of $P(x_d)$, in which the problem 64 admits at least one optimal solution. $P^*(x_d)$ is necessarily a polytope because:

- a polytope is bounded by hyperplans which can lead to edges that are polytopes
- a polytope is a convex hypervolume

The family of the optimal region $P^*(x_d)$:

$$P^*(x_d) = \left\{ (x_c, \theta) \Big| \begin{cases} \begin{bmatrix} F & G & H \end{bmatrix} \begin{bmatrix} x_c \\ \theta \\ x_d \end{bmatrix} \leq W \\ J(x_c^* = \min_{x_c}(Ax_c + Bx_d) \end{cases} \right\} \tag{66}$$

This family of spaces $P^*(x_d)$ with $x_d \in dom(x_d)$ can be described by an optimal function $Z(x_c, x_d)$.

To determine this function Z, different spaces are defined, some of which correspond to the space of definition of this function Z.

Definition 3 The family of the admissible regions for θ is defined by:

$$\Theta_a(x_d) = \left\{ \theta | \exists x_c \text{ sbj. to } \begin{bmatrix} F & G & H \end{bmatrix} \begin{bmatrix} x_c \\ \theta \\ x_d \end{bmatrix} \leq W \right\} \tag{67}$$

Definition 4 The family of the optimal regions for θ is a subset of the family $\Theta_a(x_d)$:

$$\Theta_a^*(x_d) = \left\{ \theta | \exists x_c^* \text{ sbj. to } \begin{cases} \begin{bmatrix} F & G & H \end{bmatrix} \begin{bmatrix} x_c \\ \theta \\ x_d \end{bmatrix} \leq W \\ J(x_c^*) = \min_{x_c}(Ax_c + Bx_d) \end{cases} \right\} \tag{68}$$

Definition 5 The family of the admissible regions for x_c is defined by:

$$X_a(x_d) = \left\{ x_c | \exists \theta \text{ sbj. to } \begin{bmatrix} F & G & H \end{bmatrix} \begin{bmatrix} x_c \\ \theta \\ x_d \end{bmatrix} \leq W \right\} \tag{69}$$

Definition 6 The family of the optimal regions for x_c is a subset of the family $X_a(x_d)$:

$$X_a^*(x_d) = \left\{ x_c^* | \exists \theta \text{ sbj. to } \begin{cases} \begin{bmatrix} F & G & H \end{bmatrix} \begin{bmatrix} x_c \\ \theta \\ x_d \end{bmatrix} \leq W \\ J(x_c^* = \min_{x_c}(Ax_c + Bx_d) \end{cases} \right\} \tag{70}$$

Definition 7 The objective function represents the family of optimal regions $P^*(x_d)$ which was defined in 65. It is defined by $X_a^*(x_d)$ to $\Theta_a^*(x_d)$, which were defined in 70 and 68 respectively:

$$Z(x_c, x_d) : X_a^*(x_d) \mapsto \Theta_a^*(x_d) \tag{71}$$

Definition 8 The critical region $RC_m(x_d)$ is a subset of the space $P^*(x_d)$ where the local conditions of optimality for the optimization criterion remain immutable, i.e, that the function optimizer $Z_m(x_c, x_d) : X_a^*(x_d) \mapsto \Theta_a^*(x_d)$ is unique. $RC_m(xd)$ is determined by doing the union of different optimal regions $P^*(x_d)$ which has the same optimizer function.

The purpose of the linear multi-paramatric mixed-integer programming is to characterize the variables to optimize x_c, x_d and the objective function according to θ. The principle for solving the MP-MILP is summarized by two next steps:

- First step: search in the region of parameters θ the smallest sub-space of $\mathbb{P}$ which contains the optimal region $P^*(x_d)$. Then, determine the system of linear inequalities according to θ which defines $\mathbb{P}$.

- Second step: determine the set of all critical regions: the region $\mathbb{P}$ is divided into sub-spaces $RC_m(x_d) \in P^*(x_d)$. In the critical region $RC_m(x_d)$, the objective function $Z_m^*(x_c, x_d)$ remains a unique function. After determining the family of critical regions $RC_m(x_d)$, the piecewise affine functions of $Z_m^*(x_c, x_d)$ that characterize x_c, x_d according to θ is found. After refining the critical regions by grouping sub-spaces RC_m, we can get minimal facades which characterize the critical region.

7.4 Application to the home energy management problem

After having introduced multi-parametric programming, the purpose of this section is to adapt this method to the problem of energy management. As shown before, the problem of energy management in the building can be written as:

$$\begin{aligned} J &= (A_1.z + B_1.\delta + D_1) \\ A_2.z &+ B_2.\delta + C_2.x \le C \end{aligned} \tag{72}$$

where $z \in Z$ is the set of continuous variables and $\delta \in \Delta$ is the set of binary variables resulting from the logic transformation see section 4. Uncertainties can be modelled by intervals $\theta \in \Theta$. Assuming that the uncertainties are bounded, so

$$\underline{\theta} \le \theta \le \overline{\theta} \tag{73}$$

The family of solutions of the problem taking into account the uncertainties is generated by parametric programming. To illustrate this method, two examples are proposed.

Example 1. Consider a thermal service supported by an electric heater with a maximum power of 1.5 kW. T_a is the indoor temperature and T_m is the temperature of the building envelope with an initial temperatures $T_a(0) = 22$řC and $T_m(0) = 22$řC. A simplified thermal model of a room equipped with a window and a heater has been introduced in Eq. (3). The initial temperatures are set to $T_a(0) = 21°C$, $T_m(0) = 22°C$. The thermal model of the room after discretion with a sampling time equal to 1 hour is:

$$\begin{aligned} \begin{bmatrix} T_a(k+1) \\ T_m(k+1) \end{bmatrix} &= \begin{bmatrix} 0.364 & 0.6055 \\ 0.359 & 0.625 \end{bmatrix} \begin{bmatrix} T_a(k) \\ T_m(k) \end{bmatrix} \\ &+ \begin{bmatrix} 0.0275 & 1.1966 & 0.4193 \\ 0.016 & 0.7 & 0.2434 \end{bmatrix} \begin{bmatrix} T_{ext} \\ \phi_r \\ \phi_s \end{bmatrix} \end{aligned} \tag{74}$$

Supposing that the function of thermal satisfaction is written in the form:

$$U(k) = \delta_a(k).a_1.\frac{T_{opt} - T_a(k)}{T_{opt} - T_{\min}} + (1 - \delta_a(k)).a_2.\frac{T_{opt} - T_a(k)}{T_{opt} - T_{Max}} \tag{75}$$

where:

- $\delta_a(k)$: binary variable verifying $[\delta_a(k) = 1] \Leftrightarrow [T_a(k) \le T_{opt}], \forall k$

- T_{opt}: 'ideal' room's temperature for the user.

- $[T_{\min}, T_{Max}]$: the area of the value of room's temperature.

- a_1, a_2: are two constant that reflect the different between the sensations of cold or hot.

with $T_{opt} = 22°C$, $T_{min} = 20°C$, $T_{Max} = 24°C$ and $a_1 = a_2 = 1$.

It is assumed that there was not a precise estimate of the outdoor temperature T but it is possible to set that the outdoor temperature varies within a range: $[-5°C, +5°C]$. The average energy assigned to the heater over a period of 4 hours to minimize the objective function is:

$$J = \left(\sum_{k=1}^{4} U(k) \right) \tag{76}$$

The parametric programming takes into account uncertainties on the outdoor temperature. An implementation of multi-parametric solving may be done using a toolbox called Multi Parametric Toolbox MPT with the programming interface named YALMIP solver developed by Lofberg (2004). The resolution of the example 1 takes 3.31 seconds on using a computer Pentium IV 3.4 GHz. The average energy assigned to the heater according to the temperature outside is:

$$\phi_r(i) = \begin{cases} 1.5 \text{ if } -5 \leq T_{ext} \leq -0.875 \\ -0.097 \times T_{ext} + 1.415 \text{ if } -0.875 < T_{ext} \leq 5 \end{cases} \tag{77}$$

The parametric programming divided the uncertain region into two critical regions. The first region corresponds to the zone: $-5 \leq T_{ext} \leq -0.875$. The optimal solution is to put the heater to the maximum level in order to approach the desired temperature. In the second critical region, $-0.875 \leq T_{ext} \leq 5$, the energy assigned to the heater is proportional to the outdoor temperature. The higher the outside temperature is, the less energy is assigned to the radiator. In fact, $T_{ext} = -0.875$ is the point of the system where the maximum power generated by the radiator can compensate the thermal flow lost through the building envelope.

Example 2. This example is based on example 1 but with additional uncertainties on sources. In this example, the disturbance caused by the user have been simulated. It is assumed that in the 3rd and 4th periods of the resource assignment plan, it is likely that a consumption may occur. Accordingly, the available energy during the periods 3 and 4 is between 0 and 2kWh. A parametric variable $E_{max} \in [0, 2]$ and a constraint are added as follows:

$$\phi_r(3) + \phi_r(4) \leq E_{max} \tag{78}$$

The optimal solution of the problem must be computed based on two variables $[T_{ext}, E_{max}]$. This example has still been solved using the MPT tool. This time, the solver takes 5.2 seconds. The average energy assigned for the period 1, $\phi_r(1)$, is independent of the variable E_{max}. It means that whatever happens on the energy available during periods 3 and 4, the decision to the period 1 can not improve the situation:

$$\phi_r(1) = \begin{cases} 1.5 \text{ if } \begin{bmatrix} -5 \leq T_{ext} \leq -0.875 \\ 0 \leq E_{max} \leq 2 \end{bmatrix} \\ -0.097 \times T_{ext} + 1,415 \text{ if } \begin{bmatrix} -0.875 < T_{ext} \leq 5 \\ 0 \leq E_{max} \leq 2 \end{bmatrix} \end{cases} \tag{79}$$

The energy assigned to the heater in the second period $\phi_r(2)$ is a piecewise function which consists of five different critical areas. Among these five regions (fig.9), we see that the optimal solution assigns the maximum energy to the heater in three regions. By anticipating the availability of resources in periods 3 and 4, the comfort is improved in the heating zone. This result corresponds to the conclusion found in Ha et al. (2006a). During periods 3 and 4, the
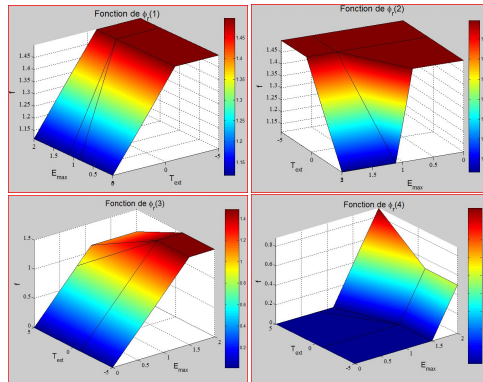
Fig. 9. Piecewise function of $\phi_r(k)$ following $[T_{ext}, E_{max}]$

consumption of radiator is less important than for the periods 1 and 2. A robust solution is obtained despite the disturbance of the resource and the outside temperature. However, in the critical region 5 (Fig.9), there is an extreme case in which it is very cold outside and there is simultaneously a large disturbance on the availability of the resource. The only solution is to put $\phi_r(k)$ to the maximum value although there is a deterioration in the comfort of user.

After generating the family of solutions at step 1, an effective solution must be chosen during step 2. Knowing that the optimal solutions of step 1 are piecewise functions limited by critical regions, therefore the procedure of selecting a solution now is to select a piecewise function. The area of research is therefore reduced and the algorithm of step 2 requires few computations. A min-max approach is used to find a robust solution among the family of solutions. A polynomial algorithm that comes in the different critical regions to find a solution that optimizes the criterion is used:

$$J^* = (Max(J(\theta))|\theta \in \mathcal{P}^*) \tag{80}$$

8. Conclusion

This chapter presents a formulation of the global home electricity management problem, which consists in adjusting the electric energy consumption/production for habitations. A service oriented point of view has been justified: housing can be seen as a set of services. A 3-layer control mechanism has been presented. The chapter focuses on the anticipative layer, which computes optimal plannings to control appliances according to inhabitant request and weather forecasts. These plannings are computed using service models that include behavioral, comfort and cost models.

The computation of the optimal plannings has been formulated as a mixed integer linear programming problem thanks to a linearization of nonlinear models. A method to decompose the whole problem into sub-problems has been presented. Then, an illustrative application example has been presented. Computation times are acceptable for small problems but it increases up to more than 24h for an example with 91 binary variables and 1792 continuous ones. Heuristics has to be developed to reduce the computation time required to get a good solution.

Even if uncertainties can be managed by the reactive layer, an approach that takes into account uncertainties model by intervals from the anticipative step has been presented. It is an adaptation of the multi-parametric programming. It leads to robust anticipative plans. But this approach is useful of biggest uncertainties because it is difficult to apprehend a large number of uncertainties because of the induced complexities.

9. References

Abras, S., Ploix, S., Pesty, S. & Jacomino, M. (2006). A multi-agent home automation system for power management, *The 3rd International Conference on Informatics in Control, Automation and Robotics*, Setubal, Portugal.

AFNOR (2006). Ergonomie des amniances thermiques , détermination analytique et interprétation du confort thermique par le calcul des indices PMV et PDD et par des critère de confort thermique local, *Norme européenne, norme française* .

Angioletti, R. & Despretz, H. (2003). Maîtrise de l'énergie dans les bâtiments -techniques, *Techniques de l'ingénieurs* .

Aubry, A., Rossi, A., Espinouse, M.-L. & Jacomino, M. (2006). Minimizing setup costs for parallel multi-purpose machines under load-balancing constraint, *European Journal of Operational Research, in press, doi:10.1016/j.ejor.2006.05.050* .

Bemporad, A. & Morari, M. (1998). Control of systems integrating logic, dynamics and constraints, *Automatica* **35**: 407–427.

Billaut, J.-C., Moukrim, A. & Sanlaville, E. (2005a). *Flexibilité et Robustesse en Ordonnancement*, Hermès Science, Paris, France.

Billaut, J.-C., Moukrim, A. & Sanlaville, E. (2005b). *Flexibilité et Robustesse en Ordonnancement*, Hermès Science, Paris, France, chapter 1.

Borrelli, F. (2002). *Discrete Time Constrained Optimal Control*, PhD thesis, Swiss Federal Institute of technilogy (EHT) Zurich.

Borrelli, F., Bemporat, A. & Morari, M. (2000). A geometric algorithme for multi-parametric linear programming, *Technical report*, Automatic Control Laboratory ETH Zurich, Switzerland.

Castro, P. M. & Grossmann, I. E. (2006). An efficient mipl model for the short-term scheduling of single stage batch plants, *Computers and Chemical Engineering* **30**: 1003–1018.

Diestel, R. (2005). *Graph Theory Third Edition*, Springer Verlag, Heidelberg.

Dubois, D., Fargier, H. & Fortemps, P. (2003). Fuzzy scheduling: Modeling flexible constraints vs. coping with incomplete knowledge, *Euroupean Journal of Operational Research* **147**: 231–252.

Dubois, D., Fortemps, P., Pirlot, M. & Prade, H. (2001). Leximin optimality and fuzzy set-theoretic operations, *European Journal of Operational Research* **130**: 20–28.

Duy Ha, L. (2007). *Un système avancé de gestion d'énergie dans le bâtiment pour coordonner production et consommation*, PhD thesis, Grenoble Institute of Technology, Grenoble, France.

Esquirol, P. & Lopez, P. (1999). *L'Ordonnancement*, Economica, chapter 5 Ordonnancement sous contraintes de ressources cummulatives, p. 87.

Gal, T. & J.Nedoma (1972). Multiparametric linear programming, *Management Science* **18**: 406–442.

Gass, S. & Saaty, T. (1955). The computatinal alogorithm for the parametric objective function, *Naval Reseach Logistices Quarterly* **2**: 39–45.

Greenberg, H. & Woodruf, D. (1998). *Advances in Computational and Stochastic Optimization, Logic Programming and Heuristic Search: Interfaces in Computer Science and Operations Research*, Kluwer Academic Publishers, Norwell, MA, USA, chapter 4.

Ha, D. L., Ploix, S., Zamai, E. & Jacomino, M. (2006a). A home automation system to improve the household energy control, *INCOM2006 12th IFAC Symposium on Information Control Problems in Manufacturing*.

Ha, D. L., Ploix, S., Zamai, E. & Jacomino, M. (2006b). Tabu search for the optimization of household energy consumption, *The 2006 IEEE International Conference on Information Reuse and Integration IEEE IRI 2006: Heuristic Systems Engineering September 16-18, 2006, Waikoloa, Hawaii, USA*.

Henze, G. P. & Dodier, R. H. (2003). Adaptive optimal control of a grid-independent photovoltaic system, *Transactions of the ASME* **125**: 34–42.

House, J. M. & Smith, T. F. (1995). Optimal control of building and hvac systems, *Proceddings of the American Control Conference, Seattle, Washington*.

ILOG (2006). CPLEX tutorial handout, *Technical report*, ILOG.

Lawler, E. & Wood, D. (1966). Branch-and-bound methods: a survey, *Operations Research* **14**: 699–719.

Lofberg, J. (2004). YALMIP : A toolbox for modeling and optimization in MATLAB, *Proceedings of the CACSD Conference*, Taipei, Taiwan. Available from `http://control.ee.ethz.ch/~joloef/yalmip.php`.

Madsen, H. (1995). Estimation of continuous-time models for the heat dynamics of a building, *Energy and Building* .

Makhorin, A. (2006). GNU linear programming kit reference manual version 4.11, *Technical report*, GNU Project.

Muselli, M., Notton, G., Poggi, P. & Louche, A. (2000). Pv-hybrid power system sizing incorporating battery storage: an analysis via simulation calculations, *Renewable Energy* **20**: 1–7.

Nathan, M. (2001). Building thermal performance analysis by using matlab/simulink, *Seventh International IBPSA Conference*, Rio de Janeiro, Brazil.

Palensky, P. & Posta, R. (1997). Demand side management in private home using lonworks, *Proceedings.1997 IEEE International Workshop on Factory Communication Systems*.

Pinto, J. M. & Grossmann, I. (1995). A continuous time mixed integer linear programming model for short term scheduling of multistage batch plants, *Industrial and Engineering Chemistry Research* **35**: 338–342.

Pinto, J. M. & Grossmann, I. E. (1998). Assignment and sequencing models for the scheduling of process systems, *Annals of Operations Research* **81**: 433–466.

Rossi, A. (2003). *Ordonnancement en milieu incertain, mise en oeuvre d'une démarche robuste*, PhD thesis, Ecole Doctorale EEATS " Electronique, Electrotechnique, Automatique & Traitement du Signal", INPGrenoble.

Wacks, K. (1993). The impact of home automation on power electronics, *Applied Power Electronics Conference and Exposition*, pp. 3 – 9.

Williams, H. P. (1993). *Model building in mathematical programming*, New York: Wiley.

Zhou, G. & Krarti, M. (2005). Parametric analysis of active and passive building thermal storage utilization, *Journal of Solar Energy Engineering* **127**: 37–46.

Passivity-Based Control and Sliding Mode Control applied to Electric Vehicles based on Fuel Cells, Supercapacitors and Batteries on the DC Link

M. Becherif[1,2], M. Y. Ayad[1], A. Henni[3], M. Wack[1], A. Aboubou[4],
A. Allag[4] and M. Sebaï[4]

[1] *SeT Laboratory, UTBM University, France*
[2] *FC-Lab fuel Cell Laboratory, UTBM University, France*
[3] *Alstom Power System, Energy Management Business, France*
[4] *LMSE Laboratory, Biskra University, Algeria*

1. Introduction

Fuel Cells (FC) produce electrical energy from an electrochemical reaction between a hydrogen-rich fuel gas and an oxidant (air or oxygen) (Kishinevsky & Zelingher, 2003) (Larminie & Dicks, 2000). They are high-current, and low-voltage sources. Their use in embedded systems becomes more interesting when using storage energy elements, like batteries, with high specific energy, and supercapacitors (SC), with high specific power. In embedded systems, the permanent source which can either be FC's or batteries must produce the limited permanent energy to ensure the system autonomy (Pischinger et al., 2006) (Moore et al., 2006) (Corrêa et al., 2003). In the transient phase, the storage devices produce the lacking power (to compensate for deficit in power required) in acceleration function, and absorbs excess power in braking function. FC's, and due to its auxiliaries, have a large time constant (several seconds) to respond to an increase or decrease in power output. The SCs are sized for the peak load requirements and are used for short duration load levelling events such as fuel starting, acceleration and braking (Rufer et al, 2004) (Thounthong et al., 2007). These short durations, events are experienced thousands of times throughout the life of the hybrid source, require relatively little energy but substantial power (Granovskii et al.,2006) (Benziger et al., 2006).

Three operating modes are defined in order to manage energy exchanges between the different power sources. In the first mode, the main source supplies energy to the storage device. In the second mode, the primary and secondary sources are required to supply energy to the load. In the third, the load supplies energy to the storage device.

In this work, we present a new concept of a hybrid DC power source using SC's as auxiliary storage device, a Proton Exchange Membrane Fuel Cell (PEMFC) as the main energy source. The source is also composed of batteries on a DC link. The general structure of the studied system is presented and a dynamic model of the overall system is given. Two control

techniques are presented. The first is based on passivity based control (PBC) (Ortega et al. 2002). The system is written in a Port Controlled Hamiltonian (PCH) form where important structural properties are exhibited (Becherif et al., 2005). Then a PBC of the system is presented which proves the global stability of the equilibrium with the proposed control laws. The second is based on nonlinear sliding mode control for the DC-DC supercapacitors converter and a linear regulation for the FC converter (Ayad et al. 2007). Finally, simulation results using Matlab are given

2. State of the art and potential application
2.1. Fuel Cells
A. Principle
The developments leading to an operational FC can be traced back to the early 1800's with Sir William Grove recognized as the discoverer in 1839.

A FC is an energy conversion device that converts the chemical energy of a fuel directly into electricity. Energy is released whenever a fuel (hydrogen) reacts chemically with the oxygen of air. The reaction occurs electrochemically and the energy is released as a combination of low-voltage DC electrical energy and heat.

Types of FCs differ principally by the type of electrolyte they utilize (Fig. 1). The type of electrolyte, which is a substance that conducts ions, determines the operating temperature, which varies widely between types.
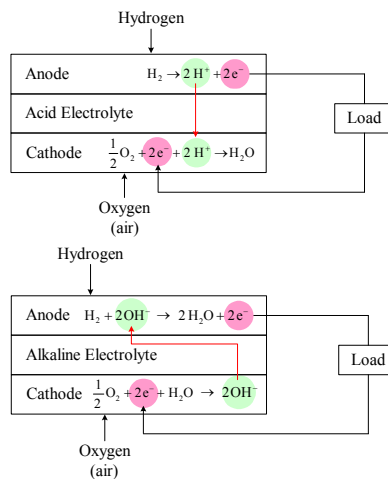

Fig. 1. Principle of acid (top) and alkaline (bottom) electrolytes fuel cells

Proton Exchange Membrane (or "solid polymer") Fuel Cells (PEMFCs) are presently the most promising type of FCs for automotive use and have been used in the majority of prototypes built to date.

The structure of a cell is represented in Fig. 2. The gases flowing along the x direction come from channels designed in the bipolar plates (thickness 1-10 mm). Vapour water is added to the gases to humidify the membrane. The diffusion layers (100-500 μm) ensure a good distribution of the gases to the reaction layers (5-50 μm). These layers constitute the

electrodes of the cell made of platinum particles, which play the role of catalyst, deposited within a carbon support on the membrane.
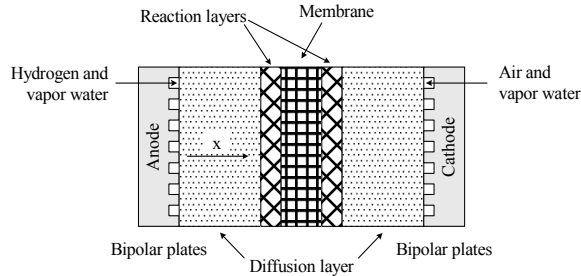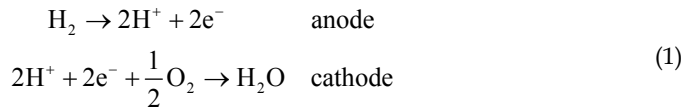

Fig. 2. Different layers of an elementary cell

Hydrogen oxidation and oxygen reduction:

$$H_2 \rightarrow 2H^+ + 2e^- \qquad \text{anode}$$

$$2H^+ + 2e^- + \frac{1}{2}O_2 \rightarrow H_2O \quad \text{cathode} \qquad (1)$$

The two electrodes are separated by the membrane (20-200 μm) which carries protons from the anode to the cathode and is impermeable to electrons. This flow of protons drags water molecules as a gradient of humidity leads to the diffusion of water according to the local humidity of the membrane. Water molecules can then go in both directions inside the membrane according to the side where the gases are humidified and to the current density which is directly linked to the proton flow through the membrane and to the water produced on the cathode side.

Electrons which appear on the anode side cannot cross the membrane and are used in the external circuit before returning to the cathode. Proton flow is directly linked to the current density:

$$J_{H^+} = \frac{i}{F} \qquad (2)$$

where F is the Faraday's constant.
The value of the output voltage of the cell is given by Gibb's free energy ΔG and is:

$$V_{rev} = -\frac{\Delta G}{2.F} \qquad (3)$$

This theoretical value is never reached, even at no load condition. For the rated current (around 0.5 A.cm^{-2}), the voltage of an elementary cell is about 0.6-0.7 V.
As the gases are supplied in excess to ensure a good operating of the cell, the non-consumed gases have to leave the FC, carrying with them the produced water.
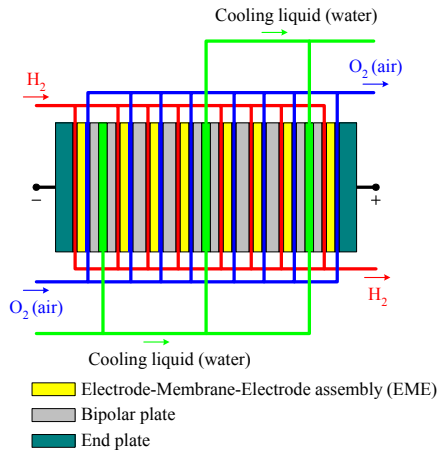
Fig. 3. External and internal connections of a PEMFC stack

Generally, a water circuit is used to impose the operating temperature of the FC (around 60-70 °C). At start up, the FC is warmed and later cooled as at the rated current nearly the same amount of energy is produced under heat form than under electrical form.

B. Modeling Fuel Cell

The output voltage of a single cell V_{FC} can be defined as the result of the following static and nonlinear expression (Larminie & Dicks, 2000):

$$V_{FC} = E - V_{act} - V_{ohm} - V_{concent} \tag{4}$$

where E is the thermodynamic potential of the cell and it represents its reversible voltage, V_{act} is the voltage drop due to the activation of the anode and of the cathode, V_{ohm} is the ohmic voltage drop, a measure of the ohmic voltage drop associated with the conduction of the protons through the solid electrolyte and electrons through the internal electronic resistances, and $V_{concent}$ represents the voltage drop resulting from the concentration or mass transportation of the reacting gases.
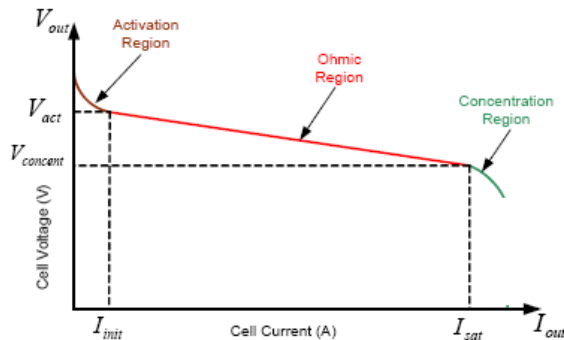

Fig. 4. A typical polarization curve for a PEMFC

In (4), the first term represents the FC open circuit voltage, while the three last terms represent reductions in this voltage to supply the useful voltage of the cell V_{FC}, for a certain operating condition. Each one of the terms can be calculated by the following equations,

$$V_{act} = A \log\left(\frac{i_{FC} - i_n}{i_0}\right)$$

$$V_{ohm} = R_m (i_{FC} - i_n) \tag{5}$$

$$V_{concent} = b \log\left(1 - \frac{i_{FC} - i_n}{i_{lim}}\right)$$

Hence, i_{FC} is the delivered current, i_0 is the exchange current, A is the slope of the Tafel line, i_{Lim} is the limiting current, B is the constant in the mass transfer, i_n is the internal current and R_m is the membrane and contact resistances.

2.2. Electric Double-layer supercapacitors
A. Principle
The basic principle of electric double-layer capacitors lies in capacitive properties of the interface between a solid electronic conductor and a liquid ionic conductor. These properties discovered by Helmholtz in 1853 lead to the possibility to store energy at solid/liquid interface. This effect is called electric double-layer, and its thickness is limited to some nanometers (Belhachemi et al., 2000).
Energy storage is of electrostatic origin, and not of electrochemical origin as in the case of accumulators. So, supercapacitors are therefore capacities, for most of marketed devices. This gives them a potentially high specific power, which is typically only one order of magnitude lower than that of classical electrolytic capacitors.
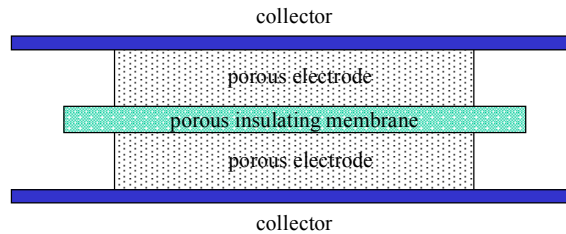

Fig. 5. Principle of assembly of the supercapacitors

In SCs, the dielectric function is performed by the electric double-layer, which is constituted of solvent molecules. They are different from the classical electrolytic capacitors mainly because they have a high surface capacitance (10-30 $\mu F.cm^{-2}$) and a low rated voltage limited by solvent decomposition (2.5 V for organic solvent). Therefore, to take advantage of electric double-layer potentialities, it is necessary to increase the contact surface area between electrode and electrolyte, without increasing the total volume of the whole.

The most widespread technology is based on activated carbons to obtain porous electrodes with high specific surface areas (1000-3000 $m^2.g^{-1}$). This allows obtaining several hundred of farads by using an elementary cell.

SCs are then constituted, as schematically presented below in Fig. 5, of:
   - two porous carbon electrodes impregnated with electrolyte,
   - a porous insulating membrane, ensuring electronic insulation and ionic conduction between electrodes,
   - metallic collectors, usually in aluminium.

B. Modeling and sizing of suparcpacitors

Many applications require that capacitors be connected together, in series and/or parallel combinations, to form a "bank" with a specific voltage and capacitance rating. The most critical parameter for all capacitors is voltage rating. So they must be protected from over voltage conditions. The realities of manufacturing result in minor variations from cell to cell. Variations in capacitance and leakage current, both on initial manufacture and over the life of the product, affect the voltage distribution. Capacitance variations affect the voltage distribution during cycling, and voltage distribution during sustained operation at a fixed voltage is influenced by leakage current variations. For this reason, an active voltage balancing circuit is employed to regulate the cell voltage.

It is common to choose a specific voltage and thus calculating the required capacitance. In analyzing any application, one first needs to determine the following system variables affecting the choice of SC,

-the maximum voltage, V_{SCMAX}

-the working (nominal) voltage, V_{SCNOM}

-the minimum allowable voltage, V_{SCMIN}

-the current requirement, I_{SC}, or the power requirement, P_{SC}

-the time of discharge, t_d

-the time constant

-the capacitance per cell, C_{SCcell}

-the cell voltage, V_{SCcell}

-the number of cell needs, n

To predict the behavior of SC voltage and current during transient state, physics-based dynamic models (a very complex charge/discharge characteristic having multiple time constants) are needed to account for the time constant due to the double-layer effects in SC. The reduced order model for a SC cell is represented in Fig. 6. It is comprised of four ideal circuit elements: a capacitor C_{SCcell}, a series resistor R_S called the equivalent series resistance (ESR), a parallel resistor R_P and a series stray inductor L of ~nH. The parallel resistor R_P models the leakage current found in all capacitors.

This leakage current varies starting from a few milliamps in a big SC under a constant current as shown in Fig. 7.

A constant discharging current is particularly useful when determining the parameters of the SC.

Nevertheless, Fig. 7 should not be used to consider sizing SCs for constant power applications, such as common power profile used in hybrid source.
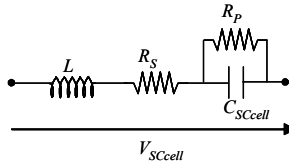
Fig. 6. Simple model of a supercapacitor cell

To estimate the minimum capacitance C_{SCMIN}, one can write an energy equation without losses (R_{ESR} neglected) as,

$$\frac{1}{2}C_{SCMIN}\left(V_{SCNOM}^2 - V_{SCMIN}^2\right) = P_{SC}t \qquad (6)$$

with

$$P_{SC}(t) = V_{SC}(t)i_{SC}(t) \qquad (7)$$

Then,

$$C_{SCMIN} = \frac{2P_{SC}t_d}{V_{SCNOM}^2 - V_{SCMIN}^2} \qquad (8)$$

From (6) and (7), the instantaneous capacitor voltage and current are described as,

$$\begin{cases} V_{SC}(t) = V_{SCNOM}\sqrt{1 - \left(1 - \left(\frac{V_{SCNOM}}{V_{SCMIN}}\right)^2\right)\frac{t}{t_d}} \\[4mm] i_{SC}(t) = \dfrac{P_{SC}}{\sqrt{1 - \left(1 - \left(\frac{V_{SCNOM}}{V_{SCMIN}}\right)^2\right)\frac{t}{t_d}}} \end{cases} \qquad (9)$$

Since the power being delivered is constant, the minimum voltage and maximum current can be determined based on the current conducting capabilities of the SC. (6) and (7) can then be rewritten as,

$$\begin{cases} V_{SCMIN} = \sqrt{V_{SCNOM}^2 - \dfrac{2P_{SC}t_d}{C_{MIN}}} \\[4mm] I_{SCMIN} = \dfrac{P_{SC}}{\sqrt{V_{SCNOM}^2 - \dfrac{2P_{SC}t_d}{C_{MIN}}}} \end{cases} \qquad (10)$$
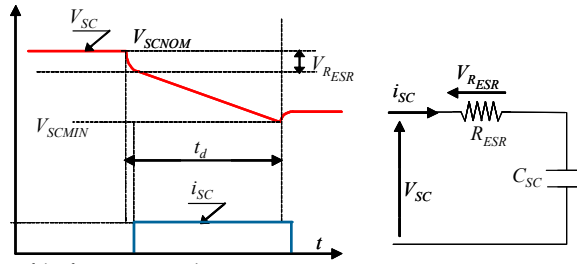
Fig. 7. Discharge profile for a SC under constant current.

The variables V_{SCMAX} and C_{SC} are indeed related by the number of cells n. The assumption is that the capacitors will never be charged above the combined maximum voltage rating of all the cells. Thus, we can introduce this relationship with the following equations,

$$\begin{cases} V_{SCMAX} = nV_{SCcell} \\ C_{SC} = \dfrac{C_{SCcell}}{n} \end{cases} \tag{11}$$

Generally, V_{SCMIN} is chosen as $V_{SCMAX}/2$, from (6), resulting in 75% of the energy being utilized from the full-of-charge (SOC^1 = 100%). In applications where high currents are drawn, the effect of the R_{ESR} has to be taken into account. The energy dissipated W_{loss} in the R_{ESR}, as well as in the cabling, and connectors could result in an under-sizing of the number of capacitors required. For this reason, knowing SC current from (6), one can theoretically calculate these losses as,

$$W_{loss} = \int_0^{t_d} i_C^2(\tau) R_{ESR} d\tau = P_{SC} R_{ESR} C_{MIN} \ln\left(\frac{V_{SCNOM}}{V_{SCMIN}}\right) \tag{12}$$

To calculate the required capacitance C_{SC}, one can rewrite (6) as,

$$\frac{1}{2} C_{SCMIN}\left(V_{SCMAX}^2 - V_{SCMIN}^2\right) = P_{SC}t + W_{loss} \tag{13}$$

From (6) and (13), one obtains

$$\begin{cases} C_{SC} = C_{SCMIN}(1 + X) \\ X = \dfrac{W_{loss}}{P_{SC}t} \end{cases} \tag{14}$$

where X is the energy ratio.
From the equations above, an iterative method is needed in order to get the desired optimum value.

---

[1] State Of Charge

C. State of the art and potential application

Developed at the end of the seventies for signal applications (for memory back-up for example), SCs had at that time a capacitance of some farads and a specific energy of about 0.5 Wh.kg^{-1}.
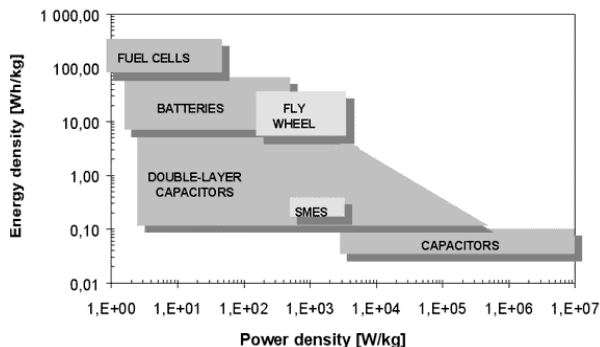

Fig. 8. Comparison between capacitors, supercapacitors, batteries and Fuel cell

High power SCs appear during the nineties and bring high power applications components with capacitance of thousand of farads and specific energy and power of several Wh.kg^{-1} and kW.kg^{-1}.

In the energy-power plan, electric double layers SCs are situated between accumulators and traditional capacitors.

Then these components can carry out two main functions:

- the function "source of energy", where SCs replace electrochemical accumulators, the main interest being an increase in reliability,

- the function "source of power", for which SCs come in complement with accumulators (or any other source limited in power), for a decrease in volume and weight of the whole system.

2.3. State of the art of battery in electric vehicles

An electric vehicle (EV) is a vehicle that runs on electricity, unlike the conventional vehicles on road today which are major consumers of fossil fuels like gasoline. This electricity can be either produced outside the vehicle and stored in a battery or produced on board with the help of FC's.

The development of EV's started as early as 1830's when the first electric carriage was invented by Robert Andersen of Scotland, which appears to be appalling, as it even precedes the invention of the internal combustion engine (ICE) based on gasoline or diesel which is prevalent today. The development of EV's was discontinued as they were not very convenient and efficient to use as they were very heavy and took a long time to recharge.

This led to the development of gasoline based vehicles as the one pound of gasoline gave equal energy as a hundred pounds of batteries and it was relatively much easier to refuel and use gazoline. However, we today face a rapid depletion of fossil fuel and a major concern over the noxious green house gases their combustion releases into the atmosphere causing long term global crisis like climatic changes and global warming. These concerns

are shifting the focus back to development of automotive vehicles which use alternative fuels for operations. The development of such vehicles has become imperative not only for the scientists but also for the governments around the globe as can be substantiated by the Kyoto Protocol which has a total of 183 countries ratifying it (As on January 2009).

A. Batteries technologies

A battery is a device which converts chemical energy directly into electricity. It is an electrochemical galvanic cell or a combination of such cells which is capable of storing chemical energy. The first battery was invented by Alessandro Volta in the form of a voltaic pile in the 1800's. Batteries can be classified as primary batteries, which once used, cannot be recharged again, and secondary batteries, which can be subjected to repeated use as they are capable of recharging by providing external electric current. Secondary batteries are more desirable for the use in vehicles, and in particular traction batteries are most commonly used by EV manufacturers. Traction batteries include Lead Acid type, Nickel and Cadmium, Lithium ion/polymer , Sodium and Nickel Chloride, Nickel and Zinc.

	Lead Acid	Ni - Cd	Ni - MH	Li – Ion	Li - polymer	Na - NiCl$_2$	Objectives
Specific Energy (Wh/Kg)	35 – 40	55	70 – 90	125	155	80	200
Specific Power (W/Kg)	80	120	200	260	315	145	400
Energy Density (Wh/m^3)	25 – 35	90	90	200	165	130	300
Cycle Life (No. of charging cycles)	300	1000	600	+ 600	+ 600	600	1000

Table 1. Comparison between different baterries technologies.

The battery for electrical vehicles should ideally provide a high autonomy (i.e. the distance covered by the vehicle for one complete discharge of the battery starting from its potential) to the vehicle and have a high specific energy, specific power and energy density (i.e. light weight, compact and capable of storing and supplying high amounts of energy and power respectively). These batteries should also have a long life cycle (i.e. they should be able to discharge to as near as it can be to being empty and recharge to full potential as many number of times as possible) without showing any significant deterioration in the performance and should recharge in minimum possible time. They should be able to operate over a considerable range of temperature and should be safe to handle, recyclable with low costs. Some of the commonly used batteries and their properties are summarized in the Table 1.

B. Principle

A battery consists of one or more voltaic cell, each voltaic cell consists of two half-cells which are connected in series by a conductive electrolyte containing anions (negatively charged ions) and cations (positively charged ions). Each half-cell includes the electrolyte and an electrode (anode or cathode). The electrode to which the anions migrate is called the anode and the electrode to which cations migrate is called the cathode. The electrolyte connecting these electrodes can be either a liquid or a solid allowing the mobility of ions.

In the redox reaction that powers the battery, reduction (addition of electrons) occurs to cations at the cathode, while oxidation (removal of electrons) occurs to anions at the anode. Many cells use two half-cells with different electrolytes. In that case each half-cell is enclosed in a container, and a separator that is porous to ions but not the bulk of the electrolytes prevents mixing. The figure 10 shows the structure of the structure of Lithium–Ion battery using a separator to differentiate between compartments of the same cell utilizing two respectively different electrolytes

Each half cell has an electromotive force (or emf), determined by its ability to drive electric current from the interior to the exterior of the cell. The net emf of the battery is the difference between the emfs of its half-cells. Thus, if the electrodes have emfs E_1 and E_2, then the net emf is $E_{cell} = E_2 - E_1$. Therefore, the net emf is the difference between the reduction potentials of the half-cell reactions.

The electrical driving force or ΔV_{Bat} across the terminals of a battery is known as the terminal voltage and is measured in volts. The terminal voltage of a battery that is neither charging nor discharging is called the open circuit voltage and equals the emf of the battery.

An ideal battery has negligible internal resistance, so it would maintain a constant terminal voltage until exhausted, then dropping to zero. If such a battery maintained 1.5 volts and stored a charge of one Coulomb then on complete discharge it would perform 1.5 Joule of work.

$$\text{Work done by battery (W)} = - \text{Charge X Potential Difference} \tag{15}$$

$$Charge = \frac{Coulomb}{Mole \quad Electrons} Moles \quad Electrons \tag{16}$$

$$W = -nFEcell \tag{17}$$

Where n is the number of moles of electrons taking part in redox, $F = 96485$ coulomb/mole is the Faraday's constant i.e. the charge carried by one mole of electrons.

The open circuit voltage, E_{cell} can be assumed to be equal to the maximum voltage that can be maintained across the battery terminals. This leads us to equating this work done to the Gibb's free energy of the system (which is the maximum work that can be done by the system)
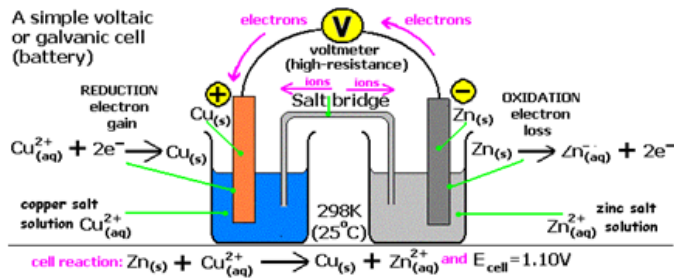
$$\Delta G = W \max = -nFEcell \tag{18}$$

Fig. 9. Showing the apparatus and reactions for a simple galvanic Electrochemical Cell
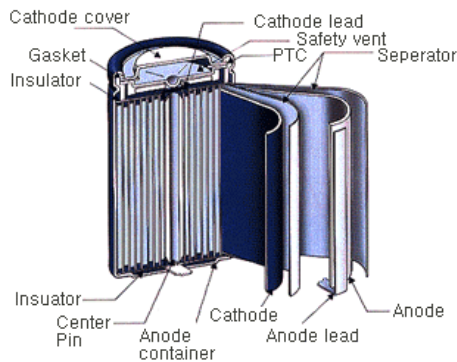

Fig. 10. Structure of Lithium-Ion Battery

C. Model of Battery

Non Idealities in Batteries: Electrochemical batteries are of great importance in many electrical systems because the chemical energy stored inside them can be converted into electrical energy and delivered to electrical systems, whenever and wherever energy is needed. A battery cell is characterized by the open-circuit potential (V_{OC}), i.e. the initial potential of a fully charged cell under no-load conditions, and the cut-off potential (V_{cut}) at which the cell is considered discharged. The electrical current obtained from a cell results from electrochemical reactions occurring at the electrode-electrolyte interface. There are two important effects which make battery performance more sensitive to the discharge profile:

- Rate Capacity Effect: At zero current, the concentration of active species in the cell is uniform at the electrode-electrolyte interface. As the current density increases the concentration deviates from the concentration exhibited at zero current and state of charge as well as voltage decrease (Rao et al., 2005)

- Recovery Effect: If the cell is allowed to relax intermittently while discharging, the voltage gets replenished due to the diffusion of active species thereby giving it more life (Rao et al., 2005)

D. Equivalent Electrical Circuit of Battery

Many electrical equivalent circuits of battery are found in literature. (Chen at al., 2006) presents an overview of some much utilized circuits to model the steady and transient behavior of a battery. The Thevenin's circuit is one of the most basic circuits used to study the transient behavior of battery is shown in figure 11.
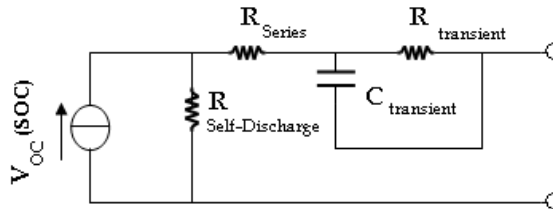

Fig. 11. Thevenin's model

It uses a series resistor (R_{series}) and an RC parallel network ($R_{transient}$ and $C_{transient}$) to predict the response of the battery to transient load events at a particular state of charge by assuming a constant open circuit voltage [V_{oc}(SOC)] is maintained. This assumption unfortunately does not help us analyze the steady-state as well as runtime variations in the battery voltage. The improvements in this model are done by adding more components in this circuit to predict the steady-state and runtime response. For example, (Salameh at al., 1992) uses a variable capacitor instead of V_{oc} (SOC) to represent nonlinear open circuit voltage and SOC, which complicates the capacitor parameter.
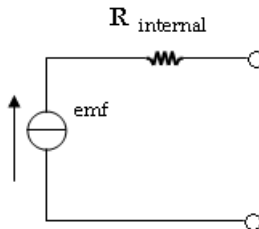

Fig. 12. Circuit showing battery emf and internal resistance $R_{internal}$

However, in our study we are mainly concerned with the recharging of this battery which occurs while breaking. The SC coupled with the battery accumulates high amount of charge when breaks are applied and this charge is then utilized to recharge the battery. Therefore, the design of the battery is kept to a simple linear model which takes into account the internal resistance ($R_{internal}$) of the battery and assumes the emf to be constant throughout the process (Figure. 12).

3. Control of the Electric Vehicles based on FC, SCs and Batteries on the DC Link

3.1 Structure of the hybrid source

As shown in Fig. 13 the studied system comprises a DC link directly supplied by batteries, a PEMFC connected to the DC link by means of a Boost converter, and a supercapacitive storage device connected to the DC link through a current reversible DC-DC converter. The function of FC and the batteries is to supply mean power to the load, whereas the storage device is used as a power source: it manages load power peaks during acceleration and braking.

The aim is to have a constant DC voltage and the challenge is to maintain a constant power working mode for the main sources (batteries and FC).

3.2. Problem formulation

The main objectives of the proposed study are:

- To compare two control techniques of the hybrid source by controlling the two DC-DC converters. The first is based on passivity control by using voltage control (on FC and current control for SC), and the second is based on sliding mode control by using current controller.

- To maintain a constant mean energy delivered by the FC, without a significant power peak, and to ensure the transient power is supplied by the SCs.

- To recover energy through the charge of the SC.

After system modelling, equilibrium points are computed in order to ensure the desired behaviour of the system. When steady state is reached, the load has to be supplied only by the FC source. So the controller has to maintain the DC bus voltage to a constant value and the SCs current has to be cancelled. During transient, the power delivered by the DC source has to be the more constant as possible (without a significant power peak), so the SCs deliver the transient power to the load. If the load provides current, the SCs recover its energy.

At equilibrium, the SC has to be charged and the current has to be equal to zero.
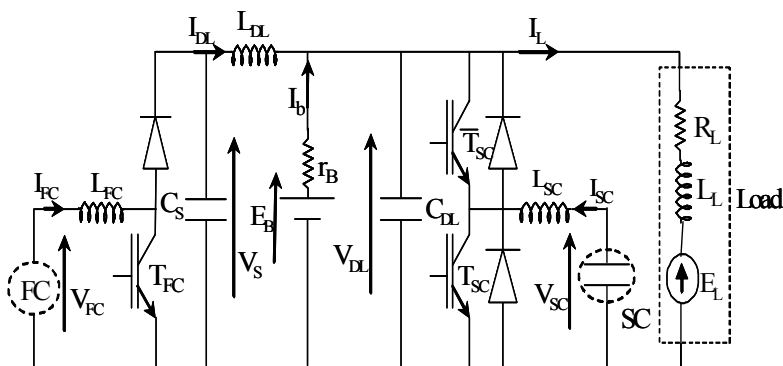

Fig. 13. Structure of the hybrid source

3.3 Port Controlled Hamiltonian System

PCH systems were introduced by van der Schaft and Maschke in the early nineties, and have since grown to become a large field of interest in the research of electrical, mechanical and electro-mechanical systems. A recent and very interesting approach in PBC is the Interconnection and Damping Assignment (IDA-PBC) method, which is a general way of stabilizing a large class of physical systems) (Ortega et al. 2002) (Becherif et al., 2005).

A. Equations of the system

The overall model of the hybrid system is written in a state space equation by choosing the following state space vector:

$$
\begin{aligned}
x &= \begin{bmatrix} x_1 & x_2 & x_3 & x_4 & x_5 & x_6 & x_7 \end{bmatrix}^T \\
&= \begin{bmatrix} V_S & I_{FC} & V_{DL} & I_{DL} & V_{SC} & I_{SC} & I_L \end{bmatrix}^T
\end{aligned}
\tag{19}
$$

The output voltage of a single cell V_{FC} can be defined as the result of the following expression:

$$
V_{FC} = E_0 - A \log\left(\frac{i_{FC} - i_n}{i_0} \right) - \left\{ R_m (i_{FC} - i_n) + B \log\left(1 - \frac{i_{FC} - i_n}{i_{Lim}} \right) \right\}
\tag{20}
$$

where E is the thermodynamic potential of the cell representing its reversible voltage, i_{FC} is the delivered current, i_o is the exchange current, A is the slope of the Tafel line, i_{Lim} is the limiting current, B is the constant in the mass transfer, i_n is the internal current and R_m is the membrane and contact resistances. Hence $V_{FC} = f(i_{FC})$.

The fourth term represents the voltage drop resulting from the concentration or mass transportation of the reacting gases.

In equation (20), the first term represents the FC open circuit voltage, while the three last terms represent reductions in this voltage to supply the useful voltage of the cell V_{FC}, for a certain operating condition. Each of the terms can be calculated by the following equations, The control vector is:

$$
\mu = \begin{bmatrix} \mu_1, & \mu_2 \end{bmatrix}^T = \begin{bmatrix} (1 - U_{FC}), & (1 - U_{SC}) \end{bmatrix}^T
$$
$$
\text{or} \quad U = \begin{bmatrix} U_{FC}, & U_{SC} \end{bmatrix}^T
\tag{21}
$$

With $V_{FC} = V_{FC}(x_2)$ given in (Larminie & Dicks, 2000). In the sequel, V_{FC} will be considered as a measured disturbance, and from physical consideration, it comes that $V_{FC} \in [0; V_d[$.

B. Equilibrium

After simple calculations the equilibrium vector is:

$$\overline{x} = \begin{bmatrix} \overline{x}_1, & \overline{x}_2, & \overline{x}_3, & \overline{x}_4, & \overline{x}_5, & \overline{x}_6, & \overline{x}_7 \end{bmatrix}^T$$

$$= \begin{bmatrix} V_d, & \left(\dfrac{V_d}{V_{FC}} \left(\dfrac{V_d}{R_L} - \dfrac{E_B - V_d}{r_B} \right) \right), & V_d, & \dfrac{V_d}{R_L} - \dfrac{E_B - V_d}{r_B}, & V_{SC}(t=0), & 0, & \dfrac{V_d}{R_L} \end{bmatrix}^T \qquad (22)$$

where V_d is the desired DC link voltage. An implicit purpose of the proposed structure shown in Fig.13 is to recover energy to charge the SC. Hence, the desired voltage $\overline{x}_5 = \overline{V}_{SC} = V_{SC}(t=0) =$ Constante.

$$\overline{\mu} = \begin{bmatrix} \overline{\mu}_1, & \overline{\mu}_2 \end{bmatrix}^T = \begin{bmatrix} \dfrac{V_{FC}}{V_d}, & \dfrac{\overline{x}_5}{V_d} \end{bmatrix}^T \qquad (23)$$

Or

$$\overline{U} = \begin{bmatrix} \overline{U}_{FC}, & \overline{U}_{SC} \end{bmatrix}^T = \begin{bmatrix} 1 - \dfrac{V_{FC}}{V_d}, & 1 - \dfrac{\overline{x}_5}{V_d} \end{bmatrix}^T \qquad (24)$$

The natural energy function of the system is:

$$H = \frac{1}{2} x^T Q x \qquad (25)$$

where

$$Q = \text{diag}\{C_S; \quad L_{Fc}; \quad C_{DL}; \quad L_{DL}; \quad C_{SC}; \quad L_{SC}; \quad L_L\}$$

is a diagonal matrix.

C. Port-Controlled Hamiltonian representation of the system

In the following, a closed loop PCH representation is given. The desired closed loop energy function is:

$$H_d = \frac{1}{2} \widetilde{x}^T Q \widetilde{x} \qquad (26)$$

Where $\widetilde{x} = x - \overline{x}$ is the new state space defining the error between the state x and its equilibrium value $\overline{x}$.

The PCH form of the studied system with the new variable $\widetilde{x}$ as a function of the gradient of the desired energy (26) is:

$$\dot{\widetilde{x}} = [\Im(\mu_1, \mu_2) - \Re]\nabla H_d + A_i(\overline{x}, \mu) \qquad (27)$$

With

$$\Im(\mu_1,\mu_2)-\Re=$$

$$
\begin{bmatrix}
0 & \dfrac{\mu_1}{C_S L_{FC}} & 0 & \dfrac{1}{C_S L_{DL}} & 0 & 0 & 0 \\[2mm]
\dfrac{-\mu_1}{C_S L_{FC}} & 0 & 0 & 0 & 0 & 0 & 0 \\[2mm]
0 & 0 & \dfrac{-1}{C_{DL}^2 r_B} & \dfrac{1}{C_{DL} L_{DL}} & 0 & \dfrac{\mu_2}{C_{DL} L_{SC}} & \dfrac{-1}{C_{DL} L_L} \\[2mm]
\dfrac{1}{C_S L_{DL}} & 0 & \dfrac{-1}{C_{DL} L_{DL}} & 0 & 0 & 0 & 0 \\[2mm]
0 & 0 & 0 & 0 & 0 & \dfrac{-1}{C_{SC} L_{SC}} & 0 \\[2mm]
0 & 0 & \dfrac{-\mu_2}{C_{DL} L_{SC}} & 0 & \dfrac{1}{C_{SC} L_{SC}} & 0 & 0 \\[2mm]
0 & 0 & \dfrac{1}{C_{DL} L_L} & 0 & 0 & 0 & \dfrac{-R_L}{L_L^2}
\end{bmatrix}
\tag{28}
$$

And

$$
\nabla H_d =
\begin{bmatrix}
C_S \tilde{x}_1 \\
L_{FC} \tilde{x}_2 \\
C_{DL} \tilde{x}_3 \\
L_{DL} \tilde{x}_4 \\
C_{SC} \tilde{x}_5 \\
L_{SC} \tilde{x}_6 \\
L_L \tilde{x}_7
\end{bmatrix}
\tag{29}
$$

$$
A_i(\bar{x},\mu)=
\begin{bmatrix}
C_S\left[-\bar{x}_4+\mu_1\bar{x}_2\right] \\
\dfrac{1}{L_{FC}}\left[V_{FC}-\mu_1\bar{x}_1\right] \\
0 \\
0 \\
0 \\
\dfrac{1}{L_{SC}}\left[\bar{x}_5-\mu_2\bar{x}_3\right] \\
0
\end{bmatrix}
\tag{30}
$$

Where

$$\Im(\mu_1,\mu_2)=-\Im^T(\mu_1,\mu_2)\tag{31}$$

is a skew symmetric matrix defining the interconnection between the state space and $\Re=\Re^T\geq 0$ is a symmetric positive semi definite matrix defining the damping of the system.

With r is a design parameter, the following control laws are proposed:

$$\mu_1=\bar{\mu}_1 \quad \text{and} \quad \mu_2=\bar{\mu}_2+r\tilde{x}_6 \tag{32}$$

Proposition 1: The origin of the closed loop PCH system (27), with the control laws (32) and (23) with the radially unbounded energy function (26), is globally stable.
Proof: The closed loop dynamic of the PCH system (27) with the laws (32) and (23) with the radially unbounded energy function (26) is:

$$\dot{\tilde{x}} = \left[\Im(\mu_1,\mu_2) - \Re'\right]\nabla H_d \tag{33}$$

where

$$\Re' = diag\left\{0;\quad 0;\quad \frac{1}{\left(C_{DL}^2 r_B\right)};\quad 0;\quad 0;\quad \frac{rV_d}{L_{SC}^2};\frac{R_L}{L_L^2}\quad\right\} = \Re'^T \geq 0 \tag{34}$$

The derivative of the desired energy function (26) along the trajectory of (33) is:

$$\dot{H}_d = \nabla H_d^T \dot{\tilde{x}} = -\nabla H_d^T \Re'\nabla H_d \leq 0 \tag{35}$$

3.4 Sliding mode control of the system

Due to the weak request on the FC, a classical PI controller is adapted for the boost converter. Because of the fast response in the transient power and the possibility to work with a variable or a constant frequency, a non-linear sliding mode control (ayad et al, 2007) which allows management of the charge and discharge of the SC tank is chosen for the DC-DC bidirectional SC converter.

The current supplied by the FC is limited to an interval [I_{MIN}, I_{MAX}]. Within this interval, the FC boost ensures the regulation of this current to its reference. But, as soon as the load current is greater than I_{MAX} or lower than I_{MIN}, the boost becomes unable to regulate the desired current. The lacking or excess current is then provided or absorbed by the storage device, hence the DC link current is kept equal to its reference level. Consequently, three modes can be defined to optimize the function of the hybrid source:
- The normal mode, for which the load current is within the interval [I_{MIN}, I_{MAX}]. In this mode, the boost ensures the regulation of the DC link current, and the control of the bidirectional SC converter leads to the charge or the discharge of SC up to a reference voltage level V_{SCREF},
- The discharge mode, for which the load current is greater than I_{MAX}. The current reference of the boost is then saturated to I_{MAX}, and the DC-DC converter ensures the regulation of the DC link current by supplying the lacking current through the SC discharge,
- The recovery mode, for which the load current is lower than I_{MIN}. The power reference of the controlled rectifier is then saturated to I_{MIN} and the DC-DC converter ensures the regulation of the DC link current by absorbing the excess current through the SC charge.

A. DC-DC Fuel Cell converter control principle

The FC current reference I_{FC}^* is generated by means of a PI current loop control on a DC link current and load current. The switching device is controlled by a hysterisis comparator.

$$I_{FC}^* = k_p\left(I_L - I_{DL}\right) + k_I \int_0^t \left(I_L - I_{DL}\right)dt \tag{36}$$

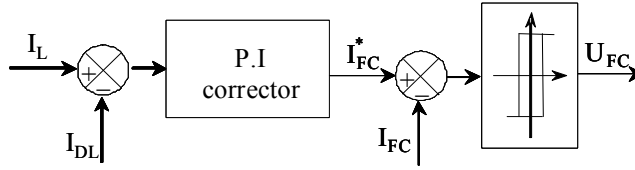where k_p and k_i are the proportional and integral gains.

Fig. 14. Control of the FC converter

B. DC-DC Supercapacitors converter control principle

To ensure proper function for the three modes, we use a sliding mode control for the bidirectional SC converter. Thus we define a sliding surface S as a function of the DC link current I_{DL}, the load current I_L, the SC voltage V_{SC}, its reference V_{SC}^* and the SC current I_{SC}:

$$S = (I_{DL} - I_L) + k_C(I_{SC} - I) \qquad (37)$$

with

$$I = k_{ps}(V_{SC} - V_{SC}^*) + k_{is}\int_0^t (V_{SC} - V_{SC}^*)dt \qquad (38)$$

With, k_{ps} and k_{is} are the proportional and integral gains.

When S < 0, the lower $T_{SC}=1$ in Fig.14 is switched on, and the upper $\overline{T}_{SC} = 0$ is switched off. When S > 0, the upper $\overline{T}_{SC} = 1$ is switched on and the lower $T_{SC}=0$ is switched off.

The FC PI controller ensures that I_{DL} tracks I_L. The SC PI controller ensures that V_{SC} tracks its reference V_{SC}^*.

k_C is the coefficient of proportionality, which ensures that the sliding surface equals zero by tracking the SC currents to its reference I when the FC controller cannot ensure I_{DL} tracks I_L.
In steady state conditions, the FC converter ensures that the first term of the sliding surface is zero, and the integral term of equation (38) implies that $V_{SC} = V_{SC}^*$. Then, imposing S = 0 leads to $I_{SC} = 0$, as far as the boost converter output current I_{DL} is not limited so that the storage element supplies energy only during power transient and I_{DL} limitation.

The general system of the DC link and the DC-DC SC converter equations can be written as:

$$\dot{X} = AX + BU + C + \xi \qquad (39)$$

With

$$X = \begin{bmatrix} V_{DL} & I_{SC} & V_{SC} & I \end{bmatrix}^T$$

And

$$A = \begin{bmatrix} -1/(r_B.C_{DL}) & 1/C_{DL} & 0 & 0 \\ -1/L_{SC} & -r_{SC}/L_{SC} & 1/L_{SC} & 0 \\ 0 & -1/C_{SC} & 0 & 0 \\ 0 & -k_{ps}/C_{SC} & k_{is} & 0 \end{bmatrix}$$

$$B = \begin{bmatrix} \dfrac{-I_{SC}}{C_{DL}} & \dfrac{V_{DL}}{L_{SC}} & 0 & 0 \end{bmatrix}^T$$

$$, \xi = \begin{bmatrix} \dfrac{(I_{DL} - I_L)}{C_{DL}} & 0 & 0 & 0 \end{bmatrix}^T \quad C = \begin{bmatrix} \dfrac{E_B}{(r_B C_{DL})} & 0 & 0 & -k_{is} V_{SC}^* \end{bmatrix}^T,$$

$$U = U_{SC}$$

If we denote

$$G = \begin{bmatrix} 0 & k_C & 0 & -k_C \end{bmatrix} \tag{40}$$

the sliding surface is then given by

$$S = C_{DL}\xi + GX \tag{41}$$

In order to set the system dynamics, we define the reaching law

$$\dot{S} = -\lambda S - K\text{sign}(S) \tag{42}$$

with

$$K = 0 \quad \text{if } \|S\| < \varepsilon \quad \text{and} \quad K = n\lambda\varepsilon \quad \text{if } \|S\| > \varepsilon \tag{43}$$

The linear term $-\lambda S(X)$ imposes the dynamics inside the error bandwidth ε. The choice of a high value of λ ($\leq f_c/2$) ensures a small static error when $\|S\| < \varepsilon$. The non-linear term $-K\text{sign}(S)$ permits to reject perturbation effects (uncertainty of the model, variations of the working conditions…). This term allows compensation high values of error $\|S\| > \varepsilon$ due to the above mentioned perturbations. The choice of a small value of ε leads to high current ripple (chattering effect) but the static error remains small. A high value of ε forces a reduction in the value of λ to ensure the stability of the system and leads to a higher static error.

Once the parameters (λ, K, ε) of the reaching law are determined, it is possible to calculate the continuous equivalent control, which allows the state trajectory on the sliding surface to be maintained. Using Equations (39), (41) and (42), we find:

$$U_{SCeq} = (GB)^{-1}\left\{-GAX - GC - \lambda GX - K\text{sign}(S) - C_{DL}\left[\dot{\xi} + \lambda\xi\right]\right\} \tag{44}$$

(37) and (39) give the equation:

$$A_{eq} = A - B(GB)^{-1}GA - B(GB)^{-1}\lambda G \tag{45}$$

This equation allows the determination of the poles of the system during the sliding motion as a function of λ and k_C. The parameters k_{is} and k_{ps} are then determined by solving S = 0.

This equation is justified by the fact that the sliding surface dynamic is much greater than the SC voltage variation.

C. Stability
Consider the following Lyapunov function:

$$V = \frac{1}{2}S^2 \tag{46}$$

Where, S is the sliding surface.
The derivative of the Lyapunov function along the trajectory of (42) in the closed loop with the control (44) gives:

$$\dot{V} = S\dot{S} = -\lambda S^2 - KS\,sign(S) \leq 0 \tag{47}$$

With $\lambda, K > 0$
Hence, the origin of the closed loop of the system (39) with the control (44) and the sliding surface (41) is asymptotically stable.

3.5 Simulation results of the hybrid source control
The whole system has been implemented in MATLAB-SIMULINK with the following parameters associated to the hybrid sources:
- FC parameters: P_{MAX} = 400 W.
- DC link parameters: V_{DL}= 24 V.
- SC parameters: C_{SC} = 3500/6 F, $V_{SC}^* = 15V$.

The results presented in this section have been carried out by connecting the hybrid source to a "R, L and E_L " load.

A. Sliding mode control applied to the hybrid source
Figures 15, 16 and 17 present the behaviour of currents I_{DL}, I_{DL}, I_{SC}, I_B and the DC link voltage V_{DL} for transient responses obtained for a transition from the normal mode to the discharge mode by using sliding mode control. The test is performed by changing sharply the e.m.f load voltage E_L in the interval of t∈[0.5 s, 1.5 s]. The load current I_L changes from 16.8 A to 25 A. The current load I_L = 16.8 A corresponds to a normal mode and the current load I_L = 25 A to a discharge mode.
At the starting of the system, only the FC provides the mean power to the load. The storage device current reference is equal to zero, we are in normal mode. In the transient state, the load current I_L became greater then the DC link current I_{DL}. The storage device current reference became positive thanks to control function which compensate this positive value by the difference between the SC voltage and its reference. We are in discharging mode. After the load variation (t > 1.5 s), the current in the DC link became equal to the load current. The SC current I_{SC} became null. We have a small variation in the batteries currents.
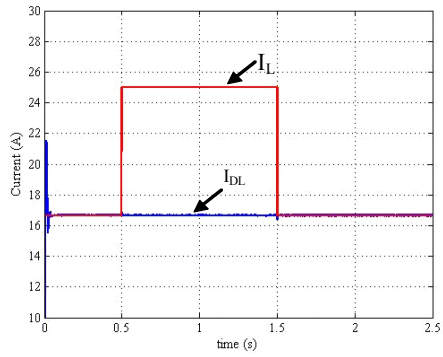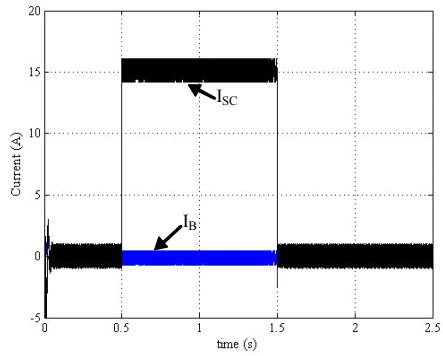
Fig. 15. Load and DC link currents
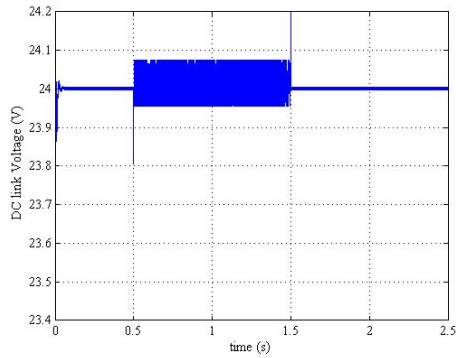

Fig. 16. SC and batteries currents

Fig. 17. DC link voltage

B. Passivity Based Control applied to the hybrid source

Figure 18 shows the FC voltage and current. Figure 19 presents the SC voltage and current response. The SC supply power to the load in the transient and in the steady state no power or energy is extracted since the current $x_6 = I_{SC}$ is null.

The positive sens of I_{SC} means that the SCs supply the load and the negative one corresponds to the recover of energy from the FC to the SC. Figure 20 presents the batteries voltage and its current. Figure 21 presents the response of the system to changes in the load current I_L. The DC Bus voltage tracks well the reference, i.e. very low overshoot and no steady state error are observed. It can be seen from this figure that the system with the proposed controller is robust towards load resistance changes. Figure 22 shows the FC Boost controller, the SC bidirectional converter controller and the changes in the Load resistance RL. U_{SC} and U_{FC} are in the set [0; 1].
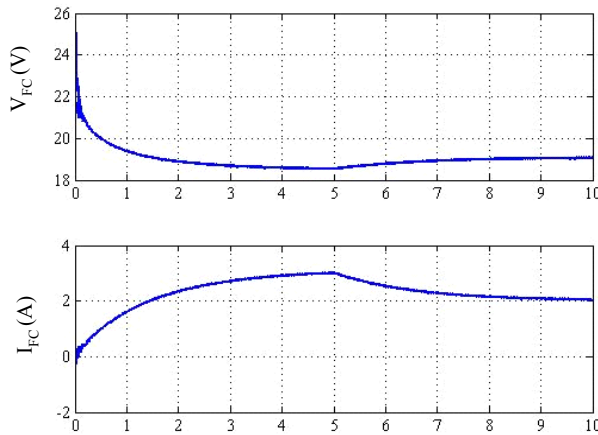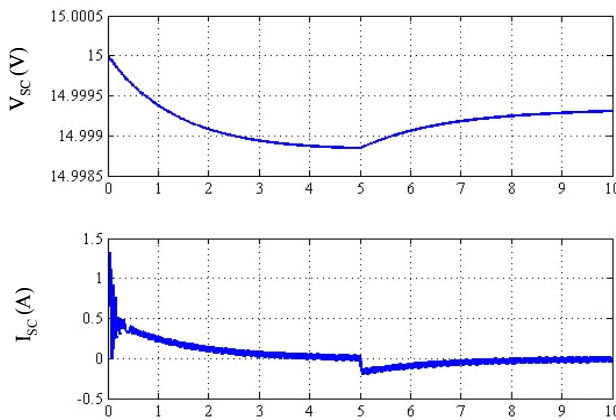

Fig. 18. FC voltage and FC current
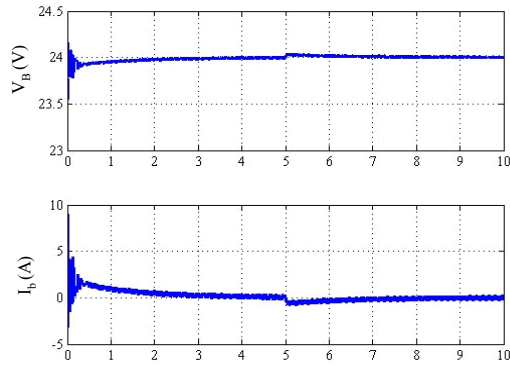

Fig. 19. SC voltage and SC current

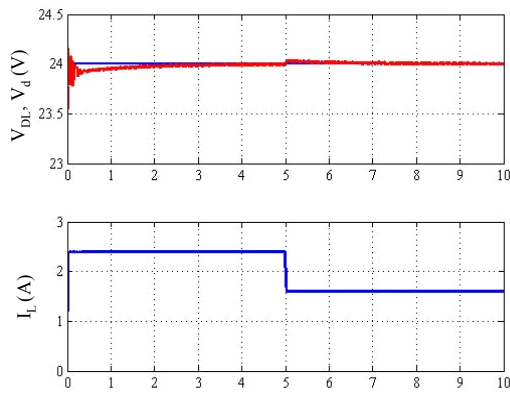Fig. 20. Batteries voltage and batteries current
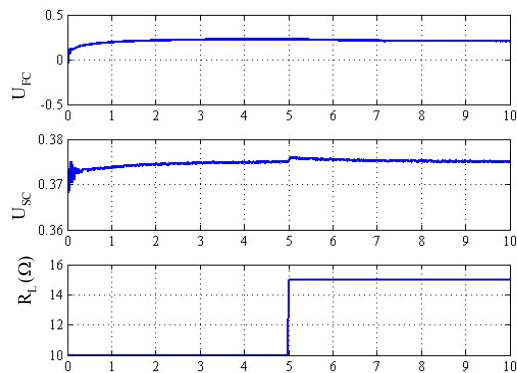

Fig.21. DC link voltage and load current

Fig. 22. (a) FC Boost control. (b) SC DC-DC (c) Load resistance change

4. Conclusion

In this paper, control principles of a hybrid DC source have been presented. This source uses the fuel cell as mean power source, SCs as auxiliary transient power source and batteries on the DC link.

Passivity Based Control and Sliding Mode Control principles have been applied and validated by simulation results. Include main findings and highlight the positive points of the simulation results and the possibility of applying this new concept in Fuel Cell applications.

PCH structure of the overall system is given exhibiting important physical properties in terms of variable interconnection and damping of the system. The problem of the DC Bus Voltage control is solved using simple linear controllers based on an IDA-PBC approach.

With the sliding mode principle control, we have a robustness control. But the sliding surface is generated in function of multiple variables: DC link voltage, SCs current and voltage.

With PBC, only two measures are needed to achieve the control aims of this complex system (the FC Voltage and the SC current), while for the Sliding mode control we need to achieve the control aims of this complex system (the FC Voltage, the SC current, the SC voltage, load and DC link currents). The sliding mode is faster in terms of response to a set point change or disruption.

The PBC control laws are completely independent from the system's parameters, and then this controller is robust towards the parameter variation. The Sliding mode controller is function of the system parameter and is therefore sensitive to there changes.

The PBC control laws are very simple to realize and produce continuous behavior while the sliding mode control is more complicated (realization of the surface and the control laws) and introduce nonlinearities by commutation.

Global Stability proofs are given and encouraging simulation results has been obtained.

Many benefits can be expected from the proposed structure such that supplying and absorbing the power picks by using SC which also allows recovering energy.

5. References

Kishinevsky, Y. & Zelingher, S. (2003). Coming clean with fuel cells, IEEE Power & Energy Magazine, vol. 1, issue: 6, Nov.-Dec. 2003, pp. 20-25.

Larminie, J. & Dicks, A. (2000). Fuel cell systems explained, Wiley, 2000.

Pischinger, S.; Schönfelder, C. & Ogrzewalla, J. (2006). Analysis of dynamic requirements for fuel cell systems for vehicle applications, J. Power Sources, vol. 154, no. 2, pp. 420-427, March 2006.

Moore, R. M.; Hauer, K. H.; Ramaswamy, S. & Cunningham, J. M. (2006). Energy utilization and efficiency analysis for hydrogen fuel cell vehicles, J. Power Sources, 2006.

Corbo, P.; Corcione, F. E.; Migliardini, F. & Veneri, O. (2006). Experimental assessment of energy-management strategies in fuel-cell propulsion systems, J. Power Sources, 2006.

Rufer, A.; Hotellier, D. & Barrade, P. (2004). A Supercapacitor-Based Energy-Storage Substation for Voltage - Compensation in Weak Transportation Networks," IEEE Trans. Power Delivery, vol. 19, no. 2, April 2004, pp. 629-636.

Thounthong, P.; Raël, S. & Davat, B. (2007). A new control strategy of fuel cell and supercapacitors association for distributed generation system, IEEE Trans. Ind. Electron, Volume 54, Issue 6, Dec. 2007 Page(s): 3225 – 3233

Corrêa, J. M.; Farret, F. A.; Gomes, J. R. & Simões, M. G. (2003). Simulation of fuel-cell stacks using a computer-controlled power rectifier with the purposes of actual high-power injection applications, IEEE Trans. Ind. App., vol. 39, no. 4, pp. 1136-1142, July/Aug. 2003.

Benziger, J. B.; Satterfield, M. B.; Hogarth, W. H. J.; Nehlsen, J. P. & Kevrekidis; I. G. (2006). The power performance curve for engineering analysis of fuel cells, J. Power Sources, 2006.

Granovskii, M.; Dincer, I. & Rosen, M. A. (2006). Environmental and economic aspects of hydrogen production and utilization in fuel cell vehicles, J. Power Sources, vol. 157, pp. 411-421, June 19, 2006

Ortega, R.; van der Schaft, A.J.; Maschke, B. & Escobar, G. (2002). Interconnection and damping assignment passivity–based control of port–controlled hamiltonian systems, Automatica, vol.38(4), pp.585–596, 2002.

Becherif, M. & Mendes, E. (2006). Stability and robustness of Disturbed- Port Controlled Hamiltonian system with Dissipation, 16th IFAC World Congress, Prague, 2005.

Becherif, M. & Ayad, M. Y. (2006). Modelling and Passivity-Based Control of Hybrid Sources: Fuel cell and Supercapacitors, *In* 41st IEEE-IAS 2006, USA.

Ayad, M. Y.; Gualous, A.; Cirrincione, M. & Miraoui, A. (2007). Study And Realization Of A Power Source Using Supercapacitors Matrix and Fuel cell, in Proc. 2nd European Ele-Drive Transportation Conference EET-2007 - Brussels, 30th May - 1st June 2007

Ayad, M. Y.; Pierfederici, S.; Raël, S. & Davat, B. (2007). Voltage Regulated Hybrid DC Source using supercapacitors, Energy Conversion and Management, Volume 48, Issue 7, July 2007, Pages 2196-2202.

Belhachemi, F.; Rael, S. & Davat, B. (2000). A Physical based model of power elctric double layer supercapacitors, IAS 2000, 35th IEEE Industry Applications Conference, Rome, 8-12 October

Rao, V.; Singhal, G.; Kumar, A. & Navet, N. (2005). Model for Embedded Systems Battery, Proceedings of the 18th International Conference on VLSI Design held jointly with 4th International Conference on Embedded Systems Design (IEEE-VLSID'05), 2005.

Chen, M.; Gabriel, A.; Rincon-Mora. (2006). Accurate Electrical Battery Model Capable of Predicting Runtime and *I–V* Performance. . *IEEE Trans. Energy Convers*, Vol. 21, No.2, pp.504-511 June 2006.

Salameh, Z.M.; Casacca, M.A. & Lynch, W.A. (1992). A mathematical model for lead-acid batteries, *IEEE Trans. Energy Convers.*, vol. 7, no. 1, pp. 93–98, Mar. 1992.

Equivalent consumption minimization strategies of series hybrid city buses

Liangfei Xu, Guijun Cao, Jianqiu Li, Fuyuan Yang, Languang Lu and Minggao Ouyang

State Key Lab of Automotive Safety and Energy, Tsinghua University
P.R.China

1. Introduction

With ever growing concerns on energy crisis and environmental issues, alternative clean and energy efficient vehicles are favoured for public applications. Internal combustion engine(ICE)-powered series hybrid buses and fuel cell (FC) hybrid buses, respectively as a near-term and long-term strategy, have a very promising application prospect.

The series hybrid vehicle utilizes an ICE/FC as the main power source and a battery/ultra capacity (UC) as the auxiliary power source. The main power source supplies the average vehicle power, and the auxiliary power source functions during accelerating and decelerating. Because the battery/UC fulfills the transient power demand fluctuations, the ICE/FC can work steadly. Thus, the durability of the fuel cell stack could be improved compared with a pure FC-powered bus in the FC series hybrid bus. And the PM and NOx can be greatly lowered in the ICE series hybrid bus compared with a traditional city bus. Besides, the ability of the energy storage source to recover braking energy enhances the fuel economy greatly.

The hybrid configuration raises the question of energy management strategy, which chooses the power split between the two. The strategy is developed to achieve system-level objectives, e.g. fuel economy, low emission and battery charge-sustaining, while satisfying system constraints.

Energy management strategies in the recent literature can be generally categorized into two types: rule-based strategies and optimal strategies. A rule based strategy can be easily implemented for the real-time applications based on heuristics (N.Jalil, N.A.Kheir & M.Salman, 1997). Such a strategy could be further improved by extracting optimal rules from optimal algorithms (S.Aoyagi, Y.Hasegawa & T.Yonekura, 2001).

Optimal strategies differ from each other in the time range. Fuel consumption in a single control cycle is minimized in an instantaneous optimal strategy (G.Paganelli, S.Delprat & T.M.Guerra, 2002). And a global optimal strategy minimises it over a whole determined driving cycle using determined dynamic programming method (DDP) (Chan Chiao Lin et al., 2003), or over a undetermined driving cycle using stochastic dynamic programming method (SDP) (Andreas Schell et al., 2005). Other strategies minimize fuel consumption over an adaptive time span, which could be adjusted on the basis of vehicular speed, pedal

positions, historical vehicle power and power forcasting in the future (Bin He, Minggao Ouyang, 2006).

From a mathematical viewpoint, the optimal problem could be solved using different methods. Energy management strategies based on DDP, SDP, fuzzy logic (Schouten N J, Salman M A & Kheir N A, 2002), neural network optimal algorithm (Amin Hajizadeh, Masoud Aliakbar Golkar, 2007), genetic algorithm (Vanessa Paladini et al., 2007) and wavelet algorithm (Xi Zhang et al., 2008) have been proposed by different researchers.

This chapter describes the implementation of an equivalent consumption minimization strategy in a FC+battery city bus and an ICE+battery city bus. It belongs to the instantaneous optimization strategies. The strategy is based on an equivalent consumption model, which was firstly proposed by Paganelli G (Paganelli G et al., 2002) to evalutate the battery electrical energy consumption. The analytical solutions to the optimal problems are given, avoiding using complex mathematical tools.

The charpter proceeds as follows. Section 2 describes the powertrain systems of the FC/ICE-powered hybrid city buses. Section3 details the equivalent consumption model. Section 4 gives the equivalent consumption minimization strategy (ECMS) on the basis of the analytical solutions. Section 5 discusses the results in the "China city bus typical cycle" testing. Section 6 is the conclusions.

2. The series hybrid powertrains

In the 11th Five-Year Plan of China, a series of hybird city buses have been developed. Fig. 1 (a) and (b) show a fuel cell city bus and a diesel engine hybrid city bus respectively.

(a)

(b)

Fig. 1. (a) Fuel cell city bus (b) Diesel engine series hybrid city bus

The series hybrid powertrain under discussion is mainly composed of a power unit (PU), an auxiliary power source and an alternating current motor, as shown in Fig. 2 (a) and (b). A Ni-MH battery has the advantage of good charging / discharging characteristics compared with a Pb-Acid battery. And it is relatively cheap compared with a Li-ion battery. Thus, a Ni-MH battery is selected as the auxiliary power source. The two kinds of city buses differ in the PU configuration. In the fuel cell hybrid bus, the PU consists of a proton exchange membrane (PEM) fuel cell system and a direct current to direct current (DC/DC) converter, as in Fig. 2 (a). In the ICE hybrid bus, the PU consists of an internal combustion engine, a generator and a rectifier, as in Fig. 2 (b).

As an electrochemical device, the PEM fuel cell system converts hydrogen energy to electrical energy directly without mechanical processes. For the city bus in Fig. 1 (a), two stacks with a rated power of 40kW are installed. The city bus is powered by an AC motor with a rated power of 100kW. In order to fulfill the peak power during accelerating, a Ni-MH battery with a rated capacity of 80A.h, and a rated open circuit voltage of 380V is utilized. The fuel cell stack, the Ni-MH battery and the AC motor are connected as in Fig. 2 (a).

Compared with the FC-powered hybrid bus, the ICE-powered hybrid bus is much more popular in the market because of the price. The city bus in Fig. 1 (b) is equipped with a diesel engine SOFIM 2.8L. It reaches its maximal torque at $1500 r.min^{-1}$. Its lowest specific fuel consumption is $210 g.kWh^{-1}$ at about $1600 r.min^{-1}$. A three-phase synchronous generator is connected with the diesel engine directly to convert the mechanical power into alternating current (AC). A three-phase rectifier is used to convert AC into direct current (DC). The AC motor and the battery are similar as in the FC city bus. The diesel engine, the generator, the rectifier, the battery and the motor are connected as in Fig. 2 (b).

Fig. 2 (a) and (b) also present the control systems of the hybrid powertrain. It is a distributed control system based on a time-triggered controller area network (TTCAN). The vehicle controller unit (VCU) is the "brain" of the control system. It receives driver commands (pedal positions, shift signals, on-off swithes et al.) through its digital/analog input channels, and sends control commands to other controllers.

In the FC+battery hybrid powertrain, the TTCAN consists of the VCU, a fuel cell controller, a DC/DC controller, a battery management system and a motor controller. The output torque of the motor and the output current of the DC/DC converter are controlled by the VCU to regulate the motor power and the fuel cell power respectively (Xu Liangfei, 2008).

In the ICE+battery hybird powertrain, the TTCAN is composed of the VCU, an engine controller, a excitation controller, a battery management system and a motor controller. The output power of the PU is controlled by a PWM signal from the VCU to the excitation controller, and the rotational speed of the diesel engine is controlled by a simulant throttle signal from the VCU to the engine controller (Cao Guijun, 2009).

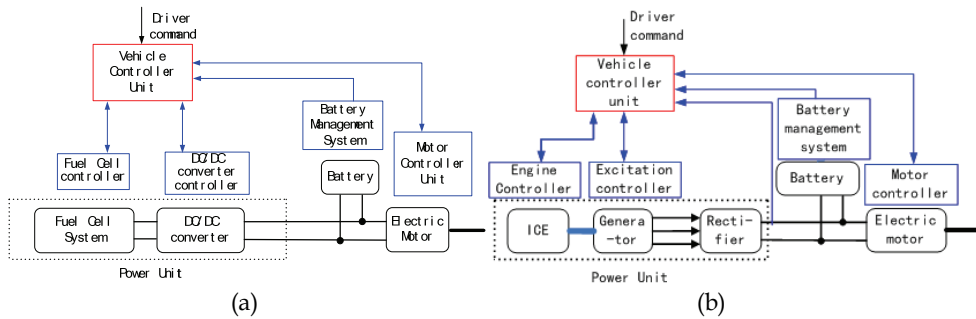Main parameters of the two city buses are presented in Table 1.

<div align="center">(a)   (b)</div>

Fig. 2. Series hybrid powertrain structure (He Bin, 2006) (a) PEM fuel cell+Ni-MH battery (b) Diesel engine+Ni-MH battery

Parameter (Unit)	Value
Fuel cell hybrid bus empty mass m (kg)	1.45×10^4
Diesel engine hybrid bus empty mass m (kg)	1.35×10^4
Frontal area A (m2)	7.5
Drag coefficient C_D	0.7
Rolling resistance coefficient	1.8×10^{-2}
Mechanical efficiency η_T (%)	95
Mass factor	1.1
PEM fuel cell rated power (kW)	80
DC/DC rated power (kW)	80
Style of the diesel engine	SOFIM 2.8L
Diesel engine lowest fuel consumption	210g.kWh^{-1}
Style of the generator	4UC224G
Rated power of the generator	68kW at 1500r.min^{-1}
Style of the rectifier	three phase full bridge uncontrollable
Power range of the rectifier (kW)	10~120
Ni-MH battery rated capacity (A.h)	80 in Fig. 1 (a), 60 in Fig. 1 (b)
Electric motor rated power (kW)	100

Table 1. Main parameters of the two hybrid city buses

3. The equivalent consumption model

The concept of equivalent fuel consumption was proposed by Paganelli et al. for an instantaneous optimization energy management strategy (Paganelli G et al., 2002). In the two kinds of series hybrid vehicles, both the PU and the battery provide energy. The electrical energy consumption of the battery is transformed into an equivalent fuel consumption to make the two comparable. If some energy is drawn from the battery at the current sample time, the battery will have to be recharged to maintain the state of charge (SOC) in the future. The energy will be provided by the PU, or by the motor in braking regeneration. That will imply extra fuel consumption. Because the operating points of the PU and the battery in the future are unknown, the average values are used to calculate the battery equivalent hydrogen consumption C_{bat}.

$$C_{bat}=\delta P_{bat}C_{pu,avg}/(\eta_{dis}\eta_{chg,avg}\ P_{pu,avg}),\ P_{bat}\geq 0 \qquad (1)$$

where:
P_{bat} is the battery power, kW.
$C_{pu,avg}$ is the PU mean fuel consumption, g.s^{-1}.
$P_{pu,avg}$ is the PU mean output power, kW.
η_{dis} is the battery discharging efficiency.
$\eta_{chg,avg}$ is the battery mean charging efficiency.
δ is a ratio factor that defines as follows.

$$\delta=E_{pu,chg}/(E_{pu,chg}+E_{recycle,chg}) \qquad (2)$$

where:
$E_{pu,chg}$ is the battery charging energy provided by the PU. $E_{recycle,chg}$ is the battery charging energy which is recycled by the electric motor. The energy should be calculated over a certain time range, depending on the working conditions. If no braking energy is recovered, $\delta=1$. If no PU energy is used to charge the battery, $\delta=0$. The battery could not only be charged by braking energy, $0<\delta\leq 1$.
If the battery is recharged at the current sample time, a discharge of the battery is required to maintain the SOC. This discharge will lead to a reduction of the fuel consumption in the future. The battery equivalent consumption can be calculated as

$$C_{bat}=P_{bat}\eta_{chg}\eta_{dis,avg}\ C_{pu,avg}/P_{pu,avg},\ P_{bat}<0 \qquad (3)$$

where:
η_{chg} is the battery recharging efficiency.
$\eta_{dis,avg}$ is the battery mean discharging efficiency.
The battery charging/discharging efficiencies are calculated based on the Rint model (V. H. Johnson, 2002), which is shown in Fig. 3. They can be formulated as

$$\begin{cases} \eta_{dis} = \dfrac{1}{2}\left(1+\sqrt{1-\dfrac{4R_{dis}P_{bat}}{U_{ocv}^2}}\right) & P_{bat} \geq 0 \\[4mm] \eta_{chg} = 2 \Big/ \left(1+\sqrt{1-\dfrac{4R_{chg}P_{bat}}{U_{ocv}^2}}\right) & P_{bat} < 0 \end{cases} \qquad (4)$$

where R_{dis} and R_{chg} are the battery discharging and charging resistance respectively, U_{ocv} is the open circuit voltage. All of them are functions of the battery SOC.

For the 80Ah Ni-MH battery, the relationship between R_{dis}/R_{chg} and SOC is shown in Fig. 3 (b), as well as the relationship between U_{ocv} and SOC. Fig. 3 (c) presents the relationship between battery efficiency and P_{bat}, SOC. Fig. 3 (d) indicates the relationship between the battery equivalent consumption and P_{bat}, SOC, where $\delta=1$.
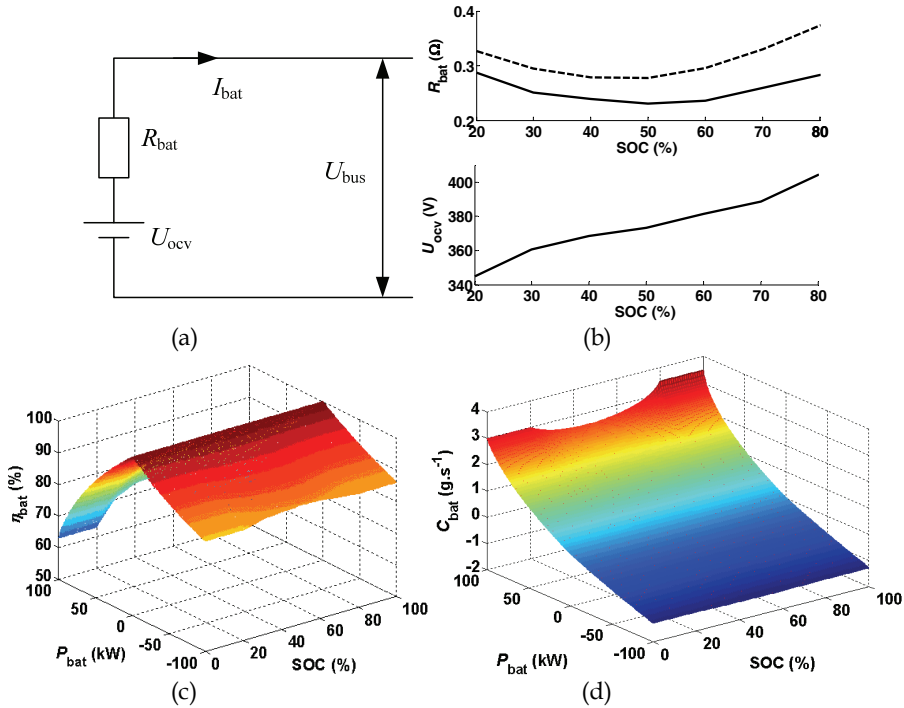

Fig. 3. (a) The battery Rint model (b) Relationship between battery resistance/open circuit voltage and SOC (solid line for charging, dashed line for discharging) (c) Battery efficiency v.s. battery power and SOC (d) Battery equivalent hydrogen consumption C_{bat} v.s. battery power and SOC, $\delta=1$.

In the fuel cell + battery hybrid powertrain, the PU is composed of the fuel cell system and the DC/DC converter. In the following equations, C_{fc} is the fuel cell hydrogen consumption, and P_{dc} is the DC/DC output power. According to the experimental data, the fuel cell hydrogen consumption C_{fc} can be expressed as

$$C_{fc} = \begin{cases} a_0 P_{dc} + a_1, & P_{dc} \geq P_{dc0} \\ b_0 P_{dc}^2 + b_1 P_{dc} + b_2, & P_{dc} < P_{dc0} \end{cases} \tag{5}$$

where a_i, b_i are fit coefficients, P_{dc0} is a critical value of P_{dc}.

The relationship between C_{fc} and P_{dc} is nonlinear when P_{dc} is smaller than the critical value P_{dc0}, and it is linear when P_{dc} is larger than P_{dc0}. Fig. 4 (a) and (b) compare the experiment curves and the fitting curves in the two cases. P_{dc0} is about 7.5kW for the hybrid powertrain under discussion.
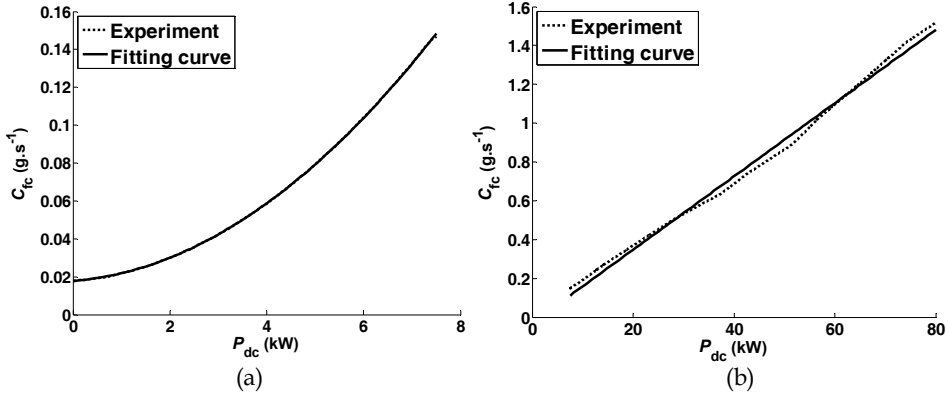

Fig. 4. (a) Relationship between fuel cell hydrogen consumption C_{fc} and DC/DC power P_{dc} when $P_{dc} \leq 7.5$kW (b) Relationship between fuel cell hydrogen consumption C_{fc} and DC/DC power P_{dc} when $P_{dc} > 7.5$kW

In the diesel engine + battery hybrid powertrain, the PU is composed of the diesel engine, the generator and the rectifier. In the following equations, C_{ice} is the diesel engine fuel consumption, and P_{rec} is the rectifier output power. The specific fuel consumption of the diesel engine is a complex function of torque and speed. Fig. 5 (a) gives an example of a TDI 1.9 L diesel engine. The engine can work at different working points when the output power is P_{ice}. Among these points there is an optimal working point, where the specific fuel consumption is minimal. The optimal working points compose an optimal curve, as shown in Fig. 5 (a). According to the optimal curve in Fig. 5 (a), we can find the relationship between the diesel engine output power P_{ice} and the minimal fuel consumption C_{ice}, as in Fig. 5 (b).

(a)   (b)
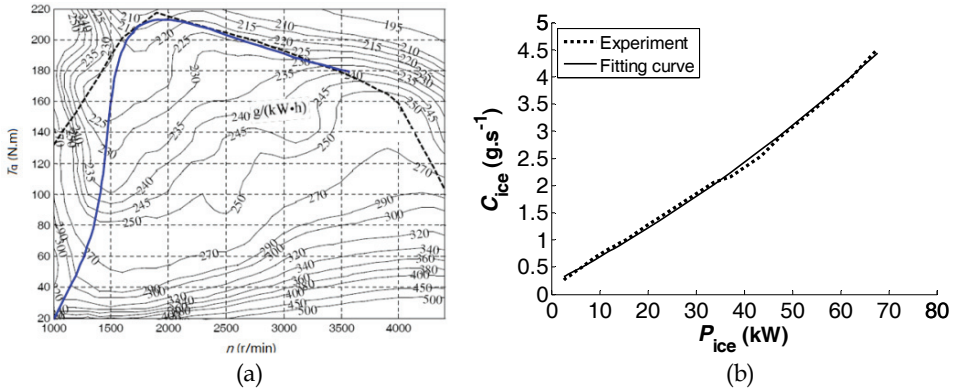
Fig. 5. (a) The relationship between specific fuel consumption, torque and rotational speed of TDI 1.9L Diesel Engine. The dashed is the external characteristic, and the solid blue line is the optimal curve. (He Bin, 2006) (b) The minimal fuel consumption when the engine output power is P_{ice}

The fitting curve in Fig. 5 (b) can be expressed as:

$$C_{ice} = c_0 P_{ice}^2 + c_1 P_{ice} + c_2 \tag{6}$$

where c_i, i=0~2 are fitting coefficients. For the TDI 1.9L engine, c_0=0.0002g.s⁻¹.kW⁻² wait

where c_i, i=0~2 are fitting coefficients. For the TDI 1.9L engine, c_0=0.0002g.s^{-1}.kW^{-2}, c_1=0.0456 g.s^{-1}.kW^{-1}, c_2=0.2036g.s^{-1}. The output power of the rectifier is calculated as:

$$P_{rec} = P_{ice}\eta_{gen}\eta_{rec} \tag{7}$$

where η_{gen} and η_{rec} are the generator and rectifier efficiencies respectively.
Then, the total fuel consumption C of the hybrid powertrain can be written as

$$C = C_{pu} + C_{bat} \tag{8}$$

4. The equivalent consumption minimization strategy (ECMS)

In the instantaneous optimization algorithm, an optimal output power of the PU is calculated to minimize the powertrain fuel consumption in one control cycle. It can be formulated mathematically as follows.

$$P_{pu,opt} = \arg\min_{P_{pu}} C = \arg\min_{P_{pu}}\left(C_{pu} + C_{bat}\right)$$

$$\text{subject to:} \begin{cases} \text{SOC}_L \leq \text{SOC} \leq \text{SOC}_H \\ U_{bus,min} \leq U_{bus} \leq U_{bus,max} \\ 0 \leq P_{pu} \leq P_{pu,max} \end{cases} \tag{9}$$

where $U_{\text{bus,min}}$ and $U_{\text{bus,max}}$ are the minimal and maximal value of bus voltage, $P_{\text{pu,max}}$ is the maximan of P_{pu}, C_{pu} equals to C_{fc} in the fuel cell hybrid bus, C_{pu} equals to C_{ice} in the diesel engine hybrid bus.

4.1 ECMS for the fuel cell hybrid powertrain

As for the fuel cell city bus under discussion, the vehicle auxiliary power P_{aux}, which is consumed by the cooling system, the electric assistant steering system et al., is about 5kW (without the air condition) or 17kW (with the air condition). Therefore, the possibility of $P_{\text{dc}}<7.5\text{kW}$ is very small. That means, the relationship between the fuel cell hydrogen consumption C_{fc} and the DC/DC power P_{dc} could be regarded as linear in most of the time. Then, the optimized problem defined in Equation (9) could be simplified and the analytic solution to the problem is as follows.

$$P_{\text{bat,opt}} = \min\left(\frac{U_{\text{ocv}}^2\left(1-\delta^2\right)}{4R_{\text{dis}}}, \frac{U_{\text{bus,min}}\left(U_{\text{ocv}}-U_{\text{bus,min}}\right)}{R_{\text{dis}}} \right) \tag{10}$$

where $P_{\text{bat,opt}}$ is the optimal battery power. If no braking energy is recovered, $\delta=1$, then $P_{\text{bat,opt}}=0$. This is because the relationship between the hydrogen consumption and the DC/DC power is linear, any charging/discharging process of the battery will cost an extra energy.

With such a strategy, the battery SOC will fluctuate around the initial value. But usually we want to keep the SOC around a target value SOC_{tg}. Thus, a balance power $P_{\text{bat,balance}}$ is defined as follows.

$$P_{\text{bat,balance}} = k\left(\text{SOC-SOC}_{\text{tg}}\right) \tag{11}$$

where k is a coefficient, $k>0$. Then, the DC/DC target power $P_{\text{dc,tg}}$ is calculated as follows.

$$P_{\text{dc,tg}} = \max\left(\min\left(P_{\text{demand}} - P_{\text{bat,opt}} - P_{\text{bat,balance}}, P_{\text{dc,max}} \right), 0 \right) \tag{12}$$

where P_{demand} is the powertrain demand power, including the electric motor power and the vehicle accessorial power. The VCU calculates the DC/DC target voltage/current according to $P_{\text{dc,tg}}$, sends the signal to the DC/DC controller through TTCAN. There is a time-delay between the DC/DC target signal and its actual output. This is because the fuel cell can't response quickly to dynamic loads. The fuel cell voltage drops with increasing current. A reactant starvation occurs at high currents and dynamic loads because the transport of reactant gases is not able to keep pace with the amount used in the reaction (Xu Liangfei et al., 2008).

4.2 ECMS for the diesel engine hybrid powertrain

According to equations (6) and (7), the relationship between the C_{ice} and P_{rec} is.

$$\begin{cases} C_{ice} = c_0' P_{rec}^2 + c_1' P_{rec} + c_2 \\ c_0' = c_0 \left(\eta_{gen} \eta_{rec} \right)^2 \\ c_1' = c_1 \eta_{gen} \eta_{rec} \end{cases} \tag{13}$$

The analytic solution for the optimized problem defined in Equation (9) can be written as follows.

$$P_{bat,opt} = \begin{cases} \dfrac{U_{bus,min} \left(U_{ocv} - U_{bus,min} \right)}{R_{dis}}, K \leq dx_{min} \\[2ex] \dfrac{U_{ocv}^2}{4R_{dis}} \left(1 - \dfrac{K^2}{a^2} \right), dx_{min} < K \leq d \\[2ex] 0, d < K \leq d / \left(\eta_{chg,avg} \eta_{dis,avg} \right) \\[2ex] \dfrac{U_{ocv}^2}{4R_{chg}} \left(1 - \dfrac{\left(K\eta_{chg,avg} \eta_{dis,avg} \right)^2}{a^2} \right), \dfrac{d}{\eta_{chg,avg} \eta_{dis,avg}} < K < \dfrac{dx_{max}}{\eta_{chg,avg} \eta_{dis,avg}} \\[2ex] -\dfrac{U_{bus,max} \left(U_{bus,max} - U_{ocv} \right)}{R_{chg}}, K \geq \dfrac{dx_{max}}{\eta_{chg,avg} \eta_{dis,avg}} \end{cases} \tag{14}$$

where d, K, x_{min}, x_{max} are coefficients defined as follows.

$$\begin{cases} d = c_1' + 2c_0' P_{demand} \\[1ex] K = \begin{cases} \delta C_{fc,avg} / \left(\eta_{dis,avg} \eta_{chg,avg} \right), P_{bat} \geq 0 \\ C_{fc,avg} / \left(\eta_{dis,avg} \eta_{chg,avg} \right), P_{bat} < 0 \end{cases} \\[2ex] x_{min} = \sqrt{1 + 4U_{bus,min} \left(U_{bus,min} - U_{ocv} \right) / \left(U_{ocv}^2 \right)} \\[1ex] x_{max} = \sqrt{1 + 4U_{bus,max} \left(U_{bus,max} - U_{ocv} \right) / \left(U_{ocv}^2 \right)} \end{cases} \tag{15}$$

Equations (14) and (15) indicate that, the battery optimal power $P_{bat,opt}$ is a function of vehicle power demand P_{demand}, battery SOC and the ratio coefficient δ. $P_{bat,opt} = f(P_{demand}, \text{SOC}, \delta)$. In real-time application, this function can be calculated and stored in the ECU memory. The target power of the rectifier $P_{rec,tg}$ is calculated using a similar formula as Equation (12).

$$P_{rec,tg} = \max \left(\min \left(P_{demand} - P_{bat,opt} - P_{bat,balance}, P_{rec,max} \right), 0 \right) \tag{16}$$

The output power of the rectifier is controlled by a PWM signal from the VCU to the excitation controller. According to $P_{rec,tg}$ and the optimal curve in Fig. 5 (a), the optimal working point (ω_{eng}, T_{eng}) can be found. The target rotational speed of the diesel engine ω_{eng} is controlled by a simulant throttle signal from the VCU to the engine controller. In order to reduce the emission during dynamic loads, there is a time-delay between the command of VCU and the actual output of the engine (He Bin, 2006).

5. Results in the cycle testing

The instantaneous optimal energy management strategies have been successfully implemented in the two hybrid city buses. The hybrid powertrains were tested on the test bench with "China city bus typical cycle". Results are presented in Fig. 6 (a)~(d).

Fig. 6 (a) and (b) presents the results of the fuel cell hybrid city bus in the cycle testing, δ = 0.6. The vehicle velocity is shown in Fig. 6 (a). The test lasts about 20mins, and the maximal speed is 60km.h^{-1}. The battery SOC was kept around 70%.

Fig. 6 (b) shows the power split between the electric motor, the battery and the PU (Fuel cell + DC/DC converter). Part of the braking energy was recycled. In this figure, P_m stands for the electric power of the motor. The electric power ranged from -50kW to 100kW. Because of the time-delay between the DC/DC target command and its actual output, the DC/DC output power changed much more slowly than the motor electric power. The battery functioned during accelerating and decelerating. It was kept charge-sustaining.

Fig. 6 (c) indicates the energy flow diagram. The hydrogen energy is calculated on the basis of its low heat value. The average efficiencies of the fuel cell system, the DC/DC converter and the electric motor were 50%, 96% and 85% respectively. About 5.5% of the whole energy was consumed by the vehicle auxiliary components, e.g. the air condition. About 45.2% of the hydrogen energy was output from the electric motor, and about 9.5% of the hydrogen energy was recycled. The battery slightly discharged. The fuel economy of the city bus was about 7.4kg.100km^{-1}.

The fuel consumption increases with δ increases. Testing results show that, their relationship is as follows.

δ=0.6, fuel economy = 7.4kg.100km^{-1};
δ=0.85, fuel economy = 8.9kg.100km^{-1};
δ=1, fuel economy = 9.7kg.100km^{-1}.

The energy flow diagram of the diesel hybrid powertrain, but not the city bus, is shown in Fig. 6 (d). The average diesel engine efficiency was about 33.5%, which is lower than the fuel cell engine. The total efficiency of the generator and the rectifier was about 85%. There were no vehicle auxiliary components, because the testing was carried out on a test bench. About 33.1% of the whole energy was output from the electric motor, and about 11% of the energy was recycled. The battery slightly discharged. As a result, the fuel economy was 30L.100km^{-1}, the NOx emission was 8.5g.km^{-1}, and the PM emission was 0.1g.km^{-1} (Cao Guijun, 2009).

6. Conclusions

This chapter proposes an Equivalent Consumption Minimization Strategy (ECMS) for the series hybrid city buses with two different powertrain configurations, Fuel cell + battery and diesel engine + battery.

An equivalent consumption model is firstly introduced, incorporating the fuel consumption of power unit and the battery equivalent consumption. The concept of the equivalent consumption is further developed compared with its origin. The ECMS is developed based on the analytical solution to the instantaneous optimization problem.

Because of the linear relationship between the fuel consumption and the DC/DC power, the battery optimal power is a function of the battery SOC and the ratio coefficient δ.

The ratio coefficient δ depends on the braking regeneration strategy. And it changes with the working conditions of the powertrain system. It is the key parameter of the ECMS, and changes with time. Besides, a battery balance power is introduced to keep the battey SOC around a target value.
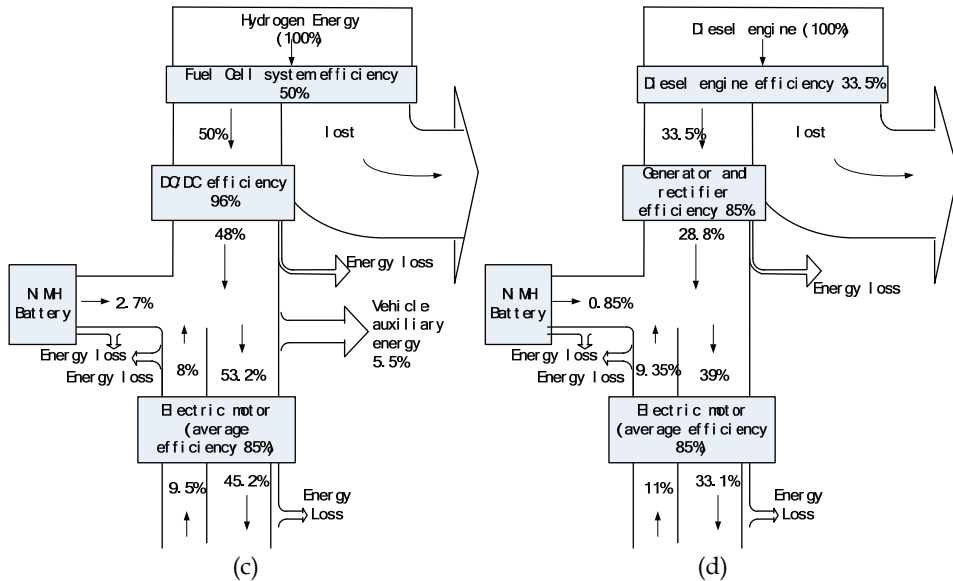

(a)

(b)

(c)   (d)
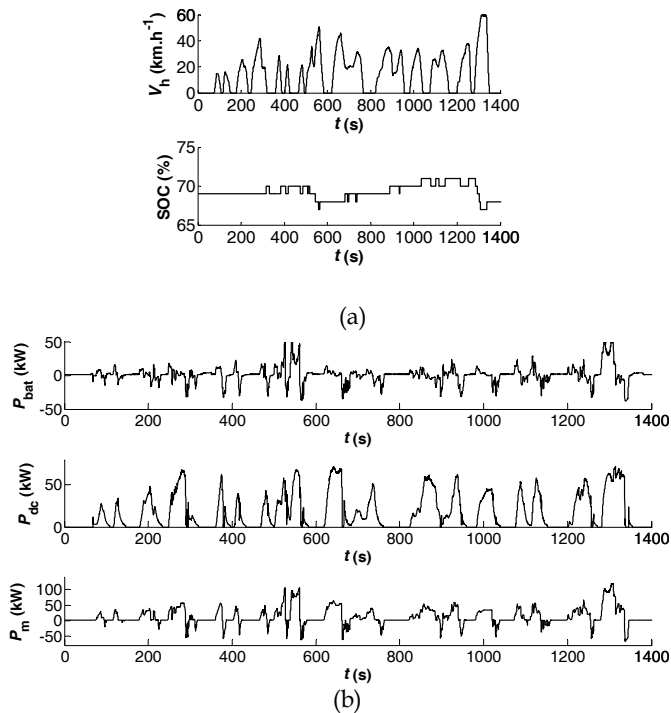
Fig. 6. (a) Vehicle velocity and the battery SOC in the "China city bus typical cycle" (b) Power split of the fuel cell hybrid city bus, $\delta = 0.6$ (c) energy flow diagram of the fuel cell hybrid city bus (d) energy flow diagram of the diesel hybrid powertrain, $\delta = 0.6$

The ECMS of the diesel hybrid powertrain is a little complex, because there is a quadratic relationship between the fuel consumption and the engine power. The battery optimal power is a function of powertrain demand power, battery SOC and the ratio coefficient δ. For the same reason, the balance power is introduced to calculate the target power of the rectifier.

The fuel cell + battery city bus was tested in the "China city bus typical cycle". Results show that, the battery SOC was kept around 70%, and the fuel economy was 7.4kg.100km^{-1}. Fuel consumption increases with the ration coefficient δ increases.
The diesel + battery powertrain was tested in lab with the same cycle. Results show that, the battery SOC was kept in balance, and the fuel economy was 30L.100km^{-1}.

In this chapter, we only consider the fuel economy in the optimal strategy. However, the fuel cell durability and the exhaust emission should also be included in the optimized strategy.

Because of the linear characteristics of the fuel cell system, the fuel economy is mainly determined by the ratio coefficient δ. It means that, the braking regeneration strategy contributes much more than the power split strategy. Thus, the primary challenge in power split strategy is to prolong the fuel cell durability, while fulfill the powertrain power demand.

The fuel economy of the diesel engine hybrid bus is determined by δ, SOC and vehicle power demand. The braking regeneration strategy is also very important. The primary challenge of the control system is to make the engine work on the optimal curve, as in Fig. 5 (a). Actually we use a feedforward + feedbackward method to control the engine working point so as to lower the fuel consumption and the exhaust emission (Cao Guijun, 2009). This control problem is valuable to be studied in future.

7. References

N., Jalil; N., A., Kheir & M., Salman. (1997). A rule-based energy management strategy for a series hybrid vehicle, *Proceedings of the American Control Conference*, pp. 689-693

S., Aoyagi; Y., Hasegawa; T., Yonekura; H., Abe. (2001). Energy efficiency improvement of series hybrid vehicle. *JSAE Review*, Vol. 22, (2001), pp. 259-264

G., Paganelli; S., Delprat; T., M., Guerra; J., Rimaux; J., J., Santin. (2002). Equivalent consumption minimization strategy for parallel hybrid powertrains. *IEEE Vehicular Technology Conference*, Vol. 4, (2002), pp. 2076-2081

C., C., Lin; H., Peng; J.,W., Grizzle; J., Kang. (2003). Power managment strategy for a parallel hybrid electric truck. *IEEE Transactions on Control Systems Technology*, Vol. 11, (2003), pp. 839-849

Andreas Schell; Huei Peng; Doanh Tran; et al. (2005). Modelling and control strategy development for fuel cell electric vehicles. *Annual Reviews in Control*, Vol. 29, No. 1, pp. 159~168

B., He; M., Yang. (2006). Optimization-based energy management of series hybrid vehicles considering transient behavior. *International Journal of Alternative Propulsion*, Vol. 1, No. 1, pp. 79~96

Schouten N., J.,; Salman M., A.,; Kheir N., A. (2007). Fuzzy Logic Control for Parallel Hybrid Vehicles. *IEEE Transactions on Control Systems Technology*, Vol. 10, No. 3, pp. 460~468

Amin Hajizadeh; Masoud Aliakbar Golkar. (2007). Intelligent power management strategy of hybrid distributed generation system. *International Journal of Electrical Power & Energy Systems*, Vol. 29, No. 10, pp. 783~795

Vanessa Paladini; Teresa Donateo; Arturo de Ris; et al. (2007). Super-capacitors fuel cell hybrid electric vehicle optimization and control strategy development. *Energy Conversion and Management*, Vol. 48, No. 1, pp. 3001~3008

Xi Zhang; Chunting Mi; Abul Masrur & David Daniszewski. (2008). Wavelet Based Power Management of Hybrid Electric Vehicles with Multiple Onboard Power Sources. *Journal of Power Sources*, Vol. 185, No. 2, pp. 1533-1543

Paganelli G., ; Delprat S., ; Guerra T., ; et al. (2002). Equivalent consumption minimization strategy for parallel hybrid powertrains. *IEEE 55th VTC*, Birmingham, Al, USA,Vol. 4, pp. 2076~2081

Xu Liangfei; Hua Jianfeng; Li Xiangjun; Meng Qingran; Li Jianqiu; Ouyang Minggao. (2008). Control strategy optimization of a hybrid fuel cell vehicle with braking energy regeneration. *IEEE Vehicle Power and Propulsion Conference*, Harbin, China, pp. 1-6

Cao Guijun. (2009).Research on the auxiliary power unit of the diesel based series hybrid electric powertrain. *PhD dissertation*, Tsinghua University, Beijing, China

He Bin. (2006). Energy management and dynamic control of series hybrid vehicles. *PhD dissertation*, Tsinghua University, Beijing, China

V., H., Johnson. (2002). Battery performance models in ADVISOR. *Journal of Power Sources*, Vol. 110, No. 2, pp. 321~329

Intelligent Energy Management in Hybrid Electric Vehicles

Hamid Khayyam[1], Abbas Kouzani[1], Saeid Nahavandi[1],
Vincenzo Marano[2] and Giorgio Rizzoni[2]
Deakin University Australia[1] and The Ohio State University USA[2]

1. Introduction

Energy management in vehicles is an important issue because it can significantly influence the performances of the vehicles. Improving energy management in vehicles can deliver important benefits such as reducing fuel consumption, decreasing emission, lower running cost, reducing noise pollution, and improving driving performance and ease of use. According to Mainins (Manins, 2000), each year more then 50 million new cars are produced in the world. However, usually only 30% to 40% of the energy produced by the engine is used to drive a car. The large energy waste of around 60% is the result of having an engine powerful enough to cope with the maximum power demand despite the fact that such power is required for only a vary small percentage of vehicles' operating time. In addition, vehicle emissions are a source of greenhouse gas pollution emitting 70% to 90% of urban air pollution (SOE, 2006). Fuel economy benchmarks and emission regulations have encouraged vehicle manufactures and researchers to investigate new technologies to enhance fuel economy and minimise emissions. The energy efficiency of vehicles can be improved by enhancing the efficiency of the vehicle. Implementing energy management strategies in classical vehicles does not fully deliver the expected benefits. Hybrid electric vehicles, on the other hand, offer a platform that can accommodate advanced energy management strategies giving rise to full realization of the stated benefits. Intelligent energy management methods can observe and learn driver behavior, environmental and vehicle conditions, and intelligently control the operation of the hybrid electric vehicle.

A Hybrid Electric Vehicle (HEV) takes advantage of an Internal Combustion Engine (ICE) and an Electric Motor (EM) to deliver fuel consumption and exhaust emission reduction. An EM is powered by on-board battery packs to drive the vehicle. From the consumers overall perspective, the HEV is essentially the same as a Conventional Vehicle (CV). Moreover, HEVs are refuelled in the same way as a CV. A HEV has the advantage over a pure Electric Vehicle (EV) in both travelling range and convenience, as there is no need to recharge the battery through a power point for long hours. Importantly, a HEV has the potential to improve fuel economy by almost 50%, while also possessing all the advantages and flexibility of a CV (Ehsani et al,. 2005). Hence, HEVs solve the problems of EVs whilst minimising the shortcoming of CVs providing the benefits of both electric and conventional

vehicles. HEVs are categorised into three groups: Series (S-HEV), Parallel (P-HEV), and Series/Parallel (S/P-HEV) as shown in Fig. 1.

In an S-HEV, there is no mechanical link between the ICE and drive train. This means that the ICE can run continuously in its preferred operating range, whereas the drivetrain is driven by an electric machine. For the electric power request, it relies on the battery plus the generator. The generator is driven by the ICE and maintains an appropriate energy level in the battery. A disadvantage of this configuration is that energy is first converted from mechanical power to electric power with the generator and then back to mechanical power by the electric machine, both introducing losses.

The P-HEV establishes a parallel connection between the ICE and the electric machine that both are allowed to give force to the drive the vehicle. The power through the EM can be positive as well as negative. This allows the EM to operate in motor mode and generator mode. At a top-level view, the P-HEV configuration looks similar to a conventional vehicle, although the EM in a conventional vehicle operates only in generator mode.

Finally, the last vehicle configuration is an S/P-HEV. It merges the topology of a series and a parallel HEV. S/P-HEVs have the highest complexity since power to the drivetrain can follow various trajectories. Recently plug-in hybrid electric vehicle (PHEV) has come to market. A PHEV is a hybrid electric vehicle that described above. The PHEV batteries can be recharged by plugging into an electric power source. A PHEV combines type of conventional hybrid electric vehicles and battery electric vehicles, possessing both an internal combustion engine and batteries for power. The desire strategy using PHEV can be employed as follows: in short distance travelling electric vehicle (EV) mode operation such as urban and for long distance travelling hybrid electric vehicle (HEV) mode operation such as highways.

The most important challenge for the development of P-HEV is the synchronization of multiple energy sources and conversion of power flow control for both the mechanical and electrical paths in optimal fuel efficiency and battery areas.The difficulty in the development of hybrid electric vehicles is the coordination of multiple sources such as mechanical and electrical. The reason why a P-HEV is considered in this work is that it has fewer disadvantages and less complexity (Kessels.J, 2007) (Ehsani et al.,2005).
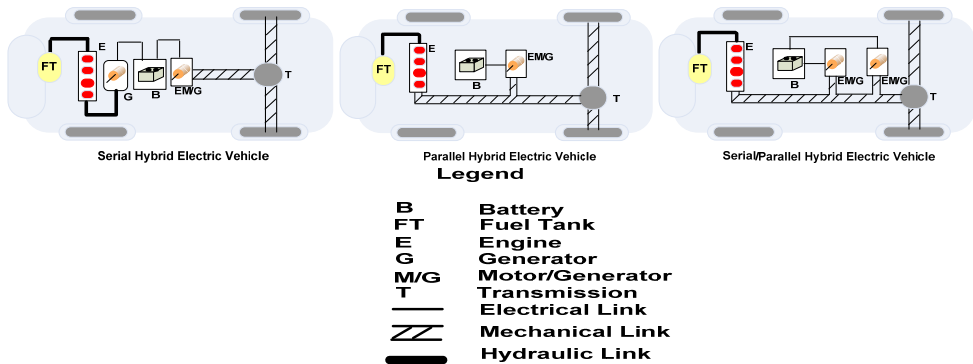

Fig. 1. Three HEVs structures.

Nevertheless, any vehicle needs to deal with uncertain factors such as environment conditions and also driver behaviour. HEVs are a highly complex systems comprising a

large number of mechanical, electronic, and electromechanical elements (Zhu et al.,2002). Hence a HEV can be considered as a Complex System (CS).

A Complex System is a system that can be analyzed into many components having relatively many relations among them, so that the behaviour of each component depends on the behaviour of others (Simon. A.H,1973).

In the real world, many problems and systems exist that are too complex or uncertain to be represented by complete and accurate mathematical models. However, such systems need to be designed, optimized, and controlled. CSs can be handled by Intelligent Systems (ISs). ISs can learn from examples, are fault tolerant, are able to deal with non-linear problems, and once trained can perform prediction and generalization at high speed. Intelligence systems have been used in diverse applications in control, robotics, pattern recognition, forecasting, medicine, power systems, manufacturing, optimization, signal processing, and social/psychological sciences. They are useful in system modelling such as in implementing complex mappings and system identification. ISs comprise areas like expert systems, artificial neural networks, genetic algorithms, fuzzy logic and various hybrid systems, which combine two or more of these techniques. ISs play an important role in modelling and prediction of the performance and control of energy and renewable energy processes. According to literature, ISs have been applied to energy and renewable energy engineering.

ISs can be developed through modelling and simulation. The modelling and simulation approach has become an essential tool for mechanical engineers and automotive researches in improving efficiency and timing of vehicle design and development, resulting in the delivery of significant cost saving as well as environmental benefits. The modelling and simulation is generally defined as mathematical realisation and computerised analysis of abstract representation of systems. The modelling and simulation helps achieve insight into the functionality of the modelled systems, and investigate the systems' behaviours and performances. The modelling and simulation is used in a variety of practical contexts relating to the design, development, and use of conventional as well as advanced vehicles including: design and evaluation of vehicle performance, fuel consumption, emission, energy storage devices, internal combustion engine, hybrid engine, accessories, composite materials, determination of drag using wind tunnel, training drivers trough virtual vehicle, collecting and analysing sensory information, identifying critical test conditions, investigating crash factors, characterising road topology, testing and analysing energy management strategies, and so on.

This work employs the modelling and simulation approach to develop an Intelligent Energy Management System (IEMS) for a P-HEV.

The main objective is to optimize fuel consumption and reduce emissions. The work involves the analysis of the role of drivetrain, energy management control strategy and the associated impacts on the fuel consumption with combined wind/drag, slope, rolling, and accessories loads.

2. Literature Review and Background

This section provides a review of the main approaches used in modelling and control of energy management of HEVs. In a CV, energy can be dissipated in a number of ways including (Kessels.J, 2007):

i.   Brake utilisation: The brake is applied by the driver to decelerate the vehicle resulting in the loss of kinetic energy in the form of heat.

    ii.   Engine start/stop: The engine often runs idle during the utilisation of vehicle resulting in an unnecessary consumption of fuel.

   iii.   Uneconomic engine operating condition: An engine often demonstrates non-   linear fuel consumption behaviour in certain operating conditions that causes an excessive use of fuel.

   iv.   Unscheduled load: Certain mechanical and electrical loads get activated outside the economic operating point of engine increasing the fuel consumption.

P-HEVs provide a platform to reduce the wasted energy. The most important challenge for the development of P-HEV is the synchronization of multiple energy sources and conversion of power flow control for both the mechanical and electrical paths. Control in HEVs is recognized as two levels of actions: supervisory control and component control. In this study supervisory control is investigated as a suitable control strategy in energy management.

The control strategy is an algorithm that is used for issuing a sequence of instructions from the vehicle central controller to operate the drivetrain of the vehicle.   The control strategy needs to monitor uncertain events. Moreover, in order to improve the system, the control strategy can provide optimized energy management. The control strategies in a P-HEV can be classified in two main groups as follows.

2.1 Rule-Based Control

The control rules techniques are based on mathematical, heuristics, and human expertise generally with an analytical knowledge of a predefined driving cycle. Control rules can be categorized in three methods.

A. Rule-Based

This method is based on an examination of the power requirements, ICE efficiency, fuel or emission maps. Human knowledge is used to design rules to split the requested power between converters. The method can be categorized into three groups: on/off control (Ehsani et al.,2005), base line control (Zhu et al.,2002) (Sciarretta et al., 2004) (Linl et al.,2004) (Lyshevski,1999) (Barsali et al., 2004) (Khayyam et al., 2008), and discrete time events (Zhang & Chen, 2001) approaches.

B. Fuzzy logic

Fuzzy logic control has a nonlinear structure that can deal with the nonlinear structure of the power split problem. Fuzzy logic has a more robust structure and offers more design flexibility. The problem with fuzzy logic is the optimization and mathematical manipulation of defuzzification system. The defuzzification process consumes memory and time in controller. Some fuzzy logic controller have been developed for HEVs including (Baumann et al., 2000) (Farrokhi & Mohebbi, 2005) (Langari &won, 2005) (Mohebbi et al.,2005) (Salman et al., 2000) (Schouten et al.,2002) (Hajimiri at al., 2008).

C. Neuro-Fuzzy

There are also combinations of fuzzy logic and artificial neural called neuro-fuzzy control (Mohebbi et al.,2005) and fuzzy discrete event control (Bathaee et al., 2005).

2.2 Optimal Control

In optimal control the controller is optimized according to a cost function of the system. Therefore, optimal control strategies are almost perfect. However, the optimal controllers are sensitive to parameter changes and also to noise. To perform the optimization process, all the dynamic and static behaviours of the system components are taken into consideration. Calculations are usually simplified by introducing assumptions which means that the solution is optimum only under the assumptions. On the other hand, the discrete time events method is simple and more robust. System behaviours are divided into discrete events. Each event is connected to another by certain rules (Mohebbi & Farrokhi, 2007).

If this optimal control is performed over a fixed driving cycle, a global optimum solution can be found. In fact, the optimal control system solution is noncasual in that it achieves the reduction of fuel consumption using information of future and past power demands. Obviously, this technique cannot be used directly for real-time energy management. Optimal control can be divided in two groups as follows.

A. Global Optimization (off line)

There are several reported solutions to achieve performance targets by optimization of a cost function representing efficiency over a drive cycle, yielding global optimal operating points. The global optimization techniques are not directly applicable for real-time problems, considering the fact that they are casual solutions. This is due to their computational complexity. Some of the global optimization methods are given below:

A.1 Neural Networks

Neural networks have the ability to be trained online or offline, but online training consumes memory in a controller. This trainability characteristic makes neural networks as a good candidate for adaptive energy management systems. As an example, the work presented in (Mohebbi &Farrokhi,2007) developed a neural network for optimal control. Prokhorov (Prokhorov D.V , 2008) used a neural network controller for improved fuel efficiency of the Toyota Prius hybrid electric vehicle. A new method to detect and mitigate a battery fault was also presented. The developed approach was based on recurrent networks and included the extended Kalman filter.

A.2 Classical Optimal Control

(Delprat et al,. 2004) used the optimal control theory based on Lewis and Syrmos (Lewis & Syrmos., 1995) work. This method is directly applied to find a global solution for the energy management problem in a parallel torque-addition arrangement. The analytical nature of this method makes it a good one. However, variation of drivetrain structure makes it difficult to find an analytical solution, compared with numerical and iterative-based methods. Some optimal control have been developed for HEVs including (Wei et al.,2007) (Pisu & Rizzoni,2007) (Musardo et al.,2007).

A.3 Linear Programming

This method can formulate the problem of optimizing the fuel efficiency as a nonlinear convex optimization problem that is approximated by a large linear program (Tate &

Boyd,1998). The approximations used for transformations and the fact that LP may not be applicable to a more sophisticated drivetrain degrade the proposed approach.

A.4 Dynamic and Stochastic Programming

Dynamic Programming (DP) method utilizes the minimizing cost function over a driving cycle. (Lin et al.,2003) demonstrated that the approach does not give a real-time solution by nature. A family of random driving cycles needs to be used to find an optimal solution.

A.5 Genetic Algorithm

The Genetic Algorithm (GA) has been used to solve a constrained nonlinear programming problem. (Piccolo et al.,2001) showed that GA is very useful for complex nonlinear optimization problems. This is because GA leads to a more accurate exploration of the solution space than a conventional gradient-based procedure. But GA dose not give the necessary view to the designer of the powertrain , unlike an analytical approach. Montazeri et al. (Montazeri et al., 2006) described the application of genetic algorithm for optimization of control parameters in P-HEV.

B. Real Time Optimization (on line)

In order to develop a cost function for real-time optimization, the following methods can be used.

B.1 Model Predictive Control

(Salman et al., 2005) utilized a look-ahead window to find a real-time predictive optimal control law. This approach can be used for superior fuel economy by previewing the driving pattern and road information.

B.2 Decoupling Control

(Barbarisi et al.,2005) proposed a novel strategy to assure acceptable drivability of the vehicle that was based on the vehicle's dynamic model. Based on the proposed decoupling methods, the controller's output is composed of different components.

B.3 Genetic-Fuzzy

The genetic-fuzzy control strategy is a fuzzy logic controller that is tuned by a genetic algorithm. Poursamad et al. (Poursamad et al.,2008) and Montazeri et al. (Montazeri et al., 2008) applied these control strategy model to minimize fuel consumption and emission.

2.3 Discussions
The presented work is focused on a control strategy to reduce fuel consumption though considering performance and driveability. Our optimal control strategy is found in two steps, first finding the control which results in the reduction of fuel consumption together and offering the best performance, and second taking vehicle driveability into consideration. Among the control strategies for the best fuel economy, dynamic programming is the only one that assures global optimality if the driving cycle is known in advance.
However, it does not apply to real-time problems. On the other hand, fuzzy logic, rule-based, and neuro-fuzzy controllers are not generally optimized, but applied to real-time

problems. If the future driving conditions of a few minutes ahead can be predicted then the optimal controller can help find a suboptimal solution.

3. Factors Involved in Energy Management of Hybrid Electric Vehicles

Bandivadekar and Heywood (Bandivadekar & Heywood, 2007) presented an analysis that shows the possibility of halving the fuel consumption of new vehicles by 2035. Enhancement in vehicle control and management strategies is considered to be an influential mean in reducing the fuel consumption of vehicles. Energy management approaches in vehicles can be realised through considering a number of factors including (Cacciabue et al., 2009): environmental conditions, driver behaviour, vehicle specifications, and intelligent transportation approach (EPA, 2004). In order to develop an energy management system, a number of models need to be implemented and used. These models are described in the following.

3.1 Main factors involved in energy management system of HEVs

A HEV can be considered as a complex system consisting of subsystems. In the development of energy management systems, model of the HEV subsystems are developed and used. Fig. 2 shows an overview of the energy management model for HEVs.
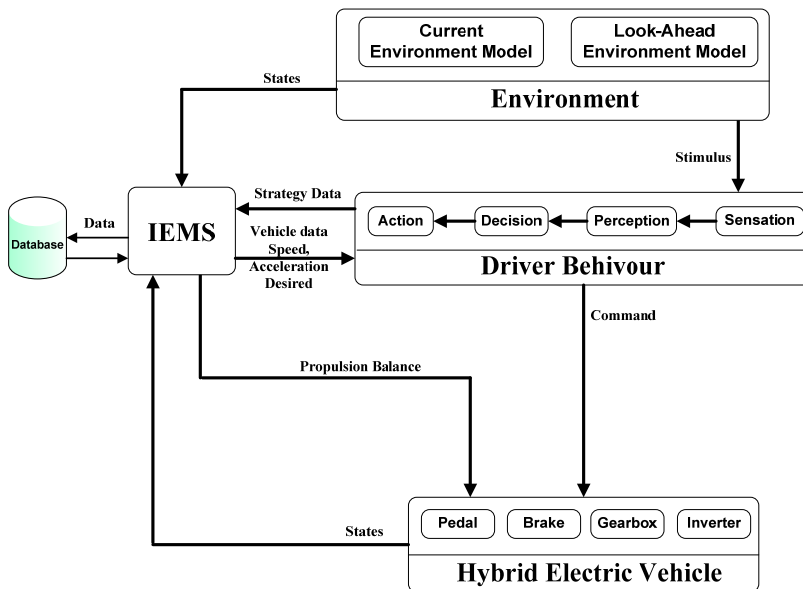

Fig. 2. Overview of the energy management model for HEVs.

3.2 Model of Environment

Among the factors that are involved in HEV systems, the environment conditions such as road geometrical specifications and wind behaviour are often unknown and uncertain during drives. The information about the geometrical specification and wind behaviour of the road

ahead of the vehicle can be used by an intelligent system to reduce fuel consumption of the vehicles (Khayyam et al., 2008). However, this information is often unavailable to the intelligent system on-board of a vehicle in real-time. Thus, utilising on-line and off-line prediction and monitoring of the geometrical specifications and wind behaviour of the road ahead of vehicles can improve their performances. Environmental information can be categorized in two groups: current and look-ahead. The data include road geometry, road friction, wind drag, and ambient temperature. It has been demonstrated that lookahead environment information can be employed by the energy management system to achieve reduction of fuel consumption (Hellstrom et al.,2009). Khayyam et al. (Khayyam et al.,2008) presented a Slope Prediction Unit (SPU) to calculate the slope angle of the road within the distance of 50-300 meters away from the vehicle. This information reduced fuel consumption about 6.1% liter/100 km during simulation. Global Positioning Systems (GPS) and Geographic Information Systems (GIS) can provide static and dynamic road information.

Current Environment Model (CEM) is an algorithm that creates data associated with environmental conditions and frictions. Look-ahead Environment model (LEM) is an algorithm that creates data associated with future environmental conditions and frictions encountered by the vehicle.

In order to model environment, a number of methods can be used. Khayyam et al. (Khayyam et al.,2009a) proposed a method that can be used to produce authentic highway height data using a set of probability distributions. They considered a highway as a complex road which can have any kind of possible geometrical variations. The presented method models highway heights by Rayleigh probabilistic distribution function. In addition, highway geometric design laws were employed to modify the created highway data making it consistent with the real highway situation. The proposed model is then used to produce a 3D realistic road. The method is called a Probabilistic Highway Modelling (PMH) technique. PMH is capable of creating artificial highway and wind data that possess statistical characteristics of real highway and wind situations. A highway is considered to contain a collection of road segments. The Poisson Probability Distribution Function (PDF) is used to produce a random number that determines the number of road segments. Segments can then have different lengths. For each segment, the exponential PDF produces a random number that represents the segment length. In addition, for each segment, two other random numbers are generated and used to form the geometry of the segment. The Rayleigh PDF is employed to produce a random number that represents the height change of the segment. Also, the Gaussian PDF is used to form a random number that gives the bend deflection change in the segment. The random numbers for height and bend could be small or large injecting varying degrees of heights and bends into different road segments. Also, highway geometric design laws are used to modify the created highway data to make it consistent with the real physical highway situation.

A wind is constructed using a collection of regions of differing lengths. A wind creation algorithm is an iterative routine. The algorithm creates wind speed and direction values for each region. The exponential PDF produces a random number that represents the region length. The Weibull PDF is employed to produce a random number that represents the wind speed value in the region. Also, the uniform PDF is used to form a random number that gives the wind direction value in the region.

The PHM can be employed in simulation of problems involving highway roads such as energy optimization of conventional and hybrid electric vehicles. Fig. 3 displays a flowchart

diagram description of the highway creation algorithm using the PHM. The result of the highway creation algorithm demonstrates in Fig. 4 that show a 3D representation of the constructed sample highway using the PHM. Fig. 5 displays a flowchart diagram description of the wind creation algorithm using the developed PHM concept.
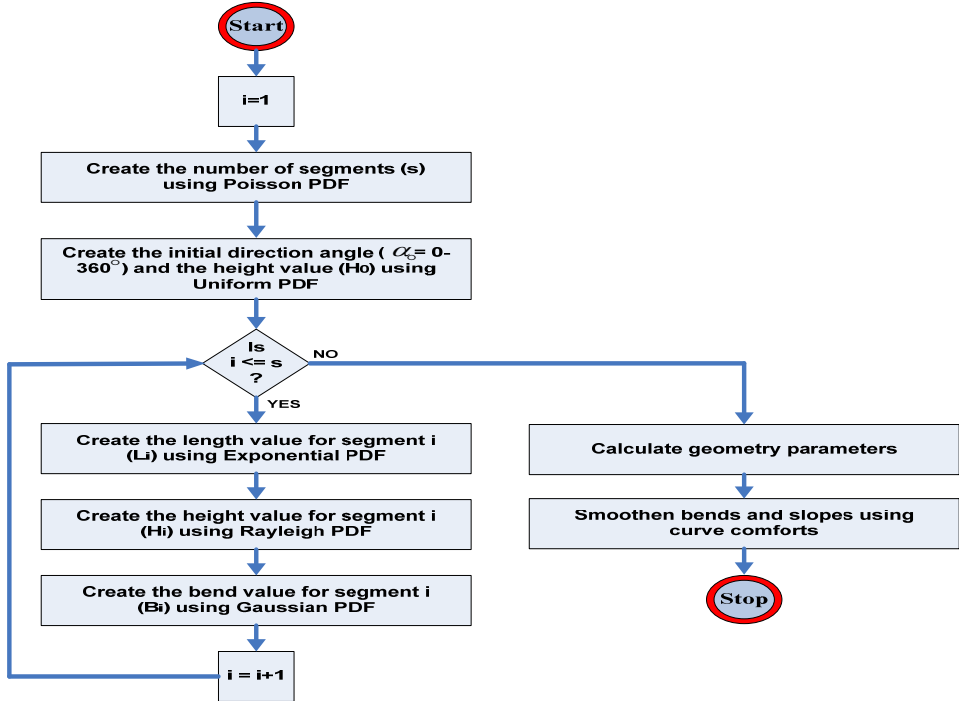

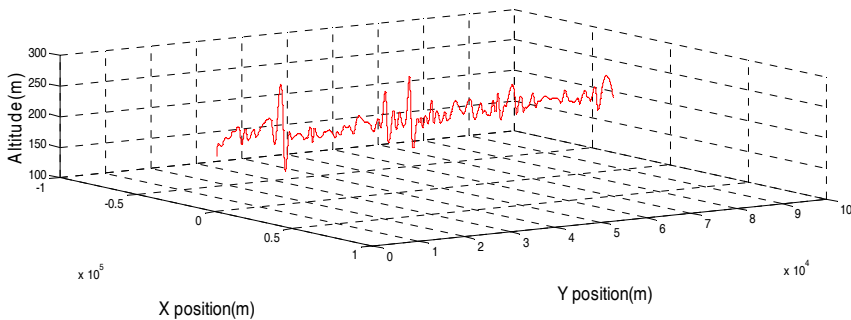Fig. 3. Highway creation algorithm using the developed PHM.

Fig. 4. 3D representation of the constructed sample highway using PMH technique.
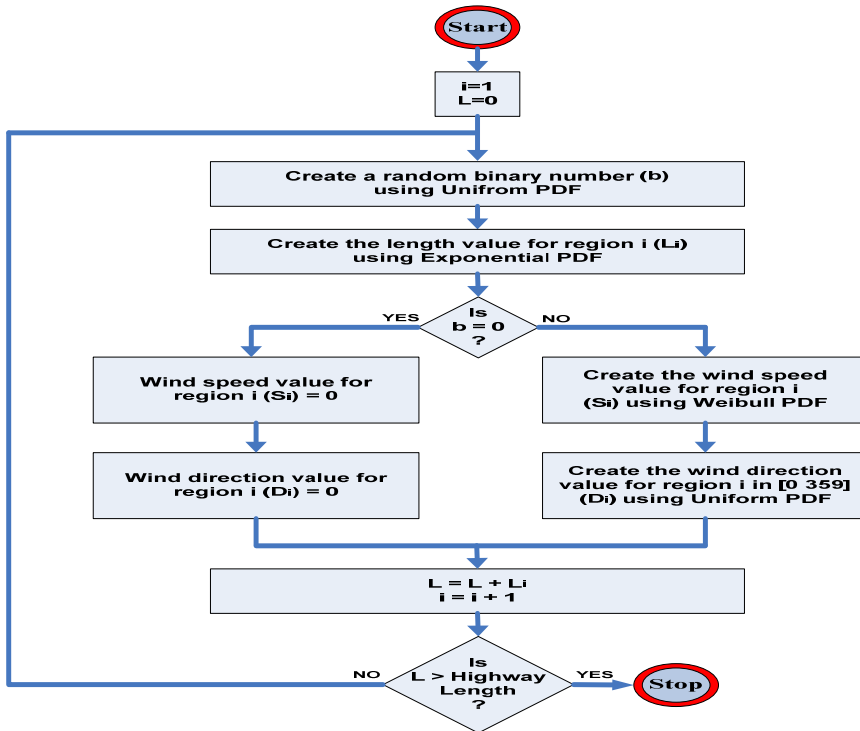
Fig. 5. Wind creation algorithm using the developed PHM.

3.3 Model of Driver

Driver behaviour has a strong influence on emissions and fuel consumption of the vehicle. Modelling driver behaviour can be done using different methods. As an example, the Driver-Vehicle-Environment (DVE) (Cacciabue, 2007) (Lin et al., 2005) method models human machine interaction and associated taxonomies for classifying human behaviour. De. Vlieger et al. (De. Vlieger et al.,2000) identified three types of driving behaviour as follows:

1- Calm driving that implies anticipating other road user's movement, traffic lights, speed limits, and avoiding hard acceleration.
2- Normal driving that implies moderate acceleration and braking.
3-Aggressive driving that implies sudden acceleration and heavy braking.

Moreover, they note that emissions obtained from aggressive driving in urban and rural traffic are much higher than those obtained from normal driving. A similar trend is observed in relation to fuel consumption. It is stated that the driving style affects the emission rate and the fuel consumption rate.

Average acceleration and Standard Deviation (SD) of acceleration over a specific driving range are used to identify the driving style. Acceleration criteria for the classification of the

driver's style are based on the acceleration ranges proposed by De Vlieger et al. (De Vlieger et al. 2000). They defined the typical ranges of average accelerations as describe in table 1.

Acceleration	Calm Driving	Normal Driving	Aggressive Driving
City Journey(m/s²)	4.85-6.9	6.98-8.6	9.15-11.8
Highway Journey(m/s²)	0.85	1.0	2.16

Table 1. Overview of the tested acceleration (De Vlieger et al., 2000).

Our objective is to use support dynamic real-time driver behaviour system in the energy management system. A driver first determines the drive strategy, selects the engine specifications, starts the vehicle motion, and controls the mass flow rate of fuel into ICE by changing the pedal, gear, brake, and clutch. Also, the driver sends this data as drive strategy to IEMS.

3.4 Model of Vehicle (Quasi-Static)

In a P-HEV, both the Internal Combustion Engine (ICE) and the Integrated Starter/Generator (ISG) can give tractive force to the wheels. Furthermore, the ISG will be used as a generator to supply the electric loads. A schematic drawing of the vehicle configuration is shown in Fig. 6.
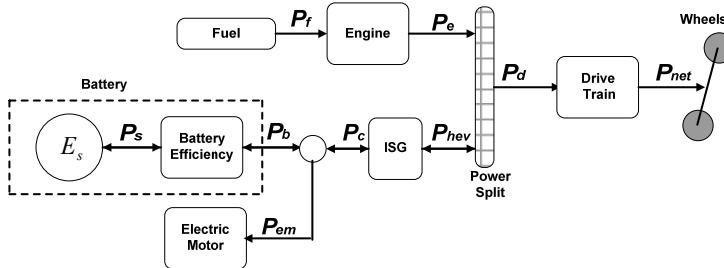

Fig. 6. P-HEV topology (Kessels.J,2007).

The power demand of the drivetrain P_d covers all the elements of the drivetrain, including the transmission and the clutch. The engine speed ω and the drivetrain torque t_d are calculated back from the vehicle speed and denote the driver's power demand:

$$P_d = \omega \tau_d \tag{1}$$

The power split device is assumed to have no energy losses and establishes the following power balance:

$$P_e = P_d + P_{hev} \tag{2}$$

Where : P_{hev} is hybrid power and P_e is engine power.

3.4.1 Conventional Vehicle Specification

A vehicle ICE can be treated as a controlled volume system whose energy balance is given as follows:

$$\dot{Q}_{combustion} = (\dot{Q}_{fuel} + \dot{Q}_{air} - \dot{Q}_{exhaust})$$
$$= P_{road-friction} + P_{drag} + P_{slope} + P_{accessory} + P_{driving} + \dot{Q}_{water/oil} + \dot{Q}_{heatloss} \tag{3}$$

In order to include all losses, Equation (3) is reformed into the following equation where the effect of different losses is taken into account by corresponding efficiencies:

$$(\dot{Q}_{combustion}) \times \eta_{otto} \times \eta_{fuel-air} \times \eta_{mechanical} \times \eta_{heat\ loss} = P_{net}$$
$$= P_{road-friction} + P_{drag} + P_{slope} + P_{accessory} + P_{driving} \tag{4}$$

where: P_{net} = Power output of engine

η_{otto} =Otto cycle efficiency= $1 - \dfrac{1}{r_c^{(\gamma-1)}}$ =0.529 (Pullkrabek,1997)

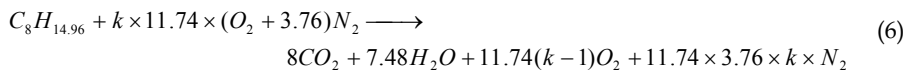$\eta_{fuel-air}$ = Real fuel air engine efficiency =0.75(Yaodong Wang,2007)

$\eta_{mechanical}$ =Mechanical efficiency=0.9 (Plint ,1997)

$\eta_{heat\ loss}$ = Heat loss efficiency=0.8 (Pullkrabek,1997)

These efficiency are depend on some variable factors and situations.They can be measured by industrial vehicle companies. In the section 3.4.3 we will select specific efficiency in our model.To calculate $\dot{Q}_{combaustion}$ Equation (3) is used:

$$\dot{Q}_{combustion} = \dot{m}_{fuel} \times q_{combustion} \tag{5}$$

where $q_{combustion}$ is the combustion energy. In this model, the fuel is assumed to be $C_n H_{1.87n}$ in (Wang et al., 2007) . The complete combustion of $C_8 H_{14.96}$ with *1+k* percent theoretical air is written as:

$$C_8 H_{14.96} + k \times 11.74 \times (O_2 + 3.76) N_2 \longrightarrow$$
$$8CO_2 + 7.48 H_2 O + 11.74(k-1)O_2 + 11.74 \times 3.76 \times k \times N_2 \tag{6}$$

If the heat transfer was accurately measured, the released energy would be 109100 kJ/kg per 8 mole of CO_2 (Heywood .B.J, 1998). The result of Equation (6) gives:

$$q_{combustion} + \sum ni\,[hf + \Delta h]i = W_{C.V.} + \sum n_e[h_f + \Delta h]_e \tag{7}$$

Where:

$$\sum n_i[h_f + \Delta h]_i = h_f C_8 H_{14.96} + 1.2 \times 11.74(O_2 + 3.76 \times N_2) = 793.23\ kJ/kg$$

Description	Type	Symbol	Value
Combustion			
Enthalpy of formation	E-F	$\overline{h}_f^{\,\circ}$	Thermodynamic tables
Sensible formation	E-F	$\Delta\,\overline{h}$	Thermodynamic tables
Combustion energy	E-F	$q_{combustion}$	38017 kJ/kg
Mass flow rate of fuel combustion	V-O	$\dot{m}_{fuel}$	kg/s
Temperature of fuel	V-S	T_{fuel}	27 °C
Temperature of air	V-S	T_{air}	27 °C
Temperature of exhaust	V-S	$T_{exhaust}$	450 °C
Engine compression ratio	E-F	r_c	8.6
Air compression ratio	E-F	γ	1.35
Ratio of nitrogen per oxygen	E-F	$r_{N2/O2}$	3.76
Excess air	V-O	$E_{excessair}$	20%
Road			
Road friction	E-F	$F_{friction}$	$C_{rolling}\,mg\cos\Phi$
Road friction coefficient	E-F	$C_{rolling}$	0. 01
Gravity acceleration	E-F	g	9.8 m/s²
Vehicle velocity	V-O	V_1	16.6 m/s
Vehicle angle	V-O	θ_1	0°
Drag			
Drag friction	E-F	F_{drag}	$C_{drag}(\theta)\times\frac{1}{2}\rho V^2 A(\theta)$
Wind angle of attack	E-F	θ_2	Random direction (0-360º)
Wind velocity	E-F	V_2	0-6 m/s
Result wind and vehicle angle	V-O	θ	Calculate in simulation IEMS
Result of wind and vehicle speed	V-O	V_t	Calculate in simulation IEMS
Result of wind and vehicle speed	V-O	V_{t-1}	Calculate in simulation IEMS
Drag coefficient (By simulation)	V-S	$C_{drag}(\theta)$	$-(0.00005)\times(\theta)+0.0097\times(\theta)+0.31$
Front surface area	V-S	$A(\theta)$	$1.8\times 1/\cos(\theta)$
Vehicle + passenger mass	V-O	m	1280 kg
Air density	E-F	ρ	1.225 kg/m³
Slope			
Slope friction	R-O	F_{slope}	$mg\sin\Phi$
Road slope angle	R-O	Φ	$-1\% \le \mathrm{atan}(\varnothing) \le +0.6\%$
Radius of Comfort requirement	R-O	R	100 m
Accessory			
Accessory	V-O	$P_{accessory}$	0-4250 watt

V-S vehicle specification; V-O vehicle operation; E-F environment factors;
R-O road condition.

Table 2. Parameters involved in energy balance equation

and

$$\sum n_e [h_f + \Delta h]e = 8CO_2[h_f + \Delta_h]CO_2 + 7.48H_2O[h_f + \Delta_h]H_2O + 11.74 \times (0.2)O_2[\Delta_h]O_2 +$$
$$11.74 \times 3.76 \times 1.2 \times N_2[\Delta_h]N_2 = 37219.70\, kJ / kg$$

and $W_{C.V} = 0$

$$q_{combustion} = |-37219.70 + 793.23| = 38017.93\ kJ / kg \tag{8}$$

Substituting the terms stated in Table 2, the mass flow rate fuel consumption of the vehicle can be calculated as follows :

$$\dot{m}_{fuel} = \frac{P_{road-friction} + P_{drag} + P_{slope} + P_{accessory} + P_{driving}}{(q_{combustion}) \times \eta_{otto} \times \eta_{fuel-air} \times \eta_{mechanical} \times \eta_{heat\ loss}} \tag{9}$$

The total fuel consumption in this process is:

$$m_{fuel} = \int_0^T \dot{m}_{fuel} \times dt \tag{10}$$

$$P_{net} = [F_{friction} + F_{drag} + F_{slope} + F_{accessory}] \times V_t + \frac{1}{\Delta t}[1/2 \times m \times (V_{t-1}^2 - V_t^2)]$$

where t is the total numbers of steps involved in the simulation.

The symbols given in these equations are described in Table 2. The acceleration of the vehicle in Δt time can be calculated as:

$$a_t = \frac{V_t - V_{t-1}}{\Delta t} = \frac{dV}{dt} \tag{11}$$

Also, the distance traversed by vehicle in Δt is:

$$X_t = \frac{1}{2} \times a_t \times \Delta t^2 + V_{t-1} \times \Delta t \tag{12}$$

3.4.2 Parallel Hybrid Electric Vehicle Specification

The ISG is mounted on the crankshaft of the ICE and therefore, it is also coupled to the drive train of the vehicle. Since the ISG model uses power based signals, it is not possible to observe speed-dependent characteristics. The ISG operates similar to the electric machine. It can operate in two modes: generator mode ($P_{hev} >= 0$) and motor mode ($P_{hev} < 0$).

The electric power net connects the ISG with the electric loads and the battery. No losses are assumed in the electrical wires, leaving the following description:

$$P_c = P_{em} + P_b \tag{13}$$

Where: P_{em} is electric machine power, P_b battery power, and P_c electric loads.

The battery model consists of two subsystems: a static efficiency block and a dynamic energy storage block, see Fig. 7. The battery model is used where the losses grow proportionally with the power during charging ($P_b > 0$) and discharging ($P_b < 0$).

The efficiency block incorporates the energy losses during charging and discharging, whereas the energy storage block keeps track of the actual energy level E_s in the battery. At this point an integrator is used:

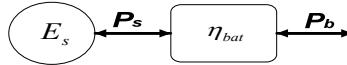$$E_s(t_e) = E_s(0) + \int_0^t P_s(t)dt \; , \; P_b = \max(\; \eta^- P_s, \frac{1}{\eta^+} P_s) \tag{14}$$

Fig. 7. Battery Model

To indicate the actual charging level of the battery, the State of Charge (SOC) is often used. However, the physical background of SOC has a strong relation with battery models based on current and voltage. Because the proposed battery model is power based, the State of Energy (SOE) is more appropriate. The SOE expresses the relative energy status as follows:

$$SOE \; = \; \frac{E_s}{E_{cap}} \times 100 \; \% \tag{15}$$

Depending on the control strategy from the EM system, three different representations of the internal battery losses are taken into account, which approximate the relation between the power P_b at the battery terminals and the net internal power P_s. Table 3 provides the specifications of the battery and EM. The battery efficiency is considered as:

$$\eta_{Batt} \; = \; 2547600 \; \Big/ \; 2881008 \; = \; 88 \; \% \tag{16}$$

Feature	Symbol	Type
Battery (NHW11)		
Cells per module		6
Total Volts	**V**max	273.6
Capacity (Amp hours)		6.5
Capacity (Watt hours)		1778.4
Electric Motor		
Operating Voltage (V)	**V**min	273
Power (W)		33000-44000

Table 3. Parameters involved in energy balance equation

3.4.3 Control strategy and optimal torque

The control strategy involves calculation of the torque produced by ICE based on various parameters such as road load and battery SOC. This includes the calculation of an optimal torque based on contending ICE parameters, and deciding the actual torque output by later modifying the optimal torque based on road load and battery SOC. The optimal torque map is shown in Fig. 8.
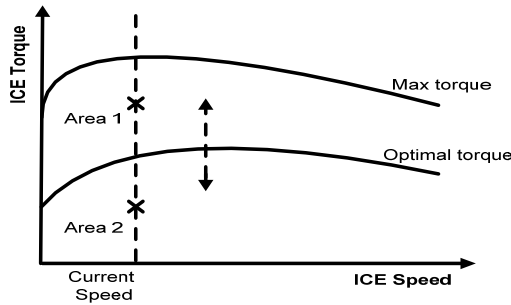
Fig. 8. Optimal torque map

At the same current speed, if the required torque is above the optimal torque (Area 1), the ICE torque should be decreased bringing it near the optimal torque point. It means that EM should be run as a motor to make up for the remaining torque, provided there is enough battery charge.

At the same current speed, if the required torque is below the optimal torque (Area 2), the ICE torque should be increased bringing it near to the optimal torque point. This is possible only if SOC is not high. We can run the EM as a generator, while running the ICE at its optimum.

In order to modeling, the following specification of engine and Motor/Inverter will be considered. Figs 9 and 10 show that the fuel converter efficiency operation and as well Motor/Inverter Efficiency.
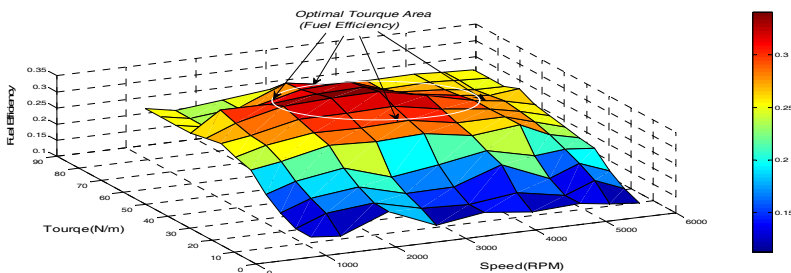

Fig. 9. Fuel Converter Operation Honda Insight 1.01 VTEC-E SI from ANL Test Data .
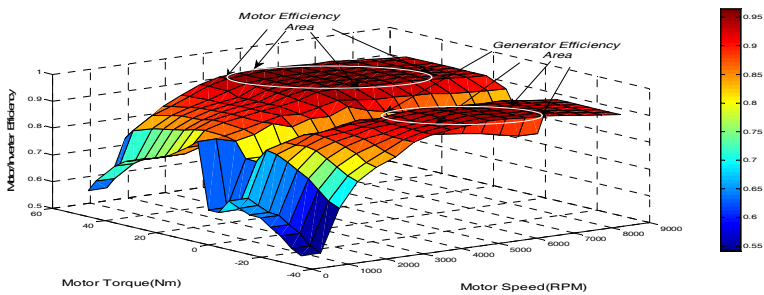

Fig. 10. Motor/Inverter Efficiency and Condition Torque Capability (Preliminary Model of Honda 10kw).

3.4.4 On-line adaptive strategy

The general control strategy for a parallel HEV can be summarized as follows (Shi et al,.2006):

i. When the speed of the vehicle is small, ICE stops and electric motor gives the driving power required which avoids higher fuel consumption and reduce emission (It is assumed that SOC is sufficient).

ii. When the speed of the vehicle is high enough, electric motor stops, ICE starts and gives the driving power required. Currently, ICE works along optimum curve depending on the cost function.

iii. If the power required is larger than what ICE can give, ICE and electric motor work together and electric motor takes additional required power from the battery (It is assumed that SOC is sufficient).

iv. If SOC of the battery drops under the safe level, ICE supplies both the energy required for travelling and extra power to charge the battery through electric motor (electric motor is at generator mode).

v. In brake state, energy floats from vehicle body to drivetrain. Electric motor works as a generator and transforms braking energy to electricity to charge the battery.

4. Intelligent System Methods in Energy Management

Intelligent energy management methods can observe and learn driver behavior, environmental and vehicle conditions, and intelligently control the operation of the hybrid vehicle. This section describes intelligent system approaches with applications to design optimization, modeling, and control of complex systems and processes.

4.1 Introduction of Complex and Uncertain System

A Complex System is (Simon. H,1973) "A system that can be analyzed into many components having relatively many relations among them, so that the behaviour of each component depends on the behaviour of others".

In the real world, we can find many problems and systems that are too complex or uncertain to be represented in complete and accurate mathematical models. And yet, we still have the need to design, optimize, or control the behaviour of such systems. Complex system can be solved by artificial intelligent systems.

Advances in intelligent systems have brought new opportunities and challenges for researchers to deal with complex and uncertain problems and systems, which could not be solved by traditional methods. Methods developed for mathematically well-defined problems with precise models may lack in autonomy and thus cannot give adequate solutions under uncertain environments (Shin &Xu, 2009). Intelligent systems are defined with high degree of autonomy, reasoning with uncertainty, higher performance, high level of abstraction, data fusion, learning and adaptation (Shoureshi & Wormley,1990).

4.2 Soft Computing Techniques

Various soft computing based techniques have emerged as useful tools for solving engineering problems that were not possible or convenient to handle by traditional methods. The soft computing techniques give computationally efficient modelling, analysis, and decision making. The techniques that belong to the soft computing include artificial neural networks (ANNs), Fuzzy sets and systems, and evolutionary computation.

4.2.1 Artificial neural networks (ANNs)

ANNs are collections of small individually interconnected processing units. Information is passed between these units along interconnections. An incoming connection has two values associated with it, an input value and a weight. The output of the unit is a function of the summed value. ANNs while implemented on computers are not programmed to perform specific tasks. Instead, they are trained with respect to data sets until they learn patterns used as inputs. Once they are trained, new patterns may be presented to them for prediction or classification. ANNs can automatically learn to recognize patterns in data from real systems or from physical models, computer programs, or other sources. They can handle many inputs and produce answers that are in a form suitable for designers.

4.2.2 Genetic Algorithms (GA)

GA is based on the way living organisms adapt to life by evolution and inheritance. GA imitates the process of evolution of population by selecting fit individuals for reproduction. Thus, GA is an optimum search technique based on the concepts of natural selection and survival of the fittest. It works with a fixed-size population of possible solutions of a problem, called individuals, which are evolving in time. A genetic algorithm utilizes three principal genetic operators: selection, crossover, and mutation.

4.2.3 Fuzzy Logic (FL)

FL is used in control engineering. It is based on reasoning which employs linguistic rules in the form of IF-THEN statements. FL provides a simplification of a control methodology description. This allows the human language to be used to describe the problem and its solutions. In many control applications, the model of the system is unknown or the input parameters are variable and unstable. In such cases, fuzzy controllers can be applied. These are more robust and cheaper than conventional PID controllers. It is also easier to understand and modify fuzzy controller rules, which not only use human operator's strategy but, are expressed in natural linguistic terms.

4.2.4 Hybrid system (HS)

Techniques	Advantage	Limitation
Expert Systems also called Knowledge-Based Systems (KBS)	-Cost reduction in achieving a complex task	-The lack of expertise
Artificial Neural Networks (ANNs)	-Most of the problems are now able to be solved -Representing I/O relationships for nonlinear systems.	-Is only a special mathematical technique
Fuzzy logic (FL)	-Applied successfully in large number of uncertain applications	-Input/output controls of process are complicated
Genetic Algorithms (GAs)	-Optimisation	-Successful for some applications
Hybrid System (ANNs & FLS), (FLS & ANNs), (GAs & FLS) and (GAs & ANNs)	-Combination technique is capable to solve all problems of engineering discipline	-No

Table 4. Intelligent system methods.

HS combines multiple soft computing methods. For example, neuro-fuzzy controllers use neural networks and fuzzy logic, whereas in a different hybrid system a neural network may be used to derive some parameters and a genetic algorithm may be used subsequently to find an optimum solution to a problem. Table 4 presents a comparison of features of soft computing methods.

5. Proposed Intelligent Energy Management System

This work employs the analysis and simulation approach to develop an Intelligent Energy Management System (IEMS) for a HEV. The overview of IEMS is shown in Fig12. IEMS calculates the energy distribution and power flows in the powertrain of the vehicle and related losses. It indicates the ways to minimises the vehicles' fuel consumption under various driving conditions. IEMS learns when it is run, and makes proper adjustments to the way it operates to ensure that fuel consumption optimisation is achieved.

The developed model includes the following components:

5.1 Look-Ahead Environment Model Unit (LEM):
This unit employs an imaging sensor and a vision algorithm to calculate the slope angle of the road ahead within the distance of 300 meters away from the vehicle, and forward this information to IEMS.

5.2 Current Environment Model Unit (CEM):
This unit employs the following data from environment situation.
   i. Current Road Slope Module (CRSM): This module specifies the actual slope angle of the road at the current location of the vehicle.
   ii. Road Friction Module (RFM): This module gives road friction coefficient, gravity acceleration, and motion angle.
   iii. Wind Drag Module (WDM): This module provides the following wind parameters: wind speed, wind direction, and drag coefficient.

5.3 Friction Management Unit (FMU):
This module obtains CEM data and also the following data to calculate and send them to IEMS.
   i. Combustion Module (CM): This module employs the combustion process from the vehicle as described in Equation (6-8), and calculates and returns the amount of combustion energy needed.
   ii. Accessory Module (AM): This module represents the accessories embedded within the vehicle such as electrical devices and air conditioning.
   iii. Vehicle Efficiencies Module (VEM): This module defines the values of the otto cycle, real fuel air engine, mechanical and heat loss efficiencies.

5.4 Battery State of Charge (SOC):
This module provides the amount of current, temperature and voltage of the battery continuously. Figure 11 displays only that the useable area of charge on the hybrid battery, displayed "empty" is about 40% and displayed "full" is about 85%.
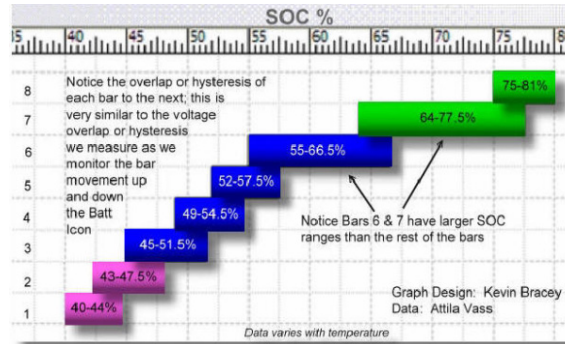
Fig. 11. The useable area of charge and discharge on the hybrid battery.

5.5 Control Strategy

In this work, the on-line adaptive strategy which was discussed in section 3.4.4, has been considered.

5.6 IEMS Algorithm

The overview of the simulation algorithm for IEMS is displayed in Fig. 13. The simulation starts with initialising several variables including normal power and primal kinetic energy for a moving vehicle. The data includes arrays of 7200 elements (steps). One iteration occurs in each step representing the time interval of 0.05 sec. Then the slope prediction data is retrieved from LEM. If the predicted slope angle is different from the current slope angle, STI block increases or decreases the power. Next, the vehicle/environment/friction data is retrieved from FMU. If the current total friction energy is different from the energy associated with the slope prediction, FTI block is triggered calculating the amount of power for all frictions. Otherwise, fuzzy logic controller (FLC) block is entered. FLC controls and optimises the fuel consumption with respect to the vehicle/efficiencies, speed, acceleration, and gear data. Also the FLC intelligently consider with drive strategy (see section 5.7) and control strategy. If the comparison is satisfied then these data will be forwarded to the next block where they overwrite the results of the previous iteration. Otherwise, the power of engine and inverter operation is corrected by decreasing or increasing. Once either of speed or acceleration is found to be greater than the desired limit, and then FLC will control the engine power and inverter operation by its algorithm. When either of speed or acceleration becomes smaller than the desired control strategy limit, the engine power is increased with regard to control strategy. In the assignment block, the old data is overwritten with the new data. The Inverter algorithm, shown in Fig. 14, synchronises the battery with EM, Gen. With regard to the battery SOC and IEMS Interpreter Load (IIL), inverter starts charging or discharging the battery in each time. It then informs the IEMS about its result via SOC. If SOC is high, and at times of high load, the generator can be switched off and EM can provide mechanical power via the battery by the inverter's instruction. The parameters of the FLC controller are optimized by genetic algorithm optimizer (GAO).
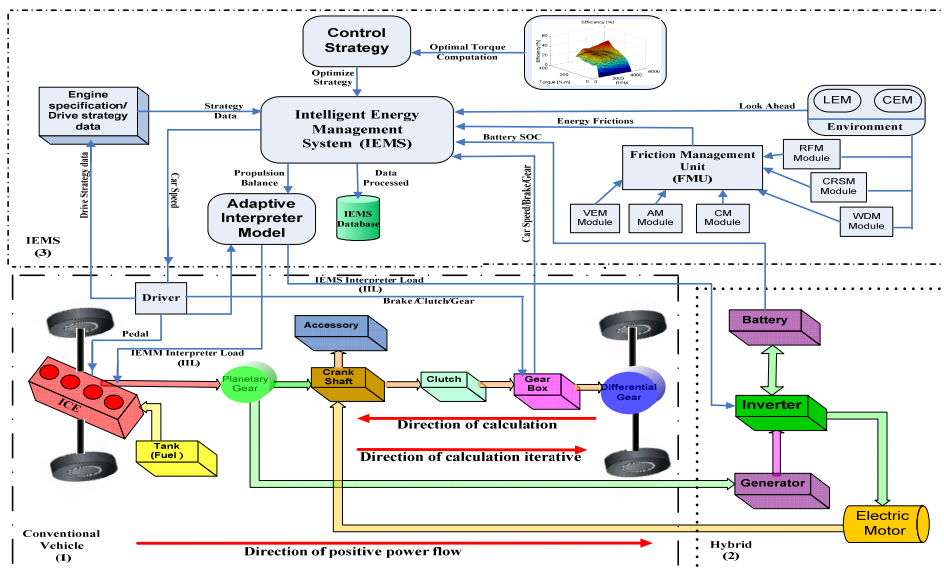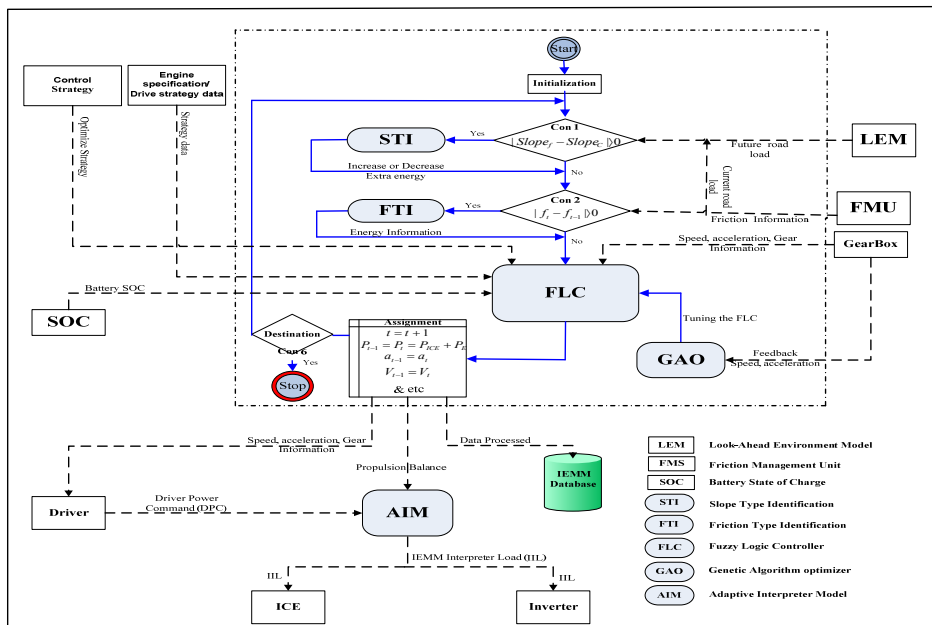
Fig. 12. Overview of the IEMS model.

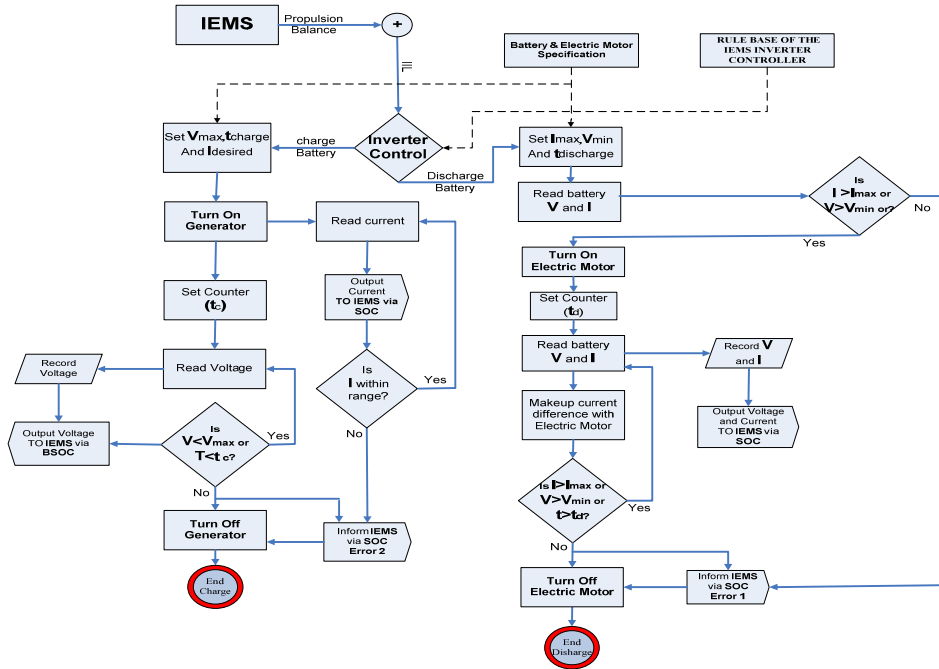Fig. 13. Overview of the IEMS algorithm.

Fig. 14. Overview of the inverter algorithm.

5.7 Engine and EM/Gen Specification and Drive Strategy

In this work, we have considered a vehicle with the engine and specification as given in Table 5.

Parameters	Min	Max	Average
Engine size (litre)	----	1.1	---------
Engine RMP (Rev/min)	3000	4000	3500
Engine power (kW)	9.8	10.5	10
Engine Torque (N/m)	25	29	27
EM/Gen RPM (Rev/min)	3000	4000	3500
EM/Gen Torque(N/m)	8	12	10

Table 5. Engine and EM/Gen specification.

We have also formulated a set of parameters called "Drive Strategy" as shown in Table 6.

Parameters	Min	Max	Average
Engine size (litre)	----	1.2	---------
Speed (m/s)	16.38	16.94	16.66
Acceleration (m/s^2)	-0.98	0.98	0.5
Travel Time	------	7200	0.05(s)
Travel Distance (m)		6000	

Table 6. Drive strategy parameters.

6. Simulation and optimization of hybrid vehicle

6.1 Simulation

6.1.1 Simulation 1

Khayyam et al (Khayyam et al, 2009b) demonstrated a Air Condition system simulation that, the vehicle was tested under sunny condition first for 1200 step for the vehicle speed around 20 m/s. Next, the fan and the air conditioning are turned on. The parameters given in Tables 7-9 were employed to achieve the comfort temperature in the cabin room for 6000 step. The air condition energy consumption shown in Fig 15(d).

Parameters	Min	Max	Normal
C.O.P	1.45	1.71	1.38
CAP (KW)	3.8	8.15	7.9
RMP (rev / min)	3000	4000	3500
Evaporator (KW)	5.51	13.93	10.90
Temperature (C) Gas R-134	0 Sub Cool	10 superheat	
Pressure (kPa) Gas R-134	310 Charge	2415 Discharge	

Table 7. Compressor specifications.

Parameters	Min	Max	Average
Volts	12.5	12.6	12.5
Amp	20	25	24
RMP (rev / min)	1000	1800	1200
Engine power (W)	250	315	300

Table 8. Blower specifications.

Parameters	Min	Max	Average
Temperature (C)	20	25.6	21.5
Humidity (%)	40	60	50
Air speed (m/s)	1	5	2.5

Table 9. Comfort cabin room specifications.

As discussed in section 3.2, some data has been created by PMH technique. The data created is associated with a slopped-windy-sunny condition. HEV was tested on this data, where the hybrid electric components were included. The road was set to be slopped with various slope angles within the range $– 1\% \leq atan(\emptyset) \leq +0.6\%$. Moreover, the environmental wind was assumed to be non-zero. The wind angle of attack, $\theta2$, was varied within the range 0 to 360°. Considering the wind velocity, however, different conditions were implemented: V2=0 to 6. The Current Environment Model (CEM) component monitored the current slope. The following parameters were also considered: road-friction, combustion, and air conditioning accessory (Table1). Fig. 15 illustrates the slope angle, wind-speed, wind direction as well as A/C energy consumption data used in the simulation.
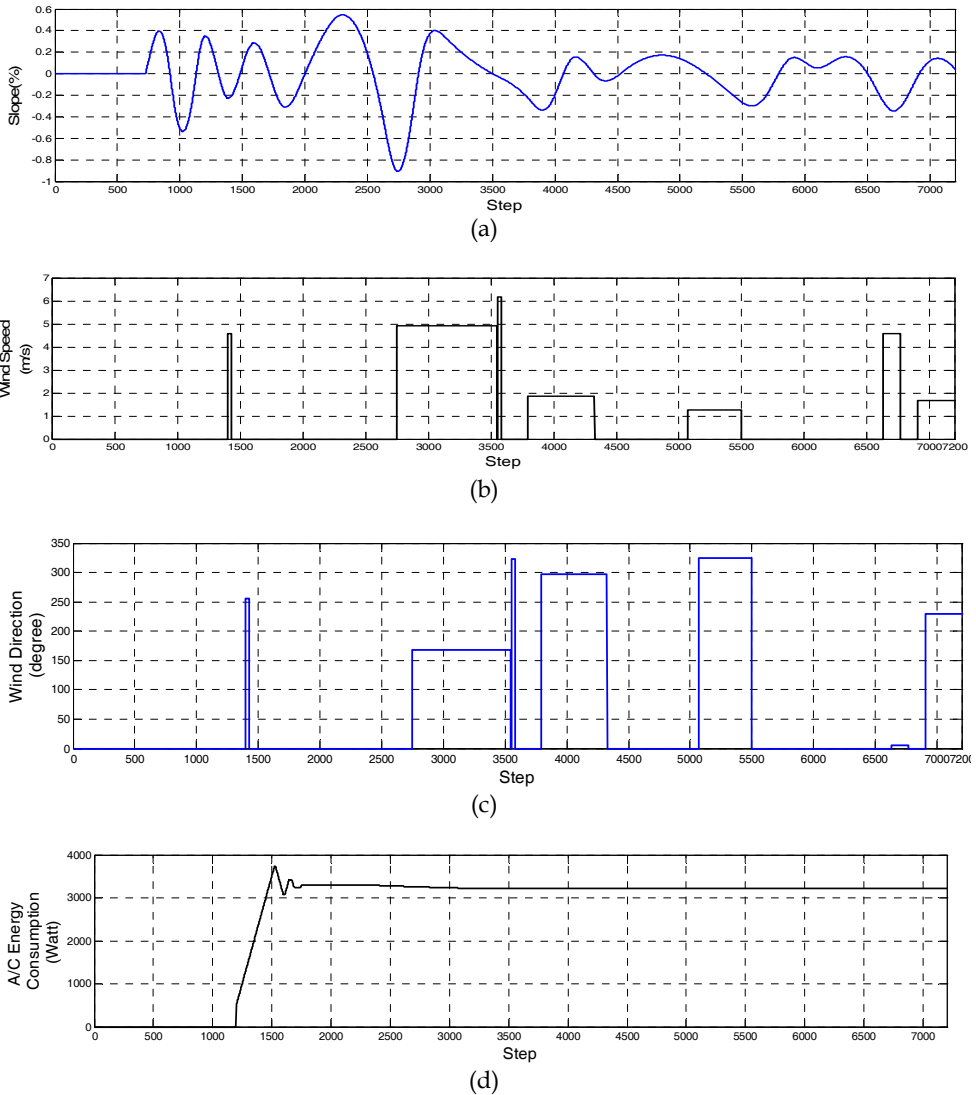
Fig. 15. (a) Slope (Road) angle data, (b) wind-speed data ,(c) wind-direction and (d) A/C energy consumption.

6.1.2 Simulation 2

IEMS-HEV was tested on a set of data associated with a slopped prediction (look-ahead within a 300 meter distance)-windy-warmed employing the hybrid electric components. The management of the battery, EM, and Gen is conducted by the inverter algorithm. This enables ICE and EM to output power simultaneously when the load is greater than 10 kW or a slope of greater than 0.1% is climbed by the vehicle. The following parameters were also

considered: road-friction, combustion, and air conditioning accessory. The predicted slope angle data is similar to the actual slope angle data.

6.2 Discussions

6.2.1 Simulation 1 Results

The power and fuel consumption results for the first simulation are shown in Fig. 16. Initially. 7800 W of energy is given to the vehicle so that the initial speed of 16.6 m/s is achieved. The energy consumption remained constant at 7800 W where the condition was flat-windless (e.g. steps 0-600). Depending on the condition of the road slope angle, the wind speed, angle of attack, and accessory energy consumption, the power consumption varied as shown in Fig. 16. The HEV was informed about the current slope by CEM.

Fig. 16 shows that the air conditioning system and slope friction have a significant impact on the fuel consumption. The reason is that it requires more fuel in a transit time. HEV can measure how much energy is needed in each step, and works out a desired fuel rate for the engine so that the power brake would not be needed. Using Equation (10), the average fuel consumption for Simulation 1 was found to be around 6.65 liter/100 km.
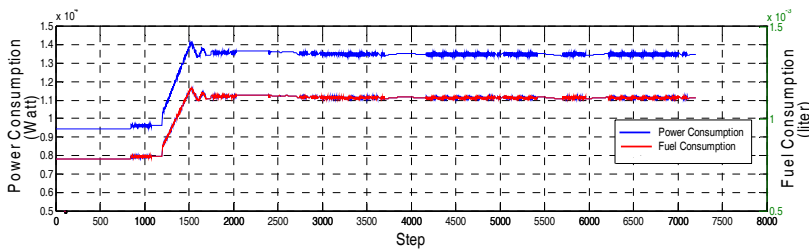

Fig. 16. Power and fuel consumption results for Simulation 1.

6.2.2 Simulation 2 Results

The power and fuel consumption results for the second simulation are shown in Fig. 17. Similarly, 7800 W of energy is initially given to the vehicle so that the initial speed of 16.6 m/s is achieved. Also, the Look-Ahead informed IEMS about any slope ahead. IEMS calculates and FLC investigates, and if the load is found to be greater than 10 kW or the slope greater than 0.1%, the propulsion balance requests ILL to switch on EM through inverter. The outcome of this simulation shows that the vehicle speed and acceleration are smoother than those of Simulation 1. Using Equation (10), the average fuel consumption for Simulation 2 was found to be around 6.11 liter/100 km. Fig. 18 shows the SOC of battery during the travel. It goes up to 85% and then comes down to the same level when used.
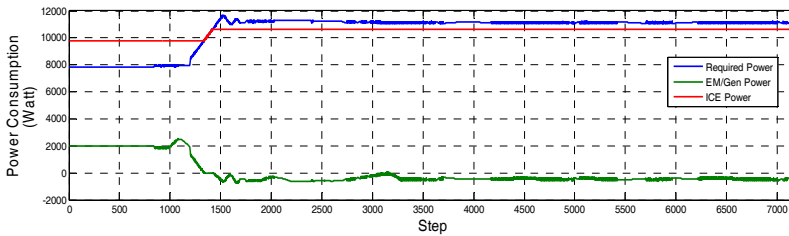
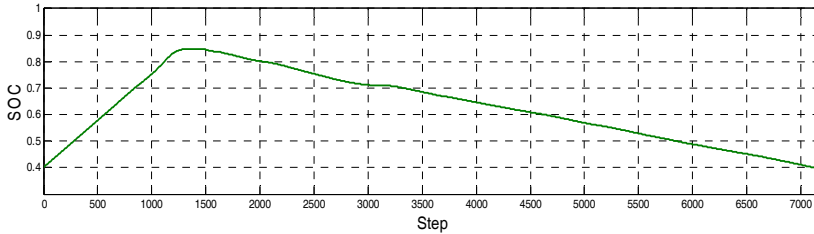Fig. 17. Power consumption results for Simulation 2.

Fig. 18. SOC of battery.

7. Conclusions

This chapter presented a description of intelligent energy management systems for hybrid electric vehicles. In addition, an intelligent energy management model for a parallel hybrid electric vehicle was described. The model takes into account the role of combined wind/drag, slope, rolling, and accessories loads to minimize the fuel consumption under various driving conditions. Two simulation studies were conducted. They show that the vehicle speed and acceleration were smoother when the hybrid section was included. The average fuel consumption for Simulation 1 and 2 were found to be around 6.65 and 6.11 liter/100 km, respectively.

8. References

A. Bandivadekar and J. Heywood,(2007) "Factor of two : halving the fuel consumption of new U.S. automobiles by 2035," Report from Laboratoy for energy and the environment (MIT), vol. LFEE,.

A. Piccolo, L. Ippolito, V. Galdi, and A. Vaccaro,(2001) "Optimization of energy flow management in hybird electric vehicles via genetic alorithms," Proc. IEEE/ASME Int. Conf. Italy, pp. 434-439,.

A. Sciarretta, M. Back, and L. Guzzella,(2004)"Optimal Control of Parallel Hybrid Electric Vehicles," IEEE Trans. on Control Systems Technology, vol. 12,.

B. M. Baumann, G. Washington, B. C. Glenn, and G. Rizzoni,(2005) "Mechatronic design and control of hybrid electric vehicles," IEEE/ASME Transactions on Mechatronics, vol. 5, pp. 58-72, 2000.

C. Musardo, G. Rizzoni, Y. Guezennec, B Staccia.(2005)"A-ECMS: An Adaptive Algorithm for Hybrid Electric Vehicle Energy Management"; European Journal of Control, Fundamental Issues in Control, Special Issue, Volume 11, Number 4-5.

C. C. Lin, H. Peng, and J. W. Grizzle,(2003) "Power management strategy for a parallel hybrid electric truck," IEEE Trans. on Control Systems Technology, vol. 11, pp. 839-849,.

C. C. Linl, H. Pengl, and J. W. Grizzle, (2004)"A Stochastic Control Strategy for Hybrid Electric Vehicles," Proceeding of the 2004 American Control Conference Boston, Massachusetts, vol. 4710-4715,.

E. D. Tate and S. P. Boyd,(1998) "Finding ultimate limits of performance for hybrid electric vehicles," SAE, vol. 00FTT-50,.

E. Hellstrom, M. Ivarsson, J. Aslund, and L. Nielsen,(2009) "Look-ahead control for heavy trucks to minimize trip time and fuel consumption," control Engineering Practice, vol. 17, pp. 245-254,.

EPA, (2004)"Assessing the emission and fuel consumption impacts of intelligent transportation system(ITS)," EPA, vol. 231, pp. 98-007,.

G. J. v. Wylen and R. E. Sonntag,(1990)"fundamentals of classical thermodynamics " vol. Third edition SI version.

G. Shi, Y. Jing, A. Xu, and J. Ma, (2006)"Study and Simulation of Based-fuzzy-logic Parallel Hybrid Electric Vehicles Control Strategy," Proceedings of the Sixth International Conference on Intelligent Systems Design and Applications pp. 280-284,.

H. Khayyam, A. Z. Kouzani, and E. J. Hu,(2008) "An intelligent energy management model for a parallel hybrid vehicle under combined loads," in IEEE International conference on vehicular electronics and safety Columbus, OH, USA 2008, pp. 145-150.

H. Khayyam, A. Z. Kouzani, and E. J. Hu,(2009b) "Reducing energy consumption of vehicle air conditioning system by an energy management system," IEEE The 4th Internationnal Green Energy Conferance Beijing, China, vol. 1

H. Khayyam, A. Z. Kouzani, H. Abdi, and S. Nahavandi,(2009a) "Modeling of highway heits for vehicle modeling and simulation " Proc. ASME/IEEE Int. Conf. MESA09 USA.

J. B. Heywood, (1998)"Internal combustion engine fundamentals," McGraw-Hill, New York,.

J. S. Won, (2003)."Intelligent energy management agent for a parallel hybrid vehicle," PhD Thesis 2003.

J. T.B.A. Kessels, (2007) "Energy Management for Automotive Power Nets," PhD thesis 2007.

L. L. Yaodong Wang, (2007)"An analytic study of applying Miller cycle to reduce Nox emission from petrol engine " Applied Thermal Engineering, vol. 27, pp. 1779-1789,.

Lewis,Frank L. & Syrmos, Vassilis L. (1995) "Optimal Control" Hohn Wiley & Sons Inc. Newyork.

M. Ehsani, Y. Gao, S. E. Gay, and A. Emadi, (2005) "Modern electric, hybrid electric, and fuel cell vehicles", New York CRC PRESS.

M. Farrokhi and M. Mohebbi, (2005) "Optimal Fuzzy Control of Parallel Hybrid Electric Vehicles," ICCAS2005 June 2-5.

M. Mohebbi and M. Farrokhi,(2007) "Adaptive neuro control of parallel hybrid electric vehicles," Int. J. Electric and Hybrid Vehicles, vol. 1,.

M. Mohebbi, M. Charkhgard, and M. Farrokhi,(2005)"Optimal neuro-fuzzy control of parallel hybrid electric vehicles," Vehicle Power and Propulsion, 2005 IEEE Conference, pp. 26-30.

M. Plint and A. Martyr,(1997) "Engine testing theory and practice," Butter worth-Heinemann British Library .

M. Salman, F. Change, and J. S. Chen,(2005) "Predictive energy management strategies for hybrid vehicles," IEEE Conf. Decision Control pp. 21-25,.

M. Salman, N. J. Schouten, and N. A. Kheir, (2000) "Control strategies for parallel hybrid vehicles", American Control Conference, vol. 1, pp. 524-528.

Manins ,P.C.(2000)."Environmental impact of the new Australian Hybrid Cars " Proceedings of the 15th International Clean Air and Environment Conference vol. 26-30, pp. 117-122,.

N. J. Schouten, M. A. Salman, and N. A. Kheir,(2002)"Fuzzy logic control for parallel hybrid vehicles," IEEE Transactions on Control Systems Technology, vol. 10, pp. 460-468, .

O. Barbarisi, E. R. Westervelt, F. Vasca, and G. Rizzoni,(2005) "Power management decoupling control for a hybrid electric vehicle," IEEE Conf on Decision and Control, Spain, pp. 2012-2017.

P. C. Cacciabue, (2007)"Modelling driver behaviour in automotive environments ": Springer 2007.

P. Pisu, G. Rizzoni, (2007) "A Comparative Study of Supervisory Control Strategies For Hybrid Electric Vehicles" IEEE Transactions on Control Systems Technology, Special Issue on Control Applications in Automotive Engineering,

Q. R. Riley, (1994)"Alternative cars in the 21 century a new personal transportaion paradigm," SAE International, vol. 1994,.

R. Langari and J.-s. W. Won, (2005)"Intelligent Energy Management Agent for a Parallel Hybrid Vehicle-Part 1 : Systsem Architecture and Design of the Driving Situation Identification Process," IEEE Trasactions on Vehicular Technology vol. 54, pp. 925-934,.

R. Shoureshi and D. Wormley,(1990) "Intelligent control systems," Final report of NSF/EPRI,.

R. Zhang and Y. Chen, (2001) "Control of hybrid dynamical systems for electric vehicles,"American Control Conference, vol. 4, pp. 2884-2889,

S. Barsali, C. Miulli, and A. Possenti, (2004)"A control strategy to minimize fuel consumption of series hybrid electric vehicles," IEEE Transaction on Energy Conversion, vol. 19, pp. 187-195,

S. Delprat, J. Lauber, T. M. Guerra, and J. Rimaux,(2004) "Control of a Parallel Hybrid Powertrain: Optimal Control," IEEE Transaction on vehicular technology, vol. 53, pp. 872-881,.

S. E. Lyshevski,(1999)"Diesel-Electric Drivetrains for Hybrid-Electric Vehicles: New Challenging Problems in Multivariable Analysis and Control," Proceedings of the 1999 IEEE International Conference on Control Applications vol. 1, pp. 840-845,.

S. M. T. Bathaee, A. H. Gastaj, S. R. Emami, and M. Mohammadian,(2005) "A fuzzy-based supervisory robust control for parallel hybrid electric vehicles," Vehicle Power and Propulsion, 2005 IEEE Conference, pp. 694-700,.

Simon, Herbert A., (1973) "The Organization of Complex Systems," in Hierarchy Theory, ed. by Howard H. Pattee, New York: George Braziller,

SOE,(2006) "Independent report to the Australian Government Minister for the Environment and Heritage " <http://www.environment.gov.au/soe/2006/publications/report/index.html>, 2006.

W. W. Pullkrabek,(1997)"Engineering fundamentals of the internal combustion engine " Prentice Hall.

X. Wei, L. Guzzella*, V. I. Utkin and G. Rizzoni, (2007) "Model-based Fuel Optimal Control of Hybrid Electric Vehicle Using Variable Structure Control Systems", ASME Transactions. Journal of Dynamic Systems, Measurement, and Control - Volume 129, Issue 1, pp. 13-19.

Y. C. Shin and C. Xu,(2009)" Intelligent Systems modeling, optimization, and control" Boca Raton : CRC Press,.

Y. Lin, P. Tang, W. J. Zhang, and Q. Yu,(2005)"Artificial neural network modelling of driver handling behaviour in a driver-vehicle-environment system," International Journal of Vehicle Design, vol. 37, pp. 24-45,.

Y. Wang, L. Lin, and A. roskily(2007). "An analytic study of applying Miller cycle to reduce Nox emission from petrol engine " Applied Thermal Engineering, vol. 27, pp. 1779-1789

Y. Zhu, Y. Chen, and Q. Chen,(2002) "Analysis and Design of an Optimal Energy Management and Control System for Hybrid Electric Vehicles," Proc. of the 19th Electric Vehicles Symposium, Busan, Korea,.

Optimal Management of Power Systems

Luca Andreassi
University of Rome "Tor Vergata"
Italy
Stefano Ubertini
University of Naples "Parthenope"
Italy

1. Introduction

The increasing energy demand along with the growing concern for environmental issues make energy saving one of the main tasks of present times and it is likely to become even more important in the next decades, as the economic growth is being pursued in developing countries, as China, India and Brazil.

As a consequence, researchers, industries and politicians are required to make significant efforts in this field. More and more stringent regulations on pollution and CO_2 emissions have been issued, which means limiting energy consumption. However, even if policy is an important tool, it cannot be the only one and it is necessary to spread the knowledge on energy systems, energy saving options and energy use rationalisation (Lopes et al., 2005). This is a prerequisite to make right choices for a more efficient use of energy, even if these choices are not mandatory from a "legal" point of view.

Being obvious that this knowledge should be transferred to all the population layers, it is important that the main energy users, as industry, realize that energy is not merely an overhead, as part of business maintenance, but actually a raw material resource required to run the business. Energy management programs should, therefore, become an integral part of the corporate strategy, to increase the business' profitability and competitiveness. Moreover, knocking down energy costs most of the times means reducing demand on the world's finite energy sources, cutting pollution and creating a healthier working environment.

The main example in this context is Japan, as the Japanese economy is the most energy efficient in the industrialized world and their improvements in energy efficiency enabled the Japanese industry to increase its output of 40% by spending the same energy in 2001 as in 1973 (Van Schijndel., 2002; Kamal, 1997). In general, the application of good energy management practices and energy-efficient equipment allow a readily achievable, cost-effective, 20% reduction in industrial consumption (Smith et al., 2007)

Energy saving can be realised through different actions on both the utilisation and the production sides (Agency for Natural Resources and Energy, 2004; Meier, 1997). However, it is really a complex task, as many factors influence energy usage, conversion and consumption and these factors are strictly connected to each other. For example, when

evaluating an action on energy consumption/conversion, one should take care of the interactions, as one measure influences the saving effect of the other measures. Accordingly that the single contributions to energy saving cannot be simply summed up because of overlapping effects. On the other hand, the combined effect can be higher than the sum of the separate effects as well. Furthermore, it is worth of noting that energy saving represents energy that is not used and, therefore, it cannot be directly measured (except in some cases as, for example, straightforward energy conversion processes).

Therefore, it is necessary to develop and apply new methodologies for total energy management in buildings and industrial plants (Cesarotti et al., 2007, Andreassi et al., 2009).

In this scenario, the installation of energy systems (characterized by multiple energy supplies and energy conversion equipments to meet energy demands) in industrial plants has become increasingly popular in recent years (i.e. combined heat and power – CHP, renewable energy systems) and their proper management becomes crucial to reduce energy costs and environmental impact.

Usually, in fact, the small power plants dedicated to buildings or power plants (nominal power ranging from some hundreds of kWs to 10 MW) are operated simply switching on and off the machines for long time intervals (i.e. night and day, winter and summer). However, the machines typically used in these systems have small thermal inertia, thus allowing quick load variation, and may be operated under partial load.

In most cases operating decisions are made by a control room dispatcher on the basis of empirical data, machine efficiency calculations and/or trial errors. Obviously, this approach cannot keep into proper account all the huge number of variables (and their interaction) affecting the energetic and economic results that may be achieved. In fact, these combined cooling, heating and power systems meet the electricity demand by running the generators and by purchasing electricity from an outside electric power company. The exhaust heat recovered from the thermal engines is reused to handle the heating load which is supplemented by boilers. Analogously, cooling load could be met by recovering heat to power absorption chiller system so providing all or a portion of the cooling load. Any other request of cooling load can be satisfied with an electric power compressor driven air conditioning system. Of course, the main objective is to achieve for each hour the most profitable operation strategy, maximizing the profitability, covering the energy demand and obtaining savings in terms of primary energy and emissions. It becomes obvious that in order to realize the greatest cost savings a proper optimization has to be performed.

In scientific literature, several criteria for the optimization of combined cooling, heating and power systems in industrial plants are available based on different management hypotheses and objective functions. The goal of the models is to optimize the operation of the energy system to maximize the return on invested capital. Many of these models do account for load operations but use simple linear relationships to describe thermodynamic and heat transfer process that can be inherently non-linear. (Arivalgan et al., 2000) presented a mixed-integer linear programming model to optimize the operation of a paper mill. It was demonstrated that the model provides the methods for determining the optimal strategy that minimizes the overall cost of energy for the process industry. (Von Spakovsky et al.,1995) used a mixed integer linear programming approach which balances the competing costs of operation and minimizes these costs subject to the operational constraints placed on the system. Main issue of the presented model is that it is useful to predict the best operating strategy for any given day. Nevertheless, the model validity was strictly dependent on the

linear behavior of the plant components. (Frangopoulos et al., 1996) employed linear programming techniques to develop an optimization procedure of a power plant supported by a thermo-economic analysis of the system. (Puttgen & MacGregor, 1996) and (Valero & Lozano, 1993), illustrate a total revenue maximization performed through linear programming subject to constraints due to conservation of mass, thermal storage restrictions and shiftable loads requirement. (Moslchi et al., 1991) divided the energy system into an electric subsystem and a steam subsystem: in the first one steam turbines generate the electricity necessary to meet the power demand, while the second one consists of boilers which use fuel and water to produce steam for industrial processes. The two subsystems were solved separately with solutions coordinated to achieve optimality of the combined systems. Finally, thermo-economics offer the most comprehensive theoretical approach to energy systems analysis where costs are concerned. It is based on the assumption that exergy is the only rational basis to assign cost. In other terms, the main issue is that costs occur and are directly related to the irreversibility taking place within each component. Accordingly thermo-economics could represent a reliable approach to power plants operation optimisation involving thermodynamic and economical aspects (Tstsaronis & Winhold,1985; Temir & Bilge, 2004; Tstsaronis & Pisa, 1994).

The purpose of this chapter is to highlight the importance of the optimal management of power plants in terms of environmental impact, fuel consumption and energy costs. This is done by presenting and applying a mathematical model to identify the optimal operating conditions of energy conversion equipments (i.e. boilers, air-conditioning systems and refrigerators, thermal engines) (Cardona & Piacentino, 2007; Doering & Lin, 1979; Kong et al., 2009; Marik et al., 2005; Kong et al., 2005). In practice, substantial energy savings and/or environmental benefits could be obtained without any action on the power plant components.

2. Main philosophy

The power plant serving an industrial or civil facility is a complex system made up of different components (i.e. primary movers, boilers, refrigerators etc.) that has to satisfy the energy requirements in terms of heat, electricity and cooling. The effectiveness of a power plant is measured through the overall efficiency, which is the ratio between the obtained usable energy (i.e. electrical and thermal energy, cooling energy) and the spent primary energy (i.e. fuel). The difference between spent and useful energy represents waste energy.

The efficiency of a power system is a combination of the components efficiency, defined as the ratio between output and input energy. The maximisation of a power plant efficiency can be, therefore, performed mainly in two ways:

-      substituting existing components with higher efficient ones;
-      running components as much efficiently as possible.

The first item is related to the existence of different ways to convert primary energy to useful energy and thus different machines and power systems in general, as reciprocating engines, gas turbines, fuel cells and so on up to renewable energy systems which, in principle, convert free available energy to useful one.

The second one is indeed related to the dependence of energy converters efficiency on several parameters, and, therefore, on the instantaneous efficiency of each component of a power plant varies with time. As these efficiency variations may be significant and the

energy demand could be satisfied with several power plant operating configurations (i.e. heat from a boiler or a cogenerator), the optimal management of a power plant is as much important as the use of efficient component, with the certain advantage of requiring limited investments.

Next we have to consider that the power produced by the energy system may be not entirely used in the structure that serves, as the electric power may be imported/exported to a utility grid. This means that the electric network acts as an energy storage system that gives and absorbs energy at different costs, defined by the electricity rate. Therefore energetic and economic optimisation do not in general coincide and the concept of power plant optimal management needs to be extended to reducing costs and not (only) primary energy consumption (i.e. maximum efficiency).

This complicates the analysis, as costs are not proportional to the energy content of a certain energy carrier (i.e. methane, gasoline, electricity etc.) and other factors need to be assessed and optimised, as the contract with the electric company. On the other hand, this makes an optimal management strategy much more attractive, as costs can be reduced (or profits can be increased) up to 10% passing from standard to optimal management.

The meaning of optimal management of a power plant is setting the power plant components operating conditions in order to satisfy the energy demand while minimising or maximising a certain objective function (i.e. energy costs/profit, pollutant emissions, fuel consumption, carbon dioxide emissions etc.). This can be done at different detail levels. In the following a simple but sufficiently accurate methodology is proposed.

Before giving the details of the proposed methodology, it is important to highlight that this chapter discusses the opportunities given by running a power system efficiently, but it presupposes that a regular maintenance of the power plant components and the prompt repair of defects are performed. Maintenance is, in fact, one of the most cost-effective methods for avoiding energy waste, as energy losses from poorly maintained or antiquated systems are often considerable. In particular, modern power systems feature sophisticated components that require regular ongoing inspections, measurements and repair for peak operating efficiency.

3. Mathematical model

The system representation can be achieved through a mathematical model which emulates the energy/mass balances existing between the power plant and the served facility. The model allows matching the industrial plant energy demands (electricity, hot water, cold, etc.) through an analysis of the system performance characteristics, taking into account the main subsystems integration issues, their operation requirements and their economic viability.

In this chapter the following equipments are investigated:
- gas engines
- gas steam boilers
- hot water boilers
- mechanical chillers
- absorption chillers

being understood that any other energy converter may be included in the proposed method. In particular, also renewable energy systems may be included in this analysis. In fact, it is true that in the case of wind or solar power generation, the main goal is to produce as much energy from the system as possible to recover the installation cost, but this electrical energy production affects the behavior of the whole energy system. For example, if a wind turbine is producing the electrical power needed by the industrial plant, it may be convenient to reduce the cogenerator load and increase the heat production in the boilers.

As the present approach is devoted to optimal management of the power plant, which is to say those equipment operating conditions (i.e. set-points) that minimize a prescribed cost function, it is not necessary to go into the detail of the equipments behavior. Therefore, all the equipments in the power plant are considered as energy converters, characterized by inputs and outputs and modelled as black-boxes. The outputs depend on the component load or setpoint. It is worth of noting that, although the output could be more than one, as in the case of a gas engine cogenerator (electricity and hot water for example), each equipment is usually defined by only one input (fuel or electric energy).

Conservation equations are considered to solve each subsystem with a quasi-steady approach (i.e. the variables are considered constant between two time steps).

Before starting the description of the numerical model equations, it is essential to introduce the feature of the variables involved in the mathematical representation.

3.1 Input and the output variables

Input variables are subdivided into two main classes, as proposed in (van Schijndel, 2002): controllable and non-controllable variables.

The non-controllable inputs are those related to the energy requirements (i.e. dependent on the industrial plant production plan or the building operation), as, at each time step, the power plant has to supply the "non controllable" energy demand.

The energetic non-controllable inputs are: the cooling demand ($\dot{Q}_{CD}$), the low temperature heat demand ($\dot{Q}_{HwD}$), the high temperature heat demand (steam) ($\dot{Q}_{SD}$) and the electricity demand (P_{ElD}).

The economic non-controllable inputs are the fuel cost (c_f) and the electricity cost. Considering that electricity can be purchased by or sold to the public network, as the power plant electricity output may be higher or lower than the electric demand, the energy costs in sale (S_{El}) and in purchase (c_{El}) are considered. There are two important factors affecting the economic inputs that need to be assessed:

-    as different electricity rates are available in the market, and the power plant operation affects the electricity demand from the net, the present methodology may be efficiently combined to a tariff analysis and contract renewal process;
-    there may be other terms that affect the energy cost and price due to public incentives, as it happens for renewable energy and high efficiency cogeneration in Europe.

The controllable inputs are the power plant component operating conditions, here uniquely determined by set points varying from 0 (representing switching off) to 1 (representing maximum load).

The total cost (TC), the electricity cost and consumption (ElC, P_{ElBal}), the fuel cost and consumption (FC, $\dot{m}_{Tf}$) are the model outputs. The optimisation procedure is performed on one or a combination of the above outputs.

3.2 The objective function

Simulations are performed pursuing the goal of optimising the equipment operation, in order to satisfy specified criterion. Currently, the following three optimization criteria are the most common:

- minimum cost of operation
- minimum fuel consumption
- minimum pollutant emissions (CO, NO_x, SO_x, Soot, CO_2)

For the last strategy different weights of the different pollutant emissions may be applied. In the present work, we have assumed that they are proportionally weighted with the Italian legislation maximum limits, as reported in section 3.8.

3.3 Modeling the power plant components

The mathematical representation of every subsystem is summarised in Table 1. Each equation is representative of the energy transformations taking place into the correspondent equipment between input and output. Efficiencies forming equations are set point dependent, according to the manufacturer specifications. In fact, the efficiency under nominal operating condition is always available and very often efficiency values at other loads are also known. It is important to keep in mind that efficiency can be limited by mechanical, chemical, or other physical parameters, or by the age and design of equipment. Therefore, deviations from producer efficiency may exist and should be taken into account.

Then, the efficiency (η) of each equipment could be represented by a polynomial function as it follows:

$$\eta = \sum a_k E^k \tag{1}$$

where E is the primary input energy and a_k is the polynomial coefficient.

Of course, the more are the known load/efficiency points, the more accurate will be the efficiency profile.

As an example, a cogenerator can be represented as a black-box where fuel is converted, through an efficiency function like (1), in electricity, thermal energy (both low and high temperature) and cooling energy, as shown in Figure 1.

In this scenario, the primary energy power equation for the gas engine is

$$P_{ge} = \dot{m} \cdot H_i \cdot SP_{ge} \tag{2}$$

This chemical power is subdivided in electrical and thermal power on the basis of the machine efficiencies (electric efficiency of the gas engine, thermal efficiency of the gas engine for steam production, thermal efficiency of the gas engine for hot water production, thermal efficiency of the gas engine for cold water production). The values of the presented efficiencies can be directly obtained by the engine manufacturer.

Equipment	Chemical power	Electrical power	Hot water power	Steam power	Cold power
Gas engine	$P_{ge} = \dot{m} \cdot H_i \cdot SP_{ge}$	$P_{elge} = P_{ge} \cdot \eta_{elge}$	$\dot{Q}_{Hwge} = P_{ge} \cdot \eta_{Hwge}$	$\dot{Q}_{Sge} = P_{ge} \cdot \eta_{Sge}$	$\dot{Q}_{Cge} = P_{ge} \cdot \eta_{Cge}$
Mechanical chiller					$\dot{Q}_{Cmc} = P_{Elmc} \cdot \eta_{Elmc}$
Absorption chiller					$\dot{Q}_{Cac} = Q_{Hwgeac} \cdot \eta_{Cac}$
Hot water boiler			$\dot{Q}_{Hwb} = \dot{m}_{fHwb} \cdot H_i \cdot \eta_{Hwb}$		
Steam boiler			$\dot{Q}_{Sb} = \dot{m}_{fSb} \cdot H_i \cdot \eta_{Sb}$		

Table 1. Subsystems mathematical characterization

The numerical results discussed in this chapter have been derived following this approach. Nevertheless, one of the main peculiarities of the presented numerical model is the flexibility. Accordingly, it is possible to easily represent the efficiency on the basis of specific driving parameters as, for example, external temperature, maintenance service level, etc. Following a similar scheme, the boilers heat production as hot water is evaluated as

$$\dot{Q}_{Hwb} = \dot{m}_{fHwb} \cdot H_i \cdot \eta_{Hwb} \tag{3}$$

and, as steam as

$$\dot{Q}_{Sb} = \dot{m}_{fSb} \cdot H_i \cdot \eta_{Sb} \tag{4}$$

Once again the boiler efficiencies can be schematized exclusively on the basis of the manufacturer data or this representation can be improved considering specific drivers. Finally, two chillers have been considered: mechanical and electric chillers. In both cases the chiller cold power production is defined on the basis of a chiller efficiency:

$$\dot{Q}_{Cmc} = P_{Elmc} \cdot \eta_{Elmc} \tag{5}$$

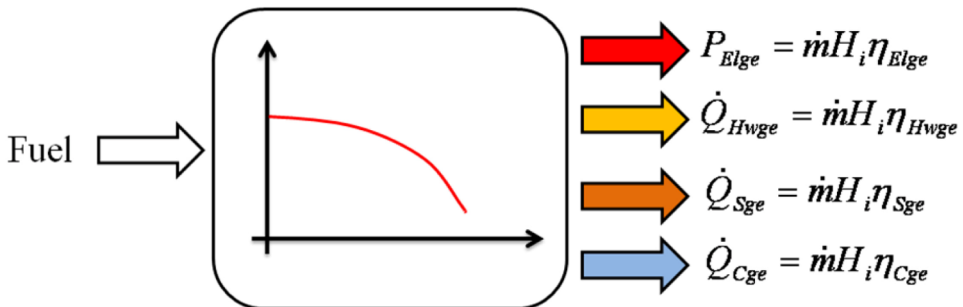$$\dot{Q}_{Cac} = \dot{Q}_{Hwgeac} \cdot \eta_{Cac} \tag{6}$$

$$P_{Elge} = \dot{m} H_i \eta_{Elge}$$
$$\dot{Q}_{Hwge} = \dot{m} H_i \eta_{Hwge}$$
$$\dot{Q}_{Sge} = \dot{m} H_i \eta_{Sge}$$
$$\dot{Q}_{Cge} = \dot{m} H_i \eta_{Cge}$$

Fig. 1. Representative model of a trigenerator.

3.5 Electricity and thermal balances

The energy model can be divided into two main submodels: the electricity balance and the thermal balance.

Considering the overall power plant and keeping into account the previous sections, the electricity balance can be expressed as follows:

$$P_{ElBal} = P_{Elge} - P_{mc} - P_{ElD} \tag{6}$$

where P_{Elge} is the gas engine electric power output, P_{mc} and P_{ElD} represent the electric power used by the mechanical chiller and the other electric needs of the facility, respectively. Of course, negative values of P_{ElBal} indicate a shortage of electricity.

Once the electricity demand (or the electricity offer to the market) is defined, it is possible to determine the electricity cost, given by:

$$ElC = s_{El} \cdot p(P_{ElBal}) + c_{El} \cdot n(P_{ElBal}) \tag{7}$$

where s_{El} and c_{El} represent the cost of electricity in sale and in purchase, respectively, and the function $p(x)$ $(n(x))$ return the value of the argument x if positive (negative), zero otherwise.

It is worth noting that the electrical efficiencies, which contribute to the definition of the terms in Equation (6), depend on the setpoint according to the manufacture specification. It is therefore clear, and it will be highlighted in the case study section, that a numerical procedure is requested as the main aim of the model is to define the optimal equipments setpoint in order to satisfy a specific request, which depends on the power outputs that, in turn, depend on the setpoint reliant efficiencies.

Electric energy is univocally defined, whereas characterizing thermal energy needs one more specification. Operating temperature must be issued to define the available thermal energy potential. Hence, in principle, infinite thermal balances would be possible.

Three balances have been distinguished in this paper: a hot water balance (T = 80°C), a steam balance (12 bars saturated steam) and a cooling balance (T = -5°C).

To evaluate the supplied fuel to the hot water boiler, a hot water balance can be written as the difference between the cogenerator hot water heat power, $\dot{Q}_{Hwge}$, and the plant hot water power demand, $\dot{Q}_{HwD}$:

$$\dot{Q}_{HwBal} = \dot{Q}_{Hwge} - \dot{Q}_{HwD} \tag{8}$$

A negative value of the balance (i.e. the hot water demand exceeds the cogenerative hot water), implies the hot water boiler usage.

The switching of the absorption chiller depends on the thermal balance (8): if positive it is possible to turn on the absorption chiller, defining the following function:

$$SW_{ac} = p\left(\text{sign}\left(\dot{Q}_{HwBal}\right)\right) \tag{9}$$

The used heat from the CHP systems to the absorption chiller can be calculated as:

$$\dot{Q}_{Hwac} = SW_{ac} \cdot \left(\dot{Q}_{HwBal} - p\left(\dot{Q}_{HwBal} - \dot{Q}_{acmax} \right) \right) \tag{10}$$

where $\dot{Q}_{acmax}$ is the maximum thermal power required by the absorption chiller. The heat demand and the gas supply of hot water boilers are then given by the following equations:

$$\dot{Q}_{Hwb} = -n\left(\dot{Q}_{HwBal} \right) \tag{11}$$

$$\dot{m}_{fHwb} = \frac{\dot{Q}_{Hwb}}{\eta_{Hwb} \times H_i} \tag{12}$$

where ρ and H_i are the density and the lower heating value of the fuel and η_{Hwb} is the hot water boiler efficiency. Analogously, the heat balance, the demand and the gas supply of steam boilers are evaluated as follows:

$$\dot{Q}_{SBal} = \dot{Q}_{Sge} - \dot{Q}_{SD} \tag{13}$$

$$\dot{Q}_{Sb} = -n\left(\dot{Q}_{SBal} \right) \tag{14}$$

$$\dot{m}_{fSb} = \frac{\dot{Q}_{Sb}}{\eta_{Sb} \times H_i} \tag{15}$$

where η_{Sb} is the steam boiler efficiency.

Finally, indicating with cop_{mc}, SP_{mc} and $\dot{Q}_{Cmc}$ the coefficient of performance, the set point and the cold power production of the mechanical chiller respectively, the cold balance and the electricity absorbed by the mechanical chiller are calculated with the following relationships:

$$\dot{Q}_{CBal} = \dot{Q}_{Cmc} + \dot{Q}_{Cac} - \dot{Q}_{CD} \tag{16}$$

$$P_{mc} = \frac{\dot{Q}_{Cmc}}{cop_{mc} \cdot SP_{mc}} \tag{17}$$

3.7 Pollutant emissions

The following pollutant emissions are considered: nitrogen oxides NO_x carbon monoxide CO, sulphur oxides SO_x, carbon dioxide, CO_2 and particulate, Soot.

Being the total mass flow rate used in the power plant given by the sum of the boilers ($\dot{m}_{bf}$) and the gas engine ($\dot{m}_{gef}$) fuel consumption, under the hypothesis that a complete oxidation occurs, the fuel mass balance reads as follows:

$$\dot{m}_{Tf} = \dot{m}_{bf} + \dot{m}_{gef} \qquad (18)$$

The SO_x and CO_2 mass flow rates are calculated as a percentage of the mass concentration of carbon, $[C]_m$, and sulphur, $[S]_m$, in the fuel supplied by the energy converters:

$$\dot{m}_{CO_2} = \frac{44}{12} \cdot [C]_m \cdot \dot{m}_{Tf} \qquad (19)$$

$$\dot{m}_{SO_x} = \frac{64}{32} \cdot [S]_m \cdot \dot{m}_{Tf} \qquad (20)$$

It is worth to note that the result of Equation (15) is only a first tentative value, as the CO_2 mass flow rate will be corrected after having evaluated the CO mass flow rate.

The other pollutant emissions (NO_x and CO) have been calculated on the basis of the equipment experimental emission data, usually given as a function of the load fraction. The pollutant emission mass flow rates for a boiler and gas engine are shown in Figures 2 and 3, respectively.

Accordingly, from a general point of view, CO and NO_x emissions are evaluated as a function of the equipment set point SP:
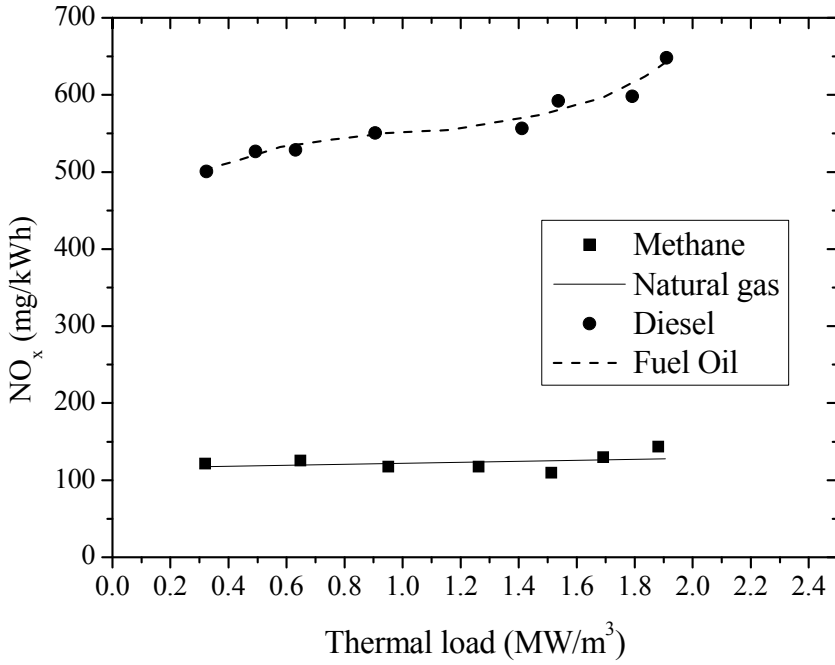
$$\dot{m}_{CO/NO_x} = f(SP) \qquad (21)$$
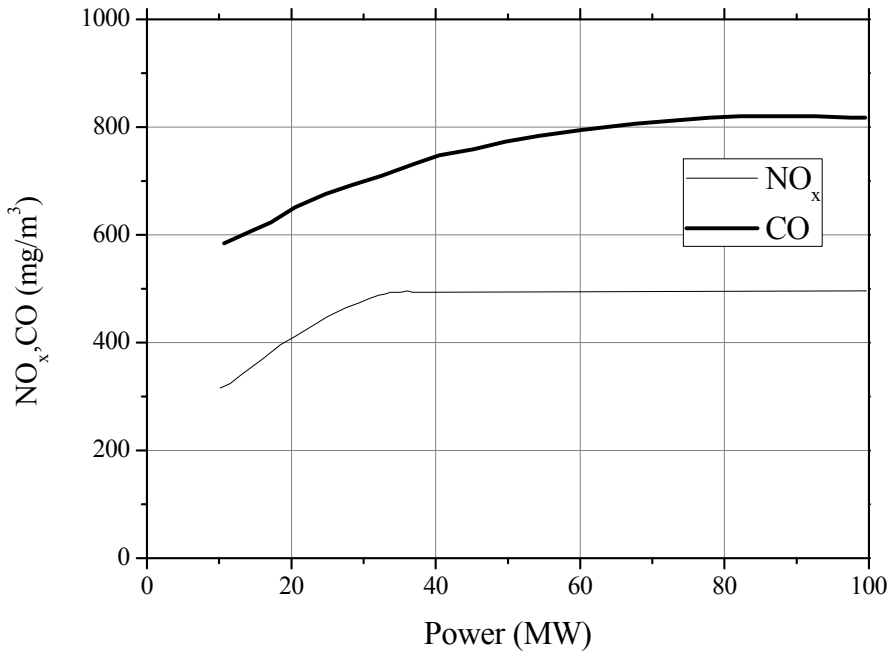
Fig. 2. NOx thermal load influence for the boilers.

Fig. 3. NOx and CO load influence for the internal combustion engine.

It must be highlighted that part of the consumed electricity could be purchased from the public network. Therefore, to minimise the pollution of the power plant on a fair basis, the emissions deriving from the production of the electric energy drawn from the public network must be estimated and taken into account. For this reason, we have introduced a polluting factor pf_{mix} (expressed in kg/kWhe) depending on the mix of the different pollutant emissions (CO, NOx, Soot, SOx) of the national power plants connected to the network:

$$pf_{mix} = kWh_e \left(0.021 \cdot pf_{CO} + 0.418 \cdot pf_{NOx} + 0.296 \cdot pf_{soot} + 0.265 \cdot pf_{SOx} \right) \tag{22}$$

The Italian polluting factors are reported in Table 2 (from ENEL s.p.a.). The coefficients multiplying each pf factor have been chosen on the basis of the current Italian environment limitations (Italian Ministry for the Environment, 2002).

pfCO	pfNOx	pfCO2	pfSOx
0.032	0.6	0.22	0.9

Table 2. 2004 italian pollutant emission factor (kg/kWh)

A similar factor exists also for carbon dioxide (i.e. related to the average electrical efficiency of the national power plants connected to the network):

$$\dot{m}_{CO_2} = pf_{CO_2} \cdot kWh_e \tag{23}$$

The carbon dioxide polluting factor, pf_{CO_2}, has been set to 0.531 $\frac{kg_{CO_2}}{kWh_e}$ according to ENEL s.p.a. data.

3.8 Economic output

The economical optimisation is performed maximising the total cost:

$$TC = ElC - FC \tag{24}$$

where ElC is the electricity cost and FC represents the total fuel cost:

$$FC = c_{bf} \cdot m_{bf} + c_{gef} \cdot m_{gef} \tag{25}$$

where c_{bf} and c_{gef} represent the boiler and the engine fuel cost, respectively. It is important to note that, even if the boilers and the internal combustion engines are both fed by natural gas, the values of c_{bf} and c_{gef} may be different (i.e. different taxes are applied if the same fuel is used for heat or electricity production). Actually, Current Italian Legislation yields a 0.25 m3/kWh of gas used in CHP defiscalisation (40 %) with respect to standard boilers (this is related to the incentive pay to improve final energy usage).

3.9 Time scale

Even if any time step may be in principle applied to the developed numerical model, the minimum time-step is defined by the time interval between the specific data available by the user on the energy loads.

The energy demand is the time integral calculation of the instantaneous power supplied by the power plant. It can be represented by a continuous function, as shown in Figure 4.

In principle, to represent the energy utilisation curve we should need an infinite number of data. In practice, the available data (i.e. energy consumption and production data) in a plant are far from being instantaneous. Moreover, such a precise data could be even useless due to the method approximations and the related foresight uncertainty.

Performing the optimisation of an energy system management requires a correct time step choice, which must be a right compromise among various effects.

For example, a small time steps guarantee accuracy, but the resulting management criterion may be applicable with difficulty, as the equipment set point adjustment could be inconsistent with the equipment specifications, both in terms of availability of an automated control system or in terms of component thermal inertia (circles in Figure 4). Moreover, the effort required to frequently change the components set point may not be justified by the effective advantage in terms of energy/money saving. It is worth noticing, in fact, that the convenience of turning on or off a thermal machine (i.e. internal combustion engine), depends on the price of electricity, and the time scale of electricity price variation are usually of the order of some hours (i.e. 4, 6, 12 hours). An example of electricity rate is given in the next section.

In this paper, four different time steps have been used, a month, half a day, four hours and one hour in order to highlight the importance of the parameter "time step" in the energy system management.
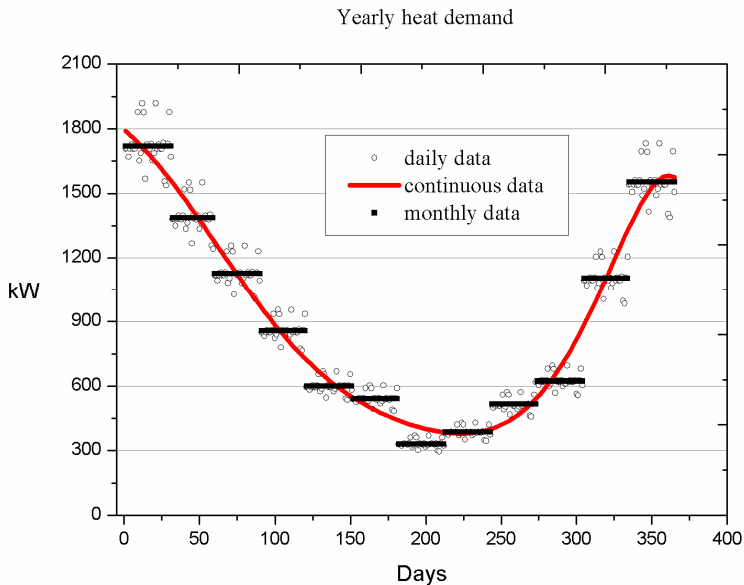

Fig. 4. Yearly thermal demand.

4. Case study

A pharmaceutical industrial plant has been selected as the case study for the present optimization procedure. The power plant consists of:

        1 natural gas internal combustion engine
        1 steam boiler
        1 hot water boiler
        1 mechanical chiller
        2 absorption chillers

The main characteristics of each component are summarized in Table 3. Energy flows and component interconnections are reported in Figure 5.

EQUIPMENT	Producer	Output	Efficiency
Gas engine	CAT	2000 kWe	0.37
Compression chiller	YORK	4200 kW	3.9
Absorption chillers	YAZAKI	500 kW	0.72
Hot water boiler	RIELLO	2500 kW	0.85
Steam boiler	RIELLO	3200 kW	0.84

Table 3. Equipment specifications
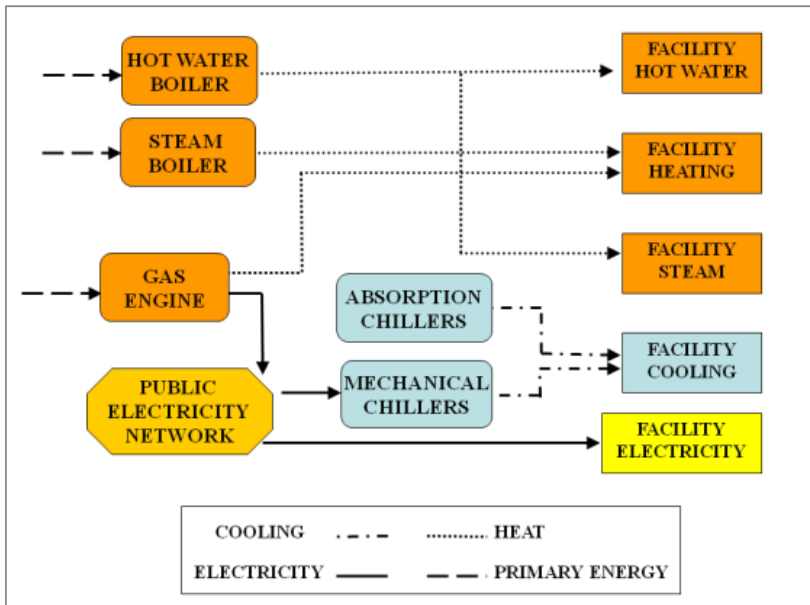
Fig. 5. Power plant energy flows and cooling installation.

The installation is designed for producing domestic hot water and heating (2.5 MW), steam (3.2 MW), cooling (4.3 MW) and electricity (1.2 MW).

The economical results and fuel usage registered in 2005, are used to validate the proposed model. In the standard operation of the power plant, the internal combustion engine is on at full power (set point equal to 1) during the day (7 am – 8 pm) and it is turned-off during the night (8 pm – 7 am). The switching on of the boilers is determined by the heat balance (i.e. heat demand minus the heat eventually available from the thermal engines). The chillers are turned on in function of the cold demand giving higher priority to the absorption chillers if there's heat available from the thermal engines (i.e. summer operation).

The operating range (set point from 0 to 1) of the machines have been discretised through steps of 0.2, being understood that the minimum set point is fixed by the manufacturer or by excessive efficiency degradation (i.e. 40% of full load for the thermal engines).

An important element for the economical optimisation is the electricity rate. In the present case, the electricity rate of the industrial plant is divided into three time bands, as shown in Table 5 (the price includes fixed contributions). Table 4 shows the year cost and consumptions summary, compared with the simulation results. A mean difference of about 2% of reported values is globally appreciable.

Year	2005	simulation	% error
Total cost (k€)	2182	2132	-2.4
Gas usage engine (m3)	1306734	1281906	-1.9
Gas usage boilers (m3)	2334173	2285155	-2.2
Public electricity cost (k€)	984	964	-2.1

Table 4. Energy aspects of the power plant

Time Bands	Price (c€/kWh)
Peak hours	14.59
Full hours	12.98
Empty hours	8.68

Table 5. Electricity rate

5. Results and discussion

The numerical method capabilities have been firstly evaluated performing three different simulations considering the same time scale and different optimisation criteria (minimum cost of operation, minimum consumption of fuel and minimum polluting emissions).

Finally, in order to highlight the numerical results dependence on the available data time scale, four simulations have been performed considering the same optimisation criterion with different time scales.

5.1 Optimisation criterion effect

The following three different optimisation strategies have been considered:

       Strategy #1: minimise the total operation cost

       Strategy #2: minimise fuel consumption

       Strategy #3: minimise polluting emissions

Each simulations has been performed using a time step of 4 hours. Table 6 compares the simulation results for the different optimization criterion.

	Strat. # 1	Strat.# 2	Strat.# 3
Total cost (k€)	1947	2094	2040
Engine fuel consumption (m3)	3405888	3167942	3283027
Boilers fuel consumptions (m3)	291359	375772	324488
Electricity cost (k€)	850	1022	956
CO2 emissions (kg)	14434458	14130819	14299282

Table 6. Four hours time step results

It is immediately detectable that in every simulation, independently from the optimization criterion, the total cost is lower than 2005, thus demonstrating that the previous standard operation was far from being the optimal one, also from an economical point of view. These results also confirm that, often, fuel consumption (i.e. CO_2 emissions) or pollutant emissions reduction, may also yield an economical advantage.

Adopting strategy #1, optimising the total cost, we could save more than the 11% of the original cost. Such an economic saving is obtainable without any installation improving (and then without any additional investment), but only with an optimal management of the power plant components. The operating conditions of the power plant components are reported in Figure 6 and Figure 7. The first graph shows the equipment utilisation factor in function of the set point, thus indicating if the components size have been properly chosen. The second graph, that shows the equipment utilisation yearly distribution, demonstrates if the equipment is characterized by a seasonal behaviour, or if it works almost constantly during the year.
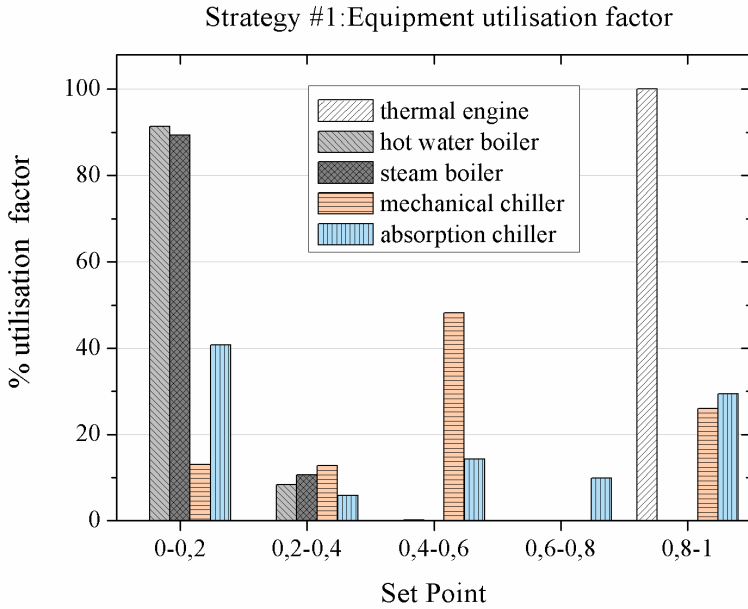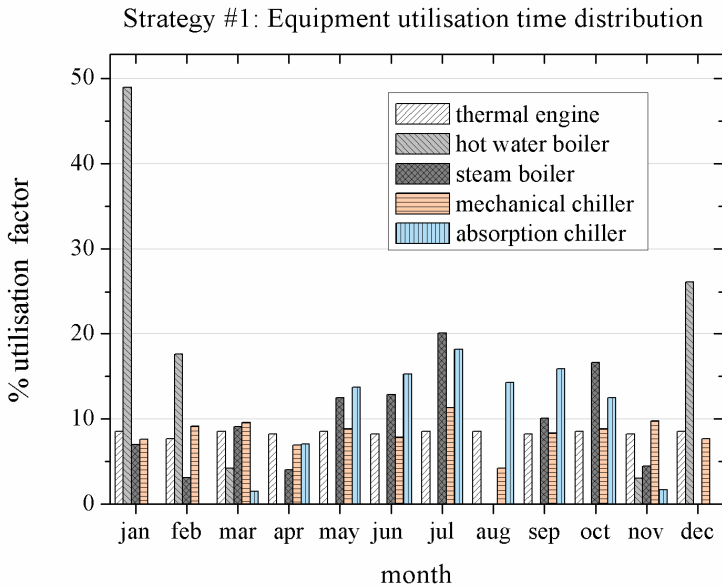
Strategy #1:Equipment utilisation factor

Fig. 6. Strategy #1: equipment utilisation factor.

Strategy #1: Equipment utilisation time distribution

Fig. 7. Strategy #1: equipment utilisation time distribution.
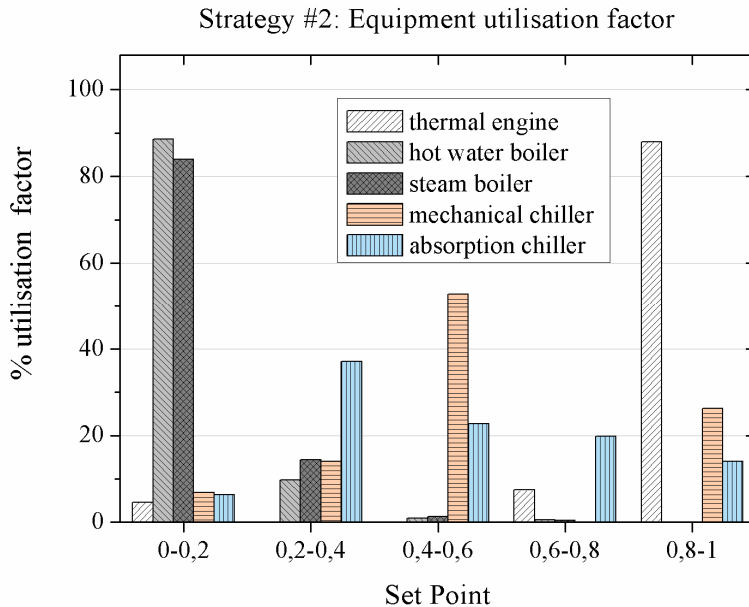
Strategy #2: Equipment utilisation factor

Fig. 8. Strategy #2: equipment utilisation factor.

The cogenerative thermal engine operates always under full load and its use is evenly distributed over the year, underlying a correct design sizing. On the other hand, the boilers are clearly over-sized, as they never work over the 40% of their capabilities. This fact can be explained observing that, originally, the power plant didn't include the cogenerator and the boilers had to satisfy the whole thermal demand. Regarding the cold production, chillers utilisation, both mechanical and absorption, is more regular over the year. Absorption chillers are turned on only during the warm months, when the heat demand is lower than the internal combustion engine heat production.

It may appear singular that minimising the fuel consumption (strategy #2) does not yield the economical optimisation. This is related to the fact that the natural gas cost depends on its usage (see eq. 25), and in particular it is reduced for CHP utilisation. Therefore, it may be economically convenient to consume more gas for CHP operation. On the other hand, when the target is the carbon dioxide emissions minimisation, the high efficiency of the boiler together with a low electricity request may lead to a lower thermal engine utilisation. Comparing Figure 6 and Figure 8, in fact, it is possible to notice that strategy #2 requires a greater use of the boiler with respect to strategy #1. In addition, it can be appreciated a more uniform equipment utilisation over the year. Moreover, the economic optimisation leads a reduction of the thermal engine utilisation as the electricity rate is such that in some periods the electricity purchase from the public network is more convenient than the auto-production. The thermal engine is even turned off in August, during the industrial plant summer closure. These results also highlight the significant effects of the electricity and gas rates on the optimal management of the power plant.(Figure 9)
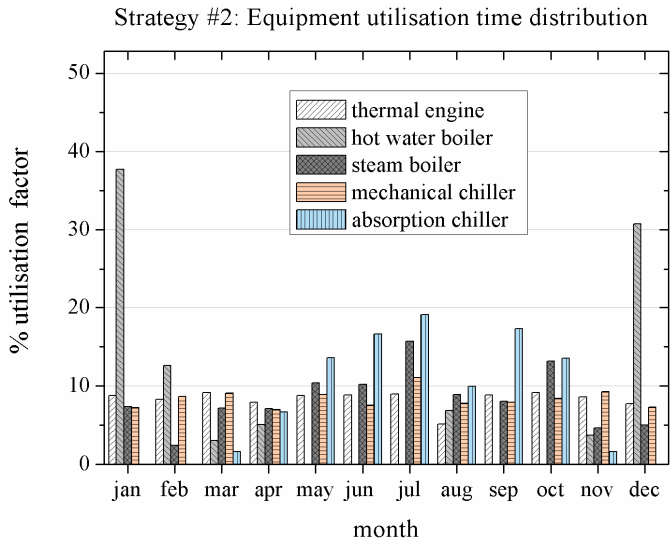
Strategy #2: Equipment utilisation time distribution

Fig. 9. Strategy #2: equipment utilisation time distribution.

Finally, considering the pollutant emissions as the target function to be minimised, the result is a compromise between the first two strategies, as primarily a function of the environmental impact of the CHP under full load and part load operations. The power plant components operation with strategy #3 is shown in Figure 10 and Figure 11.
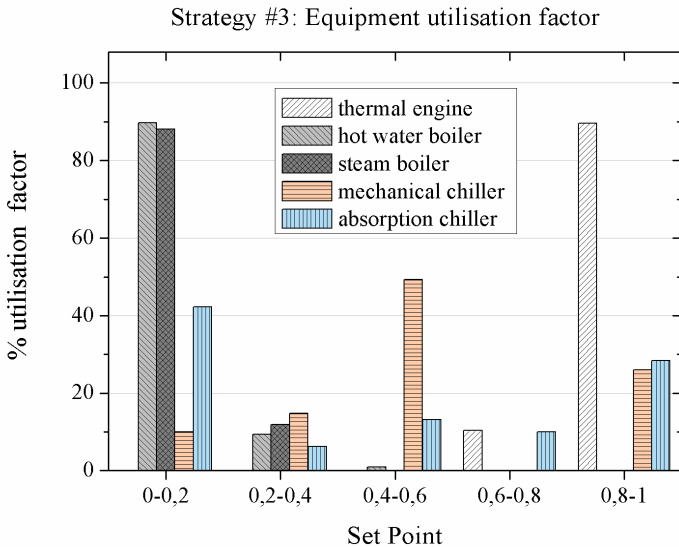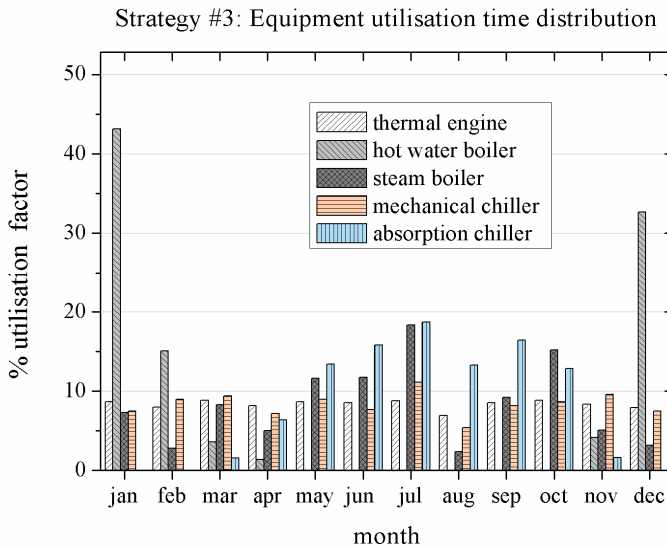
Strategy #3: Equipment utilisation factor

Fig. 10. Strategy #3: equipment utilisation factor.

Strategy #3: Equipment utilisation time distribution

Fig. 11. Strategy #3: equipment utilisation time distribution.

5.1 Time scale effect

In this paragraph, the optimisation strategy #2 results performed on four different time scales are presented. Yearly global results are summarised in Table 7.

	Monthly	12h	4h	1 h
Total cost (k€)	1921	2008	2094	2103
Engine gas usage (m3)	3349123	3195003	3167942	3162428
Boilers gas usage (m3)	274246	352955	375772	390128
Net electricity cost (k€)	844	938	1022	1031
CO2 emissions (kg)	13806563	14086093	14130819	14148523

Table 7. Optimisation results using different time steps

Firstly, as expected, reducing the time-step leads to a fuel consumption reduction, as the optimisation becomes more accurate. Considering that the minimum time-step is determined by the time-scale of energy consumption data, the more frequent is the measurement of fuel and electricity consumption the more accurate is the present methodology.

As the fuel consumption reduces, the total cost rises, such as boilers gas usage, public electricity cost and carbon dioxide emissions. This fact can be easily related to the lower usage of the thermal engine, which means that a greater part of the electric energy demand have to be satisfied by the public network and the boilers have to compensate for the lower

heat production by cogeneration. In the matter of CO2, even if boilers efficiencies are higher than the engine one, the emissions are increased because of the fuel mix utilization in public electricity production instead of natural gas only.

As reported in Table 8, mean and variance values of the equipment installation set points decrease as the time step raises, with the exception of the engine mean set point. This is related both to the increased energy demand variation and the higher efficiency of the boilers. Considering the negligible gain (0.003 % as reported in Table 8) observed changing the time step from 4 h to 1h time step and the effort required (both technological and managerial) to make a frequent control of the power plant components, it may be counterproductive to use very small time-steps. It must be also noticed that using a little time step forces a frequent regulation of the equipment set point, thus producing losses that cannot be predicted by the present quasi-steady numerical model. As an example over two weeks, Figure 12 shows how reducing the time step the steam boiler set points vary around its mean value, represented respectively by the bigger time step.

		1 h	4 h	12 h	Month
Thermal engine	mean	0,88	0,93	0,94	0,946
	variance	0,052	0,05	0,04	0,003
Hot water boiler	mean	0,057	0,056	0,053	0,042
	variance	0,016	0,013	0,012	0,006
Steam boiler	mean	0,12	0,12	0,1	0,076
	variance	0,011	0,01	0,009	0,005
Mechanical chiller	mean	0,59	0,57	0,56	0,53
	variance	0,084	0,083	0,081	0,02
Absorption chillers	mean	0,45	0,44	0,41	0,35
	variance	0,155	0,15	0,13	0,09

Table 8. Mean and variance of the equipment installation set points with strategy #2 using different time stepping

Considering the plant regulation point of view, the above results show that with manual power management (which means that the machines are manually regulated and therefore not compatible with small time-steps) it is still possible to achieve impressive results in terms of energy saving. Alternatively, with automatic power management, which theoretically allows a continuous regulation, extra-savings could be obtained.
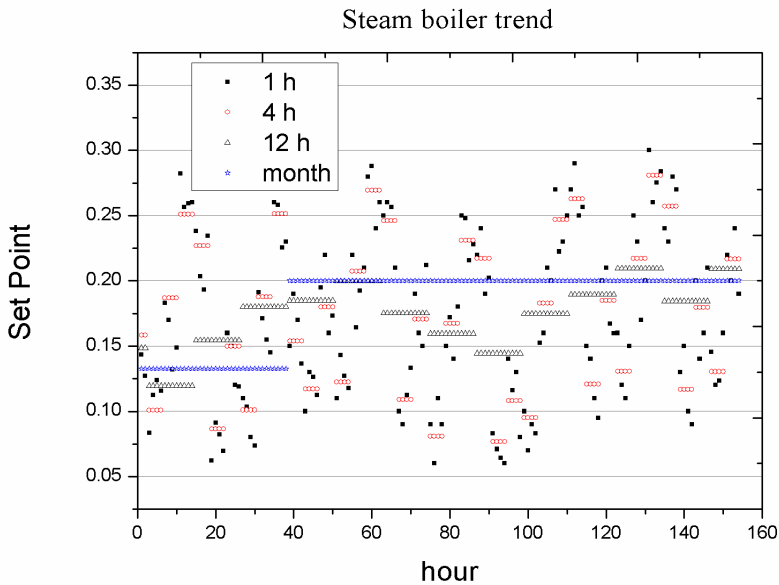
Fig. 12. Two weeks steam boiler set points.

6. Calculating or measuring the energy demand

The facility energy demand, which represent the first of the non-controllable input variables, may be obtained through historical data (i.e. energy bills) or may be directly measured or may result from a combination of the two. The present numerical results clearly highlight that the energy demand data availability is crucial to the success of implementing the proposed methodology, as the time-scale detail on the energy demand data determines the minimum time step between different set points and therefore the effective gain.

It is also important to notice that making the consumption profile on historical data , as done for the present case study, may lead to wrong conclusions and non-economic actions, as energy consumption may significantly vary from year to year, as it is related to several factors as production volume, ambient temperature, daylight length etc.

Therefore, to be effective, the present procedure should be coupled to a real-time energy monitoring system. With modern computers, in fact, the optimisation could be calculated in short times, similar to or smaller than a typical model time-step, thus giving the equipment setpoints "real-time". Moreover, if the proposed computational procedure is combined to an automatic system to control the equipment set-points, the optimisation could be performed in real-time.

The energy demand from the served facility may be also obtained through another mathematical model, which is in turn built on the basis of historical or measured data. This requires the construction of a consumption model: modeling the industrial plant energy consumption in function of its major affecting factors (i.e. energy drivers), as production volume, temperature, daylight length etc. This model should give the expected consumption in function of time and, again, the time-step should be as small as possible in order to have

reliable predictions and to distinguish the plant consumption and the energy drivers variation within the time bands of the energy rate. This could be done by installing a measuring system to record both energy consumption and energy drivers. The meters position within the plant is particularly important in order to correlate the energy consumption to the energy drivers (i.e. different production lines). Therefore, a preliminary analysis based, for example, on the nominal power and the utilization factor of the single machines should be performed in order to build a meters tree.

7. Conclusions

The present chapter discusses the importance of energy systems proper management to reduce energy costs and environmental impact. A numerical model for the optimal management of a power plant in buildings and industrial plants is presented. The model allows evaluating different operating strategies for the power plant components. The different strategies are defined on the basis of a pure economic optimisation (minimisation of total cost) and/or of an energetic optimisation (minimisation of fuel consumption) and/or of an environmental optimisation (minimisation of pollutant emissions). All these strategies have been applied to an energy system serving a pharmaceutical industrial plant demonstrating that, independently from the optimisation criterion, a significant gain can be obtained with respect to the standard operation with every objective function (cost, fuel consumption or pollutant emissions).

Furthermore, given the same optimisation criterion, remarkable differences are observed when varying the time-step, highlighting that the accuracy of the numerical results is strictly dependent on the detail level of the external inputs. In particular, the time-step dependence shows on one hand the importance of continuously monitoring the energy consumption (data available with a high frequency) and on the other hand the uselessness of using very small time scales for the energy system regulation.

The main advantages of the described model are that it is time efficient and its effectiveness is guaranteed whatever is the input data detail. Obviously, the more detailed are the input data, the more accurate are the numerical results. Nevertheless, even using monthly data it has been possible to suggest a cost reducing operating strategy. Moreover, in the presence of an energy consumption monitoring system, the proposed methodology could allow a real-time calculation of the optimal equipment setpoints.

8. References

Agency for Natural Resources and Energy, January 2004, http://www.enecho.meti.go.jp.

Andreassi L., Ciminelli M.V., Feola M. & Ubertini S. (2009) Innovative Method for Energy Management: Modelling and Optimal Operation of Energy Systems *Energy and Buildings* Volume 41 pp. 436-444

Arivalgan A., Raghavendra B.G. & Rao A.R.K.. (2000) Integrated energy optimization model for a cogeneration in Brazil: two case studies. *Applied Energy* Volume 67 pages 245-263

Cardona E. & Piacentino A. (2007) Optimal design of CHCP plants in the civil sector by thermoeconomics. *Applied Energy* Vol. 84 pages 729-748

Cesarotti V., Ciminelli M.V., Di Silvio B., FedeleT. & Introna V. (2007) Energy Budgeting and Control for Industrial Plant through Consumption Analysis and Monitoring, *Proceedings of European Power and Energy Systems EuroPES 2007*

Doering R.D.& Lin B.W. (1979) Optimum operation of a total energy plant. *Computers & Operations Research* Vol.6 pages 33-38

Frangopoulos C.A., Lygeros A.L., Markou C.T. & Kaloritis P.(1996) Thermoeconomic operation optimization of the Hellenic Aspropyrgos Refinery combined cycle cogeneration system, *Applied Thermal Eng*. Volume 16 pages 949-958

Italian Ministry for the Environment, ''Recepimento della direttiva 1999/30/CE del Consiglio del 22 aprile 1999 concernente i valori limite di qualita` dell'aria ambiente per il biossido di zolfo, il biossido di azoto, gli ossidi di azoto, le particelle e il piombo e della direttiva 2000/69/CE relativa ai valori limite di qualita` aria ambiente per il benzene ed il monossido di carbonio'', Gazzetta Ufficiale Supplemento Ordinario, 2002, p. 87.

Kamal W.A. (1997) Improving energy efficiency—the cost-effective way to mitigate global warming. *Energy Conservation and Management* 38 1, pp. 39–59.

Kong X.Q, Wang R.Z. &Huang X.H. (2005) Energy optimization model for a CCHP system with available gas turbines. *Applied Thermal Engineering.* Vol. 25 pages 377-391

Kong X.Q., Wang R.Z., Li Y. & Huang X.H. (2009) Optimal operation of a micro-combined cooling, heating and power system driven by a gas engine. *Energy Conversion and Management.* Vol. 50 pages 530-538

Lopes L., Hokoi S., Miura H.& Shuhei K.(2005) Energy efficiency and energy savings in Japanese residential buildings—research methodology and surveyed results, *Energy and Buildings* 37 698–706

Marik K., Schindler Z. &. Stluka P. (2008) Decision Support tools for advanced energy management. *Energy*. Vol. 33 pages 858-873

Meier A.K. (1997) Observed Savings from Appliance Efficiency Standards *Energy and Buildings*, 26 111-117

Moslchi K., Khade, M. & Bernal R. (1991) Optimization of multiplant cogeneration system operation including electric and steam network, *IEEE Trans Power Syst* **6** (2) pp. 484–490

Puttgen H.B. & MacGregor P.R. (1996) Optimum scheduling procedure for cogenerating small power producing facilities. *Proceedings IEEE Trans Power Syst* Vol. 4 pages 957-964

Smith, C.B.; Capehart B.L. & Rohrer Jr. (2007) Industrial Energy Efficiency and Energy Management, in *Energy Management and conservation* handbook. **ISBN:**9781420044294

Tstsaronis G. & Winhold M. (1985) Exoergonomic analysis and evaluation of energy conversion plants. I: A new methodology. II: Analysis of a coal-fired steam power plant. *Energy* Volume 10 pages 81-84

Tstsaronis G. & Pisa J. (1994) Exoergonomic evaluation and optimization of energy systems – application to the CGAM problem. *Energy* Volume 19 pages 287-321

Temir G. & Bilge D. (2004). Thermoeconomic analysis of a trigeneration system. *Applied Therm. Eng*. Volume 24, pages 2689-2699

Valero A. & Lozano M. (1993) Theory of the exergetic cost. *Energy* Vol. 18, pages 939-960

Van Schijndel A.W.M. (2002), Optimal operation of a power plant *Energy and Buildings* 34 1055-1065.

Von Spakovsky M.R:, Curtil V. &, Batato M. (1995) Performance optimization of a gas turbine cogeneration/heat pump facility with thermal storage. *Journal of Engineering of Gas Turbines and Power*, Volume 117 pages 2-9

9. Nomenclature

E	Primary energy	(E)
ElC	Annual electricity cost	(k€)
FC	Annul fuel cost	(k€)
H_i	Lower heating value	(kJ/kg)
P_{ElBal}	Electricity balance	(W)
P_{Elge}	Gas engine electric power production	(W)
P_{ElD}	Electricity demand	(W)
P_{ge}	Chemical power consumption in the gas engine	(W)
P_{mc}	Mechanical chiller electric power consumption	(W)
$\dot{Q}_{ac\max}$	Absorption chiller (maximum) heat consumption	(W)
$\dot{Q}_{Cac}$	Absorption chiller cold power production	(W)
$\dot{Q}_{CBal}$	Cold balance	(W)
$\dot{Q}_{CD}$	Cold demand	(W)
$\dot{Q}_{Cge}$	Gas engine cold power production	(W)
$\dot{Q}_{Cmc}$	Mechanical chiller cold power production	(W)
$\dot{Q}_{Hwac}$	Heat power from gas engine to absorption chiller	(W)
$\dot{Q}_{HwBal}$	Hot water balance	(W)
$\dot{Q}_{Hwb}$	Boilers heat production as hot water	(W)
$\dot{Q}_{HwD}$	Hot water demand	(W)
$\dot{Q}_{Hwge}$	Gas engine heat production as hot water	(W)
$\dot{Q}_{Sb}$	Boilers heat production as steam	(W)
$\dot{Q}_{SBal}$	Steam balance	(W)
$\dot{Q}_{SD}$	Steam demand	(W)

$\dot{Q}_{Sge}$	Gas engine heat production as steam	(W)
SP_{ge}	Gas engine set point	
SP_{mc}	Mechanical chiller set point	
SW_{ac}	Switch of supply heat of absorption chiller (0 or 1)	
TC	Total annual cost	(k€)
c_{bf}	Boilers fuel cost	(€/kg)
c_{gef}	Gas engine fuel cost	(€/kg)
c_{El}	Cost of electricity	(€/J)
cop_{ac}	Coefficient of performance of the absorption chiller	
cop_{mc}	Coefficient of performance of the mechanical chiller	
m_{bf}	Fuel mass consumption in the boilers	(kg)
m_{gef}	Fuel mass consumption in the gas engine	(kg)
$\dot{m}_{bf}$	Fuel mass flow rate in the boilers	(kg/s)
$\dot{m}_{CO}$	CO mass flow rate	(kg/s)
$\dot{m}_{CO_2}$	CO2 mass flow rate	(kg/s)
$\dot{m}_{fHwb}$	Hot water boiler fuel consumption	(kg/s)
$\dot{m}_{fSb}$	Steam water boiler fuel consumption	(kg/s)
$\dot{m}_{gef}$	Fuel mass flow rate in the gas engine	(kg/s)
$\dot{m}_{NO_x}$	NOx mass flow rate	(kg/s)
$\dot{m}_{SO_x}$	SOx mass flow rate	(kg/s)
$\dot{m}_{Tf}$	Total fuel mass flow rate	(kg/s)
pf_{CO}	CO polluting factor	
pf_{CO_2}	CO2 polluting factor	
pf_{mix}	Global polluting factor	
pf_{NO_x}	NOx polluting factor	
pf_{soot}	Soot polluting factor	
pf_{SO_x}	SOx polluting factor	

Energy Management

Alaa Mohd

The University of South Westphalia, Campus Soest
Germany

1. Introduction

Fossil fuels are currently the major source of energy in the world. However, as the world is considering more economical and environmentally friendly alternative energy generation systems, the global energy mix is becoming more complex. Factors forcing these considerations are (a) the increasing demand for electric power by both developed and developing countries, (b) many developing countries lacking the resources to build power plants and distribution networks, (c) some industrialized countries facing insufficient power generation and (d) greenhouse gas emission and climate change concerns. Renewable energy sources such as wind turbines, photovoltaic solar systems, solar-thermo power, biomass power plants, fuel cells, gas micro-turbines, hydropower turbines, combined heat and power (CHP) micro-turbines and hybrid power systems will be part of future power generation systems.

A new trend in power systems is developing toward distributed generation (DG), which means that energy conversion systems (ECSs) are situated close to energy consumers and large units are substituted by smaller ones. For the consumer the potential lower cost, higher service reliability, high power quality, increased energy efficiency, and energy independence are all reasons for interest in distributed energy resources (DERs). The use of renewable distributed energy generation and "green power" can also provide a significant environmental benefit. This is also driven by an increasingly strained transmission and distribution infrastructure as new lines lag behind demand and to reduce overall system losses in transmission and distribution. Other motives are the increased need for reliability and security in electricity supply, high power quality needed by an increasing number of activities requiring UPS like systems and to prevent or delay the expansion of central generation stations by supplying the growing loads locally (McDowall 2007; Brabandere October, 2006).

Nevertheless, all of these sources require interfacing units to provide the necessary crossing point to the grid. The core of these interfacing units is power electronics technologies since they are fundamentally multifunctional and can provide not only their principle interfacing function but various utility functions as well. The inverter is considered an essential component at the grid side of such systems due to the wide range of functions it has to perform. It has to convert the DC voltage to sinusoidal current for use by the grid in addition to act as the interface between the ECSs, the local loads and the grid. It also has to

handle the variations in the electricity it receives due to varying levels of generation by the renewable energy sources (RESs), varying loads and varying grid voltages. Inverters influence the frequency and the voltage of the grid and seem to be the main universal modular building block of future smart grids mainly at low and medium voltage levels.

The main problem associated with that is the development of general, flexible, integrated, and hierarchical control strategy for DERs to be integrated into the dynamic grid control and management procedures of electrical power supply systems (primary control, frequency and power control, voltage and reactive power control) through flexible power electronics namely inverters.

2. Distributed Generation

Currently, there is no consensus on how the distributed generation (DG) should be exactly defined (Purchala, Belmans et al. 2006). A very good overview of the different definitions proposed in the literature is given in (Pepermans, Driesen et al. 2005). In general, distributed generation describes electric power generation that is geographically distributed or spread out across the grid, generally smaller in scale than traditional power plants and located closer to the load, often on customers' property. Distributed generation is characterized by some or all of the following features:

- Small to medium size, geographically distributed power plants
- Intermittent input resource, e.g., wind, solar
- Stand-alone or interface at the distribution or sub-transmission level
- Utilize site-specific energy sources, e.g., wind turbines require a sustained wind speed of 20 km/hour. To meet this requirement they are located on mountain passes or the coast
- Located near the loads
- Integration of energy storage and control with power generation

Technologies those are involved in Distributed Generation include but are not limited to: Photovoltaic, Wind energy conversion systems, Mini and micro hydro, Geothermal plants, Tidal and wave energy conversion, Fuel cell, Solar-thermal-electric conversion, Biomass, Micro and mini turbines, Energy storage technologies, including flow and regular batteries, pump-storage hydro, flywheels and thermal energy storage.

The idea behind DG is not a new concept. In the early days of electricity generation, DG was the rule, not the exception (Driesen and Belmans 2006). However, technological evolutions and economical reasons developed the current system with its huge power generation plants, transmission and distribution grids. An overview of Distributed Generation is illustrated in Fig. 1.2.

In the last decade, technological innovation, economical reasons and the environmental policy renew the interest in Distributed Generation. The major reasons for that are:

- To reduce dependency on conventional power resources
- To reduce emissions and environmental impact
- Market liberalization
- Improve power quality and reliability

- Progress in DG technologies especially RESs
- To reduce transmission costs and losses
- To increase system security by distributing the energy plants instead of concentrating them in few locations making them easy targets for attacking
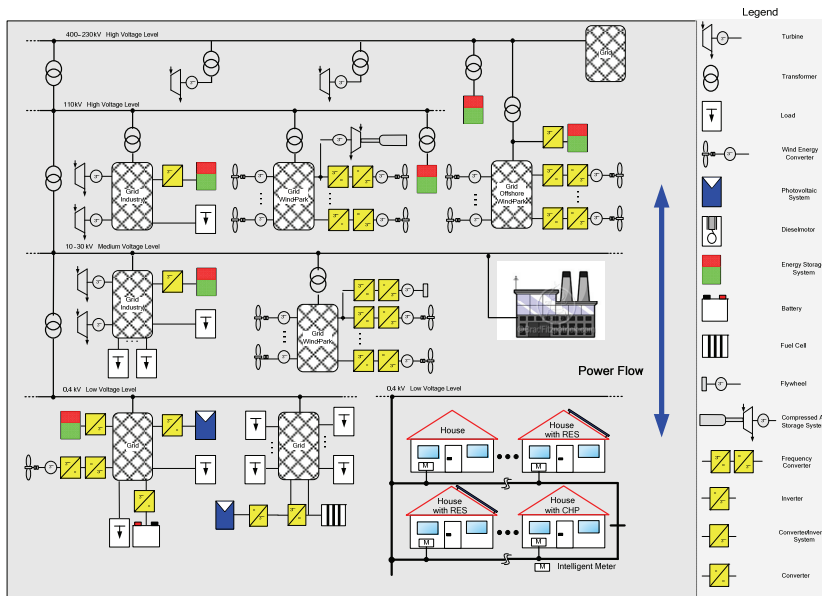

Fig. 1. Principal supply strategy of distributed Generation.

Distributed generation is becoming an increasing important part of the power infrastructure and the energy mix and is leading the transition to future Smart Grids. This is as well one of European Commission targets in order to increase the efficiency, safety and reliability of European electricity transmission and distribution systems and to remove obstacles to the large-scale integration of distributed and renewable energy sources.

3. Future Power Supply Systems (Smart Grids)

Energy plays a vital role in the development of any nation. The current electricity infrastructure in most countries consists of bulk centrally located power plants connected to highly meshed transmission networks. However, new trend is developing toward distributed energy generation, which means that energy conversion systems (ECSs) will be situated close to energy consumers and the few large units will be substituted by many smaller ones. For the consumer the potential lower cost, higher service reliability, high power quality, increased energy efficiency, and energy independence are all reasons for the increasing interest in what is called "Smart Grids".

Although the "Smart Grid" term was used for a while, there is no agreement on its definition. It is still a vision, a vision that is achievable and will turn into reality in near

future. One of the best and general definitions of a smart grid is presented in (Energy 2007). Smart grid is an intelligent, auto-balancing, self-monitoring power grid that accepts any source of fuel (coal, sun, wind) and transforms it into a consumer's end use (heat, light, warm water) with minimal human intervention. It is a system that will allow society to optimize the use of RESs and minimize our collective environmental footprint. It is a grid that has the ability to sense when a part of its system is overloaded and reroute power to reduce that overload and prevent a potential outage situation; a grid that enables real-time communication between the consumer and utility allowing to optimize a consumer's energy usage based on environmental and/or price preferences (Energy 2007).

3.1 Drivers Towards Smart Grids

Many factors are influencing the shape of our future electricity networks including climate change, aging infrastructure and fossil fuels running out. According to the International Energy Agency (IEA) Global investments required in the energy sector for 2003-2030 are an estimated $16 trillion. In Europe alone, some €500 billion worth of investment will be needed to upgrade the electricity transmission and distribution infrastructure. The following are the main drivers towards Smart Grids (Hatziagyriou 2008; Ipakchi 2007):

- *The Market:* Providing benefits to the customers by increasing competition between companies in the market. Competition has led many utilities to divest generation assets, agree to mergers and acquisitions, and diversify their product portfolios. This will give the customers a wider choice of services and lower electricity prices.

- *Environmental regulations:* Another significant driver concerns the regulation of the environmental, public health, and safety consequences of electricity production, delivery, and use. The greenhouse gases contribute to climate change, which is recognised to be one of the greatest environmental and economic challenges facing humanity. To meet these environmental policies, rapid deployment of highly effective, unobtrusive, low-environmental-impact grid technologies is required.

- *Lack of resources:* Energy is the main pillar for any modern society. Countries without adequate reserves of fossil fuels are facing increasing concerns for primary energy availability. Currently approximately 50% within EU is imported from politically unstable countries.

- *Security:* The need to secure the electric system from threats of terrorism and extreme weather events are having their effect as well. Techniques must exist for identifying occurrences, restoring systems quickly after disruptions, and providing services during public emergencies. This is why electricity grids should be redesigned to cope with the new rule.

- *Aging infrastructure:* The aging infrastructure (Europe and USA) of electricity generation plants, transmission and distribution networks is increasingly threatening security, reliability and quality of supply. The most efficient way to solve this is by integrating innovative solutions, technologies and grid architectures.

- *New generation technologies (Distributed Generation):* These forms of generation have different characteristics from traditional plants. Apart from large wind farms and large hydropower plants, this type of generation tends to have much smaller

electricity outputs than the traditional type. Some of the newer technologies also exhibit greater intermittency. However, existing transmission and distribution networks, were not initially designed to incorporate these kinds of generation technology in the scale that is required today.

- *Advanced power electronics:* Power electronics allow precise and rapid switching of electrical power. Power electronics are at the heart of the interface between energy generation and the electrical grid. This power conversion interface-necessary to integrate direct current or asynchronous sources with the alternating current grid-is a significant component of energy systems.
- *Information and communication technologies (ICT):* The application of ICT to automate various functions such as meter reading, billing, transmission and distribution operations, outage restoration, pricing, and status reporting. The ability to monitor real-time operations and implement automated control algorithms in response to changing system conditions is just beginning to be used in electricity (2003). Distributed intelligence, including "smart" appliances, could drive the co-development of the future architecture.

3.2 Key Challenges for Smart Grids

Even though many drivers for smart grids and their benefits are obvious, there are many challenges and barriers standing in the way and should be cracked first. These include:

- *Standardisation:* Design and development of a modular standardised architecture of modern power electronic systems for linking distributed energy converting systems (DECSs) (i.e. PV, wind energy converters, fuel cells, diesel generators and batteries) to conventional grids and to isolated grids on the basis of modular power electronic topologies which fulfil the requirements for integration into the dynamic control system of the grid (Ortjohann and Omari 2004).
- *Advance communication layer:* Development and implementation of a general communication layer model for simple and quick incorporation of DECSs in the grid and its superimposed online control system
- *Non-technical challenges:* Issues such as pricing, incentives, decision priorities, risk responsibility and insurance for new technologies adaptation, interconnection standards, regulatory control and addressing barriers. This also includes, finding a profitable business model, attracting resources and developing better public policies (Nigim and Lee 2007).

4. State of the Art

This section presents the state-of-the-art of power electronic inverters control used currently in electrical systems. Different system architectures, their modes of operation, management and control strategies will be analysed. Advantages and disadvantages will be discussed. Though, it is not easy to give a general view at the state of the art for the research area since it is rapid and going in different directions. The focus here will be on the main streams in low voltage grids especially paralleled power electronics inverters. Inverters are often paralleled to construct power systems in order to improve performance or to achieve a high system rating. Parallel operation of inverters offers also higher reliability over a single

centralized source because in case one inverter fails the remained (n-1) modules can deliver the needed power to the load. This is as well driven by the increase of RESs such as photovoltaic and wind. There are many techniques to parallel inverters which are already suggested in the literature, they can be categorized to the following main approaches:

1)   Master/Slave Control Techniques
2)   Current/Power Deviation (Sharing) Control Techniques
3)   Frequency and Voltage Droop Control Techniques
     a) Adopting Conventional Frequency/Voltage Droop Control
     b) Opposite Frequency/Voltage Droop Control
     c) Droop Control in Combination with Other Methods

4.1 Master/Slave Control Techniques

The Master/Slave control method uses a voltage controlled inverter as a master unit and current controlled inverters as the slave units. The master unit maintains the output voltage sinusoidal, and generates proper current commands for the slave units (Prodanovic, Green et al. 2000; Tuladhar 2000; Ritwik Majumder , Arindam Ghosh et al. 2007).

One of the Master/Slave configuration is the scheme suggested in (Chen, Chu et al. 1995; Jiann-Fuh Chen and Chu 1995) , see Fig. 2, which is a combination of voltage-controlled and current-controlled PWM inverters for parallel operation of a single-phase uninterruptible power supply (UPS). The voltage-controlled inverter (master) is developed to keep a constant sinusoidal wave output voltage. The current-controlled inverter units are operated as slave controlled to track the distributive current. The inverters do not need a PLL circuit for synchronization and gives a good load sharing. However, the system is not redundant since it has a single point of failure.
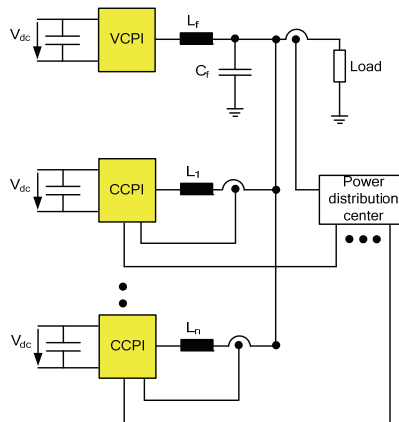
Fig. 2. Combined voltage and current controlled inverters (Jiann-Fuh Chen and Chu 1995).

A comparable scheme is also presented in (K Siri, C.Q. Lee et al. 1992) but it needs even more interconnection since it is sharing the voltage and current signals. In (Holtz and Werner 1990) the system is redundant by extended monitoring of the status and the

operating conditions of all power electronic equipment. Each block of the UPS system is monitored by two independent microcomputers that process the same data. The microcomputers are part of a redundant distributed monitoring system that is separately interlinked by two serial data buses through which they communicate. They establish a hierarchy among the participating blocks by defining one of the healthy inverter blocks as the master.

The scheme proposed in (Petruzziello 1990), see Fig. 3., is based on the Master/Slave configuration but is using a rotating priority window which provides random selection of a new master and therefore results in true redundancy and increase reliability.
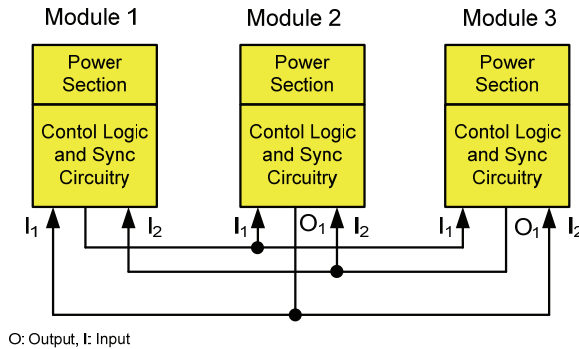
Fig. 3. Proposed Master/Slave configuration in (Petruzziello 1990)

In (Van Der Broeck and Boeke 1998) the system is also redundant since a status line is used to decide about the master inverter using a logical circuit (flip-flop), if the master is disconnected one slave becomes automatically the master. The auto-master-slave control presented in (Pei, Jiang et al. 2004) is designed to let the unit with highest output real power act as a master of real power and derives the reference frequency, the others have to follow as slaves. The regulation of the reactive power is similar, the highest output reactive power module acts as master of reactive power and adjusts the voltage reference amplitude.

In (Lopes 2004; J.A.P.Lopes, Moreira et al. 2006) the paper focus on operation of the microgrid when it becomes isolated under different condition. This was investigated for two main control strategies, single master operation where a voltage source inverter (VSI) can be used as voltage reference when the main power supply is lost; all the other inverters can then be operated in PQ mode. And multi-master operation where more than one inverter are operated as a VSI, other PQ inverters may also coexist. In more recent papers (Prodanovic, Green et al. 2000; T.C. Green and Prodanovic 2007; Prodanovic Oct. 2006) an enhanced approach is introduced, the master inverter is replaced by a central control block which controls the output voltages and can influence the output current of the different units, this is sometimes called central mode control or distributed control. This means that the voltage magnitude, frequency and power sharing are controlled centrally (commands are distributed through a low bandwidth communication channels to the inverters) and other issues such as harmonic suppression are done locally, see Fig. 4.
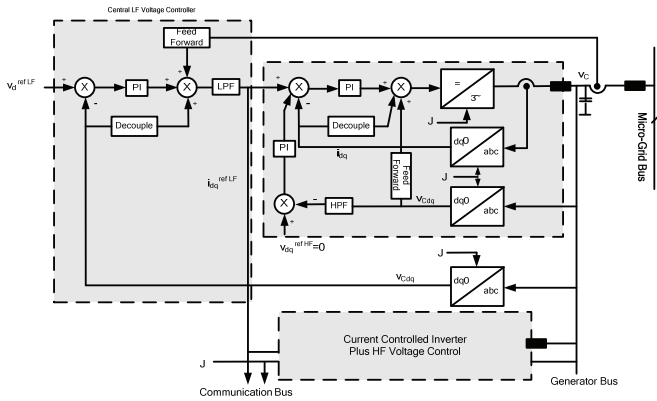
Fig. 4. Proposed distributed control configuration in (T.C. Green and Prodanovic 2007).

4.2 Current/Power Deviation (Sharing) Control Techniques

In this control technique the total load current is measured and divided by the number of units in the system to obtain the average unit current. The actual current from each unit is measured and the difference from the average value is calculated to generate the control signal for the load sharing (Tuladhar 2000). In the approach suggested in (T.Kawabata and S.Higashino 1988), see Fig. 5, the voltage controller adjusts the small voltage deviation and keeps the voltage constant. The ΔI signal is detected and given to the current loop as a correction factor, and the ΔP signal controls the phase of the reference sine wave. A very good load sharing can be obtained. Transient response is very good due to the feed forward control signal (Tuladhar 2000).
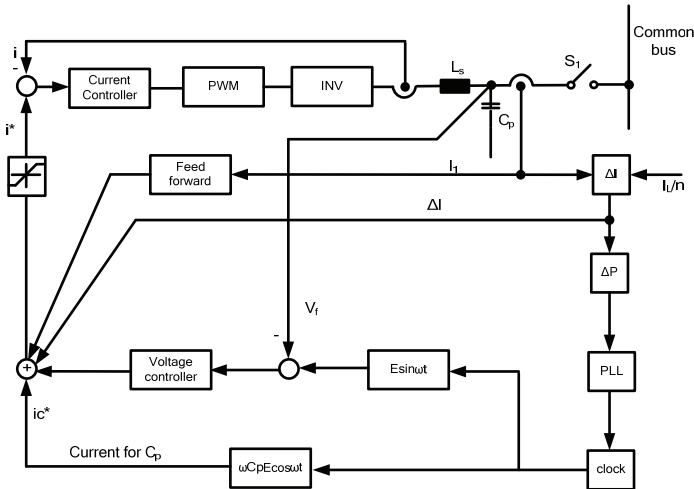
Fig. 5. Proposed parallel operation of inverter with current minor loop (T.Kawabata and S.Higashino 1988).

In (Huang 2006) circular chain control (3C) strategy is proposed, see below Fig. 6., all the modules have the same circuit configuration, and each module includes an inner current loop and an outer voltage loop control. With the 3C strategy, the modules are in circular chain connection and each module has an inner current loop control to track the inductor current of its previous module, achieving an equal current distribution.
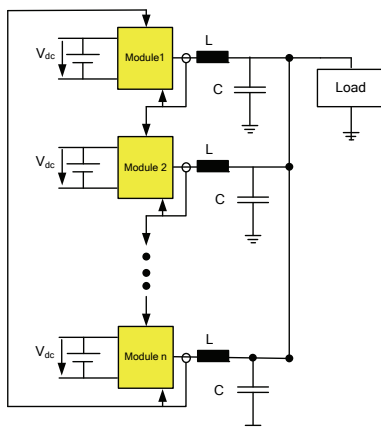
Fig. 6. The proposed circular chain control (3C) strategy (Huang 2006).

Authors of (Hanaoka 2003) proposed an inverter current feed-forward compensation which makes the output impedance resistive rather than inductive in order to get a precise load sharing. In (Hyun 2006) the paper goes further based on the approach introduced in (Hanaoka 2003) and proposes a solution to the noise problem of harmonic circulating currents due to PWM non-synchronization which is affecting the load sharing precision. This is done in (S. Tamai 1991) using a digital control algorithm. The digital voltage controller, which has high-speed current control as a minor loop, provides low voltage distortion even for nonlinear loads. Output current of each UPS module is controlled to share the total load current equally and the voltage reference command of each inverter is controlled to balance the load current. In (H.Oshima, Y.Miyazaya et al. 1991; W.Hoffmann, R.Bugyi et al. 1993; Lee, Kim et al. 1998) similar approaches are suggested. In (Qinglin, Zhongying et al. 2006) the focus is on developing a solution for the effect of DC offset between paralleled inverters and its effect on the circulating currents. In (Xing, Huang et al. 2002) the authors suggest two-line share bus connecting all inverters, one for current sharing control and the other to adjust the voltage reference.

4.3 Frequency and Voltage Droop Control Techniques
Many methods were found in the literature and can be roughly categorized into the following:

       a.   Adopting Conventional Frequency/Voltage Droop Control
       b.   Opposite Frequency/Voltage Droop Control
       c.   Droop Control in Combination with Other Methods

a.   Adopting Conventional Frequency/Voltage Droop Control

In (C.-C. Hua) the paper proposes a control technique for operating two or more single phase inverter modules in parallel with no auxiliary interconnections. In the proposed parallel inverter system, each module includes an inner current loop and an outer voltage loop controls, see Fig. 7. This technique is similar to the conventional frequency/voltage droop concept; uses frequency and fundamental voltage droop to allow all independent inverters to share the load in proportion to their capacities.
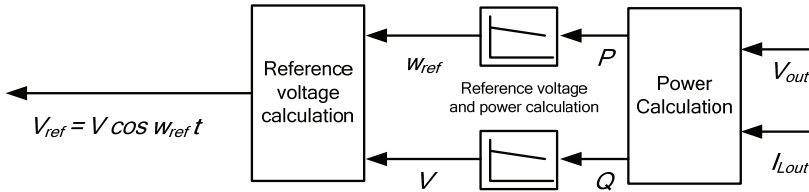
Fig. 7. Reference voltage and power calculation (C.-C. Hua).

In (M. C. Chandorkar 1993) scheme for controlling parallel-connected inverters in a stand-alone AC supply system is presented, see Fig. 8. This scheme is suitable for control of inverters in distributed source environments such as in isolated AC systems, large and UPS systems, PV systems connected to AC grids. Active and reactive power sharing between inverters can be achieved by controlling the power angle (by means of frequency), and the fundamental inverter voltage magnitude. Simulation results obtained for large units using Gate turn-off (GTO) thyristor switches. The control is done in the d-q reference frame; an inverter flux vector is formed by integrating the voltage space vector. The choice of the switching vectors is essentially accomplished by hysteresis comparators for the set values and then using a look-up table to choose the correct inverter output voltage vector. The considerations for developing the look-up table are dealt with in (Noguchi 1986). However, the inductance connected between the inverter and the load makes the output impedance high. Therefore, the voltage regulation as well as the voltage waveform quality is not good under load change conditions as well as a nonlinear load condition. The authors explain the same concept but with focusing in control issues of UPS systems in (M. C. Chandorkar, Divan et al. 1994).
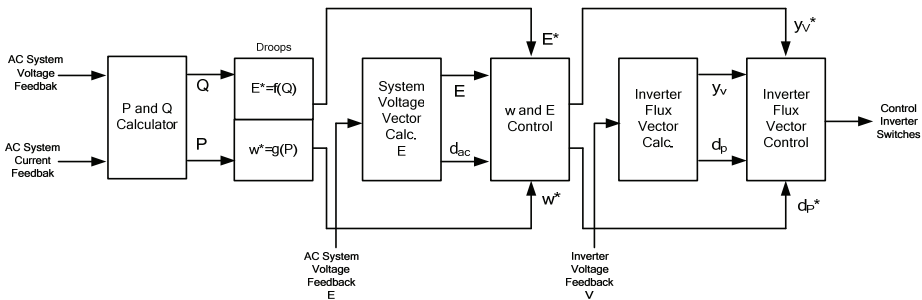
Fig. 8. Inverter control scheme (M. C. Chandorkar 1993).

In (Hauck Matthias 2000; Matthias and Helmut 2002) the inverse droop equations are used to control the inverter, see Fig. 9. The inverter is able to work in parallel with a constant-voltage constant-frequency system, as well as with other inverters or also in stand-alone mode. There is no communication interface needed. The different power sources can share the load also under unbalanced conditions. Very good load sharing is achieved by using an outer control loop with active and reactive power controller, for which the set point variables are derived out of droops. Furthermore, a relatively big inductance is used in the LC filter and a small decoupling reactance is used to decouple the inverter from other voltage sources. The interface inductance make the voltage source converters (VSCs) less sensitive to disturbances on the load bus (M. Chandorkar 1994; Sao and Lehn 2005).
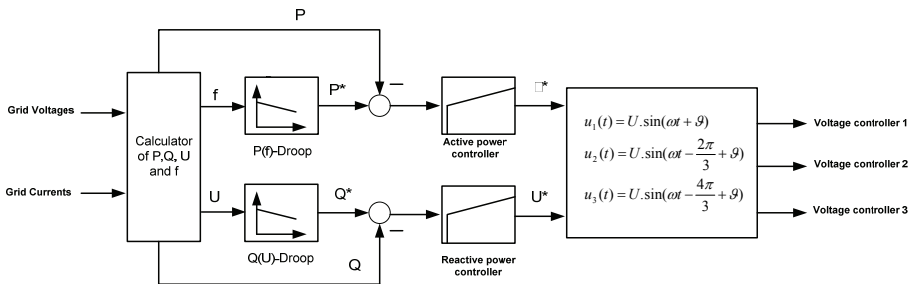
Fig. 9. Inverter control scheme proposed in (Hauck Matthias 2000; Matthias and Helmut 2002).

In (C.K. Sao) an interesting autonomous load-sharing technique for parallel connected three-phase voltage source converters is presented. This paper focuses on an improvement to the conventional frequency droop scheme for real power sharing and the development of a new reactive power-sharing scheme. The improved frequency droop scheme computes and sets the phase angle of the VSC instead of its frequency. It allows the operator to tune the real power sharing controller to achieve desired system response without compromising frequency regulation by adding an integral gain into the real power control. The proposed reactive power sharing scheme introduces integral control of the load bus voltage, combined with a reference that is drooped against reactive power output. This causes two VSCs on a common load bus to share the reactive load exactly in the presence of mismatched interface inductors if the line impedances are much smaller than the interface reactors (assuming short lines). Moreover, in the proposed reactive power control, the integrator gain can be varied to achieve the desired speed of response without affecting voltage regulation.

In (Engler 2000; A. Engler, M. Meinh et al. 2003; A. Engler, M. Meinhardt et al. 2004) the author discusses the application of conventional droops for voltage source inverters and categorize the system components to form a modular AC-hybrid power system. Then in (Engler 2006) by the same author an investigation of what is called opposite droop (active power/voltage and reactive power/frequency droop) control is carried out. The focus is on the need of different droop functions for different types of grids. In (Engler 2006) it is found that for high voltage (mainly inductive) grids the regular droop functions can be used also for distributed generation systems. For low voltage (mainly resistive) grids, so-called opposite droop functions could be used instead but the regular droop functions are advantageous since it allows connectivity to higher voltage levels and power sharing also

with rotating generators (A. Engler and Soultanis; Engler 2005; Karlsson, Björnstedt et al. 2005; Engler 2006).

A microgrid control was introduced and implemented in (Lasseter 2002; Robert Lasseter and Piagi 2006; Lasseter 2007; Piagi and Lasseter June 2006), the microgrid has two critical components, the static switch and the micro-source. The static switch has the ability to autonomously island the microgrid from disturbances such as faults or power quality events. After islanding, the reconnection of the microgrid is achieved autonomously after the tripping event is no longer present. This synchronization is achieved by using the frequency difference between the islanded microgrid and the utility grid insuring a transient free operation without having to match frequency and phase angles at the connection point. Each micro-source can seamlessly balance the power on the islanded microgrid using a power vs. frequency droop controller. This frequency droop also insures that the microgrid frequency is different from the grid to facilitate reconnection to the utility. The introduced micro-source control is shown in Fig. 10.
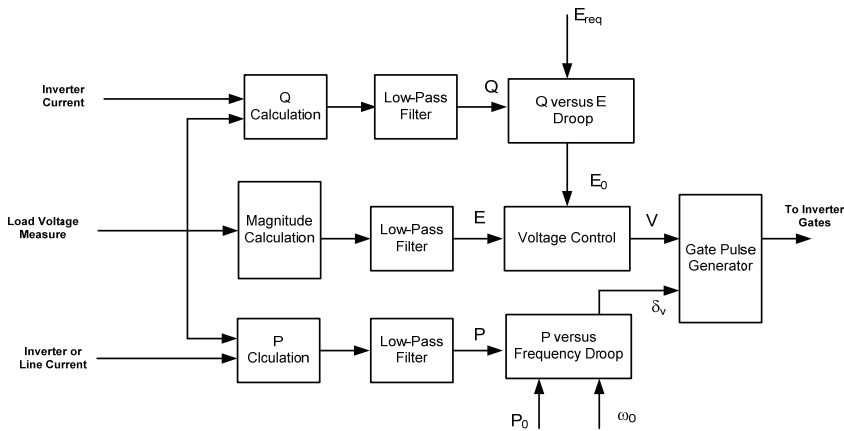
Fig. 10. Inverter control scheme proposed in (Lasseter 2002; Robert Lasseter and Piagi 2006; Lasseter 2007; Piagi and Lasseter June 2006).

The authors of (Ritwik Majumder , Arindam Ghosh et al. 2007) present a scheme for controlling parallel connected inverters using droop sharing method in a standalone ac system. The scheme proposed a PI regulator to determine the set points for generator angle and flux. The dynamic response of the system is investigated under different impedance load conditions especially motor loads. Paper (Maria Brucoli and Green 2006) analyzes the fault behaviour of four wire paralleled inverters (in droop mode) based on their control methodology.

b.   Opposite Frequency/Voltage Droop Control

In (Karlsson, Björnstedt et al. 2005; Guerrero, Berbel et al. 2006) the method selected here is to modify the droop functions of the source converters so that the regular droop functions are used in the steady-state case and opposite droops are used in transients, see Fig. 11. Note that here $\omega_{ref} = \omega_n$ and $v_{ref} = V_n$. The steady-state droop functions are according to:

$$p_s^* = K_\omega(\omega_{ref} - \omega)$$ (1)

$$q_s^* = K_v(v_{ref} - v_q)$$ (2)

where p_S^* and q_S^* are the active and reactive power references (index s denotes source converter, e.g. unit 1). K is the droop gain (slope). For the transient droop functions according to:

$$p_s^* = K_v(v_{ref} - v_q)$$ (3)

$$q_s^* = -K_\omega(\omega_{ref} - \omega)$$ (4)

where $\omega_{ref} = \omega^*$ and $v_{ref} = v^*$
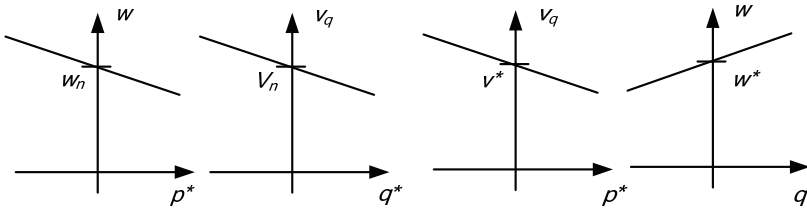
Fig. 11. Conventional droop functions (left) and transient droop functions (right) (Karlsson, Björnstedt et al. 2005; Guerrero, Berbel et al. 2006).

In this method the load-sharing is acceptable for the investigated, highly resistive, network. Still, in the case of line inductance in the same order of magnitude as the converter output filter inductance there can be a considerable degradation of power quality in terms of voltage disturbance. The origin of this degradation is the LC-circuit formed by the line inductance and the converter AC side capacitors. Furthermore, using this approach it is not possible to connect with the high level voltage which is using the regular conventional droop functions. In (Guerrero J.M, García de Vicuña et al. 2003; Guerrero, Vicuña et al. 2004; Guerrero, Berbel et al. 2006; Guerrero 2006; Guerrero 2005) the authors focus on the transient behaviour of parallel connected UPS inverters, they claim that damping and oscillatory phenomena of phase shift difference between the paralleled inverters could cause instabilities, and a large transient circulating current that can overload and damage the paralleled inverters. To overcome this they proposed using a method called "droop/boost" control scheme which adds integral-derivative terms to the droop function. This can be seen in Fig. 12. Stable steady-state frequency and phase and a good dynamic response are obtained. Further, virtual output impedance is proposed in order to reduce the line impedance impact and to properly share nonlinear loads, this is done using a high pass filter, the filter gain and pole values of this must be carefully chosen. Furthermore, the test results shown are considering a short resistive line, but the method is not taking into consideration what happens if the distance between the inverters is considerable, which is normally the case in distributed generation were an inductive impedance component appears. Nevertheless, when an inverter is connected suddenly to the common AC bus, a

current peak appears due to the initial phase error (Guerrero 2006). Compatibility problems are expected because of the opposite droop scheme (if synch generator will be included). The characteristic and the scheme are shown below:

$$E = E^* - nP - n_d \frac{dP}{dt} \tag{5}$$
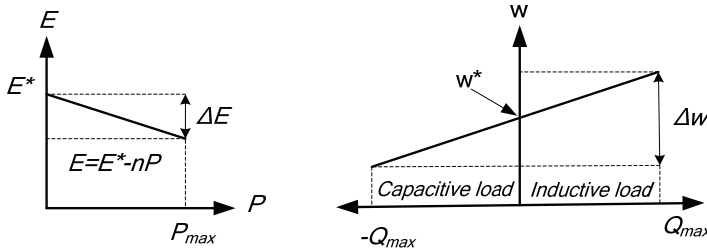
$$\omega = \omega^* - mQ - m_d \frac{dQ}{dt} \tag{6}$$

Fig. 12. Static droop/boost characteristics for resistive output impedance (Guerrero J.M, García de Vicuña et al. 2003; Guerrero, Vicuña et al. 2004; Guerrero, Berbel et al. 2006; Guerrero 2006; Guerrero 2005).

Where P is active power, Q is reactive power, E is output voltage, ω is angular frequency and m and n are the droop coefficients for the frequency and amplitude, respectively. As an addition in (Guerrero 2006) a soft-start is included to avoid the initial current peak as well as a bank of band pass filters in order to share the significant output-current harmonics. In more recent papers (Guerrero, Berbel et al. 2007; Josep M. Guerrero, Juan C. Vásquez et al. 2007) the authors use the conventional droop equations for a microgrid too.

$$E = E^* - n(Q - Q^*) \tag{7}$$

$$\omega = \omega^* - m(P - P^*) \tag{8}$$

c.   Droop Control in Combination with Other Methods

In (Brabandere, Bolsens et al. 2004; K. De Brabandere, A. Woyte et al. 2004; De Brabandere, Vanthournout et al. 2007; Brabandere October, 2006) each inverter supplies a current that is the result of the voltage difference between a reference AC voltage source and the grid voltage across a virtual impedance with real and/or imaginary parts. This is shown in Fig. 13. The reference AC voltage source is synchronized with the grid, with a phase shift, depending on the difference between nominal and real grid frequency. This method behaviour is equal to the normal existing droop control methods except that, short-circuit behaviour is better since it is controlling the active and reactive currents and not the power. It behaves also better in case of a non-negligible line resistance.
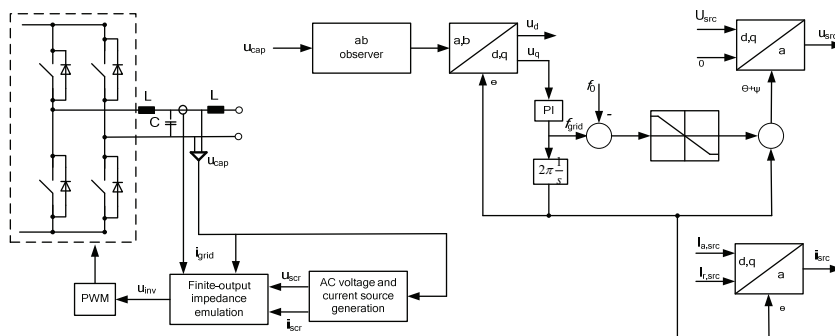
Fig. 13. Overall scheme for the proposed droop control method (Brabandere, Bolsens et al. 2004; K. De Brabandere, A. Woyte et al. 2004; De Brabandere, Vanthournout et al. 2007; Brabandere October, 2006).

In (E. Hoff 2004; T.Skjellnes, A.Skjellnes et al. 2002) novel fast control loops that adjust the output impedance of the closed-loop inverters is used in order to ensure resistive behaviour with the purpose to share the harmonic current content properly. In the measurements part a notch filter is added to remove the unwanted harmonics, it seems that without this filter the voltage regulator will not work efficiently. Furthermore, the control is done in the αβ-coordinates using a discrete controller.

The author of (Mihalache 2003) discusses the problem of inverters with very low output impedance (such as those employing resonant controllers) directly connected in parallel through a near zero impedance cable. Low total harmonic distortion (THD) content and good current sharing are simultaneously obtained by controlling the load angle through an least mean square estimator and by synthesizing a variable inductance in series with the output impedance of the inverter, while the harmonic current sharing is achieved by controlling the gain of the resonant controllers at the selected frequencies.

The authors of (Ernane Antonio Alves Coelho, Cortizo et al. 2000; Ernane Antonio Alves Coelho, Porfirio Cabaleiro Cortizo et al. 2002) introduced fast control loops that adjust the output impedance of the closed-loop inverters in order to ensure inductive behaviour with the purpose to share the harmonic current content properly. The paper presents a small-signal analysis for parallel-connected inverters in stand-alone AC power systems. The control approaches have an inherent trade-off between voltage regulation and power sharing (Guerrero, Berbel et al. 2006).

The signal injection technique proposed by (A. Tuladhar 1998; Tuladhar 2000) is not dependent in the plant parameters and can share reactive power even if the VSCs have not perfectly matched output inductors by having each VSC inject a non-60-Hz signal and use it as a means of sharing a common load with other VSCs on the network. However, the circuitry required to measure the small real power output variations due to the injected signal adds to the complexity of the control (C.K. Sao). Moreover, the controllers use an algorithm which is too complicated to calculate the current harmonic content, the harmonic current sharing is achieved at the expense of reducing the stability of the system (Guerrero J.M, García de Vicuña et al. 2003).
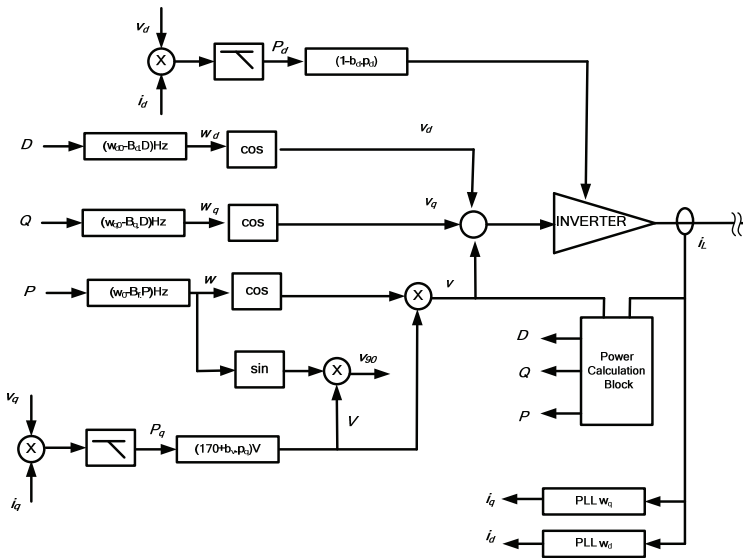
Fig. 14. Schematic diagram of implementing the signal injection technique (Tuladhar 2000).

In (Marwali, Jung et al. 2004) the proposed control method uses low-bandwidth data communication signals between each generation system in addition to the locally measurable feedback signals. The focus is on systems of distributed resources that can switch from grid connection to island operation without causing problems for critical loads. This is achieved by combining two control methods: droop control method and average power control method. In this method, the sharing of real and reactive powers between each DGS is implemented by two independent control variables: power angle and inverter output voltage amplitude. However, adding external communication can be considered as a drawback. Such communications increase the complexity and reduce the reliability, since the power balance and the system stability rely on these signals (Guerrero, Berbel et al. 2006). In (Glauser, Keller et al. 2000; Chen, Kang et al. 2004) a communication bus is used in addition to the conventional droop, it has to trigger all inverters to measure their load sharing parameters at the same line period, this is used to correct the load sharing calculation.

4.4 Discussion

The master/slave control configuration has many good characteristics. The inverters do not need a PLL circuit for synchronisation and give a good load sharing. The line impedance of the interconnecting lines does not affect the load sharing and the system is also easily expandable. There are, however, a few serious disadvantages. One of the major disadvantages is that most of these systems are not truly redundant, and have a single point of failure, the master unit. Another disadvantage of this configuration is that the stability of the system depends upon the number of slave units in the system (Tuladhar 2000). Furthermore, all these master/slave techniques, need communication and control interconnections, so they are less reliable for a distributed power supply system.

The current/power deviation (sharing) control techniques have excellent features. It has a very good load sharing, transient response and can reduce circulating currents between the inverters. There are as well some drawbacks. It is not easily expandable due to the need for measuring the load current and the need to know the number of inverters in the system. The needed interconnection makes the system less reliable and not truly redundant and distributed.

Droop control methods are based on local measurements of the network state variables which makes them truly distributed and give them an absolute redundancy as they do not depend on cables/communication for reliable operation. It has many desirable features such as expandability, modularity flexibility and redundancy. Nevertheless, the droop control concept has some limitations including frequency and amplitude deviations, slow transient response and possibility of circulating current among inverters due to wire impedance mismatches between inverter output and load bus and/or voltage/current sensor measurement error mismatches.

Each of these control techniques has its own characteristics, objectives, limits and appropriate uses. That often makes it difficult to adapt one control scheme for all applications. However, a deep understanding of these control techniques will help in enhancing them and though will improve the design and implementation of future distributed modular grid architectures.

5. The Proposed Smart Grid Philosophy

A general philosophy to supply electric energy in isolated power systems through power electronic inverters is introduced in (Omari 2005) and is extended here. The basic system philosophy is illustrated through Fig. 15. The power produced by the ECS is fed through the DC-to-DC converter and after that this DC power is fed to the grid through the inverter. The inverter produces an AC output of a specific voltage magnitude and frequency. The intermediate capacitance is used to decouple the DC current flowing to the input terminal of the grid-inverter from the DC current flowing from the DC-to-DC converters of the ECS side.
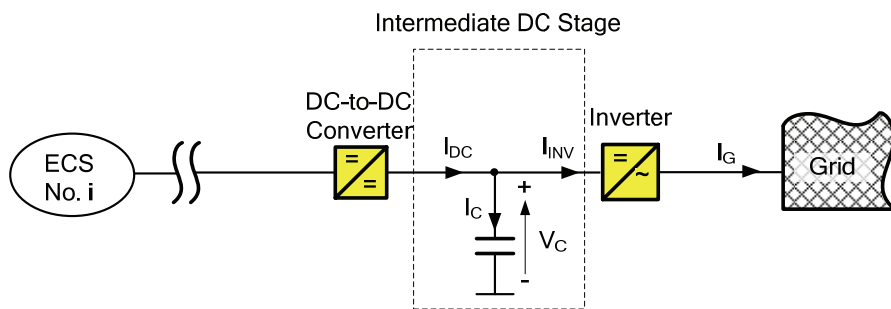

Fig. 15. System overview of the intermediate DC stage.

The mismatches between these two currents result in variations in the voltage across the intermediate capacitance caused by changes in the capacitor's current. This can be expressed using the following equation:

$$V_C = \frac{1}{C}\int I_C dt + V_{C,0} = \frac{1}{C}\int \left(I_{DC} - I_{INV}\right)dt + V_{C,0} \tag{9}$$

Where the voltage across the intermediate capacitance is V_C, the output current of the DC/DC converter is I_{DC} and the input current to the inverter is I_{INV}.

These voltage variations can be utilised to control the power flow. The size of the capacitor is determined depending on the maximum possible mismatches between power production and power consumption. The voltage variations across the capacitor should be kept within the allowable ranges.

This intermediate DC stage has two important characteristics. First, it provides a decoupling between the voltages across the terminals of the ECSs from one side and the grid voltage from the other side. Second, it provides a decoupling between the frequency of the ECSs (in the case of AC energy conversion systems) from one side and the grid frequency from the other side. In this philosophy the power flow from an energy conversion source (ECS) into the grid may be driven by the grid or by the ECS itself as summarised in Fig. 16.
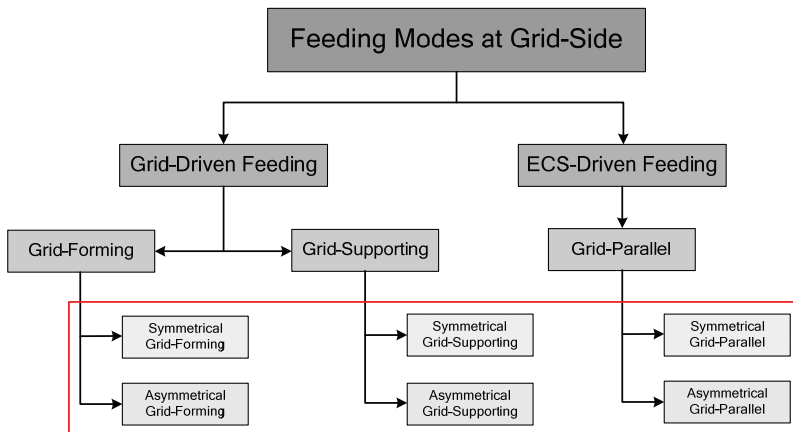
Fig. 16. A general definition of feeding modes for DER.

In a grid-driven feeding mode the flow of power from the ECS to the grid is controlled according to the requirements of the grid while in an ECS-driven feeding mode, the flow of power is controlled according to the requirements of the ECS itself. In the second case, ECSs are normally controlled to maximise their power production despite the requirements of the grid. The grid-driven feeding mode represents the active integration case while the ECSs-driven feeding mode represents the passive one. A grid-driven feeding mode may be realised through two different cases: grid-forming case and grid-supporting case, while an ECS-driven feeding mode may be realised through a grid-parallel case.

An ECS in a grid-forming case is responsible for establishing the voltage and the frequency of the grid (state variables) and maintaining them (Omari 2005). This is done by increasing or decreasing its power production in order to keep the power balance in the electrical system.

An ECS in a grid-supporting case produces predefined amounts of power which are normally specified by a management unit. Therefore, the power production in such a case is

not a function of the power imbalances in the grid. Nevertheless, the predefined amounts of power for these units may be adjusted. The management system may change the reference values according to the system's requirements and the units' own qualifications. The control strategy of the intermediate DC circuit is derived from the feeding modes definition. Therefore, in the grid-driven feeding mode the voltage across the capacitor is kept within the allowable ranges through controlling I_{DC} current while keeping I_{INV} free to change, see Fig. 17.
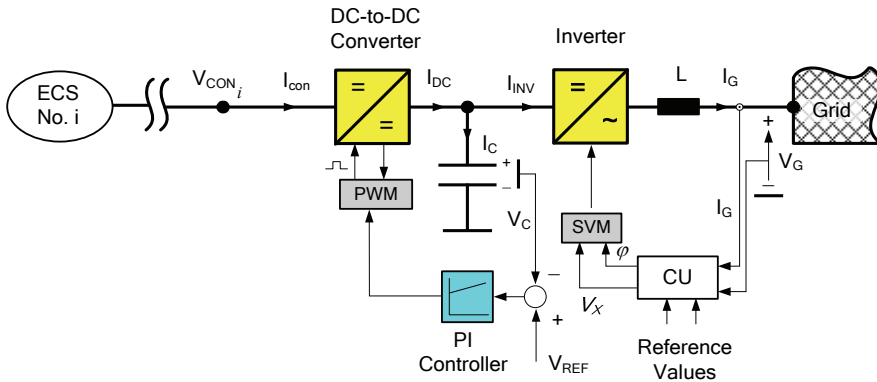
Fig. 17. General control of a system operating in a grid-driven feeding mode (Forming, Supporting).

An ECS in a grid-parallel case is a power production unit that is not controlled according to the requirements of the electrical system. RES's such as wind energy converters and photovoltaic systems may be used to feed their maximum power into the grid (standard applications in conventional grids). In such a case, these systems are considered as grid parallel units. For the ECSs-driven feeding mode control strategy the vice versa applies, I_{INV} is controlled and I_{DC} is free to change, see Fig. 18.
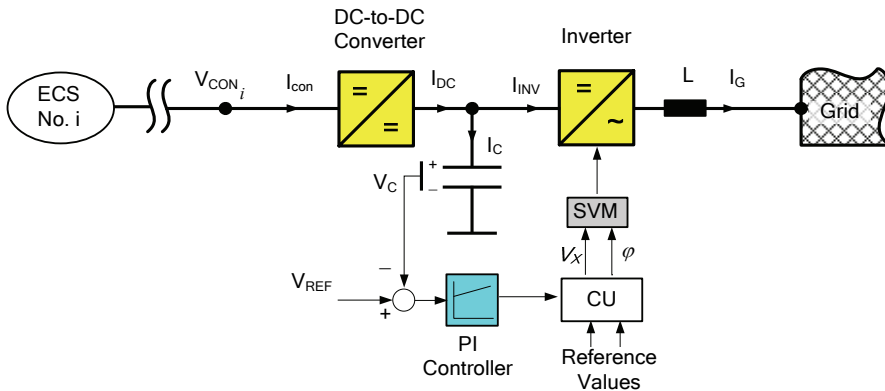
Fig. 18. General control of a system operating in ECSs-driven feeding mode (parallel).

5.1 Inverter Topologies

To articulate the control strategies in relation to power electronic devices a short introduction of the different used three-phase inverter topologies is given.

    a)   Three-phase, Three-leg Voltage Source Inverters

Three single-phase half-bridge inverters can be connected in parallel to form the three phase inverter configuration, one leg for each phase, see Fig. 19. The gating signals of single-phase inverters should be advanced or delayed by 120 degree with respect to each other in order to obtain three-phase balanced voltages (Rashid 1995). In this case it requires that the three currents are a balanced three-phase set. However, this topology can be used to feed balanced loads only.
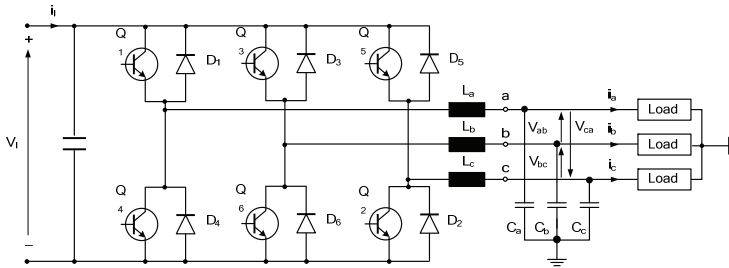
Fig. 19. Three leg inverter (balanced output).

Two configurations able to generate three-phase asymmetrical signals will be discussed. These are: The three-leg neutral point built by capacitors and the four-leg inverter with a controlled neutral point by the fourth leg.

    b)   Three-phase, Three-leg, Four-wire Voltage Source Inverters

Three-phase inverters with neutral point are an evolution from the single-phase ones. Three half-bridge single-phase inverters joined together can be seen as a three-phase neutral point inverter, see Fig. 20, where each output feeds one phase. This topology can be used to feed balanced or unbalanced loads. In case of unbalanced loads, the sum of the output currents i_a, i_b, and i_c will not be zero and the neutral current will flow in the connection between the neutral point and the mid-point of the capacitive divider (G. Seguier and Labrique 1993; Said El-Barbari and Hofmann 2000; Omari 2005). To maintain a symmetrical voltage across the two capacitors an adequate power electronic and a voltage stage management are needed, this will not be taken further into discussion.
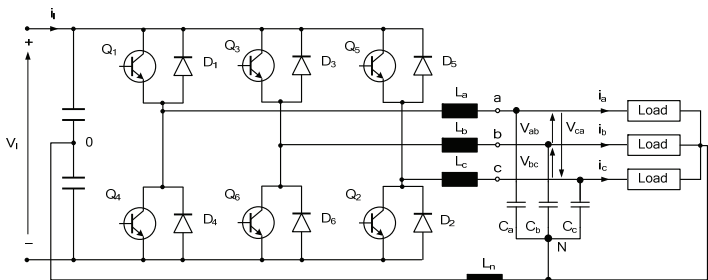

Fig. 20. Three-leg inverter with a neutral point.

c) Three-phase, Four-leg Voltage Source Inverters

The general power electronic topology of the four-legged inverter is shown in Fig. 21. The goal of the three-phase four-leg inverter is to supply a desired sinusoidal output voltage waveform to the load for all load conditions and transients. By tying the load neutral point to the mid-point of the fourth leg, it can handle the neutral current caused by an unbalanced load. A balanced output voltage can be achieved due to the tightly regulated neutral point. The additional neutral inductor L_n is optional. It can reduce switching frequency ripple (Zhang 1998). A four leg inverter can produce sixteen switching states. This enlarges the space vector modulation to three-dimensional (3-D-SVM), for a four-leg voltage source inverter the representation of the phase voltage space vectors is done in the α,β,γ space.

Compared with the four-leg inverter, the three-leg four-wire inverter has a lower number of semiconductor switches and the control function can be built like three individual single line inverters. However, the four-leg inverter still has the advantages of higher utilization of the DC link voltage. This is because the maximum available peak value of the line-to-neutral output voltage in the three-leg four-wire inverter is equal to half the value of the dc link voltage while the maximum amplitude of the line-to-line voltage with a four-leg inverter is equal to the dc bus voltage. Moreover, the high unbalanced current flowing through the dc link capacitors of the three-leg four-wire inverter requires higher capacitance (Zhang, Boroyevich et al. 1997; Maria Brucoli and Green 2006). So, the four-leg inverter has small DC link capacitor as no zero sequence current flow across the DC link capacitor and has an additional degree of freedom due to the fourth leg (Said El-Barbari and Hofmann 2000; E. Ortjohann 2006; E.Ortjohann, A.Mohd et al. 2006).
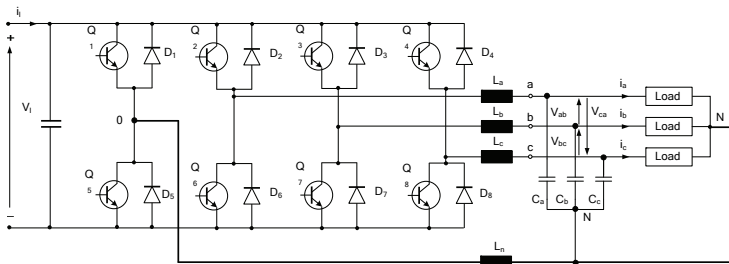

Fig. 21. Four-leg inverter.

In general, three-leg inverter will use the two-dimensional space vector modulation (2-D-SVM). On the other hand, the three-leg inverter with neutral point and the four leg inverter will extend the space vector modulation to three-dimensional (3-D-SVM) making the selection of the modulation vectors more complex. The 3-D-SVM of three-leg with neutral point inverter differ from that of the four leg inverter. Nevertheless, the control strategies are similar. Both the control strategies and the SVM algorithms will be discussed in detail in the following sections.

5.2 Inverter Control

In the following sections, the known control strategies of symmetrical inverters will be briefly reviewed; Further details can be found in (Omari 2005). Afterwards, the proposed control strategies for the asymmetrical inverters will be introduced, these were published in papers (Egon Ortjohann, Mohd et al. 2006; E.Ortjohann, A.Mohd et al. 2006).

5.2.1 Symmetrical Grid Forming

The control strategy of a three-phase inverter in grid forming mode for balanced load is shown in Fig. 22. The inverter in this case determines the voltage and the frequency of the grid. There is one inner current control loop and a second voltage control loop. Both loops use only the d-component. The q-component of the current cannot be influenced since the reactive part is depending on the load condition. Therefore, the q-component is not considered in this case. The reference angle for the dq-transformation is taken from the reference frequency.
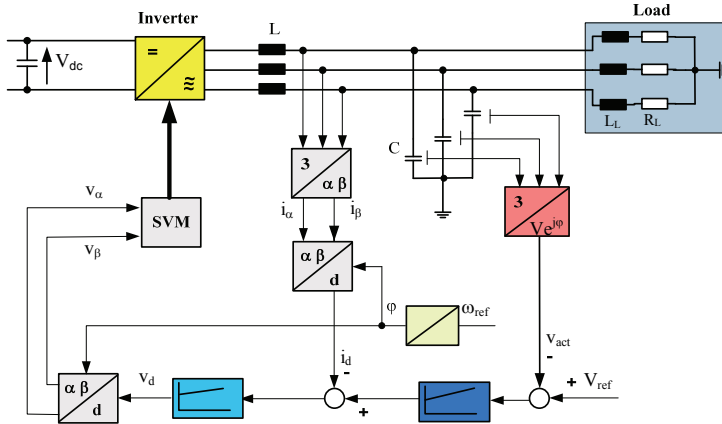
Fig. 22. Inverter in grid forming mode for balanced loads.

5.2.2 Symmetrical Grid Supporting
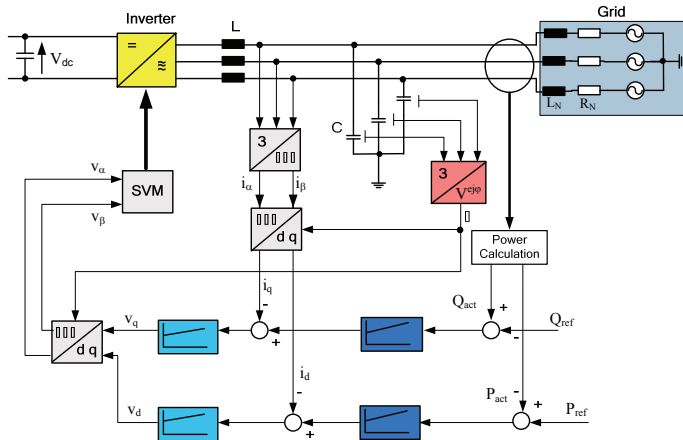
Fig. 23. P, Q-controlled inverter in grid supporting mode for balanced loads.

The grid supporting unit for balanced loads feeds the grid with a specified amount of power, which might be active, reactive, or a combination of both, see Fig. 23. The control

strategy for the grid supporting unit using active and reactive power has four controllers, two for the current (i_d and i_q), and two for the power (P and Q). Active power, *P*, is controlled by the real part of the grid current "i_d", while reactive power, *Q*, is controlled by the imaginary part "i_q". Synchronization is implemented by the generation of the angle for the dq transformation from the voltage on the grid. Other control strategies for the grid supporting mode can be implemented straight forward through controlling the real and the imaginary components of the grid current or the magnitude of the voltage and the active component of the power fed into the grid.

5.2.3 Symmetrical Grid Parallel

In the case of grid-parallel feeding mode, see Fig. 24, all of the produced active power by the ECS is passed to the grid through the inverter. The active power management is done in this application by the control of the voltage of the DC stage. The reactive power control is similar to the grid supporting case.
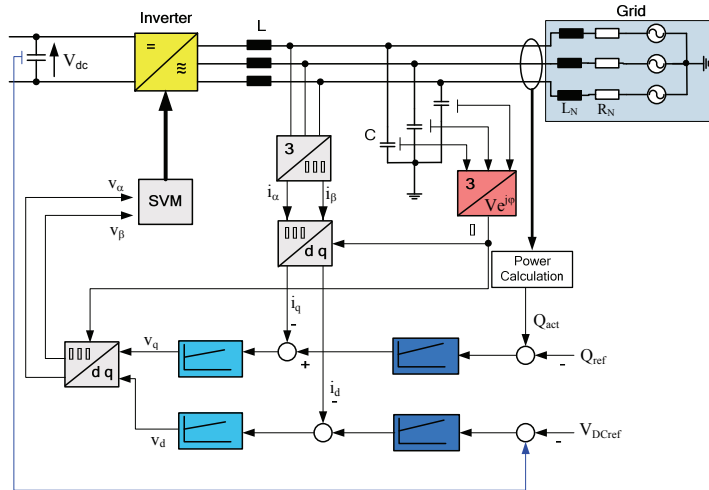

Fig. 24. Q-controlled inverter in grid parallel mode.

5.2.4 Asymmetrical Grid Forming

As a grid forming unit the inverter has to provide both the voltage and the frequency of the grid. This is done as following: The voltage and the current sensed values are transformed from the abc-frame to the positive-negative-zero dq sequence components. The controller block comprises current and voltage PI controllers for each component. Six controllers are needed for the voltage and the current components of the load. For the controller only the *d*-component of the positive sequence $V_{p\_d\_ref}$ is considered. The other reference values are set to zero since the inverter has to supply symmetrical three phase voltage. The output reference values from the control unit are transformed to the αβγ-space and the SVM block uses them to calculate the pulse pattern for the switches (Egon Ortjohann, Mohd et al. 2006). Fig. 25 shows an inverter in grid forming mode for unbalanced loads. The control functions can be also described as vectors according to the following definition:

$$[V_{pn0\_dq\_ref}] = \begin{bmatrix} V_{p\_d\_ref} \\ V_{p\_q\_ref} \\ V_{n\_d\_ref} \\ V_{n\_q\_ref} \\ V_{0\_d\_ref} \\ V_{0\_q\_ref} \end{bmatrix} \qquad [V_{pn0\_dq\_act}] = \begin{bmatrix} V_{p\_d\_act} \\ V_{p\_q\_act} \\ V_{n\_d\_act} \\ V_{n\_q\_act} \\ V_{0\_d\_act} \\ V_{0\_q\_act} \end{bmatrix} \qquad (10)$$
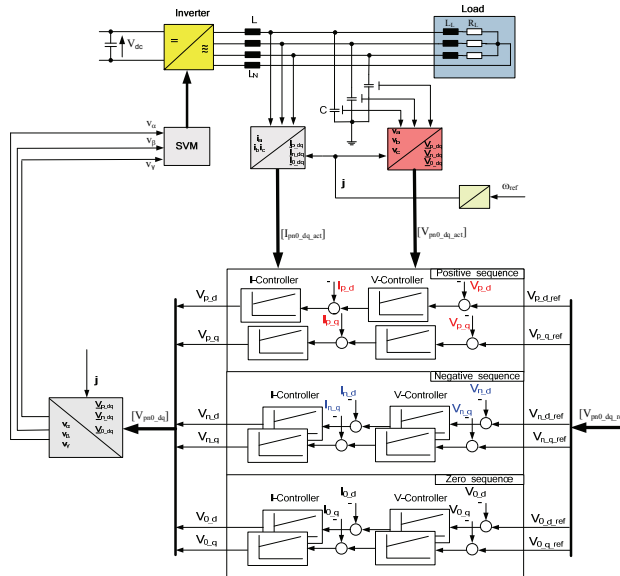
$$[V_{pn0\_dq}] = \begin{bmatrix} V_{p\_d} \\ V_{p\_q} \\ V_{n\_d} \\ V_{n\_q} \\ V_{0\_d} \\ V_{0\_q} \end{bmatrix} \qquad [I_{pn0\_dq\_act}] = \begin{bmatrix} I_{p\_d\_act} \\ I_{p\_q\_act} \\ I_{n\_d\_act} \\ I_{n\_q\_act} \\ I_{0\_d\_act} \\ I_{0\_q\_act} \end{bmatrix} \qquad (11)$$

Fig. 25. Inverter in grid forming mode for unbalanced loads.

5.2.5 Asymmetrical Grid Supporting

The asymmetrical grid supporting unit has to supply the grid with a specified amount of power, which might be active, reactive, or a combination of both as mentioned before. Synchronisation with the grid voltage is done by the voltage reference angle which has to be generated as in the symmetrical grid supporting mode. The desired amount of power has to be set by a management unit in positive, negative and zero sequence components. The

power controller block generates a reference signal for the current controller. The current controller is delivering a reference voltage signal represented by positive, negative and zero sequence components. These reference values have to be transformed (composed) to the αβγ-space vector and the SVM block uses them to calculate the pulse pattern for the switches (Egon Ortjohann, Mohd et al. 2006). Fig. 26 shows a P, Q-controlled Inverter in grid supporting mode for unbalanced loads, the control functions can be also described as vectors according to the following definition:

$$[P_{pn0\_ref}] = \begin{bmatrix} P_{p\_ref} \\ P_{n\_ref} \\ P_{0\_ref} \end{bmatrix} \qquad [Q_{pn0\_ref}] = \begin{bmatrix} Q_{p\_ref} \\ Q_{n\_ref} \\ Q_{0\_ref} \end{bmatrix} \qquad (12)$$

$$[P_{pn0\_act}] = \begin{bmatrix} P_{p\_act} \\ P_{n\_act} \\ P_{0\_act} \end{bmatrix} \qquad [Q_{pn0\_act}] = \begin{bmatrix} Q_{p\_act} \\ Q_{n\_act} \\ Q_{0\_act} \end{bmatrix} \qquad (13)$$

$$[I_{pn0\_d\_act}] = \begin{bmatrix} I_{p\_d\_act} \\ I_{n\_d\_act} \\ I_{0\_d\_act} \end{bmatrix} \qquad [I_{pn0\_q\_act}] = \begin{bmatrix} I_{p\_q\_act} \\ I_{n\_q\_act} \\ I_{0\_q\_act} \end{bmatrix} \qquad (14)$$

$$[V_{pn0\_d}] = \begin{bmatrix} V_{p\_d} \\ V_{n\_d} \\ V_{0\_d} \end{bmatrix} \qquad [V_{pn0\_q}] = \begin{bmatrix} V_{p\_q} \\ V_{n\_q} \\ V_{0\_q} \end{bmatrix} \qquad (15)$$

Other control strategies can be implemented simply through the real and the imaginary components of the grid current or the magnitude of the voltage and the active component of the power fed into the grid.
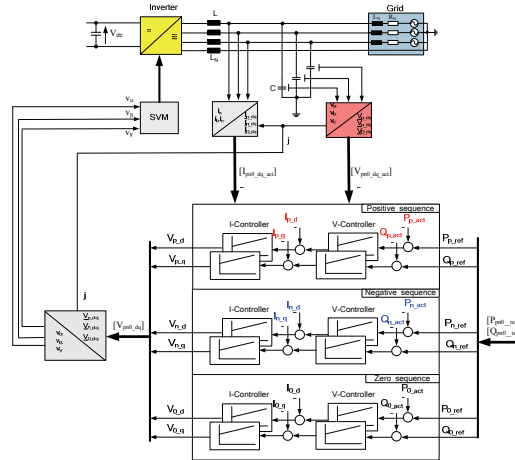
Fig. 26. P, Q-controlled Inverter in grid supporting mode for unbalanced loads.

5.2.6 Asymmetrical Grid Parallel

Obviously, in the case of asymmetrical grid-parallel unit, shown in Fig. 27, the values that can be controlled are the flow of the reactive power or reactive current to the grid. In comparison to the asymmetrical grid supporting remarkable is the active power control using V_{dc} and:

$$[P_{n0\_ref}] = \begin{bmatrix} P_{n\_ref} \\ P_{0\_ref} \end{bmatrix} \qquad [P_{n0\_act}] = \begin{bmatrix} P_{n\_act} \\ P_{0\_act} \end{bmatrix} \tag{16}$$
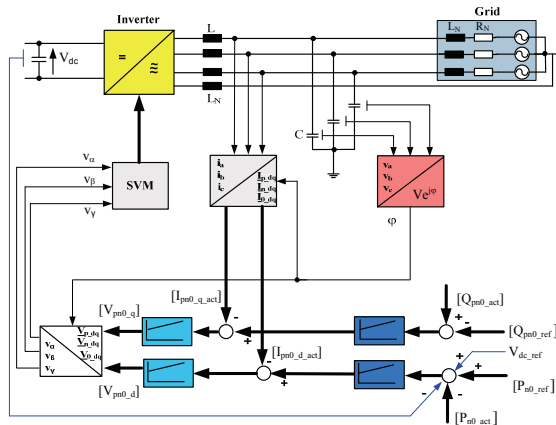
Fig. 27. Inverter in grid parallel mode for unbalanced loads.

This section presented the system components developed for the smart grid. Including the general feeding architecture was presented and discussed. Then it presents the main power electronic element of the philosophy, the inverter, showing the different topologies used. Finally, the operating principles and control techniques for these inverters were presented. This included novel standardized advanced control concept for four-wire inverters (three-leg four-wire and four-leg) using symmetrical components based on sequence decomposition to supply balanced/unbalanced loads. The principle idea is to control the positive, negative and zero sequence components. Controlling (eliminating) the negative and zero sequence components helps expanding the inverter based systems by increasing the distribution network efficiency (consequently leads to less losses and results in enhancing the power quality). This can be used for shunt active filters' applications and also grant the opportunity to supply unbalanced loads which mean supplying single and three phase loads using the same source.

6. The Proposed Smart Grid philosophy "Operation, control, and management"

In the previous section, the principles of the proposed smart grid philosophy and its components have been introduced. In this chapter, the operation, control, application and management of this philosophy are going to be presented.

Even though, most of the current approaches to build future smart power systems are trying to introduce one-size-fits-all solution but the fact is that each system (customer) needs are different and various approaches are needed to fit their exact specifications. This chapter will introduce varied opportunities of control functions for three-phase inverters used to feed passive/active grids including different topologies to feed balanced/unbalanced loads.
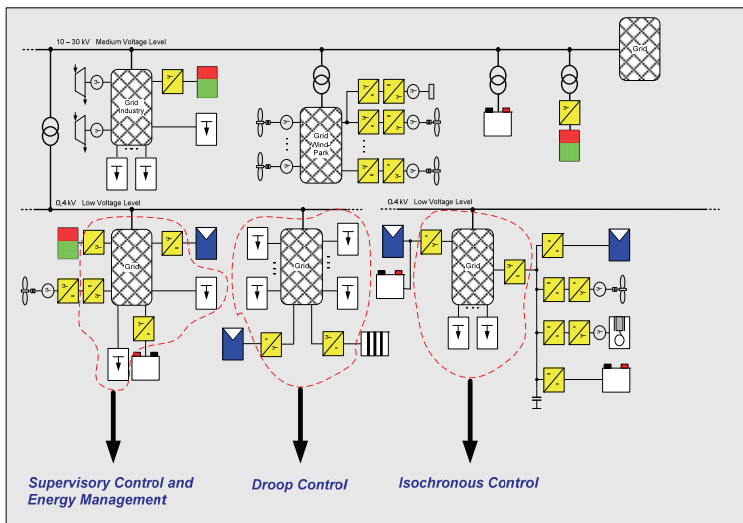

Fig. 28. The control philosophy (example).

The proposed philosophy will develop different and various robust control approaches for a realistic distributed power system with power electronics inverters as front-end, see Fig. 28. These control strategies should guarantee real modularity, higher reliability and avoid a single point of failure to qualify to be standardised. The proposed control architecture should maintain three phase voltages and frequency in the grid within certain defined limits and has to provide power sharing between the units according to their ratings and user settings.

The electrical energy produced by ECSs may be fed into the electrical grid according to one of two possible feeding modes. In the first mode, the amount of electrical energy fed into the grid is specified according to the grid requirements. This mode is denoted as a "Grid-driven feeding mode". In the second mode, the ECSs specify the amount of energy fed into the grid. This mode is denoted as an "ECSs-driven feeding mode". Fig. 29 presents a diagram showing the structure of the control functions proposed in this research study. These control strategies will be launched in this chapter.

The system philosophy under discussion is also characterised by an intermediate DC stage between the energy sources from one side and the electrical grid from the other side. From the DC-DC converters' side, it connects to the ECSs and from the main inverter's side it connects to the electrical grid, see chapter three. However, in order to simplify the analysis, the ECSs-side (the generation sources such as PV and fuel cells) are represented using a DC voltage source.
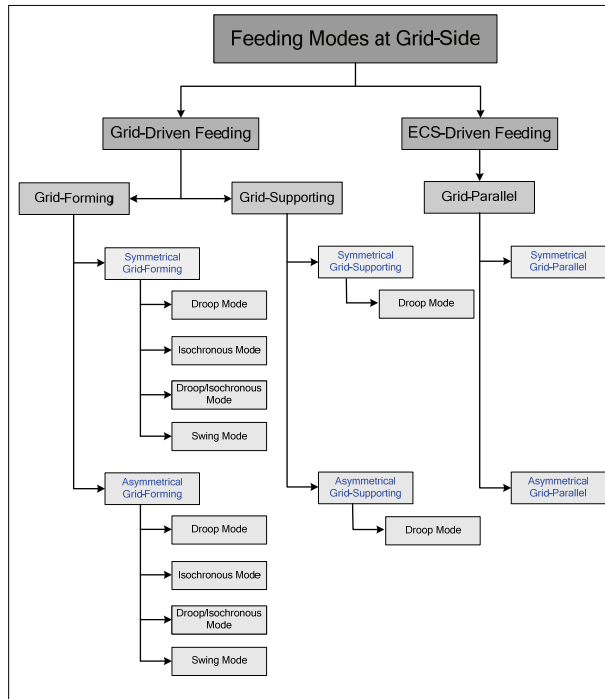

Fig. 29. Feeding modes at the grid side.

Based on the modes proposed in Fig. 29. many scenarios can be obtained. The key scenarios are taken into account in this research study as shown in Fig. 30. The proposed philosophy has two main categories. The first category is the Multi-inverter Three-wire system and the second is the Multi-inverter Four-wire system. For each of these categories different control scenarios will be proposed and explored.
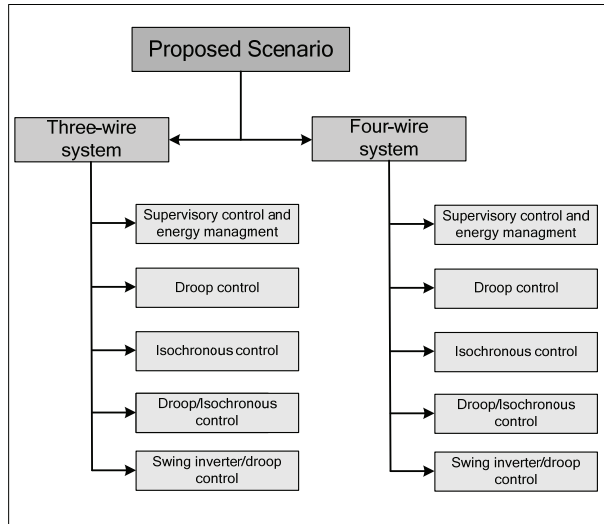

Fig. 30. The proposed scenarios.

6.1 Multi-inverter Three-wire System Control Philosophy

Since the inverters are relatively stiff sources, with unique value of open circuit frequency and voltage (due to components tolerance), large circulating currents would result if they were simply paralleled without additional control. This can be done based on information available locally at the inverter (state variables) for example using droops to make the system less stiff or using data communication such as in supervisory controlled systems. Recently data communication between units became easy realized by the rapid advances in the field of communication. However, it is preferred that communication of information will be used to enhance system performance but must not be critical for system operation. The following sections will introduce modular approaches to parallel inverters using different methodologies.

6.1.1 Supervisory Control and Energy Management Scenario

The specific aim of this concept is to develop a standardised control strategy for a realistic distributed power system with power electronics inverters as front-end. The proposed control architecture will maintain the three phase voltages and frequencies in the grid precisely and will provide power sharing between the units according to their ratings, meteorological parameters, economical dispatch prospective (can include real-time pricing) and user settings. This allows total energy optimization. The designed system can include inverter units of different power rating, distributed at various locations feeding distributed

unequal loads taking into account dissimilar line impedances between them to insure true expandability and generation placement flexibility. This means that the types, sizes, and numbers of the inverters, and the size and nature of the electrical loads may all vary without the need to alter the control strategy. The amount of data exchange can be small if it includes only basic measurements and set points but will increase proportionally as more functions are added. The proposed structure is shown in Fig. 31. It is worthy to note that the source do not have to be a single ECS and could be a hybrid power system (HPS).

The supervisory control is responsible for units dispatching, load management, and power optimization. It can include also many functions like meteorological forecasting and demand side management as illustrated in (Osama Omari, Egon Ortjohann et al. 2007). It can also manage an intelligent switch or a feeder to the main grid or to other mini-grids. The current and voltage control are done locally at the inverters according to the definition introduced in chapter three. Moreover, the proposed control can be implemented not only in distribution system of isolated grid systems, but also in the interconnected power systems (some times called on-grid micro-grid).
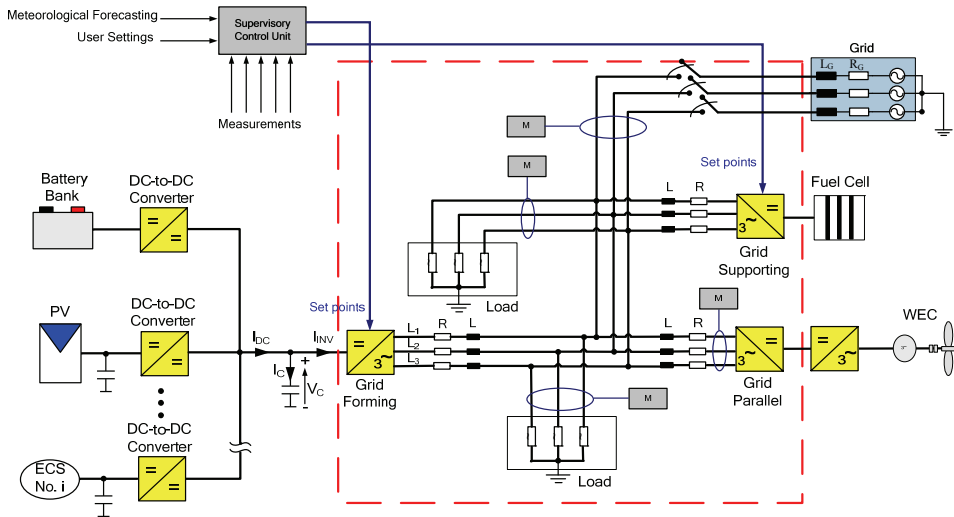

Fig. 31. Overview of supervisory control and energy management proposed system structure.

The control functions of the inverters are shown in Fig. 32 As mentioned in section 5, each grid mode has its own character for controlling the inverter. The grid forming contains inner current control loop and outer voltage control loop. The reference voltage is given to control the voltage of the system. The angular speed related to the frequency of the system is also set as constant ($2\pi f$). The control loop produce the voltage of d-axis which will be transformed to $\alpha\beta$ frame, the angle is required for that. These voltages in $\alpha\beta$ frame are supplied to the SVM to calculate the switching sequence and periods. In the next step the inverter supplies the three-phase currents to the system through the LC filter. The output currents will be measured to feed the signal to the inner current loop. The voltages across the capacitor are also measured to feed the outer control loop.
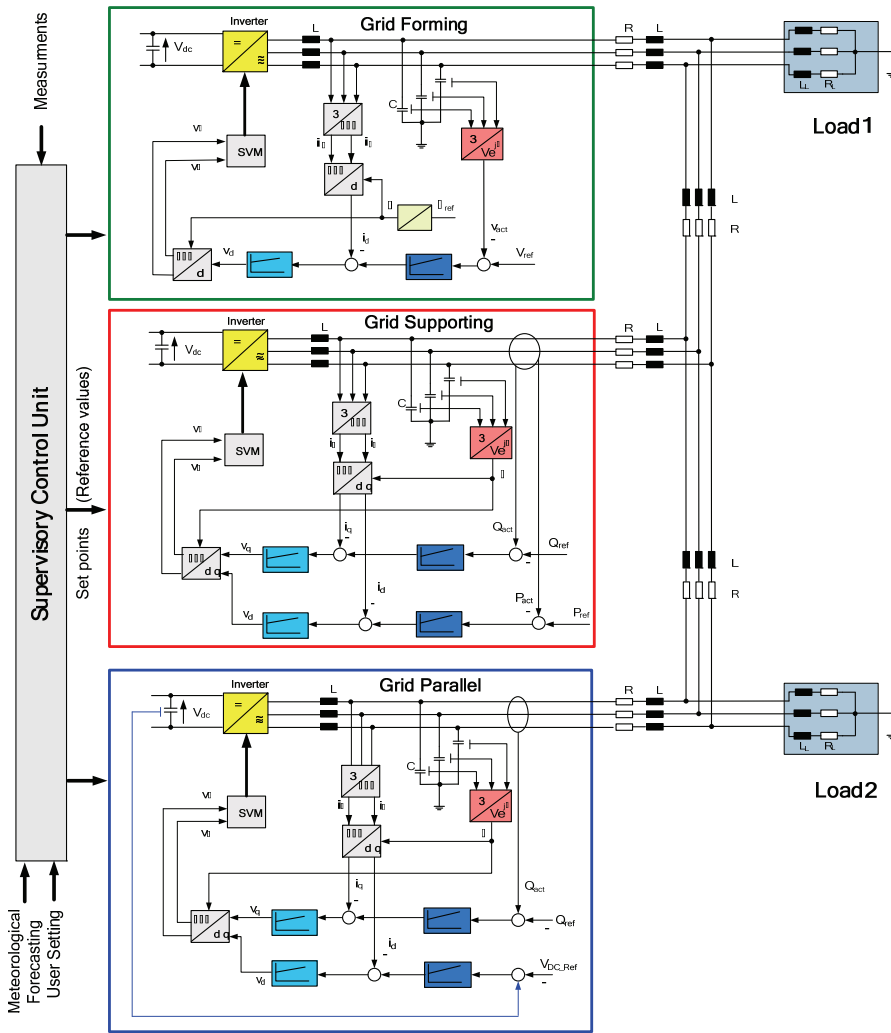
Fig. 32. Supervisory control and energy management scenario.

As stated previously, the responsibility of the grid supporting mode is to maintain the system power balance. The reference power of the grid supporting inverter is calculated in the supervisory unit based on other inverters in the system (grid forming and parallel modes) and loads. Moreover, it depends also on the pre-setting percentages or algorithms used in the supervisory control to manage the power balance. The reference values of P_{GS} and Q_{GS} are calculated based on that. In the simplest case, the set values can be adjusted by the percentage value ($GS_{percent}$) and the active power load (P_{load}) and reactive power load (Q_{load}). As a simple example, the set values of active and reactive power can be calculated via equations 17 and 18 respectively:

$$P_{GS\_ref} = \frac{\left(\sum_{i=1}^{n} P_{load_i} - \sum_{j=1}^{m} P_{GP_j}\right) \times GS_{percent}}{100} \qquad (17)$$

$$Q_{GS\_ref} = \frac{\left(\sum_{i=1}^{n} Q_{load_i} - \sum_{j=1}^{m} Q_{GP_j}\right) \times GS_{percent}}{100} \qquad (18)$$

Where, $\sum_{i=1}^{n} P_{load_i}$ and $\sum_{i=1}^{n} Q_{load_i}$ are the summation of the active and reactive power of load in the system, where, n is the number of loads and i is the counter. $\sum_{j=1}^{m} P_{GP_j}$ and $\sum_{j=1}^{m} Q_{GP_j}$ are the summation of the active and reactive power of grid parallel units in the system, where, m is the number of grid parallel units and j is the counter.

This means that the amount of power needed is deducted from the power of the grid parallel units since they cannot be influenced by the grid, the rest is shared between the grid forming and supporting according to the percentage $GS_{percent}$. This percentage can be calculated according to an algorithm based on the units' ratings, meteorological parameters, economical dispatch prospective and user settings but this will not be taken into discussion over here since its out of the scope of this study. This was demonstrated in (Osama Omari, Egon Ortjohann et al. 2007).

After the actual active and reactive power of the grid supporting mode is passed to the outer loop of the controllers, another inner current control loop is used. The current of d-axis is used to control the active power signal and the current of q-axis is used to control the reactive power signal.

The grid parallel mode is used to produce maximum amount of active power and can sometimes supply certain amount of reactive power to the system. In the voltage control loop, there are two reference inputs, voltage reference and reactive power reference. There are three inputs measured to calculate the new reference for I_d and I_q controllers. These are first, the DC intermediate stage which will be passed through the voltage controller to feed into the inner current loop for I_d controller; based on that the new reference of the voltage is established. The second input, is the three-phase voltage measured from the line. The three-phase voltage is transformed into dq-frame and the angle of the voltage can be measured from voltage of q-axis (V_q). The voltage magnitude is fed to the I_q controller which is compared to the reactive set value to get the new reference value for I_q controller. Third, the actual output current values measured are used by I_d and I_q controllers of the inner control loop. The current signals are transformed into dq-frame. After the controlled signals passed through the I_d and I_q controllers, both signals are added with the actual values of the voltage in dq-frame and then transformed into $\alpha\beta$ frame to control the inverter's output.

It should be also noticed that as a grid parallel unit, if the system frequency is rising too high the inverter's output should be reduced or set to zero (disconnected).

The following simulation case study is carried using MATLAB/Simulink to validate the proposed inverter supervisory control approach. The supervisory control is responsible for units dispatching, load management, and power optimization. However, the current and voltage control are done locally at the inverters according to the definition introduced before. The proposed control can be implemented in isolated grid as well as in interconnected power systems. In this case study there are three inverters operating in grid forming mode, grid supporting mode and grid parallel mode respectively. They are connected in parallel to supply two loads including steps as shown in Fig. 33.

The first load step is at t=1 second and the second load step is at t=1.5 second. At t=2 seconds, the active power of the grid parallel unit is stepped up from 14 kW to 21 kW. The frequency response of the system is shown in Fig. 34. At t=1 second, when the load is increased the frequency will drop. In the other hand at t=1.5 second, the load is decreased and then the frequency will rise. At t=2 second, the grid parallel gives more power to the system. As a response and to keep the frequency constant, the grid forming and supporting inverters will supply less power to the system.

Fig. 35 shows the active power response of the inverters and loads from 0.5 second to 2.5 seconds. At the first step (t=1 second), active power of load one is increased as shown in Fig. 35. Consequently, the active power of grid forming and grid supporting inverters are increased to balance with the increased load. The grid supporting takes 30 percent of the load as pre-set (This is the result based on the optimization algorithm). The active power of the grid parallel unit supplied to the system is the same. At second step (t=1.5 second), the active power of load two is decreased. The active power of the grid forming and grid supporting inverters are decreased, while the active power of the grid parallel inverter is still the same. At last step (2 second), the grid parallel is set to give more active power to the system.
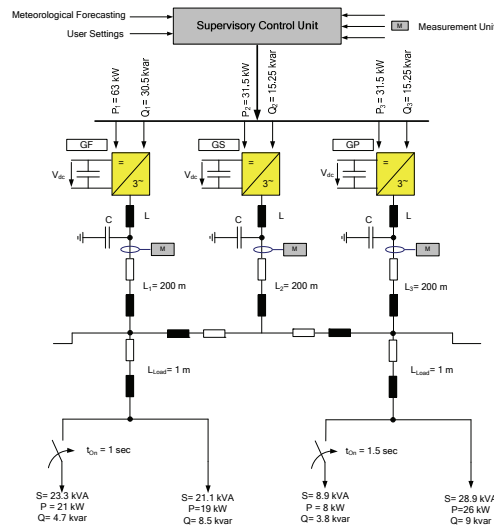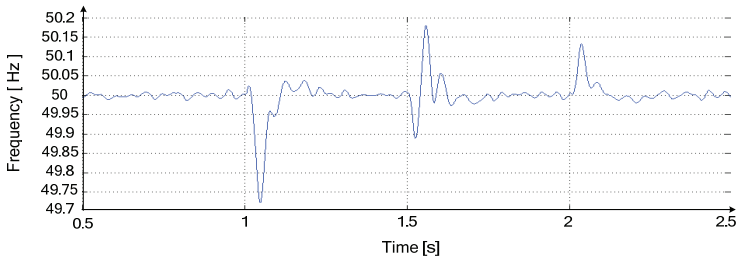

Fig. 33. Case Study.

Fig. 34. The system frequency.

Therefore, the active power of the grid parallel inverter will increase and as a response both active power of grid forming and grid supporting inverters will be signaled to decrease since the load is kept constant. The exact values are shown in Table II and confirm the system active power balance.

The reactive power behavior of the inverters is similar to the active power. The difference is that the grid parallel inverter is set only to give more active power to the system and is not contributing to the reactive power balance. Therefore, it is not affecting the reactive power of the grid parallel unit at the last step as shown in Fig. 36; loads are almost the same. The exact values are shown in Table 2 and confirm the system reactive power balance.
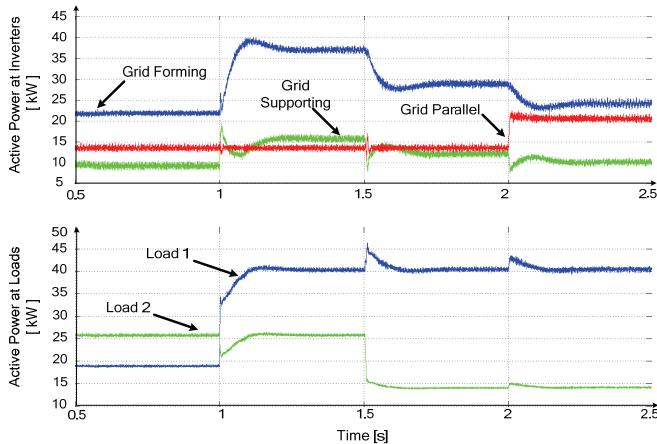

Fig. 35. The active power.

Time (s)	$P_{load\,1}$	$P_{load\,2}$	ΣP_{load}	GF	GS	GP
0 – 1.0	19	26	45	21.7	9.3	14
1.0 – 1.5	40	26	66	36.8	15.6	14
1.5 – 2.0	40	14	54	28	12.5	14
2.0 – 2.5	40	14	54	23.6	9.9	21

Table 1. Active power (kW)
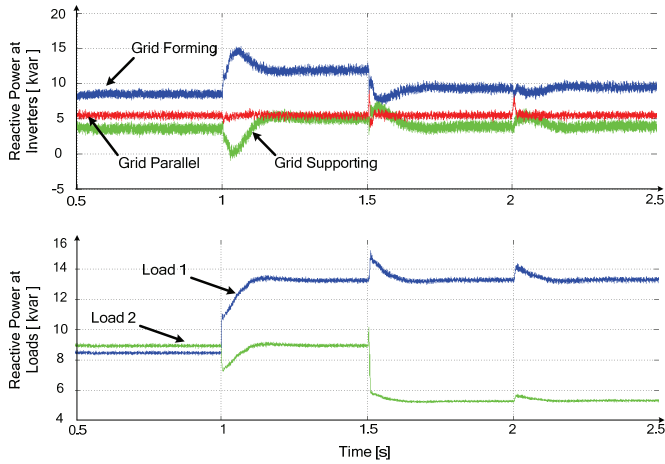
Fig. 36. The reactive power.

Time (s)	$Q_{load\ 1}$	$Q_{load\ 2}$	ΣQ_{load}	GF	GS	GP
0 – 1.0	8.5	9	17.5	8.4	3.8	5.5
1.0 – 1.5	13.2	9	22.2	11.9	5.1	5.5
1.5 – 2.0	13.2	5.2	18.4	9.3	3.87	5.5
2.0 – 2.5	13.2	5.2	18.4	9.3	3.87	5.5

Table 2. Reactive power (kvar)

Having a look at Fig. 37 we can see the response of the grid forming inverter to the load increase at t=1 second. The inverter will hold voltage constant and the current will increase to satisfy the load demand. Another example is the responses of the grid supporting inverter shown in Fig. 38, when the load decreases, which is the case at t=1.5 seconds. We can see that the voltage will stay constant as forced by the grid forming inverter while the supplied current will decrease as signaled by the supervisory unit.

Since the grid parallel unit is not dependent on the load and is not actively dispatchable by the grid we can see in Fig. 39 that it does not respond to the load steps in the grid and instead of that keeps supplying the same amount of current all the time. This matches the definition of grid parallel inverter since it is not actively controlled by the grid.

Having a look at the load voltage and current response at t=1 second when a step happens, see Fig. 40, we can see that the voltage is kept constant all the time by the system and is restored rapidly in case of any load step. This shows the controller capabilities to supply a high power quality.
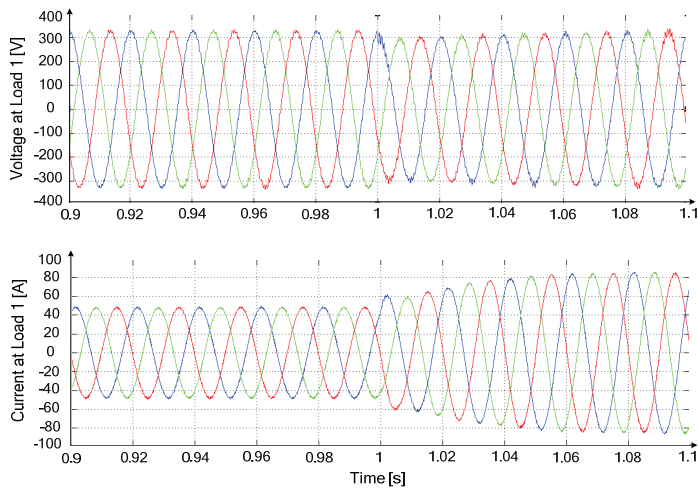
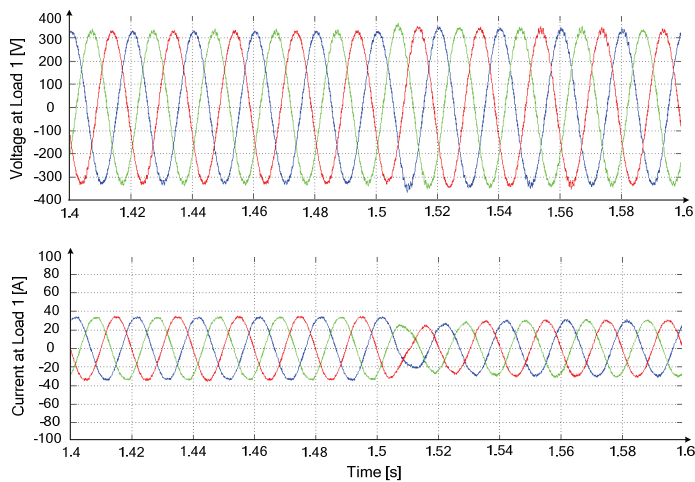Fig. 37. Voltage and current of grid forming at first step.

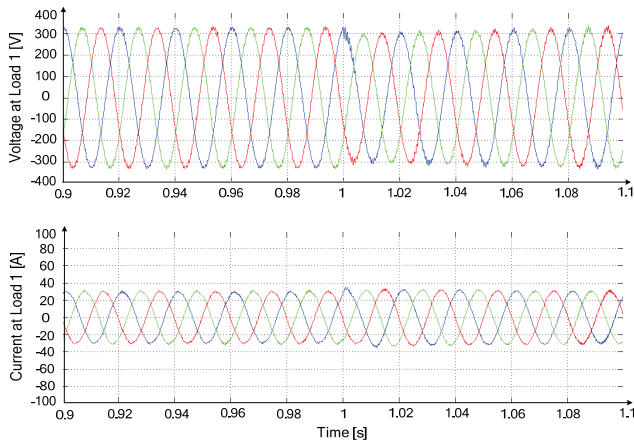Fig. 38. Voltage and current of grid supporting at second step.

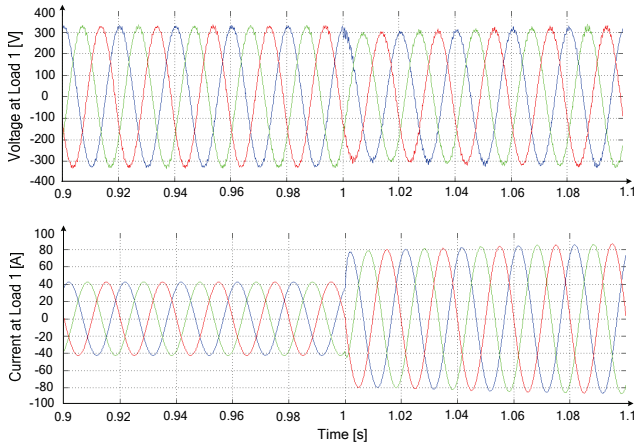Fig. 39. Voltage and current of grid parallel at first step.

Fig. 40. Voltage and current at load one during first step.

7. Conclusion

Our present and future power network situation requires extra flexibility in the integration of distributed generation more than ever. Mainly for the small and medium energy converting systems including intelligent control and advanced power electronics conversion systems.

This research study showed the visibility of various methods of forming an electric power supply system by paralleling power electronic inverters. These methods foundation is based on the conventional grid control methodologies. This research addressed mainly the control issues related to future modular distributed power systems with flexible power electronics inverters as front-end.

This work introduced a variety of standardized modular architectures and techniques for distributed intelligence and smart power systems control that can be used to build an electric power supply system by paralleling power electronic inverters. It launched different and various robust control approaches based on the feeding mode definition for a realistic distributed power system with power electronics inverters as front-end. These control strategies guarantee real modularity, high reliability and true redundancy. The proposed control architectures maintain the three phase voltages and frequencies in the grid within certain limits and provide power sharing between the units according to their ratings.

The research led to an original philosophy for supervisory control and energy management of an Inverter-based modular smart grid for distributed generation applications. The method developed is based on the feeding modes definition and supports the active integration of the inverters (energy converting systems & renewable energy sources). The main control tasks (voltage/frequency control) are done locally at the inverters to guarantee modularity and to minimize communication bandwidth requirements. The supervisory control is used for dispatching and optimization control. It can also include real time pricing and meteorological forecasting. The concept was developed and tested for three-phase, three-wire and four-wire systems.

In this study, the general control functions and the system behaviour have been investigated. With this investigation it has been shown that the realisation of smart power systems in general through the new system philosophy is possible and advantageous.

8. References

GRID 2030 :National Vision for Electricity's Second 100 Years (2003)., United States Department of Energy.

Vision and Strategy for Europe's Electricity Networks of the Future (2006).. E. Commission. Luxembourg.

A. Engler, M. Meinh, et al. (2003). New V/f-Statics controlled Battery Inverter: Sunny Island - the key component for AC-Coupled Hybrid Systems and Mini Grids. 2nd European PV Hybrid and Mini-Grid Conference Kassel

A. Engler, M. Meinhardt, et al. (2004). Pure AC-Coupling - The Concept for Simplified Design of Scalable PV-Hybrid Systems Using Voltage / Frequency Statics Controlled Battery Inverters 14th International Photovoltaic Science and Engineering Conference (PVSEC-14), Bangkok.

A. Engler and N. Soultanis Droop control in LV-Grids. International Conference Future Power Systems, Amsterdam, Niederlande.

A. Tuladhar, H. J., T. Unger, and K. Mauch (1998). Control of parallel inverters in distributed ac power systems with consideration of the line impedance effect. APEC

Brabandere, K. D. (October, 2006). Voltage and frequency droop control in low voltage grids by distributed generators with inverter frond-end Departement Elektrotechniek. Leuven, Katholieke Universiteit Leuven.

Brabandere, K. D., B. Bolsens, et al. (2004). A Voltage and Frequency Droop Control Method for Parallel Inverters. the 35th IEEE PESC Conference, Aachen, Germany.

C.-C. Hua, K.-A. L., and J.-R. Lin, Parallel operation of inverters for distributed photovoltaic power supply system. IEEE Annual Power Electronics Specialists Conference.

C.K. Sao, P. W. L. "Autonomous Load Sharing of Voltage Source Converters." EEE Transactions on Power Delivery 20(2): 1009-1016.

Chen, J.-F., C.-L. Chu, et al. (1995). Modular parallel three-phase inverter system. Proceedings of the IEEE International Symposium on Industrial Electronics.

Chen, X., Y. Kang, et al. (2004). Operation, control technique of parallel connected high power three-phase inverters. The 4th International Power Electronics and Motion Control Conference.

De Brabandere, K., K. Vanthournout, et al. (2007). Control of Microgrids. IEEE Power Engineering Society General Meeting, Tampa,Florida.

Driesen, J. and R. Belmans (2006). Distributed generation: challenges and possible solutions. IEEE 2006 Power Engineering Society General Meeting.

E. Hoff, T. S., L. Norum (2004). Paralleled Three-phase Inverters. NORPIE '04, Nordic Workshop on Power and Industrial Electronics.

E. Ortjohann, A. M., N. Hamsic, D. Morton , O. Omari (2006). Advanced Control Strategy for Three-Phase Grid Inverters with Unbalanced Loads for PV/Hybrid Power Systems. 21th European PV Solar Energy Conference, Dresden.

E.Ortjohann, A.Mohd, et al. (2006). Control and Representation of Three-Phase Asymmetrical Signals Used by Modular Inverters to Feed Unbalanced Loads in Hybrid Power Systems. The Great Wall World Renewable Energy Forum (GWREF), Beijing, China.

Egon Ortjohann, A. Mohd, et al. (2006). Advanced Control Strategy for Three-Phase Grid Inverters with Unbalanced Loads for PV/Hybrid Power Systems. 21th European PV Solar Energy Conference, Dresden.

Energy, X. (2007). "Xcel Energy Smart Grid: A White Paper." Denver Business Journal.

Engler, A. (2000). Control of Parallel Operating Battery Inverters. Photovoltaic Hybrid Power Systems Conference, Aix-en-Provence.

Engler, A. (2005). "Applicability of droops in low voltage grids." International Journal of Distributed Energy Resources 1(1).

Engler, A. (2006). APPLICABILITY OF DROOPS IN LOW VOLTAGE GRIDS. 3rd European PV-Hybrid and Mini-Grid Conference, Aix en Provence, France.

Ernane Antonio Alves Coelho, Cortizo, et al. (2000). Small Signal Stability for Parallel Connected Inverters in Stand-Alone AC Supply Systems. THE IEEE INDUSTRY APPLICATIONS CONFERENCE, CONFERENCE RECORD OF THE IEEE INDUSTRY APPLICATIONS CONFERENCE.

Ernane Antonio Alves Coelho, Porfirio Cabaleiro Cortizo, et al. (2002). "Small-signal stability for parallel-connected inverters in stand-alone AC supply systems." IEEE Trans on Industry applications(38(2):533-542.).

G. Seguier and F. Labrique (1993). Power Electronic Converters, DC-AC Conversion. Heidelberg, Germany, Springer-Verlag.

Glauser, H.-P., M. Keller, et al. (2000). New inverter module with digital control for parallel operation. The Third International Telecommunications Energy Special Conference.

Guerrero J.M, García de Vicuña, et al. (2003). A Wireless Controller for Parallel Inverters in Distributed Online UPS Systems. THE 29TH ANUAL CONFERENCE OF THE IEEE INDUSTRIAL ELECTRONICS SOCIETY.

Guerrero, J. M., N. Berbel, et al. (2007). control of line-interactive UPS connected in parallel forming a microgrid. IEEE International Symposium on Industrial Electronics, Vigo, Spain.

Guerrero, J. M., N. d. V. Berbel, et al. (2006). Droop control method for the parallel operation of online uninterruptible power systems using resistive output impedance. Applied Power Electronics Conference and Exposition, APEC '06. Twenty-First Annual IEEE.

Guerrero, J. M., L. G. d. Vicuña, et al. (2004). "A wireless controller to enhance dynamic performance of parallel inverters in distributed generation systems." IEEE Trans.Power Electron. 19(5): 1205-1212.

Guerrero, J. M. B., Nestor Matas, Jose de Vicuna, Luis Garcia Miret, Jaume (2006). Decentralized Control for Parallel Operation of Distributed Generation Inverters in Microgrids Using Resistive Output Impedance. 32nd Annual Conference on IEEE Industrial Electronics, IECON 2006, Paris, France.

Guerrero, J. M. M., J.; de Vicuna, L.G.; Berbel, N.; Sosa, J. (2005). Wireless-control strategy for parallel operation of distributed generation inverters. Industrial Electronics, 2005. ISIE 2005.

Guerrero, J. M. M., J.; Garcia De Vicunagarcia De Vicuna, L.; Castilla, M.; Miret, J. (2006). "Wireless-Control Strategy for Parallel Operation of Distributed-Generation Inverters." IEEE Transactions on Industrial Electronics 53(5): 1461 - 1470.

H.Oshima, Y.Miyazaya, et al. (1991). Parallel redundant UPS with instantaneous PWM control. 13th International Telecommunications Energy Conference.

Hanaoka, H. N., M.; Yanagisawa, M. (2003). Development of a novel parallel redundant UPS. The 25th International Telecommunications Energy Conference.

Hatziagyriou, N. (2008). Microgrids: the key to unlock distributed energy resources. IEEE power and enegy 6: 26-29.

Hauck Matthias , S. H. (2000). "Wechselrichter problemlos parallel betreiben " Elektronik H.12/2000: 120-124.

Holtz, J. and K.-H. Werner (1990). "Multi-inverter UPS system with redundant load sharing control." IEEE Transactions on Industrial Electronics Industrial Electronics 37(6): 506-513.

Huang, B. (2006). Stability of Distribution Systems with a Large Penetration of Distributed Generation. Fakultät für Elektrotechnik und Informationtechnik. Dortmund, University of Dortmund. Dr.-Ing.

Hyun, K.-H. K. D.-S. (2006). A High Performance DSP Voltage Controller with PWM Synchronization for Parallel Operation of UPS Systems. 37th IEEE Power Electronics Specialists Conference.

Ipakchi, A. (2007). Implementing the Smart Grid: Enterprise Information Integration. Grid-Interop Forum, Albuquerque, NM.

J.A.P.Lopes, C. L. Moreira, et al. (2006). "Defining control strategies for MicroGrids islanded operation." IEEE Transactions on Power Systems 21(2): 916 - 924.

Jiann-Fuh Chen and C.-L. Chu (1995). "Combination voltage-controlled and current-controlled PWM invertersfor UPS parallel operation." IEEE Transactions on Power Electronics 10(5): 547 - 558.

Josep M. Guerrero, Juan C. Vásquez, et al. (2007). Parallel Operation of Uninterruptible Power Supply Systems in MicroGrids. EPE 2007, Aalborg, Denmark.

K Siri, C.Q. Lee, et al. (1992). "Current distribution control for parallel connected converters." IEEE Transactions on Aerospace and Electronic Systems 28(3): 841 - 851.

K. De Brabandere, A. Woyte, et al. (2004). Prevemtion of inverter voltage tripping in high density PV grids. 19th EU-PVSEC, Paris, France.

Karlsson, P., J. Björnstedt, et al. (2005). Stability of Voltage and Frequency Control in Distributed Generation Based on Parallel-Connected Converters Feeding Constant Power Loads. EPE, Dresden, Germany.

Lasseter, R. H. (2002). MicroGrids. Power Engineering Society Winter Meeting.

Lasseter, R. H. (2007). "Microgrids and Distributed Generation." Journal of Energy Engineering.

Lee, C. S., S. K. Kim, et al. (1998). Parallel UPS with a instantaneous current sharing control. Proceedings of the 24th Annual Conference of the IEEE Industrial Electronics Society, Aachen, Germany.

Lopes, J. P. (2004). MICROGRIDS Large Scale Integration of Microgeneration to Low Voltage Grids-Emergency Strategies and Algorithms.

M. C. Chandorkar, D. M. Divan, et al. (1994). Control of distributed ups systems. IEEE Annual Power Electronics Specialists Conference.

M. C. Chandorkar, D. D., R. Adapa (1993). "Control of Parallel Connected Inverters in Standalone ac Supply Systems." IEEE Transactions on Industry Applications 29(1).

M. Chandorkar, D. D., Y. Hu and B. Banerjee (1994). Novel architectures and control for distributed UPS systems. Applied Power Electronics Conference and Exposition, Orlando, FL, USA.

Maria Brucoli and T. C. Green (2006). Fault Response of Inverter Dominated Microgrids. 2nd International Conference on Integration of Renewable and Distributed Energy Resources, Napa, California, USA.

Marwali, M. N., J.-W. Jung, et al. (2004). "Control of Distributed Generation Systems,Part II: Load Sharing Control." IEEE TRANSACTIONS ON POWER ELECTRONICS 19(6).

Matthias, H. and S. Helmut (2002). Control of a Three-Phase Inverter Feeding an Unbalanced Load and Working in Parallel with Other Power Sources. EPE-PEMC Dubrovnik.

McDowall, J. A. (2007). Status and Outlook of the Energy Storage Market. PES 2007, Tampa.

Mihalache, L. (2003). Paralleling control technique with no intercommunication signals for resonant controller-based inverters. 38th IAS Annual Meeting Industry Applications Conference.

Nigim, K. and W.-J. Lee (2007). Micro Grid Integration Opportunities and Challanges. IEEE PES 2007, Tampa, FL.

Noguchi, I. T. a. T. (1986). "A new quick-response and high-efficiency control strategy of an induction motor." IEEE Trans. Industry Applications, IA(22): 820-827.

Omari, O. (2005). Conceptual Development of a General Supply Philosophy for Isolated Electrical Power Systems. Soest, Germany, South Westphalia University of Applied Sciences. PhD.

Ortjohann, E. and O. Omari (2004). Advanced Integration of Distributed Electricity Generators into Conventional Electric Networks Including Control, Management, and Communication Strategies. Soest.

Osama Omari, Egon Ortjohann, et al. (2007). An Online Control Strategy for DC Coupled Hybrid Power Systems. IEEE PES general meeting, Tampa, Florida.

Pei, Y., G. Jiang, et al. (2004). Auto-master-slave control technique of parallel inverters in distributed AC power systems and UPS. IEEE 35th Annual Power Electronics Specialists Conference.

Pepermans, G., J. Driesen, et al. (2005). "Distributed generation: definition, benefits and issues." Energy Policy 33: 787-798.

Petruzziello, Z., G Joos (1990). A novel approach to paralleling of power converter units with true redundancy. 21st Annual IEEE Power Electronics Specialists Conference, San Antonio, TX, USA.

Piagi, P. and R. H. Lasseter (June 2006). Autonomous Control of Microgrids. IEEE PES Meeting, Montreal.

Prodanovic, M., T. C. Green, et al. (2000). A survey of control methods for three-phase inverters in parallel connection. Eighth International Conference on Power Electronics and Variable Speed Drives.

Prodanovic, M. G., T.C. (Oct. 2006). "High-Quality Power Generation Through Distributed Control of a Power Park Microgrid." IEEE Transactions on Industrial Electronics 53(5): 1471-1482.

Purchala, K., R. Belmans, et al. (2006). Distributed generation and the grid integration issues. E. S. E. C. A. o. F. E. D. a. G. o. E. E. a. i. S. o. Supply.

Qinglin, Z., C. Zhongying, et al. (2006). Improved Control for Parallel Inverter with Current-Sharing Control Scheme. CES/IEEE 5th International Power Electronics and Motion Control Conference.

Rashid, M. H. (1995). Power Electronics Handbook: Devices, Circuits and Applications.

Ritwik Majumder , Arindam Ghosh , et al. (2007). Load Sharing with Parallel Inverters in Distributed Generation and Power System Stability. Smart Systems 2007 "Technology, Systems and Innovation".

Robert Lasseter and P. Piagi (2006). Control and Design of Microgrid Components. P. P. 06-03, University of Wisconsin-Madison.

S Tamai, M. K. (1991). Parallel operation of digital controlled UPS system. International Conference on Industrial Electronics, Control and Instrumentation.

Said El-Barbari and W. Hofmann (2000). Digital Control of a Four Leg Inverter for Standalone Photovoltaic Systems with Unbalanced Load. IECON 2000. 26th Annual Conference of the IEEE.

Sao, C. K. and P. W. Lehn (2005). "Autonomous Load Sharing of Voltage Source Converters." IEEE Transactions on Power Delivery 20(2): 1009-1016.

T.C. Green and M. Prodanovic (2007). "Control of inverter-based micro-grids." Electric Power Systems Research 77(9): 1204-1213

T.Kawabata and S.Higashino (1988). "Parallel operation of voltage source inverters." IEEE Transactions on Industrial Electronics Industry Applications 24(2): 281-287.

T.Skjellnes, A.Skjellnes, et al. (2002). Load Sharing for Parallel Inverters without Communication. Nordic Workshop on Power and Industrial Electronics (Norpie 2002), Stockholm, Sweden.

Tuladhar, A. (2000). Advanced control techniques for parallel inverter operation without control interconnections. Dept of electrical and computer engineering, The University of British Columbia. Doctor of Philosophy.

Van Der Broeck, H. and U. Boeke (1998). A simple method for parallel operation of inverters. Twentieth International Telecommunications Energy Conference, . INTELEC. .

W.Hoffmann, R.Bugyi, et al. (1993). PWM inverter for parallel operation as high quality AC source intelecommunication. 15th International Telecommunications Energy Conference, 1993. INTELEC '93. , Paris, France.

Xing, Y., L. P. Huang, et al. (2002). A decoupling control method for inverters in parallel operation. International Conference on Power System Technology, PowerCon 2002.

Zhang, R. (1998). High performance power converter systems for nonlinear and unbalanced load/source. Faculty of the Virginia Polytechnic Institute and State University. Virginia. PhD.

Zhang, R., D. P. Boroyevich, et al. (1997). A three-phase inverter with a neutral leg with space vector modulation. Twelfth Annual Applied Power Electronics Conference and Exposition,.